Università Politecnica delle Marche
Scuola di Dottorato di Ricerca in Scienze dell'Ingegneria
Curriculum in Ingegneria Civile, Ambientale, Edile e Architettura

---

Effect of the rejuvenators on the mechanical and performance characteristics of Hot Recycled Mix Asphalt

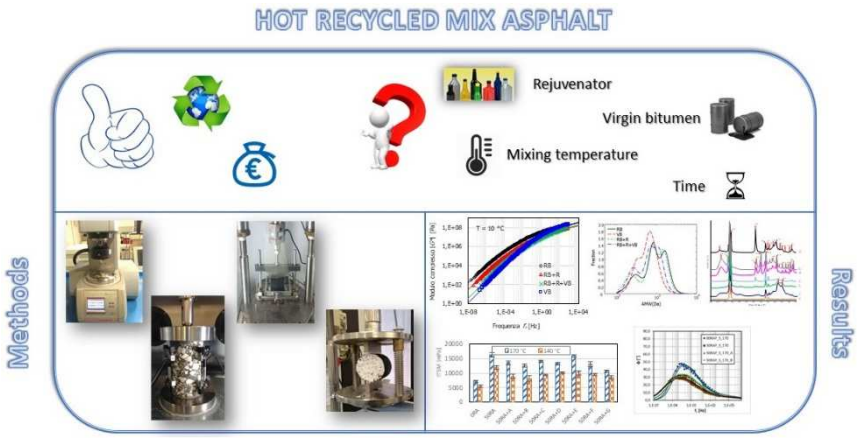

Ph.D. Dissertation of:
Emiliano Prosperi

Advisor:
Prof. Maurizio Bocci

Curriculum supervisor:
Prof. Francesco Fatone

Università Politecnica delle Marche
Scuola di Dottorato di Ricerca in Scienze dell'Ingegneria
Curriculum in Ingegneria Civile, Ambientale, Edile e Architettura

---

Effect of the rejuvenators on the mechanical and performance characteristics of Hot Recycled Mix Asphalt

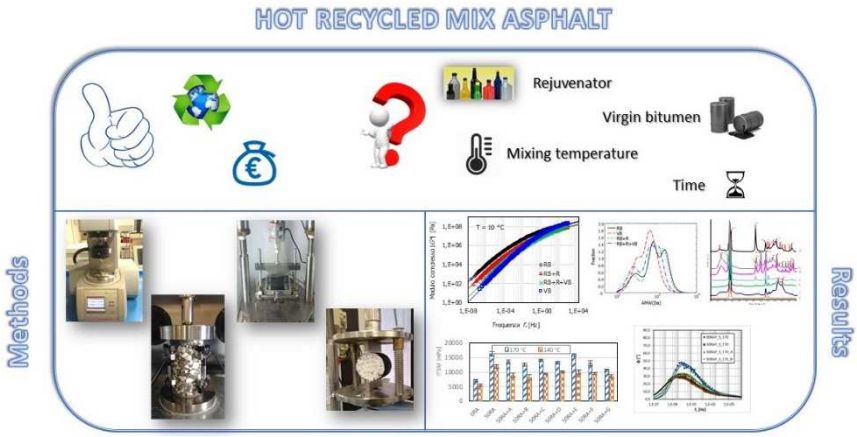

Ph.D. Dissertation of:
Emiliano Prosperi

Advisor:
Prof. Maurizio Bocci

Curriculum supervisor:
Prof. Francesco Fatone

Università Politecnica delle Marche
Dipartimento di Ingegneria Civile, Edile e Ambientale
Via Brecce Bianche — 60131 - Ancona, Italy

To my Family

Acknowledgements

The PhD research work could have never been completed without the help of some fundamental people that supported me for the entire duration of my program.

First, I wish to express my sincere gratitude to my Advisor Professor Maurizio Bocci, invaluable guide and reference point, always available to encourage and support. An admirable example to follow for my future work and personal life, a few minutes with him is equivalent to years of study, given the fundamental advice he can give thanks to his enormous experience in the road field.

A special thanks also goes to prof. Edoardo Bocci, for his enormous patience and availability at all hours of the day, every day. Without his fundamental help everything would have been more difficult and less interesting.

A loving mention goes to all the colleagues Lorenzo Paolo Ingrassia, Xiaotian Jiang, Elena Gaudenzi, Sara Spadoni, Simone D'Angelo, Vittoria Grilli and Simona Caimmi. They worked along with me during this experience with always useful advice and sincere friendship. Particular mentions go to Davide Ragni and Chiara Mignini, they act like big brothers to me, they taught me a lot during these years continuing even after their graduation. A very special thanks goes to my teammate Carlo Carpani, with whom, in addition to having shared a lot of work together, a great friendship was also born that will last forever.

My sincere appreciation goes to the staff of the department ICEA (infrastructure area): Stefania Mercuri, Nicola Agostinacchio, Gabriele Galli and, especially, Pierluigi Priori.

Thanks to the research group at the Polytechnic University of Marche in Ancona, for the scientific and personal support offered me. Thanks to all of them.

The final and most heartfelt thanks to all my Family for giving me the possibility to reach this precious goal. With their daily highly esteemed example and support, my girlfriend Laura and my parents gave me the strength to face all the challenges faced day after day.

This work is dedicated to all of them.

Abstract

Nowadays, one of the main challenges to face up is the development of a circular economy. For this purpose, in the road sector, many economic and environmental benefits encourage the use of the Reclaimed Asphalt Pavement (RAP) to produce new Hot Mix Asphalt (HMA). Such material, together with an important cost and landfill issues reduction, leads to a considerable saving of natural resources, thanks to the re-use of both materials contained into it (aggregates and bitumen). Despite several benefits in using RAP with the Hot-Recycling technique, many issues also arise. Some of the main problems are its isogeneity (both from aggregate gradation and bitumen content) and the difficulties in defining and ensuring the correct heating of the recycled material from a logistical (needing to adapt existing plants) technical (necessity to limit the aging of both virgin and recycled bitumen) and environmental point of view (CO_2 emission). Moreover, the aged and brittle bitumen contained into RAP leads to the reduction of the workability and the performance of the Hot Recycled Mix Asphalt (HRMA) with the consequent and inevitable need to add additives called rejuvenators. All these issues explain why in Italy and all around the world, there are still many limitations on the percentage of RAP that can be re-used in hot recycling techniques. Recently, research has been moving on trying to develop solutions to allow the 100% reuse of RAP even with the hot technique, thus guaranteeing the continuous and circular recycling.

In this context, the main purpose of this PhD research activity is to study and analyse the rheological, mechanical and performance characteristics of HRMA changing the type of rejuvenator, the distillation process of the virgin bitumen, the pre-heating and mixing temperature and the loose mixture time spent in the oven after the mixing process.

Based on the experimental findings, it can be stated that the use of a high RAP content (equal to 50%), without compromising the properties of the HRMA is possible if the production and compaction process, the origin and the properties of the RAP material, the virgin bitumen and the rejuvenator are properly selected. In particular, it was found out that using a reasonably low mixing temperature (enough to make the bitumen workable) and a good straight-run virgin bitumen plays a fundamental role in the production of an HRMA that achieves optimal rheological and mechanical characteristics and is therefore durable over time without suffering from cracking issues. Moreover, the analysis of the effects of a second aging of the rejuvenated bitumen led to the conclusion that the re-aging induces a bitumen having rheological characteristics almost comparable to those of a virgin bitumen first time aged. Thus, the possibility to reuse the rejuvenated bitumen for the production of new asphalt pavements is achieved.

Sommario

Una delle principali sfide da fronteggiare ai giorni nostri è sicuramente quella di garantire un'economia quanto più possibile circolare. Per questo motivo, in ambito stradale, molteplici benefici economico-ambientali incoraggiano l'uso di fresato (RAP), proveniente dalla demolizione di vecchie pavimentazioni stradali, da introdurre nella produzione di nuovo conglomerato bituminoso a caldo. Tale materiale permette, insieme ad una netta riduzione dei costi di produzione e dei problemi di smaltimento, anche un notevole risparmio delle risorse naturali, grazie allo sfruttamento di entrambi i materiali con cui il RAP è composto (aggregati e bitume). A fronte dei tali vantaggi nell'utilizzare il fresato nella tecnica a caldo, ci sono anche alcune problematiche da fronteggiare, come la sua disomogeneità (sia dal punto di vista della granulometria che del contenuto di bitume), la difficoltà nel garantire e definire un corretto riscaldamento del RAP, sia dal punto di vista logistico (con la necessità di adeguare gli impianti esistenti) che tecnico (occorre limitare l'invecchiamento del bitume vergine e di quello presente nel RAP) che ambientale (con problematiche di emissione di fumi). Inoltre, il bitume contenuto nel fresato risulta essere invecchiato e quindi rigido-fragile, con la conseguente necessità di dover impiegare additivi rigeneranti. Tale invecchiamento del bitume provoca ovviamente una riduzione sia della lavorabilità che delle prestazioni del conglomerato bituminoso di recupero. Tutto ciò fa sì che in Italia e nel mondo ci siano tutt'ora delle limitazioni sulla percentuale di RAP utilizzabile nel riciclaggio a caldo. Negli ultimi anni la ricerca si sta muovendo cercando di studiare queste problematiche, trovando delle soluzioni per arrivare a poter riutilizzare il 100% di fresato anche con la tecnica a caldo garantendo quindi un riciclo continuo e circolare.

In questo contesto, l'attività di dottorato ha come scopo principale quello di studiare ed analizzare le proprietà reologiche, meccaniche e prestazionali del conglomerato bituminoso riciclato a caldo al variare della tipologia di additivo rigenerante, del processo produttivo del bitume vergine, della temperatura di produzione della miscela ed infine del tempo di permanenza in forno della miscela sfusa dopo la fase di miscelazione.

Sulla base delle evidenze sperimentali ottenute si può affermare che l'impiego di un elevato contenuto di RAP (pari al 50%) è possibile, senza l'insorgenza di effetti dannosi sulla miscela finale se la tecnica di produzione e compattazione, la provenienza e le proprietà del RAP, del bitume vergine e dell'additivo rigenerante sono selezionate e scelte opportunamente. In particolare, usare una ragionevolmente bassa temperatura di miscelazione (sufficiente da rendere il bitume lavorabile) ed un buon bitume primario comporta la produzione di un conglomerato bituminoso riciclato a caldo con ottime proprietà reologiche e meccaniche tali da essere duraturo nel tempo senza soffrire di problemi fessurativi. Inoltre, l'analisi degli effetti del successivo invecchiamento del bitume rigenerato ha portato a concludere che tale re-invecchiamento produce un bitume aventi caratteristiche reologiche pressoché comparabili a quelle di un bitume vergine invecchiato per la prima volta, confermando così la possibilità di riutilizzare il bitume rigenerato per la produzione di nuove pavimentazioni stradali.

Contents

List of Figures

List of Tables

Introduction

Chapter 1. Background and problem statement

During the last decades, the term sustainability is widely used all over the world in several different fields. There is no universally agreed definition of this word. In fact, there are many different viewpoints on this concept and on how it can be achieved.

Nowadays, because of the environmental and social problems societies around the world are facing, sustainability has been increasingly used in a specific way and, it is usually defined as the processes and actions through which humankind avoids the depletion of natural resources, in order to keep an ecological balance that doesn't allow the quality of life of modern societies to decrease. However, the most appropriate definition of sustainability was given by Bruntland in a final report (1987) called *"Our Common Future"*. He defined defines sustainable development as: "*the development that meets the needs of the present without compromising the ability of future generations to meet their own needs*".

The principles of sustainability are the foundations of what this concept represents. In particular, the sustainability is determined by the combination of three fundamental pillars:

- environmental sustainability: ecological integrity is maintained, all of earth's environmental systems are kept in balance while natural resources within them are consumed by humans at a rate where they are able to replenish themselves;
- economic sustainability: the ability of the human communities across the globe to maintain their independence and have access to the resources that they require, financial and other, to meet their needs. Economic systems are intact, and activities are available to everyone, such as secure sources of livelihood;
- social sustainability: the universal human rights and basic necessities must be attainable by all people, who have access to enough resources in order to keep their families and communities healthy and secure. Healthy communities have just leaders who ensure personal, labour and cultural rights are respected and all people are protected from discrimination.

Therefore, it is obvious that the design and construction process of a new structure/infrastructure must follow and consider its sustainability. In Italy, the concept of sustainable construction is resumed by the D.P.R. n.207/2010 "Regolamento dei Lavori Pubblici", which explicit the need to inspire the design to more advanced principles of environmental protection, related to the concept of sustainability. In particular, the above-mentioned decree states: "[…] *la progettazione deve essere informata a principi di sostenibilità ambientale nel rispetto, tra l'altro, della minimizzazione dell'impegno di risorse materiali e di massimo riutilizzo delle risorse naturali impegnate dall'intervento e dalla massima manutenibilità, miglioramento del rendimento energetico, durabilità dei materiali e dei componenti, sostituibilità degli elementi, compatibilità tecnica ed ambientale dei materiali ed agevole controllabilità delle prestazioni dell'intervento nel tempo* […]".

Therefore, new strategies, policies and integrated assessments about the environmental issue are needed.

The most used solution to reach sustainability is recycling, which implies environmental (reduction in the consumption of natural resources, energy and landfill spaces) and economic benefits (costs saving for new materials, disposal and transport).

In the sector of road pavement engineering, the easiest way to promote the recycling is to encourage the use of Reclaimed Asphalt Pavement (RAP). RAP is defined as removed and/or reprocessed pavement material composed of bitumen and aggregates.

Despite many issues the use of high amounts of RAP in road construction is already a reality in many countries. For instance, Germany, United States, Netherlands and Japan have started to manufacture mixtures with 100% RAP in the asphalt plants, which successfully inaugurates the concept of 'total recycling' in pavement engineering (Al Mamun *et al.* 2020). However, the percentage of re-used RAP has grown gradually in all the countries around the world (Tarsi *et al.* 2020).

Four methods: hot in-plant recycling, hot in-place recycling, cold in-plant recycling, and cold in-place recycling allow RAP recycling in new asphalt mixtures, determining the saving of virgin resources and the progressive cyclic reuse of this waste material, in a sustainable and circularly economic way (Zaumanis and Mallick 2015).

Cold recycling consists of blending RAP with bitumen emulsion (or foamed bitumen), Portland cement, water and, in some cases, virgin aggregate (Kuchiishi *et al.* 2019). Since RAP is not heated, it is typically supposed to behave as a ''black'' aggregate, meaning that the bitumen in the RAP does not have binding properties and is considered as a solid. Differently, hot recycling consists of including the RAP in new hot mix asphalt (HMA). Through its heating or by contact with hot virgin aggregate, the bitumen in the RAP softens and can interact, in some way, with the other HMA components (virgin aggregates, virgin binder and rejuvenator) (Bocci and Prosperi 2020). This represents the most profitable reuse method because both the solid and binding components of the RAP can be recovered. However, since RAP comes from old pavements and contains aged bitumen, there are many issues on the performance of the HMA including hot recycled RAP (also called Hot Recycled Mix Asphalt – HRMA). In particular, a stiffer and more brittle mix is produced when using RAP (Ahmad *et al.* 2020). For this reason, road agencies usually limit the maximum amount of RAP that can be recycled in new hot mixes (Zaumanis *et al.* 2016). With the aim of solving this issue, many products worldwide have been used with the function of rejuvenating agents, which allow restoring (fully or partly) the mechanical properties that the RAP binder loses with aging (Tarsi *et al.* 2020). Several additives have been used as rejuvenators, including bio-oils (Zaumanis, Mallick, Poulikakos, *et al.* 2014, Król *et al.* 2016, Bocci *et al.* 2017, Elkashef *et al.* 2019), waste minerals (Dony *et al.* 2013, Farooq *et al.* 2018, Joni *et al.* 2019, Li *et al.* 2019) or vegetable (Gong *et al.* 2016, Gökalp and Emre Uz 2019, Noor *et al.* 2020) oils. Since the amounts of RAP in HRMA are steadily increasing and many products have been proposed as rejuvenating agents, a thorough understanding of how they modify the

properties of the aged bitumen is required, leading more and more researchers to deeply investigate this aspect in the last years (Walther *et al.* 2020)

As well as the type and content of the rejuvenators (Zaumanis, Mallick, Poulikakos, *et al.* 2014, Bocci *et al.* 2017), the mechanical properties of the HRMA depend on other factors such as the amount of RAP (Kamil Arshad *et al.* 2018); the content, type and aging degree of the bitumen contained into the RAP (Ozer *et al.* 2009, Reyes-Ortiz *et al.* 2012, De Lira *et al.* 2015); the degree of binder activation and blending (Lo Presti *et al.* 2020); the RAP heating procedure during HRMA production (Bocci, Prosperi, Mair, *et al.* 2020, Ma *et al.* 2020) and the type of the virgin bitumen used (neat or polymer-modified, soft binders) (Tarsi *et al.* 2020). However, two further variables influence the performance of HRMA but that is often neglected or underestimated: the virgin bitumen production process and the HRMA manufacturing temperature.

Regarding the type of virgin binder used, a recent study shows that virgin bitumens having the same Performance Grade (PG) but obtained from different oil sources will not always lead to mixtures that perform the same (Mogawer *et al.* 2020). Moreover, together with the oil source (Holýa and Remišováa 2019, Li *et al.* 2020) (that can hardly be managed even by the refineries), also the type of distillation process to which the crude oil is subjected can influence the characteristics of the final mixture.

During the distillation, the various phases of the crude oil are separated due to the difference in its boiling and condensing temperatures (Paliukaitė *et al.* 2014). A typical distillation process involves a first step in which the lighter components are separated, subjecting the crude oil to a temperature of about 350 °C at atmospheric pressure. The residue of the first step is subjected to a higher temperature, around 350-425 °C, under a controlled pressure ranging from 1 kPa to 10 kPa. The residue of the second process is called straight-run bitumen (Giavarini 1981). Moreover, if the residue of this second process is subjected to another step of thermal distillation at temperatures between 455 °C and 510 °C, visbreaker bitumen is produced (Speight 2012). Vis-breaking allows refineries to reduce the amount of the residue produced, as it allows the further recovery of lighter products such as diesel and gas. This penalizes the quality of the bitumen that is obtained, which is more rigid, brittle and susceptible to aging (Giavarini and Saporito 1989). Giavarini (Giavarini 1984) studied visbreaker (VB) and straight-run (SR) bitumens obtained from the same crude oil. He repeated tests such as penetration and softening immediately and after 1 year, during which all bitumens were subjected to the same treatment (i.e. controlled heating to simulate aging) and stored under the same conditions in the laboratory. He found out that the effect of aging was much more pronounced for the VB. In particular, starting from average penetration values of 175 dmm and 155 dmm for the SR and VB bitumen respectively, the average penetration decrease for the VB binder was more than 90 dmm, against about 40 dmm for the SR. Moreover, the penetration index, which was originally about the same for both kinds of bitumen, became appreciably lower for the VB, indicating that the characteristics of VB products change significantly during storage.

Summarizing, the products derived from visbreaking show higher temperature susceptibility, lower oxidation resistance and more rapid changes in properties. Considering the amount of VB bitumens that are marketed in Europe, more detailed and recent information is needed on the differences between such binders and straight-run ones, and on the correlations between the severity of the visbreaking process and the stability of the bitumen. Very often, pavement technologists distinguish bitumen only by penetration index or PG, without considering the distillation process from which it derives, which greatly affects the characteristics of HMA and its aging.

Temperature plays an essential role in bitumen aging, as it can accelerate chemical modifications (Hofko, Cannone Falchetto, *et al.* 2017). For this reason, it is fundamental to avoid bitumen overheating, which means containing the temperatures during HMA manufacturing. In particular, this can cause a more severe short-term aging for both virgin and RAP binders (Lolly *et al.* 2017), leading to stiffer and excessively brittle mixtures. In the HMA plants, the virgin aggregates are often overheated, as a function of the target mix temperature, the RAP content and the temperature and humidity of the RAP when it is introduced into the mix. The stronger the aggregate overheating is, the more severe is the thermal shock for the bitumen when it meets the aggregate particles. Moreover, also the effectiveness of the rejuvenators can be influenced by the temperature at which the HRMA is produced. On the other hand, a low mix temperature can result in poor workability and therefore in a high air voids content, reflecting on a higher risk of moisture damage, raveling, rutting and cracking (Khan *et al.* 2013a).

Based on the above-mentioned discussions, since recycling old removed pavement plays a fundamental role on promoting sustainability, the aim of the work presented in this Ph.D thesis is to investigate the influence of the type of virgin bitumen distillation process, the kind of rejuvenator and the temperature during HRMA mixing on the mechanical and performance characteristics of the Hot Recycled Mix Asphalt.

Chapter 2. Literary review

2.1. RAP: experiences, benefits and issues

During the last years, the amount of re-used RAP is significantly increasing. Currently, a RAP content ranging between 15–20% wt. is a standard practice for the production of new asphalt mixtures (Tarsi *et al.* 2020). However, as this content is still inadequate, multiple studies are still in progress to be able to bring it up to 50% or even 100% in order to obtain a complete circular economy.

Talking about the recycling of bituminous mixtures, the most efficient country is Japan. A recent survey shows that there are about 1150 asphalt plants in Japan, serving more than 90% of the country and producing about 55 million tons of HMA annually. Of those 55 million tons, about 41.9 million tons contain RAP. Moreover, RAP content in Japan asphalt mixtures increased from 33% (2000) to 47% (2013). The average RAP contents are similar in colder and warmer regions and range from 20%–60% (West and Copeland 2015).

Similarly, the recent survey of the National Asphalt Pavement Association (NAPA) showed that in USA, more than 99% wt. of the available RAP in 2018 were re-used, resulting the most recycled product among American States. In particular, from the 2018 to 2019 construction season, the amount of RAP used in HMA/WMA increased from 82.2 million to 89.2 million tons. The average percent RAP used in asphalt mixtures remained the same at 21.1 percent in 2018 and 2019. Moreover, approximately 97% of the re-used RAP was recycled in new asphalt mixtures, while 3% was re-used in other civil engineering applications. For this reasons, the average quantity of RAP landfilled was almost zero in 2018 (Brett *et al.* 2019).

In Europe, the monitoring of the use of the RAP is provided by the European Asphalt Pavement Association (EAPA). In particular, in 2018, out of the 49.5 million tonnes of reclaimed asphalt available in these countries, 76% was re-used in the manufacture of new asphalt mixes and 20% was recycled in unbound road layers and other civil engineering applications. This means that only 4% was put to landfill or used it in other and unknown applications. RAP is mainly used in HMA, Warm Mix Asphalt (WMA) and Cold Mix Asphalt (CMA) mixtures. However, a remarkable percentage (more than 20%) of RAP was used as aggregates for unbound layers, and 8.4% wt. was landfilled. It should be taken into account that, since the use of RAP is highly dependent on national regulations, the European data are very variable from country to country (EAPA 2018).

Hereafter, a table showing the comparison of RAP uses in the USA and Europe in 2018 is provided (EAPA 2018, Brett *et al.* 2019). The main differences between the American and European practices regard the quantity of RAP introduced in new HMA/WMA mixes and the quantity used for unbound layers. Moreover, it is evident that cold recycling technology is significantly more used in Europe than USA. However, it must be considered that the European data of the RAP used in CMA mixes reflect the use of RAP by a limited number

of nations; in fact, most EU nations do not still introduce RAP in CMA mixtures. Lastly, regarding the landfill disposal, a very high quantity of old pavement are disposes in Europe (compared to USA). Hence, the following table highlights that the European states should exploit more the recycled aggregates potential.

All over the world, there are limitations to the amounts of RAP used in different road layers. For countries which use Superpave mixes, the maximum allowable RAP content in the wearing course is 10% to 15%, and 50% in the other layers (Al-Shujairi *et al.* 2021).

	EUROPE	**USA**
RAP used in WMA/HMA	51.4 %	81.3 %
RAP used in CMA	3.8 %	0.3 %
RAP used for unbound layers	17.0 %	6.3 %
RAP used for other purposes	2.0 %	2.0 %
RAP landfilled	9.6 %	almost 0 %

Table 1 - differences on the use of RAP between Europe and USA (Tarsi et al. 2020)

Using RAP (hot/warm technique), in constructing new pavements leads to a couple of main benefits: economical ad environmental advantages (Baghaee Moghaddam and Baaj 2016). Martins Zaumanis et al. compared the costs of conventional asphalt mixtures to those of asphalt mixtures containing RAP. Considering different percentages of RAP (from 0 to 100%), they stated that, since more than 50% of the final cost of HMA is related to the binder cost, using 50% RAP materials resulted in decreasing the construction cost by almost 30%. Moreover, by utilizing 100% RAP material the construction cost can be reduced by 50–70% (Zaumanis, Mallick, and Frank 2014b).

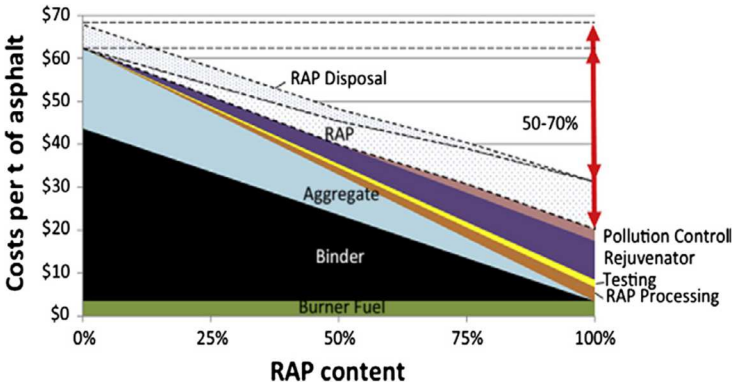

Figure 1 - Costs of materials in hot mix recycling (Zaumanis, Mallick, and Frank 2014b)

On the other hand, there are three different environmental benefits of reusing RAP. First of all, it is a valid solution to reduce waste road construction materials by adding them in new road construction works (Baghaee Moghaddam and Baaj 2016). This induces savings in raw materials (asphalt binder and aggregates). Moreover, even the energy consumptions and emissions were reduced by using RAP materials in HRMA (reduction of the extraction and transportation of virgin material) (Lee *et al.* 2012). As another environmental benefit is the reduction of the landfill space required (West 2010).

Despite the benefits listed above and that several studies have shown the possibility to produce asphalt mixtures with high (50% wt. and more) amount of RAP, the national specifications and the practical issues limit the common practice to go beyond the average RAP content of 15–30% wt. The major disadvantages using RAP materials can be summarized in four categories: the quality and the homogeneity of the RAP aggregates, the technology of the production plant, the mix design methodology and the performances of the final mix containing RAP (Tarsi *et al.* 2020).

In order to assess the quality and homogeneity of the RAP, it needs to be controlled frequently (Lee *et al.* 2015). The basic principle for ensuring good performing HRMA is to apply the same requirements to the RAP fractions as those that are specified for virgin aggregates (Willis *et al.* 2012). However, due to the milling operation, excessive fines are generated, and it becomes very difficult to fulfil the gradation requirements. This limits the maximum content of RAP material to which it can be used (Rathore *et al.* 2019). Moreover, due to their higher surface area, the finer particles bring to the recycled mixtures a higher amount of aged binder and a higher moisture content (Newcomb *et al.* 2007). A recent survey showed that RAP gradation is general more consistent than that of virgin aggregates (West 2015). However, since RAP is milled from different roads using different techniques, its inhomogeneity has been reported as a problem (Rathore *et al.* 2019). The ideal production process should allow the use of RAP coming from only a single source (intended as pavement layer). Moreover, the quality of the removed asphalt materials from pavements also depends on the milling machine, its speed and milling depth: good milling operations guarantee a high quality of RAP (Van Den Kerkhof 2015). Therefore, keeping different milling projects in different stockpiles leads to the increase of the consistency of the removed asphalt material (West and Copeland 2015). Recently, (Tebaldi *et al.* 2018) presents a new characterization procedure for RAP materials, intended for use in new, rehabilitated and maintenance related construction activities for asphalt pavements. The aim of this characterization procedure is to develop a fingerprint method for RAP and to determine and obtain parameters that can enhance the reliability of design procedures for HRMA.

Together with the RAP properties, even the recycling technique has a crucial role to obtain agood recycled mixtures and consequently suitable field performance. Regarding the hot recycling process, RAP represents a percentage of the total amount of materials around 10 to 50% to be mixed with aggregates and bitumen preventively heated at high temperature. Two different production methods can be adopted:

- in plant recycling: the milled material is moved from the old pavement location to the plant site where it is processed through crushing and screening to discard foreign matters and clumps too large. Then, it is usually sieved and divided in more fractions prior to being re-used. Thanks to the higher possibility to monitor and control the milled material prior to be re-introduced in the production process, this method avoids high variability of RAP and guarantees a better quality and a more uniform homogeneity of the final mixture. Moreover, it provides the advantage of having higher flexibility in the production sequences that can be adapted according to several requirements and different types of mixture. At the same time, this method has few drawbacks mainly related to the higher costs due to the transport and the stocking of the milled material in the plant where it is necessary to ensure a big amount of appropriate spaces;
- in place recycling: in this case, all the production activities (milling, mixing, compaction) are implemented directly in field using specific equipments. Lower control of the milled materials and the quality of the production process have to be considered. However, these drawbacks are balanced by higher economic benefits and shorter production time. The so produced mixtures are usually employed to build binder or base layers, depending on type and volume of traffic (Tebaldi *et al.* 2012).

The choice to adopt the in plant production process is mainly determined by the following factors:

- type of application: the in plant recycling is usually taken into account when the recycled material is used to build a new layer of the pavement;
- in site material: since high quality and good properties are required for surface layers, when they are produced with milled material, the variability usually related to RAP can justify a pre-treatment that can be realized only in plant.

One of the most important issues to face in in plant hot recycling is the management of the milled product during the mixing process. With respect to the batch plant, RAP can be heated and dumped into the mixture using different solutions (Dharmesh 2015):

- adding cold RAP through a simple RAP ring into the drier at its exit end after the burner to avoid flame affecting the RAP material. This way one can add up to about 15% RAP which can go over the screen with little maintenance care;
- adding cold RAP to the hot elevator just after the fresh material discharge from the drum. This method can handle up to 15% RAP and can go over the screen with little maintenance care;
- adding cold RAP directly into the pug mill. This method is called as RAC and can go up to about 30% RAP. The RAP does not go over the screen, but the 70% fresh material goes through the screen and weighing system of batch mix plant.

- adding RAP in the drum at a point around mid-way. The drum has very special arrangement inside to protect flame from coming in contact with RAP material. This drier drum can handle up to 40 to 45% of RAP.
- adding RAP heated in a separate heating and drying drum with burner to heat RAP up to certain temperature and then add this hot RAP into the pugmill mixer with fresh hot aggregates. This method can handle up to 60% RAP. The hot RAP does not go through the screen, but the fresh aggregates go through the screen and weighing process;
- a Swiss company has recently developed special recycling drum which can heat the RAP material up to final mix temperature and can handle nearly 100% RAP. Entire material does not go over the screen.

On the other hand, in a continuous plant, whether single drum or double drum, because there is no screening of hot mix done in the plant, the cold RAP material is added to the drier drum through a special RAP ring which allows feeding of the RAP material in a rotating drum. Because this is not a batch mix plant and does not have screening and weighing of hot aggregates, the amount of RAP that can be added depends upon the heat transfer and flame protection systems given in the drier drum design (Milad *et al.* 2020).

To achieve a HRMA having good mechanical and performance characteristics, homogeneous distribution of rejuvenator and good diffusion into reclaimed asphalt binder film has to be ensured (Zaumanis *et al.* 2019). A recent study ranked ten potential locations for rejuvenator addition in asphalt plant in terms of pavement performance, plant operation, and environmental safety. The two most promising were compared in full-scale study: spraying of rejuvenator on cold reclaimed asphalt on the feeding belt before heating versus addition of rejuvenator to hot reclaimed asphalt in mixer. The results showed that passing through the extreme temperatures in the RAP heating drum does not increase chemical aging of the rejuvenated binder. Moreover, a benefit of early rejuvenator addition is that it provides a longer residing time of rejuvenator on the binder and thus potentially may allow higher binder activation and better blending of RAP binder with rejuvenator and virgin binder (Zaumanis *et al.* 2018).

Since temperature plays an essential role in bitumen aging,(Hofko, Cannone Falchetto, *et al.* 2017), it is fundamental to avoid bitumen overheating, which means containing the temperatures during HMA manufacturing. In particular, this can cause a more severe short-term aging for both virgin and RAP binders (Lolly *et al.* 2017), leading to stiffer and excessively brittle mixtures. In the HMA plants, the virgin aggregates are often overheated, as a function of the target mix temperature, the RAP content and the temperature and humidity of the RAP when it is introduced into the mix. The stronger the aggregate overheating is, the more severe is the thermal shock for the bitumen when it meets the aggregate particles. Moreover, also the effectiveness of the rejuvenators can be influenced by the temperature at which the HRMA is produced. On the other hand, a low mix

temperature can result in poor workability and therefore in a high air voids content, reflecting on a higher risk of moisture damage, raveling, rutting and cracking (Khan *et al.* 2013b).

The mix design of HRMA has to meet the same criteria as HMA containing only virgin material (Willis *et al.* 2012). However, the traditional model needs to be uploaded in case of HRMA made with high amount of recycled material. Its inhomogeneity forces the designers to constantly monitor the RAP gradation and bitumen content adapting the mix design accordingly. Moreover, the RAP binder contributes to the rheological properties and the total content of the final blended binder. Therefore, the rheological characteristics of the aged binder must be analysed, and the rejuvenator content must be adapted. It should be pointed out that a low dosage of rejuvenator leads to a mixture having cracking and fatigue damages, while an excessive quantity of additive leads to a HRMA with rutting issues. Despite most of road agencies regulations assume a full blending between aged and virgin binder (Copeland 2011), recent studies stated that only a portion of the RAP binder is available and can act as a binder in the new formulation (Zhou *et al.* 2011, Lo Presti *et al.* 2020). Thus, another aspect to take into account in the mix design is the amount of bitumen that reactivates and can act like a binder (degree of blending and degree of activation) (Lo Presti *et al.* 2020).

The increase of RAP content in new formulations leads to an increase in the stiffness of the final mixture (Ozer *et al.* 2009) strictly related to the stiffness of the aged binder contained into it. Since asphalt mixtures having excessive stiffness are less resistant to cracking due to fatigue or thermal load, many of road agencies are reluctant to use large quantities of RAP (Willis *et al.* 2012). However, several recent studies stated that, using appropriate mix design and recycling techniques, it is possibile do produce an HRMA with mechanical and performance properties comparable, or even better, than those of an HMA produced with only virgin materials (Karlsson and Isacsson 2006, Zhou *et al.* 2011, Mogawer *et al.* 2012, Tran *et al.* 2012, Grilli *et al.* 2013, Zaumanis and Mallick 2014, Zaumanis *et al.* 2016, Wu *et al.* 2020).

2.2. Rejuvenating agents

During the last decades, a lot of studies tried to estimate the efficacy of different rejuvenators. According to the literature, there are many different sources from which we can obtain rejuvenators. In general, according to their nature, rejuvenators can be classified in additives derived from oil and biological additives. For instance, Zaumanis et al. (Zaumanis, Mallick, and Frank 2014a) and Dony et al. (Dony *et al.* 2013) stated that although the two categories may show differences, both additives can be used successfully to soften the aged bitumen and allow the fulfillment of the requirements in terms of penetration, softening point and rheological characteristic.

Besides fuels and bitumens, rejuvenators able to improve the properties of an aged binder are often produced from the processing of crude oil. These products include aromatic extracts, paraffinic oils, naphthenic oils and spent motor oils (Behnood 2019). These petroleum products have been the main agents used for many years to improve the characteristics of

aged bitumen. In recent decades, research has moved towards finding materials with rejuvenating effects for an aged bitumen having a lower cost and being environmentally sustainable. They are called bio-rejuvenators and they are products such as tall oil, rapeseed oil, soybean oil, sunflower oil, corn oil, used cooking oil, castor oil residues and organic oils. Several studies promote these rejuvenators, highlighting that they are able to restore the original properties of bitumen being eco-sustainable at the same time.

Among the numerous researches carried out during the last decades, the most relevant and suitable are reported hereafter together with a brief description of the used rejuvenators and the main results.

Bocci et al. (Bocci *et al.* 2017, n.d.) and Grilli et al. (Grilli *et al.* 2015) focused on the evaluation of the mechanical and performance characteristics of HMA made with a high amount of RAP and a bio-rejuvenator. They found out that, using appropriate dosages of this additive, acceptable performance, similar to those reached with virgin materials can be achieved. Thus, the evaluation of the correct dosage of rejuvenators plays a fundamental role in order to obtain a mixture that can easily meet the specifications.

Krol et al. (Król *et al.* 2016) and Somé et al. (Somé *et al.* 2016) evaluated the effects of several vegetable oils (rapeseed oil, soybean oil, sunflower oil, flaxseed oil) on the mechanical characteristics of bitumen and mixes. Furthermore, they also developed chemical processes to make new additives. These researches aimed to improve the performance of bituminous binders using only very cheap raw materials.

Zargar et al. (Zargar *et al.* 2012) studied the possibility to use waste cooking oil (WCO) as a rejuvenator in aged bitumen. They highlighted that, adding a specific dosage of this additive, the same values of penetration index, softening point and viscosity of a virgin bitumen can be obtained. Moreover, increasing the amount of WCO these properties can be further improved. Gökalp and Emre Uz (Gökalp and Emre Uz 2019) confirmed that using WCO leads to improvements in penetration index, viscosity and fatigue resistance.

During the last years, many studies compared the effect of WCO with respect to waste engine oils (WEO) in restoring the original properties of an aged bitumen. In particular, Joni et al. (Joni *et al.* 2019) stated that the effect of WCO is greater than that of WEO on the properties of an aged binder, therefore, to obtain the same results, the required amount of WEO to be added is greater than that of WCO. Li et al. (Li *et al.* 2019) confirmed that both WCO and WEO have rejuvenating properties, but WCO has higher efficacy than WEO, which implies the use of higher dosages. Moreover, Al Mamun et al. (Al Mamun *et al.* 2020) investigated different contents of RAP and WCO/WEO rejuvenators. Differently from the previous studies, they noted that WEO allows a higher reduction of indirect tensile strength and stiffness with respect to WCO, under the same dosage, but WCO allows a higher content of RAP to be recycled.

The differences between bio-additives and aromatic additives were also studied from a molecular point of view by FTIR. Noor et al. (Noor *et al.* 2020) showed that using biological additives involves the increase of particular functional groups (C = O) in bitumen. Moreover,

Cavalli et al. (Cavalli *et al.* 2018) stated that using rejuvenators such as seed oil or tall oil can increase the carbonyl and sulphoxide indices since they contain functional groups C=O and S = O. Investigating the performance of these indices is a good way to qualitatively understand the effects of a rejuvenating agent on an aged binder. Zhang et al. (Zhang, You, *et al.* 2019), through the analysis of the carbonyl, sulphoxide and aromatic indices, assessed the degree of aging and rejuvenation of some mixtures including bio-additives.

Zeng et al. (Zeng *et al.* 2018) tested castor oil as a rejuvenating agent and they found out that using this additive it is possible to obtain an improvement of the rheological properties of the aged binder.

The studies carried out by Elkashef et al. (Elkashef *et al.* 2019) and Nayak and Sahoo (Nayak and Sahoo 2017) focused on the use of soybean oil and Pongamia oil. They concluded that both products are good rejuvenators, capable of restoring the rheological properties that the binder lost with aging.

Kehzen et al. (Kezhen *et al.* 2020) tried to evaluate the tung oil (also called "China wood oil") as an additive, showing how its addition improves the elasticity of an aged binder. In addition, with suitable amounts of tung oil, good performances of the mixture at high temperatures are also ensured.

Several studies regard the effects of rejuvenators engineered and "built" in the laboratory. In particular, Zhang et al. (Zhang, Sun, *et al.* 2019) tested a rejuvenating agent made of rubber oil, plasticizers and surfactants and demonstrated that the blend of these ingredients allows the binder to recover the malleability and ductility lost during the aging processes. Rzek et al. (Rzek *et al.* 2020) obtained a rejuvenator by modifying pyrolytic condensate of scrap tires with tire crumb. The results confirmed that the addition of this product improved the properties of the binder. Moreover, mechanical, and rheological tests showed that the amount of RAP can reach up to 60% when this engineered rejuvenator is added to the mixture.

Zaumanis et al. (Zaumanis *et al.* 2013, Zaumanis, Mallick, and Frank 2014a, Zaumanis, Mallick, Poulikakos, *et al.* 2014) tested the rejuvenating effect of many products of both biological and hydrocarbon nature, such as cotton seed oil, vegetable oil, used cooking oil, used motor oil, aromatic extract, distilled tall oil, distilled tall oil, exhausted motor oil, naphthenic oil and aromatic extract.

Radenberg et al. (Radenberg *et al.* 2016) carried out a study testing 21 different types of rejuvenators commonly used in the road sector; the products were distinguished between "rheologically effective" and "chemically effective". While the former led to an increase in the maltenic phase, the latter reversed the effects of the oxidation process in the agglomerated compounds.

The following table presents recent publications concerning the use of additives to rejuvenate the aged bitumen in the RAP. For a correct understanding, a brief description of the nature of the additives tested is also included.

Additive	Dosage*	Description	References
Tall oil	4-20%	Tall oil is an organic product deriving from the Kraft process: procedure for converting wood into wood pulp, the main component of the paper. It contains fatty acids, acid resins and surfactants.	(Bearsley and Haverkamp 2007, Zaumanis *et al.* 2013, Zaumanis, Mallick, and Frank 2014a, Zaumanis, Mallick, Poulikakos, *et al.* 2014, Bocci *et al.* 2017, Mokhtari *et al.* 2017)
Exhausted vegetable cooking oil (mix of the main oils used for frying)	1-20%	The chemical composition of these additives mainly contains fatty acids and methyl esters, with both oleophilic and hydrophilic properties	(Asli *et al.* 2012, Zargar *et al.* 2012, Zaumanis *et al.* 2013, Zaumanis, Mallick, Poulikakos, *et al.* 2014, Hugener *et al.* 2014, Maharaj *et al.* 2015, Azahar *et al.* 2016, Gong *et al.* 2016, Osmari *et al.* 2017, Gökalp and Emre Uz 2019, Li *et al.* 2019, Al Mamun *et al.* 2020, Noor *et al.* 2020)
Sunflower oil	5-9%	It is the oil extracted from sunflower seeds. Contains triglycerides, with a high content of linoleic acid. It has a high content of polyunsaturated fatty acids.	(Król *et al.* 2016, Somé *et al.* 2016, Cavalli *et al.* 2018)
Linseed oil	6-9%	It is the oil obtained by squeezing previously dried or toasted flax seeds. It is mainly composed of triglycerides. It is one of the vegetable oils with the highest concentration of acidolinolenic acid.	(Król *et al.* 2016, Somé *et al.* 2016)

Soybean oil	6-9%	It is obtained by extraction from soybeans through a special process called “crushing” with the use of chemical solvents. It too is mainly composed of triglycerides.	(Król *et al.* 2016, Somé *et al.* 2016, Elkashef *et al.* 2019)
Rapeseed oil	1,5-9%	It is a vegetable oil produced from rapeseed seeds. It occurs naturally in many varieties. The resulting oil, therefore, depends on the characteristics of the rapeseed from which it is extracted. The chemical composition includes fatty acids and methyl esters.	(Król *et al.* 2016, Somé *et al.* 2016, Kowalski *et al.* 2017)
Castor oil	5-50%	It is very valuable vegetable oil, which is extracted from the seeds of the castor plant. It is mainly composed of acylglycerides and the main fatty acid present is ricinoleic acid.	(Nayak and Sahoo 2017, Zeng *et al.* 2018)
Pongamia oil	5-15%	It is a fixed oil derived from the seeds of the Millettia pinnata tree. Typically, Pongamia oil is made up of glycerides, especially triglycerides. It is considered a fluxing agent rather than a rejuvenator.	(Nayak and Sahoo 2017)
Tung oil	2-8%	Also called China wood oil, it is the oil extracted from the Aleurites fordii seeds. It is mainly composed of triglycerides and is considered a	(Kezhen *et al.* 2020)

		drying oil with extremely short polymerization times.	
Cashew oil	5%	It is an oil that derives from natural resins that fill the interstitial spaces of the honeycomb structure of the cashew shell. The resin is made up of 80-85% of anacardial acids (o-pentadeca dienylsalicylic acid) and the remaining fraction of cardol and methylcardol.	(Cavalli *et al.* 2018)
Corn oil	1,5-9%	It is an oil extracted from the germs of the seeds of Zea mays, a graminaceous native to North America. It has a composition similar to sunflower oil, very rich in linoleic acid. It is mainly composed of triglycerides	(Zhao *et al.* 2018)
Cotton seed oil	12%	It is the vegetable oil extracted from the seeds of cotton plants. It is mainly composed of triglycerides.	(Zaumanis, Mallick, and Frank 2014a)
Oleic acid	2,5-4,5%	It is an 18-carbon monounsaturated carboxylic acid of the omega-9 series. In the form of triglyceride, it is an important component of animal fats and is the most abundant constituent of the majority of vegetable oils.	(Ali *et al.* 2016a)

Organic oil from wood waste	2-12,4%	A very wide range of types of timber can be used such as Red Maple, Magnolia, Balsam, Poplar, Linden, Beech and Pine	(Borghi *et al.* 2017, Yang *et al.* 2017)
Vegetable waste fat	12%	Material composed of waste grease produced by catering processes	(Zaumanis, Mallick, Poulikakos, *et al.* 2014)
Pig manure	2-10%	It is the product of the fermentation of pig manure mixed with solid material used as bedding	(Borghi *et al.* 2017, Yang *et al.* 2017, Pahlavan *et al.* 2019)
Algae additive	10%	This is a bio-oil extracted from algae leaves or blooms through pyrolysis and it is rich in phenolic compounds.	(Pahlavan *et al.* 2019)
Waste engine oil	1-20%	It is the waste lubricating oil used by engines. It is mainly produced from paraffinic oil.	(Romera *et al.* 2006, Dony *et al.* 2013, Zaumanis *et al.* 2013, Zaumanis, Mallick, and Frank 2014a, Farooq *et al.* 2018, Fernandes *et al.* 2018, Joni *et al.* 2019, Li *et al.* 2019, Al Mamun *et al.* 2020)
Rubber powder from pyrolysis of used tires	5-12%	Pyrolysis is a thermochemical decomposition process of organic materials, obtained by applying heat and in the complete absence of an oxidizing agent. The pyrolytic product from tires pyrolysis contains high concentrations of polycyclic aromatic hydrocarbons	(Avsenik *et al.* 2016, Rzek *et al.* 2020)

Aromatic extract	5-9%	Aromatic extracts are refined products from crude oil and constitute one of the most traditional classes of rejuvenators. Their chemical structure includes aromatic polar rings.	(Garcia *et al.* 2010, Zaumanis *et al.* 2013, Zaumanis, Mallick, and Frank 2014a, Mogawer *et al.* 2015)
Naphthenic oil	50-400%	Naphthenic oils are high-quality pure naphthenic mineral bases, obtained by hydrogen refining of selected crude oil.	(Zaumanis *et al.* 2013)
"Soft" bitumen	5%	Bitumen with a high penetration value and low stiffness. It is typically classified as a fluxing agent since it does not restore the physical and chemical properties of the aged binder. However, this binder can lead to a decrease in bitumen blend viscosity.	(Chen *et al.* 2015, Ameri *et al.* 2018)
*** The dosages refer to the weight of the aged bitumen**			

Table 2 - Most used additives, biological (grey) and derived from oil (white) used to rejuvenate aged bitumen.

2.3. Bitumen aging and rejuvenation chemistry: processes, materials and analyses

In the scientific literature, there are several studies concerning the aging and rejuvenation of bitumen. In particular, most of the studies are focused on how "improved" (in terms of performance or even environmental friendship) bituminous binders behave with aging and when blended with aged bitumen from RAP. For instance, the use of polymer-modified bitumen is one of the hottest topics in this field (Polacco *et al.* 2015). Bitumen including elastomeric or plastomeric polymers experiences different changes with aging with respect to the neat bitumen, as a function of the polymer type and content (Wang *et al.* 2019, Celauro *et al.* 2020, Cuciniello *et al.* 2021, Feng *et al.* 2021, Sun *et al.* 2021). Moreover, it is a theme of research whether RAP including polymer-modified bitumen is recyclable as the RAP

containing neat bitumen, in terms of final mix performance and emission during mix production (Rodriguez-Fernandez *et al.* 2020, Lin *et al.* 2021). Another technique to increase the bitumen performance, which is actually investigated in terms of aging behavior, deals with the use of nanomaterials as modifiers, such as fumed silica, clay, diatomite, titanium dioxide, graphene and carbon nanotubes (Liu *et al.* 2017, Cheraghian and Wistuba 2020, 2021, Anwar *et al.* 2021, Dell'Antonio Cadorin, N. Victor Staub de Melo *et al.* 2021, Han *et al.* 2021, Moretti *et al.* 2021). However, there are still some gaps of knowledge on the understanding of neat bitumen aging phenomena, particularly from a chemical point of view. Many researchers have been trying to fill these gaps in the last 5 years. As shown in Table 3 and Fig. 3, the search for the keywords "bitumen" (or "asphalt", in the American dictionary), and "aging" or "rejuvenation" in the Scopus database has provided several occurrences when associated with chemical analyses. More than half of these publications come from Chinese authors (first author), but many studies have been carried out also in North America (United States and Canada) and Europe.

Keywords	**Papers published since 2016**
"Bitumen/Asphalt", "Aging", "AFM"	114
"Bitumen/Asphalt", "Aging", "Chemistry"	71
"Bitumen/Asphalt", "Aging", "Chromatography"	115
"Bitumen/Asphalt", "Aging", "FTIR"	395
Total number of papers of bitumen aging chemistry	589
"Bitumen/Asphalt", "Rejuvenation", "AFM"	24
"Bitumen/Asphalt", "Rejuvenation", "Chemistry"	15
"Bitumen/Asphalt", "Rejuvenation", "Chromatography"	29
"Bitumen/Asphalt", "Rejuvenation", "FTIR"	73
Total number of papers of bitumen rejuvenation chemistry	121

Table 3 - Number of papers indexed by Scopus in the period 2016-2021 on the theme of bitumen aging/rejuvenation chemistry (date of the research 2021-05-27)

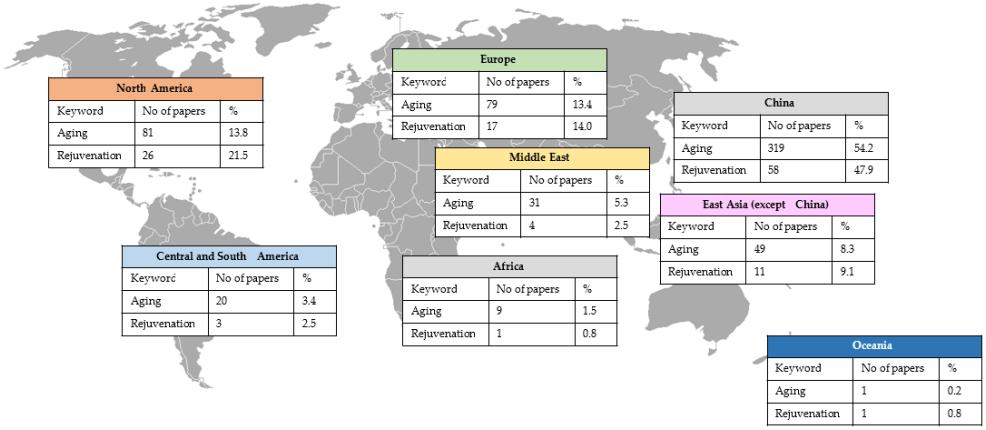

Figure 2 - Origin of the papers indexed by Scopus in the period 2016-2021 on the theme of bitumen ag-ing/rejuvenation chemistry.

2.3.1. Bitumen chemistry

Bitumen is the visco-elasto-plastic material obtained through crude oil distillation. Basically, during this process, the various phases of the crude oil are separated due to the difference in its boiling and condensing temperatures (Paliukaitė *et al.* 2014). A typical distillation process involves a first step in which the lighter components are separated, subjecting the crude oil to a temperature of about 350 °C at atmospheric pressure. The residue of the first step is subjected to a higher temperature, around 350-425 °C, under a controlled pressure ranging from 1 kPa to 10 kPa (de Klerk 2020). The residue of the second process is called straight-run bitumen (Giavarini 1981). Moreover, if the residue of this second process is subjected to another process of thermal distillation at temperatures between 455 °C and 510 °C, visbreaker bitumen is produced (Speight 2012). Vis-breaking allows refineries to reduce the amount of the residue produced, as it allows the further recovery of lighter products such as diesel and gas. This penalizes the quality of the bitumen that is obtained, which is more rigid, brittle and susceptible to aging (Giavarini 1984, Giavarini and Saporito 1989).

2.3.1.1. Basic characterization

The bitumen composition is strictly related to the characteristics of the starting crude oil, particularly on its age and the depth from which it is extracted. The study of bitumen chemical composition is very tricky because it contains many chemical elements. Although bitumen is mainly composed of hydrogen (8-12% by weight) and carbon (80-88% by weight), which together give a hydrocarbon content of about 90%, heteroatoms as nitrogen (0-2% by weight), oxygen (0-2% by weight) and sulfur (0-9 % by weight) are also present. Moreover,

there can also be traces of heavy metals such as nickel and vanadium, with the order of hundreds of parts per million (Mortazavi and Moulthrop 1993).

The hydrocarbons (C+H) can be classified, according to the type of bond between the carbon atoms, into:

- saturated: only simple bonds are present between the carbon atoms;
- unsaturated: double or triple bonds are present.

The heteroatoms (N, S, O) can be found in the correspondence of the unsaturated bonds. When combined with carbon, these can cause an imbalance of the electrochemical forces that gives polarity to the molecule. Therefore, the heteroatoms, despite being present in small percentages, have the ability to make the unsaturated molecules more active, influencing the bitumen rheological properties (Petersen 1984).

2.3.1.2. Chemical-structural analysis – SARA analysis

To interpret bitumen properties from its chemistry it is necessary to consider it on different scales and not only at a global level. In fact, bitumen can be described as several central structures consisting of polyaromatic assemblies containing a various number of molten rings, saturated polycyclic structures and combinations. Saturated hydrocarbon side chains, which are characterized by different dimensions and patterns, are linked to these central assemblies. Therefore, the number of possible isomers is almost unlimited. This is the reason why bitumen is characterized by millions of different molecules and none of these is present in such a high quantity to isolate and characterize it. Therefore, a chemical-structural analysis is more useful and appropriate to understand bitumen composition and mechanical behavior (Redelius and Soenen 2015).

The chemical-structural analysis has progressed with fractionation techniques, through which it is possible to separate the bitumen molecules into chemical groups according to the dimensions or the soluble properties in various kinds of solvents (polar, apolar or aromatic). Over the years, the fractionation techniques applied to bitumen have undergone a series of advances that have led to increasingly interesting results, clarifying more and more the structure of the material and therefore allowing a deeper understanding of the bitumen chemical composition.

In 1836, Boussingault separated two components of bitumen by distillation. He obtained two fractions named “petrolenes” (85% by weight) and “asphaltene” (15% by weight). Given the similar H/C ratio of the two fractions, he thought that asphaltene could derive from the oxidation of petrolene (Boussingault 1837). A few decades later, Richardson made his contribution defining “asphaltenes” as the part of the bitumen insoluble in naphtha but soluble in carbon tetrachloride (CCl_4). Moreover, he introduced the “carbeni” and the “carboids”, respectively soluble and insoluble in CS_2. (Richardson 1910).

Kayser, in 1897, used three solvents, chloroform, ether and alcohol, to obtain three bitumen fractions (Krishnan and Rajagopal 2003). Hoiberg achieved greater success in 1939 when he achieved the separation of the maltenes in resins (precipitate) and oils (soluble part) (Rostler 1965). Corbett proposed a method to further split the maltenes and obtaining three categories: saturated, aromatics and resins (Corbett 1969). Therefore, he managed to separate the bitumen into the 4 fractions that are still considered today in the chromatographic analysis: Saturated, Aromatic, Resins and Asphaltenes (SARA). Hence the SARA terminology is obtained by joining the initials of each fraction.

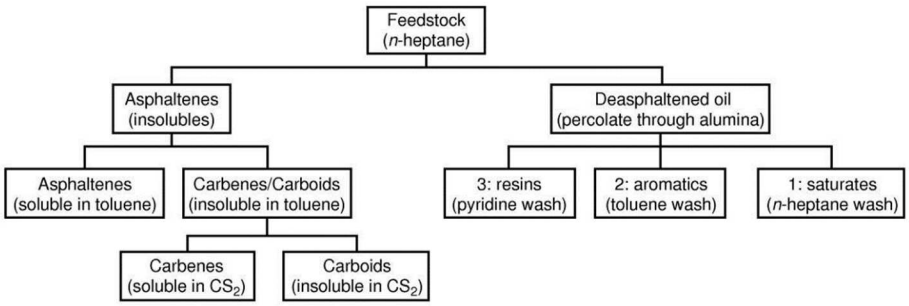

Figure 3- Bitumen composition (reprinted from Reference (Lesueur 2009) with the permission of Elsevier).

Nowadays, the process defined by ASTM D-4124 (American Society for Testing and Materials 2018) is divided into several steps. The first consists of the separation of asphaltenes with precipitation of n-heptane. Afterward, the maltenes in a solution of n-heptane are poured into a chromatographic column to separate the saturates; then, the aromatics are separated using 100% toluene and a 50/50 blend of toluene and methanol; finally, the resins are obtained using trichloroethylene.

Several methods are available to obtain the SARA fractions (Leroy 1989, Ecker 2001), but despite the proportions depend on the origins of the raw material, the use of different techniques gives slightly different results. Therefore, to compare different varieties of bitumen according to the SARA fractions, the use of the same fractionation method is always a good practice. A deeper description of the four distinct fractions is provided below.

Saturates represent about 5-15% by weight of bitumen and consist of an almost transparent liquid. They are mainly composed of aliphatic (branched, linear and cyclic hydrocarbons) and have no polarity (rare aromatic rings or polar atoms). They function as a jellying agent for bitumen components, as they favour asphaltene flocculation and therefore the bitumen solid-elastic phase.

Aromatics represent about 30-45% by weight of bitumen and consist of a yellow-red oily liquid. They contain one or more aromatic rings and act as solvents for the peptized asphaltenes.

Asphaltenes represent about 5-20% by weight of bitumen and consist of a dark powder (Speight 2004). They have many aromatic rings and polar compounds. They are the main component associated with bitumen stiffness and viscosity (Branthaver, J.F. Petersen, J.C. Robertson, R.E. Duvall, J.J. Kim, S.S. Harnsberger, P.M. Et Al 1994).

Resins represent about 30-45% by weight of bitumen and consist of a black solid. They are similar to asphaltenes in terms of composition but they have a higher polarity (Koots and Speight 1975). They are the component that is associated with the bitumen stability as they behave as act as flocculent agents for the asphaltenes.

The bitumen behavior is determined by the relative amount of the components but especially by the compatibility and the interactions among these homogeneous fractions.

2.3.1.3. Colloidal system

Several models were proposed to understand the rheological properties of the bitumen through its chemical composition. Although Rosinger had thought about a colloidal structure for bitumen in 1914 (Rosinger 1914), today this intuition is attributed to Nellesteyn, who described the bituminous colloidal system in 1924 (Nellensteyn 1924). They described bitumen as the dispersion of asphaltene micelles (solid) in an oily phase (fluid) thanks to the presence of peptizing agents. The first description of the colloidal system is a structure determined by asphaltenes micelles immersed in a maltene solution. In particular, the asphaltenes are covered by the maltenic polar part (resins), which acts as a peptizing agent for the asphaltenes themselves and everything is immersed in the so-called oils, flocculating agents for asphaltenes.

In the following years, Pfeiffer and Saal (Pfeiffer and Saal 1940) introduced the difference between two colloidal systems (sol and gel), which represent the two colloidal limit systems for all the bitumen.

In particular, if resins keep asphaltenes highly peptized (or dispersed) in the oily phase so that micelles are not interacting, the associated bitumen is characterized by a sol model. This model results in a very viscous (not elastic) behavior at low temperatures and a Newtonian liquid behavior at high temperatures. Whereas, if resins are not very effective in peptizing asphaltenes, which become fully interconnected, a gel model is obtained. This model results in a not-Newtonian fluid (viscoelastic) behavior at high temperatures and elastic solid behavior at low temperatures.

Most of the bitumen shows intermediate characteristics between these two structures, which represent the limit cases. The coexistence of the sol-type micelles and the gel structure as a function of temperature and aggregation state of micelles (ratio among asphaltenes, resins, aromatics and saturates) is defined as a gel-sol model.

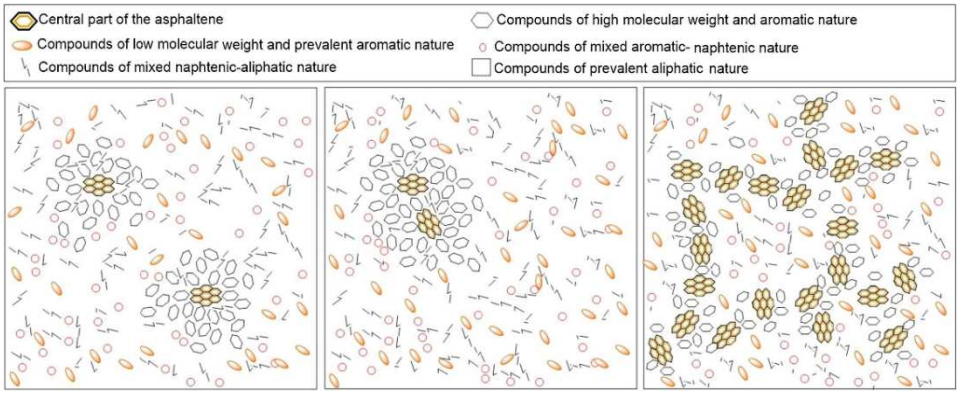

Figure 4- Schematic representation of the colloidal model of bitumen: (a) sol, (b) flocculated asphaltene micelles, (c) gel. (reprinted from Reference (Behnood and Modiri Gharehveran 2019) with the permission of Elsevier).

In 1971, Gaestel et al. (Gaestel *et al.* 1971) introduced the concept of Colloidal Index (CI) or Instability Index, whose empirical expression is reported below.

$$\mathrm{CI} = \frac{\text{Asphaltenes} + \text{Saturates}}{\text{Aromatics} + \text{Resins}}$$

Generally, this index has a value between 0.5 and 2.7 for the most used bitumen. The bitumen shows a clear gel behavior if the colloidal index is greater than 1.2 while the behavior is closer to a sol model if the colloidal index is lower than 0.7.

2.3.1.4. Test methodologies to investigate bitumen chemistry

Nowadays, a wide variety of methodologies is available to analyze the chemical properties of bitumen. Each technique has some issues because the results are different as a function of the nature of the binder and the process conditions under which it is analyzed. Therefore, to deeply investigate the chemical properties of bitumen, it is a good practice to combine multiple chemical tests, together with a rheological and traditional characterization.

The most frequently used techniques for the chemical analysis of bitumen are summarized in Table 4 and described hereafter.

Technique	Type of analysis	Parameters used
AFM: Atomic Force Microscope	Microscopic	Microstructure and micro-mechanical properties of bitumen
FTIR: Fourier Transform Infrared spectroscopy	Chemical	Quantity of carbonyl and sulphoxide groups

TLC-FID: Thin Film Chromatography with Flame Ionization Detection	Chemical	Saturated, aromatic, asphaltene and resin content
HP-GPC: Gel Permeation High-Pressure Chromatography	Chemical	Number of chemical groups and molecular weights

Table 4 - Most frequently used techniques for the chemical analysis of a bitumen

2.3.1.4.1. Atomic Force Microscope (AFM)

The AFM test is a non-destructive analysis that allows representing the surface morphology of a bitumen sample, as well as information regarding stiffness, cohesion and molecular interactions at a microscopic level. The fundamental principle on which this test is based is very easy to understand. The device is equipped with a flexible cantilever, which is linked to a piezoelectric component and has a tip at the extremity. During the test, the tip slides on the bitumen surface while its position is measured through a laser system and the resistance to the tip movement, which depends on the distance between atoms, is registered. By coupling this information, a detailed scansion of the bitumen sample surface at a microscopic (atomic) scale is collected (Li *et al.* 2020).

The AFM technique allows the identification of three major phases of different rheology and composition:

- catana phase or bee phase, which are a sort of hills in the undulated pattern of the AFM image;
- peri phase (from Greek peri = around) surrounding the bees and characterized by a certain roughness;
- para phase (from Greek para = neighbor) next to the peri phase and typically flat (Masson *et al.* 2006, Fischer *et al.* 2014, Tarpoudi Baheri *et al.* 2020).

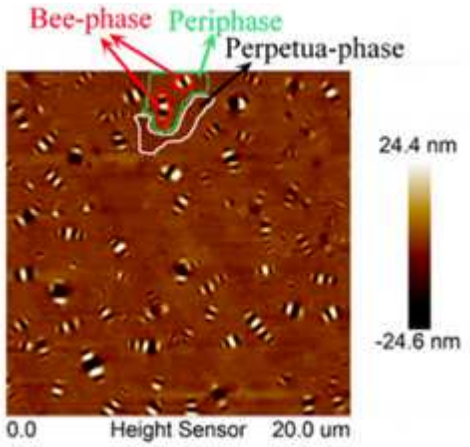

Figure 5 - Three major phases of the superficial morphological representation of bitumen (reprinted from Reference (Yang et al. 2018)).

2.3.1.4.2. Fourier Transform Infrared (FTIR) spectroscopy

FTIR spectroscopy is widespread technology for the identification and analysis of organic compounds. In particular, FTIR is a method for determining the molecular structure of a material by measuring the atom oscillations (rotations and vibrations). During the test, infrared radiations hit the sample, whose atomic functional groups absorb part of these radiations. In particular, the specific wavenumber of the absorbed radiation is a function of the vibration mode of the functional group. Through the application of the Fourier Transform, the absorbance spectrum of the sample is obtained.

Each functional group has different vibration modes, whose number is related to the number of atoms and type of bond. For instance, the symmetrical molecules that include two atoms (e.g. diatomic nitrogen N_2) have no absorption in the IR spectrum while asymmetrical diatomic molecules (e.g. carbon monoxide CO) have. For more complex functional groups, e.g. methylene ($-CH_2$), the vibration modes (Fig. 6) include six types of oscillations (Fahrenfort and Visser 1962).

The bitumen characterization through FTIR spectroscopy provides different information. The analysis of the peak position in the spectrum allows the identification of the functional groups. Moreover, the height of the peaks allows the quantification of the functional group concentration (Hou *et al.* 2018).

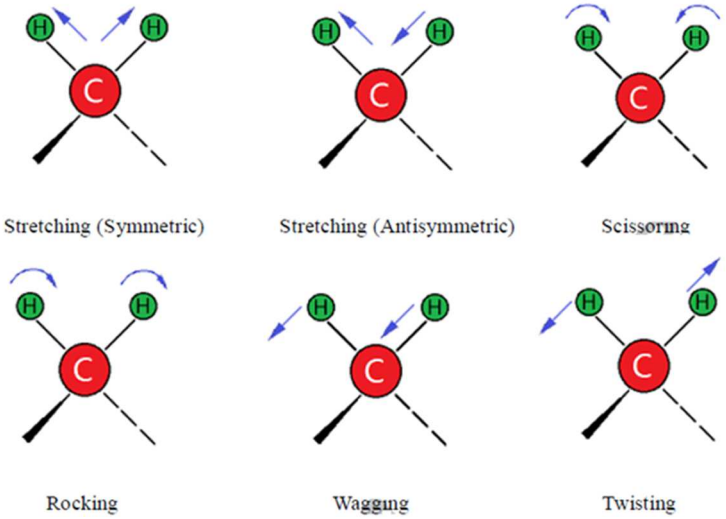

Figure 6 - Vibration modes of the methylene group (-CH2) (reprinted from Reference (Hou et al. 2018) with the permission of Elsevier).

2.3.1.4.3. TLC-FID: Thin Film Chromatography with Flame Ionization Detection

The TLC–FID is used to quantify the content of each SARA fraction in a bitumen. The bitumen is initially blended with cyclohexane solvent and a small amount of solution is put on a quartz rod named chromarod. Then, the procedure is repeated using three more solvents (n-hexane, toluene, dichloromethane). The separated fractions, i.e. asphaltenes, resins, aromatics and saturates, are located in the chromarod series respectively at 0 cm, 2.5 cm, 5 cm and 10 cm, as a function of the decreasing polarity. Finally, the chromarod is analyzed by the Flame Ionization Detection (FID), which step by step ionizes the different zones, corresponding to the four SARA fractions, and allows the estimation of their percentage in the bitumen (Sharma and Yen 1994, Masson *et al.* 2001).

2.3.1.4.4. HP-GPC: Gel permeation high-pressure chromatography FID: Thin Film Chromatography with Flame Ionization Detection

HC-GPC is a test method that allows quantifying the molecular size distribution of bitumen. The binder sample is dissolved in tetrahydrofuran (THF) and the solution is put in a column for chromatographic analysis. Gel (stationary phase) is used as a stabilizing agent that slows down the permeation of light components, while the high pressure allows increasing the test speed and the separation efficiency.

Typically, thirteen slices of the chromatographic pattern are assumed in order to discriminate between large (slices 1-5), medium (slices 6-9) and small (slices 10-13) molecular sizes (Xiao and Amirkhanian 2009).

The molecular weight can be represented in terms of average molecular weight by molecule weight (M_w) and average molecular weight by molecule number (M_n). In addition to M_w and M_n, also their ratio (M_w/M_n), defined as "molecular weight dispersion index", is often considered in the study of bitumen molecular size distribution (Li *et al.* 2020).

2.3.2. Bitumen aging

Bitumen aging is defined as the series of chemical transformations that the material undergoes and that results in the variation of its physical characteristics (Roberts *et al.* 1996a). In general, two different aging processes, namely short-term aging and long-term aging, are identified.

Short-term aging is the phenomenon that bitumen suffers during HMA manufacturing (mixing, hauling, paving and compacting) because of the high processing temperatures (> 150 °C). Long-term aging is the phenomenon that interests bitumen during the entire service life of the mix, which is subjected to traffic and environmental stresses. The severity of this process is mainly related to the bitumen exposition to air, which depends on the mix air voids and the position of the HMA layer within the pavement structure (Lesueur 2009).

Despite some studies (Thurston and Knowles 1941, Traxler 1963) identified several variables that affect bitumen aging the most widely recognized mechanisms include:

- Physical and steric hardening (reversible mechanisms);
- Loss of low-weight components (volatiles) by evaporation;
- Oxidation, with the consequent changes at the molecular level that cause a change in the SARA fractions.

The oxidation and evaporation of volatiles, which are irreversible processes, are accelerated during the HMA production and paving when the bitumen is hot (Miró *et al.* 2015). When the mix reaches the air temperature, the evaporation of volatiles becomes much less influent while oxidation continues in the long-term aging. Furthermore, the greater importance of oxidation compared to that of physical hardening is given by the different nature of these processes: oxidation is irreversible while physical hardening can be recovered. For these reasons, oxidation is considered the main process in the aging of bitumen.

These mechanisms are described in detail in the following sections.

2.3.2.1. Physical and steric hardening

The physical hardening deals with the changes in the bitumen viscoelastic properties due to the material cooling below the glass transition region. However, the process does not entail any change in the chemical structure and is reversed when the bitumen is re-heated to air

temperatures (Hesp *et al.* 2007). Assuming that the material volume consists of the volume of the oscillating molecules and the free volume between the molecules (Struik 1978) (Ferry 1980a), when the bitumen temperature decreases, both molecular mobility and free volume reduces, maintaining the same proportion between occupied and free volume. When the glass transition temperature is reached, the free volume decrease becomes slower than the decrease of molecule oscillation, entailing a kind of "over-hardening" for the bitumen (Santagata *et al.* 2016).

Physical hardening should not be confused with steric hardening. Steric hardening is a chemical process for which the bitumen molecules rearrange and form wax compounds in the maltenes, due to the presence of linear alkanes in the asphaltenes (Tauste *et al.* 2018). The process happens at intermediate temperatures but takes a three-times longer time than physical hardening (Frolov *et al.* 2016). Even steric hardening is reversible, as it can be while the previous one occurs within 1–2 days at temperatures below the glass transition temperature of bitumens (−35/−15°C), the latter is manifested at room temperature, require days or even weeks. The steric hardening is related to the inner reorganization of the binder molecules: it is associated with the formation of ordered structures by waxes in the maltenes phase that is influenced by the linear alkanes present in the asphaltenes fraction. It is a reversible process because can be removed by heating or mechanical work (Fernández-Gómez and Rondón Quintana, H. Reyes 2013).

2.3.2.2. Evaporation of the volatile components al and steric hardening

The evaporation of saturated and aromatic components has been also reported as an aging mechanism of bitumen. In particular, this phenomenon is mainly related to short-term aging as it depends on the temperature to which the bitumen is subjected during the mixing and installation phases (Bocci, Prosperi, Mair, *et al.* 2020). It has been quantified that the loss of volatiles can be twice for a temperature increase of 10 °C during HMA manufacturing at the plant (Hunter *et al.* 2015). The volatile evaporation causes the unbalancing of the SARA fractions, determining the predominance of resins and asphaltenes over saturates and aromatics. Consequently, the bitumen results harder, stiffer, more viscous and more fragile. The evaporation of volatile compounds is an irreversible mechanism that significantly affects bitumen aging, even if to a lower extent than the oxidation process (Zupanick and Baselice 1997).

2.3.2.3. Oxidation

Thurston and Knowles, in 1941, demonstrated how bitumen components, in particular asphaltenes and resins, absorb oxygen (Thurston and Knowles 1941). It is widely accepted today to consider the oxidative process of bitumen as the most important mechanism that happens during aging.

Bitumen oxidation is an irreversible process that deals with the "capture" of oxygen atoms by the bitumen components (particularly the asphaltenes), which undergo an alteration of their chemical characteristics. Moreover, this aging process could be photo-catalyzed in the

case of the bitumen in pavement surface layers, in particular for polymer-modified binders (Petersen 2009). As oxidation is due and depends on the access of oxygen in the mixture, the voids content, the HMA layer depth, the bitumen content and the presence of cracking are factors that can influence the quantity of bitumen exposed, and therefore the quantity of potentially aged bitumen.

Within bitumen morphology, oxidation includes dehydrogenation, the reaction of the alkyl sulfides into sulphoxides, the reaction of the benzyl carbons into ketones, which in turn form carboxylic acids with dicarboxylic anhydride. These reactions can be quantitatively determined by the functional group analysis through FTIR spectroscopy. A typical infrared spectrogram is shown in Fig. 7. The absorbance bands around 1690 cm^{-1} are due to the increase in C = O bonds (carbonyl groups), e.g. ketones, carboxylic acids and anhydrides, while those around 1030 cm^{-1} are due to the increase in S = O bonds (sulphoxide groups). Consequently, the peak areas of the two wavenumbers can be considered as concentration measurements of carbonyl compounds and sulphoxides, respectively (Lu and Isacsson 2002).

It is important to highlight that the carbonyls, ketones and sulfoxides generated through oxidation are characterized by a marked polarity. So, they associate with the polar groups in the bitumen forming agglomerates with a high molecular weight (Cortés *et al.* 2010). These large and "heavy" clusters, which typically involve the asphaltene fraction, determine the reduction of the molecular mobility within the bitumen colloidal system, resulting in increased viscosity, stiffness and brittleness (Tarsi *et al.* 2018).

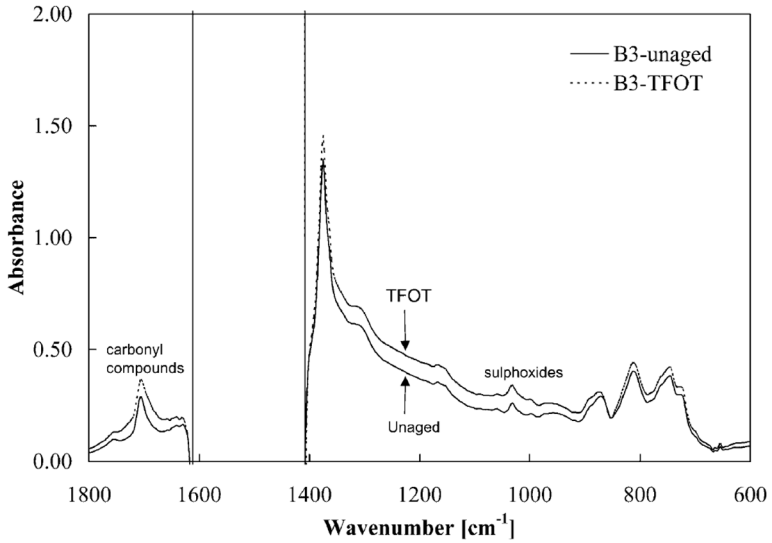

Figure 7 - Effect of aging on bitumen FTIR spectrogram (reprinted from Reference (Lu and Isacsson 2002) with the permission of Elsevier).

Temperature is a key factor in the oxidation phenomenon. In particular, the degree of oxidation is doubled every time the temperature increases by 10 °C (after 100 °C) (Hunter *et al.* 2015). The influence of temperature was also observed in the laboratory by Lu et al. (Lu *et al.* 2008). They noted that it takes 4-8 longer times to obtain the same aging when the PAV temperature is decreased from 100 to 75 °C.

As previously said, the oxidation reaction can be promoted and accelerated when the bitumen functional groups are excited by UV radiations. This issue has been neglected for many years as it only involves the upper pavement layer, because of the low ability of the radiations to penetrate in depth. However, the amplifying effect on the aging of the bituminous binder due to ultraviolet radiation should be considered, particularly in the most exposed surfaces of geographic regions characterized by high levels of solar radiation and humidity (Wu *et al.* 2010). Many authors associated the increase in bitumen viscosity, as a consequence of oxidation, with the number of radiations that invested the material (Afanasieva *et al.* 2002, Martinez and Caicedo 2005, Zeng *et al.* 2015). In particular, Zeng et al. (Zeng *et al.* 2015) observed the detrimental effects of ultraviolet radiation in association with the high temperatures in promoting oxidation. Afanasieva et al. (Afanasieva *et al.* 2002) specified that bitumen is highly oxidized when subjected to radiations with a wavelength coinciding with the UVB range (280-315 nm).

2.3.2.4. Laboratory aging methods

To date, the most frequently used methodologies to age bitumens are the thin film oven test (TFOT), rolling thin film oven test (RTFOT), pressure aging vessel (PAV) and ultraviolet test (UV). Most of them are often characterized by increases in temperature, oxygen pressure or a combination of these two in order to generate the aging conditions, as close as possible to the conditions in which real bitumen can be found. While the first two methodologies are mainly adopted to reproduce short-term aging, which occurs during storage, mixing, hauling and laying of an HMA, the last ones can simulate long-term aging that occurs during the service life of the pavement.

2.3.2.5. Laboratory aging assessment methods: general results

As regarding the different SARA fractions, aging can generally be summarized as follows:

- the saturates remain almost unchanged;
- the aromatics decrease;
- the resins get a little increase;
- the asphaltenes increase.

In particular, the general effect of oxidation is the shift of each SARA fraction towards the next component in the polarity scale. As explained before, the four bitumen fractions are ranked, as a function of the increasing polarity, in saturates, aromatics, resins and asphaltenes. Actually, the saturates only show little changes between the unaged and long-term aged

binder, so they can be considered an unreactive fraction [27]. The next fractions, aromatics and resins, oxidize and respectively shift into resins and asphaltenes. As aromatics evolve in resins but there is poor supply from the saturates (which are mainly inert), a global decrease of the aromatic content with aging is observed. Differently, the resin content only experiences a slight increase or decrease since there is the contemporary uptake of the oxidized resins into asphaltenes and of the oxidized aromatics into resins (Mirwald *et al.* 2020). The relationship between resins and asphaltenes plays a crucial role in aging: the asphaltene fraction is the component that grows the most; at the same time, the resin content increases with a lower extent, facilitating the mutual contacts between asphaltenes. When the ratio between aromatics and resins is not high enough to allow the peptization of the asphaltene micelles, or when the solvation capacity of the system is insufficient, the micelles tend to bond to each other (Mastrofini and Scarsella 2000). This determines the formation of larger irregular structures in which voids are present (filled by the external liquid of the component micelles). Thus, in terms of colloidal models, aged bitumen tends to assume a GEL structure causing a stiffer and more brittle behavior (A. E. Martin 2015). The decrease of the maltenes affects the stability of the colloidal system and determines the flocculation of the asphaltenes. Moreover, the higher amount of asphaltenes increase the propensity of the asphaltenes themselves to micellization and agglomeration (Fini *et al.* 2016). Li et al. (Li *et al.* 2020) quantified the variation of SARA fractions during aging. In this study, five different bitumens were separated into the SARA fractions before and after aging. Fig. 8 highlights how, during aging, the asphaltenes increase while the contents of aromatics and resins decrease. Moreover, the amount of saturates tends to remain stable. This phenomenon was investigated in terms of the colloidal index (CI), which proved to grow with aging, particularly in the long-term step.

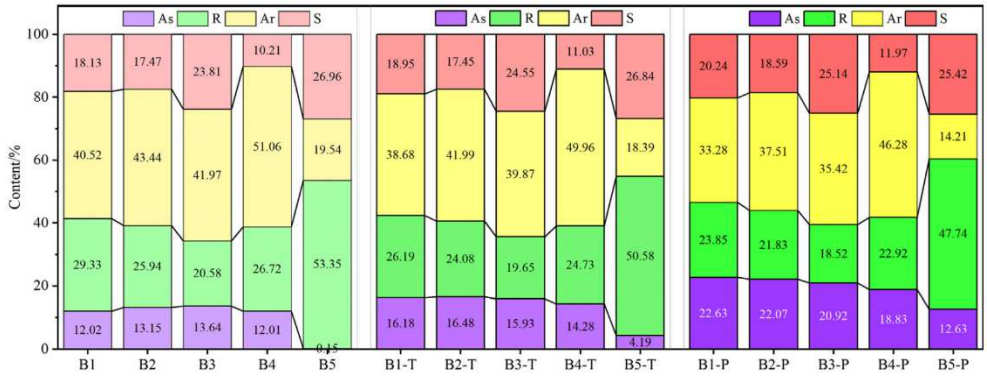

Figure 8 - Proportion of bitumen SARA fractions with aging (reprinted from Reference (Li et al. 2020) with the permission of Elsevier).

Mirwald et al. (Mirwald *et al.* 2020) tried to evaluate (using FTIR), not only the changes in quantities but also the chemical modifications within individual SARA fractions during

aging. In particular, an unaged bitumen and three long-term aged bitumens were separated into their SARA fractions, which were subsequently analyzed through FTIR spectroscopy. The absorbance spectra showed that:

- The saturates spectrum remains unchanged, confirming that this fraction is lowlily affected by aging;
- The aromatic spectrum shows some changes (an increase of the peaks in the carbonyl band, main aromatic band and across the entire fingerprint area) but no significant increase in sulfoxides;
- The interpretation of the resin spectrum is complex, because of the position of this fraction in the polarity gradient. In general, aging results in uptake from 2-quinolones and carbonyls into ketones and in the growth of the sulfoxides content;
- The asphaltenes spectrum shows significant variations in the fingerprint area. In particular, the aging determines an increase in sulfoxides (1030 cm^{-1}), main aromatic (1600 cm^{-1}) and carbonyl (1700 cm^{-1}) peaks.

Thus, the increase of the carbonyls regards the aromatics and the resins while the increase of the sulfoxides interests the resins and the asphaltenes. Using GPC, Li et al. evaluated the molecular weight of the bitumen components (Li *et al.* 2020). Table 5 shows that the molecular weight increases when moving from saturates to aromatics, to resins and asphaltenes. In particular, the saturates have the shortest molecular chains, denoting an approximate structure. Differently, the asphaltenes have the longest chains and the most complex structure. In addition, they include a higher number of polar groups that are lowly sensitive to temperature changes. So, when the asphaltene content increases the bitumen tends to maintain its mechanical properties (stiffness, viscosity) even when increasing temperature (Li *et al.* 2020).

Component	M_n	M_w	M_w/M_n	Features
Saturated (S)	506	673	1,329	Low molecular region
Aromatics (Ar)	648	1220	1,882	Transition region
Resins (R)	907	2761	3,045	Transition region
Asphaltenes (As)	1898	14660	7,725	High molecular region

Table 5 - Molecular weight of the bitumen SARA fractions (reprinted from Reference (Li et al. 2020) with the permission of Elsevier).

FTIR spectroscopy has been used for many years to analyze the bituminous binders (Mikhailenko *et al.* 2016a), particularly to investigate the polymer modification mechanisms and the effects of aging. Table 6 summarizes the main changes noticed in the bitumen FTIR spectrum as a consequence of aging.

Chemical group	Bond	Approximate wavenumber (cm^{-1})	Change with aging	References
Sulphoxide	S = O	1030	Increase	(Lamontagne *et al.* 2001, Karlsson and Isacsson 2003a, Chávez-Valencia *et al.* 2007, Mouillet *et al.* 2008, Hou *et al.* 2018, Noor *et al.* 2020)
Carbonyl	C = O	1690	Increase	
Aliphatics (plan deformation)	CH_2, CH_3	1460, 1375	Small decrease	
Aromatics	C =C	1600	Small increase	(Lamontagne *et al.* 2001, Mouillet *et al.* 2008, Tachon 2008)
Aliphatics (asymmetric or symmetric stretching	CH_2, CH_3	2923, 2853	Small decrease	(Tachon 2008, Araújo *et al.* 2011)
Polarity	O - H	3450	Increase	(Tachon 2008, Araújo *et al.* 2011)

Table 6 - Change of key FTIR bands during aging

The more significant changes in the FTIR spectrum associated with bitumen oxidation are the rise carbonyl C=O (1690 cm^{-1}) and sulfoxide S=O (at 1030 cm^{-1}) bands. This has been observed in both laboratory (Mouillet *et al.* 2008) (Siddiqui and Ali 1999) and site (Lamontagne *et al.* 2001) (Chávez-Valencia *et al.* 2007) aged bitumen. In particular, the work by Mouillet et al. (Mouillet *et al.* 2008) specified that increases in the S=O and C=O bands are mainly related to short-term aging and long-term aging, respectively. Even the aromatic C=C band (1600 cm^{-1}) shows a slight increase that is associated with the increase of the resins and especially the asphaltenes, which include condensed aromatic rings. The polarity band (around 3450 cm^{-1}) is highly marked in the spectra of resin and asphaltene components, but this has not been exactly associated with the bitumen aging process (Tachon 2008). Finally, the aliphatic CH_2 and CH_3 bands showed a slight decrease with increasing aging (Araújo *et al.* 2011).

In order to quantify the effects of bitumen oxidation, two indices have been introduced:

- Carbonyl index: $I_{C=O} = \frac{A_{1690}}{Aref}$

- Sulphoxide index: $I_{S=O} = \frac{A_{1030}}{Aref}$

where A_{1690} is the area of the C=O peak centered at 1690 cm^{-1}, is the area of the S=O peak centered at centered at 1030 cm^{-1} and A_{ref} is the area of the reference ethylene and methyl peaks, respectively centered at 1460 and 1375 cm^{-1} (Dony *et al.* 2017).

With the aim to estimate the effects of bitumen aging on its properties, the variation of the indices in unaged, short-term and long-term aged bitumen can be calculated. When increasing the aging, the heights and the areas of the peaks in correspondence of the wave numbers of 1690 cm^{-1} and 1030 cm^{-1} (respectively for the carbonyl C=O and sulphoxide S=O bands) increase, so also the two indices increase (Nivitha *et al.* 2015, Mikhailenko *et al.* 2016b, Gabrielle do Nascimiento Camargo *et al.* 2020, Yan *et al.* 2020). Moreover, a recent study (Poulikakos *et al.* 2019) proposed the Chemical Aging Index (CAI), calculated as $I_{C=O}$ plus $I_{S=O}$, in order to better understand the variation of both indices during aging.

Regarding the AFM test, changes of the particular bee-shaped structure can be used to investigate the aging process. Nowadays there is still some discussion about the nature and conformation of these structures. There is a certain agreement that the bee-structures are associated with wax crystallization (Santos *et al.* 2016). For this reason, it was hypothesized that the "bees" are correlated to the asphaltenes (Lu *et al.* 2005, Hofko *et al.* 2016). The study by dos Santos et al. (dos Santos *et al.* n.d.) demonstrated that the valleys, due to their lower thickness and roughness, are less strong than the hills. Other studies proposed that the formation of the bee structure is associated not only with asphaltenes but also with resins and aromatics, and so are strictly correlated to the bitumen performance (Bearsley *et al.* 2004, Cavalli *et al.* 2019). One more point of discussion is related to the presence of these phases in the whole bitumen volume or only on the surface (Ganter *et al.* 2020).

Li et al. (Li *et al.* 2020) tried to identify the changes in the bee structures during short- and long-term aging in different bitumens. Before aging, these show the distinct elliptic bee structures, which are short and thick. After aging, different behaviors were observed for the various bitumens. In general, the bee structures became larger and irregular when increasing the aging level. In addition, peculiar phenomena happened in the AFM diagrams, such as the increase of the bee stripes number or the formation of sunk regions, columnar peaks, blocky structures or cracks.

A study by Lu et al. (Lu *et al.* 2021) investigated wax-including bitumens in comparison with a non-waxy bitumen using AFM. They noted that aging determined a decrease in the number and an increase in the dimensions of the bee structures in the bitumen with wax, probably because of the highly increased stiffness of the aged binder and/or the reduced compatibility between the saturated crystalline fraction and the more polar bitumen matrix. On the other hand, for a non-waxy bitumen, no structure was observed either on the unaged and PAV aged state. Moreover, after the 60h long PAV aging the content of asphaltenes increased from 22% to almost 25%. This demonstrated that asphaltenes are not the fraction responsible for the structures unless they contain n-heptane insoluble crystallizable materials.

Zhang et al. (Zhang *et al.* 2020) also studied the aging effect on the bee structures. They confirmed that aging entails an increase in the bee structure number, dimension and roughness (Fig. 9), which is associated with a contemporary decrease of the penetration and increase of the ring&ball softening point and viscosity.

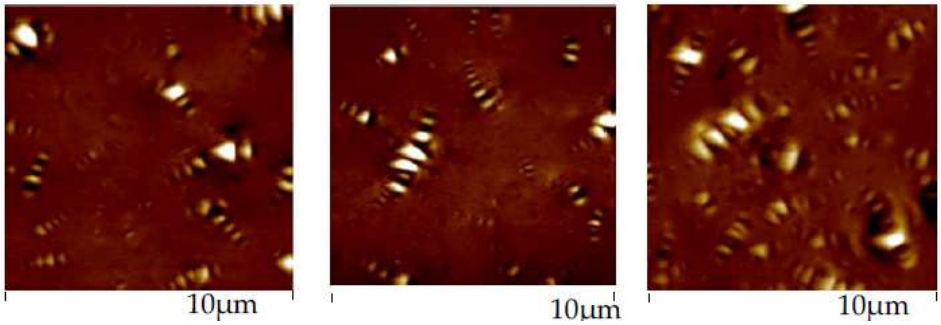

Figure 9 - AFM images of unaged, short-term aged and long-term aged bitumen (reprinted from Reference (Zhang et al. 2020)).

2.3.3. Bitumen rejuvenation

Including RAP in HMA requires a careful study of the mixture, because its mechanical properties are strongly conditioned by the presence of the aged bitumen contained into RAP. In particular, improper use of RAP can lead to premature cracking linked to the excessive stiffness of the bitumen (thermal and fatigue cracking) (Mannan *et al.* 2015b, Solanki *et al.* 2015, Coleri and Sreedhar 2019, Wu *et al.* 2020). In order to achieve the proper mechanical properties for the HMA, additives are included in the mixture. In the following paragraph, the concept of rejuvenator is provided, clarifying which are the main distinctions within this category and explaining the benefits associated with their use.

A rejuvenator is that agent that allows renovating the properties that the bitumen loses with aging (Roberts *et al.* 1996b). Thus, rejuvenators should reduce aged bitumen viscosity and stiffness and improve ductility (Loise *et al.* 2019). However, the several products that can be used for this aim may act at a different level, e.g. in the colloidal system or the chemical morphology. The literature does not seem very clear about this; the term "rejuvenator" is often used for any additive without specifying what the effective mechanisms of action in bitumen are. According to different authors (Tabatabaee and Kurth 2017a, Loise *et al.* 2019, De Bock *et al.* 2020), rejuvenators can be classified, based on the effect, in:

- Softening agents (also called fluidifying agents or rheological rejuvenators), which include:
    - Incompatible softeners, which mainly have a viscosity lowering effect;

    - Soluble softeners, which restore the balance in the SARA composition by re-enriching the maltene fraction;
- Real rejuvenators or compatibilizers, which help to renovate the physical and chemical characteristics of the bitumen through the disruption of the intermolecular associations between the asphaltenes.

The softening agents are usually based on extracts of lubricating oils. Slurry oil, flux oil and lube stock belong to this category. They include a proper content of maltenic, naphthenic or aromatic components aiming to rebalance the SARA fractions of the aged binder, characterized by a lower concentration of maltenes. The softening agent allows an increase in bitumen ductility and a decrease in viscosity and brittleness by merely supplying oily components to maltene fraction, but does not achieve ant change in the complex structure. The real rejuvenators are additives that allow restoring both the physical and chemical properties of bitumen. In particular, they are able to restore the agglomeration condition of asphaltenes to their original state by promoting their re-dispersion. Regarding the composition, real rejuvenators should have a high content of aromatics, which allows keeping the asphaltenes dispersed and low content of saturates, which have poor compatibility with the asphaltenes.

The efficacy of the rejuvenation process is strictly related to the adequate dispersion within the aged bitumen. Lee et al. first faced this aspect claiming that a mechanical mixing could allow a uniform distribution (Lee *et al.* 1983). A few years before, Carpenter and Wolosick divided the diffusion of a rejuvenator into an aged binder into 4 different steps: in the first phase, the rejuvenator forms a low viscosity layer around the particles of aggregates covered with aged bitumen. Then, the additive starts to penetrate the binder by softening it. In the third phase, the rejuvenator penetrates the aged bitumen, and the viscosity of the internal and external surfaces gradually decreases. Finally, in the last phase, over time, the rejuvenator manages to reach all the aged bitumen (Carpenter and Wolosick 1980). Noureldin and Wood (Noureldin and Wood 1987) and Huang et al. (Huang *et al.* 2005) confirmed this theory some years later. Karlsson and Isacsson (Karlsson and Isacsson 2003b), found out that the diffusion of the rejuvenator into the aged bitumen is mainly influenced by the viscosity of the maltene phase. So, it can be facilitated by raising the temperature or adding oil (Oliver 1975).

2.3.3.1. Rejuvenating mechanisms

As previously explained, aging determines morphological changes in the bitumen: in particular, it causes more intense molecular interactions by introducing polar groups which lead to an increase of the colloidal agglomerates into the bitumen volume. As the molecular structure strongly influences the rheological properties, any alteration of the balances and interactions of the polar and non-polar components in the bitumen can determine a modification of the thermal and mechanical properties in a mixture.

From a chemo-morphological point of view, rejuvenation is the inverse process of aging. True rejuvenation breaks the molecular aggregations and rebalances the SARA fractions, leading to an improvement in the rheological properties of the bitumen (Pahlavan, Hung, *et*

al. 2018). Remembering the classification made in the previous section, real rejuvenators are additives capable of both replenishing the lost volatile components and flaking the large agglomerates of asphaltenes in much smaller compounds. The studies by Pahlavan et al. (Pahlavan, Hung, *et al.* 2018, Pahlavan, Mousavi, *et al.* 2018, Pahlavan *et al.* 2019), which explain in detail the effect of rejuvenation in the aged bitumen morphology, are summarized hereafter.

The approach adopted by Pahlavan et al. to investigate the rejuvenating process is based on molecular dynamics (MD) simulation and quantum mechanical studies through density functional theory (DFT). It starts from the analysis of the asphaltene monomer and the related oxidized dimer, which consists of a structure resulting from the interaction of two monomers of asphaltenes.

The electrons of the C=O groups located around the oxidized asphaltenes (red dots in Fig. 10) change the distribution of π electrons on these flat-shaped molecules. This determines an insufficiency of electrons at the π bonds in the central part of the asphaltenes with a consequent decrease of the repulsive forces between the asphaltenes. This decrease leads to the formation of the dimer (two asphaltene monomers).

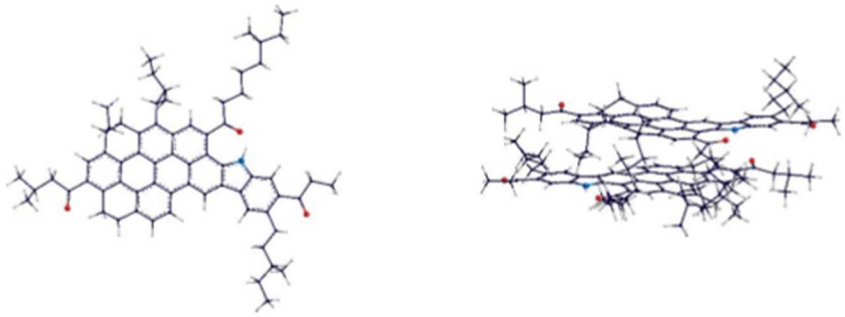

Figure 10 - Asphaltene monomer (left) and dimer (right) molecular structures in the oxidized state (reprinted with permission from (Pahlavan et al. 2019), Copyright 2019, American Chemical Society).

The forces that control the degree of asphaltenes stacking are concentrated in the aromatic motifs present in the asphaltenes. Fig. 11 shows the most probable sites of interaction between a rejuvenator and an asphaltene dimer. The zones A, B and C represent the areas where the rejuvenator likely finds a lower opposition by the hydrocarbon chains when it approaches the dimer. In these regions, the rejuvenation process happens in two steps that the author named “lock and key” step and “intercalating” step. The first step (“lock and key”) interests zones A and B, where the adhesion between the asphaltenes in the dimer is stronger due to the polar groups. When the rejuvenator reaches the zones, it detaches the aromatic ring planes allowing access to more additive. In particular, the rejuvenator can intercalate in zone C, previously less accessible, and further deagglomerate the dimer by physically imposing a

hindrance between the asphaltenes. The effectiveness of this second step depends on the chemistry of the rejuvenator. If the additive has polar properties, it creates interference on the Van der Waals forces that keep the polyaromatic cores stuck. However, the efficacy is higher if the additive has hydrocarbons with donor CH sites, which can interact with the π electrons in the asphaltenes and thus disrupt the bound of the dimer.

Of course, the rejuvenating effect of an additive is higher if it achieves both the steps, in particular, because the "intercalating" is noticeably facilitated when preceded by the "lock and key".

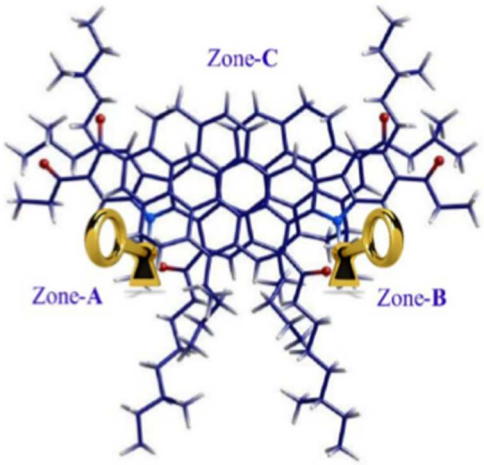

Figure 11 - More likely interaction sites for biological rejuvenator with an asphaltene dimer (reprinted with permission from (Pahlavan et al. 2019), Copyright 2019, American Chemical Society).

Fig. 12 shows the side views of the dimer before and after rejuvenation. The simulation allowed observing an increase in the distance between the asphaltene sheets when the rejuvenator is used. In particular, in zones A and B (on the right in the side views) the increase of the gap between the polyaromatic cores was higher than in zone C (on the left in the side views).

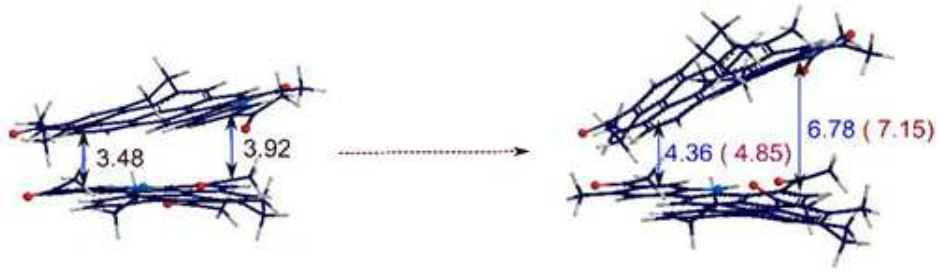

Figure 12 - Intermolecular gaps between the aromatic rings in zones A-B and C for an oxidized dimer before (left) and after (right) rejuvenation. Blue and red numbers indicate the distances (in Å) achieved with 2 different rejuvenators (Reprinted with permission

2.3.3.2. Laboratory rejuvenating assessment methods: general results

As mentioned in the previous chapters, one way to evaluate the aging and rejuvenation of bitumen is to monitor the progress of the four SARA fractions. With oxidative aging, aromatics and resins are converted into asphaltenes leading to an increase in the contacts between the micelles in the colloidal system, increasing bitumen stiffness. The application of rejuvenators should increase the maltene content of the aged binder and consequently restore the proportions of the system.

In this regard, Zadshir et al. (Zadshir *et al.* 2018) tested an aged bitumen (RTFOT and 2 PAV) rejuvenated using three additives with different nature: the first additive is based on organic oil from pig manure (BB), the second derives from vegetable oils (VB) and the third is hydrocarbon-based (PB). The chemical composition of the biological additive (BB) shows that it is characterized by a high content of asphaltenes and resins and a low content of saturates and aromatic (Fig. 13). The high content of resins stabilizes the asphaltenes and the relative micelles of the colloidal system, but the addition of further asphaltenes is typically discouraged in favor of a higher content of aromatics.

Despite the structure of bio-based asphaltenes is different from that of hydrocarbon-based asphaltenes (Xu *et al.* 2014), the lack of aromatics and abundance of asphaltenes do not tend to rebalance the SARA composition. Conversely, the vegetable oil (VB) additive shows a great content of resins and aromatics, with low percentages of saturated and asphaltenes. The high number of aromatic components can balance the maltenic fraction lost during the aging process causing an increase in the colloidal stability of the aged binder. Lastly, the hydrocarbon-based additive (PB) is characterized by a large percentage of aromatics and a lower percentage of asphaltenes in comparison with that relating to the biological binder (BB).

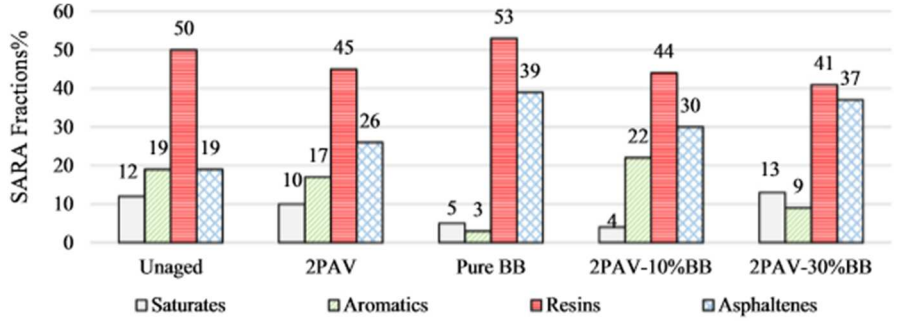

(**a**)

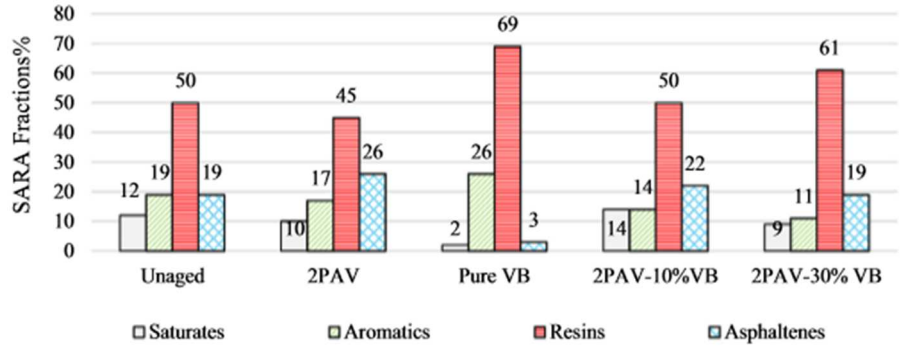

(**b**)

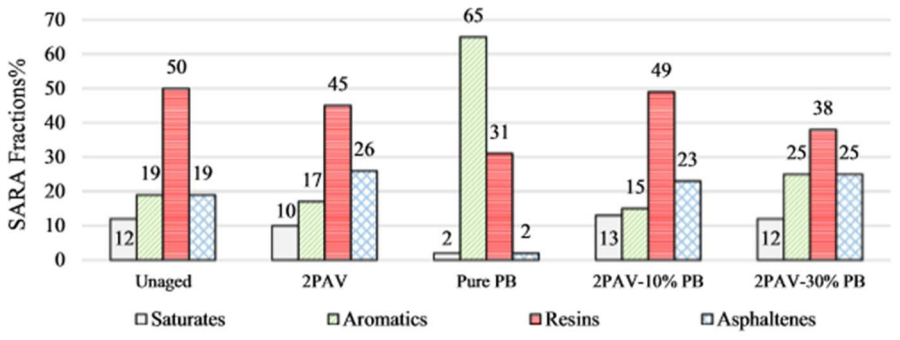

(**c**)

Figure 13 - SARA fractions of virgin binder, aged binder, additives and rejuvenated binder: a) biological additive, b) vegetable oil, c) hydrocarbon-based additive (reprinted from Reference (Zadshir et al. 2018) with the permission of Elsevier).

The evolution of the percentages of the SARA fractions using these rejuvenators can also be analyzed by monitoring the Colloidal Index (CI). In particular:

- adding the biological rejuvenator (BB) (10% by weight) causes a decrease in the CI from 0.61 of the binder aged to 0.51 (bringing it back to values similar to that of virgin bitumen). However, by increasing the percentage of the same additive up to 30%, the index increases to the unit value (exceeding even that of the aged binder without additives);
- adding the vegetable oil-based additive (VB) a progressive decrease in the index by increasing the percentage of rejuvenator comes out. This means that the stability of the binder is increased as the additive dosage increases. With an additive content of 30%, a CI lower than that of virgin bitumen is reached.
- adding the hydrocarbon-based rejuvenator (PB) the percentage of asphaltenes decreases and this leads to a slight decrease in the CI. Increasing the percentage of additive from 10% to 30% there is not a further decrease.

From the comparison between the three rejuvenators, it is clear that the content of resins and aromatics brought by the additives plays a fundamental role in the process. Resins are more effective than aromatics because of the high polarity and ability to disperse the asphaltenes micelles in the maltenic phase and consequently stabilize the colloidal system.

A very important aspect to consider in the rejuvenating process is the amount of additive that has to be introduced into the aged bitumen to ensure the greatest benefit to the process. The results of CI help to find an optimal rejuvenator content for each type of additive. However, it must be considered that for some products, as in the case of the biological additive, due to the different nature of the asphaltene molecules that compose it, the CI may increase with increasing rejuvenator dosage, but an improvement in physical and rheological behavior of the bitumen is still achieved.

The same study (Zadshir *et al.* 2018) also investigated the molecular size distribution of the rejuvenated bitumens through GPC. The results show that:

- the large molecules (LMS) increase from 83% for the non-aged binder to 87% for the aged binder, at the expense of the percentage of medium-sized molecules (MMS), which is reduced by 14% to 10%. The increase in LMS is a consequence of the increase in the number of asphaltenes in the system and their agglomeration.
- the addition of a rejuvenator tends to decrease the percentage of larger LMS molecules by increasing the presence of medium-sized molecules (MMS).

Further conclusions, related to the GPC test, were also obtained by Cao et al. (Cao *et al.* 2018a), they tested the effects of waste cooking oil as a rejuvenator for aged bitumen. The main conclusions obtained in this study are the following:

- the aged binder gets higher Mw and Mn values than the virgin one, denoting the formation of larger molecules in the binder during the aging process. Compared to

the virgin bitumen, the higher poly-dispersion of the aged binder indicates that there is a greater distribution of molecular weights.

- adding waste cooking oil with different dosages there is no chemical reaction between the additive and the aged binder. The decrease in Mw and the poly-dispersion is due to a physical dilution.

Fig. 14 shows the curves obtained by the GPC of the virgin aged and subsequently rejuvenated bitumen with different dosages of additive.

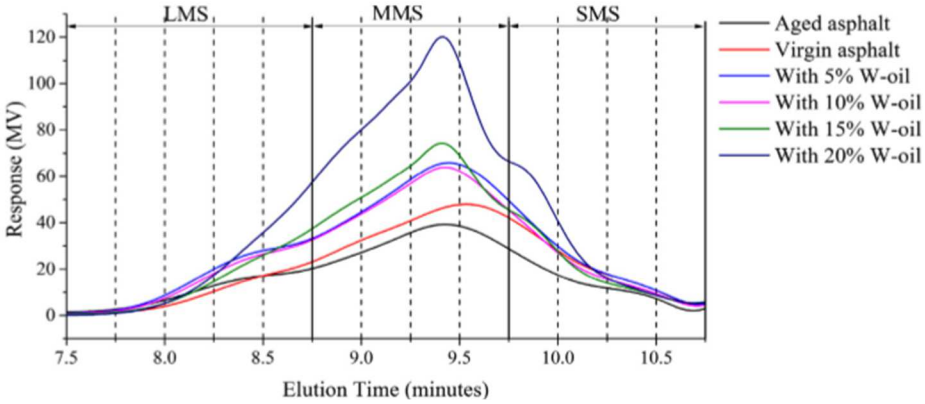

Figure 14 - GPC curves of the regenerated binder with different dosages of waste cooking oil (reprinted from Reference (Cao et al. 2018) with the permission of Elsevier).

Compared to the virgin binder (red line), the aged one (black line) has a higher percentage of LMS compared to a lower SMS and MMS. Adding the waste cooking oil, the LMS tends to decrease; the typical LMS concentration of the virgin binder can be recovered by adding 20% additive. Increasing the percentage of waste cooking oil, MMS greatly increase and SMS decrease. However, the percentage of MMS and SMS cannot be brought back to the original values of the virgin binder. Therefore, it can be concluded that by adding waste cooking oil, the distribution of the molecular size cannot be totally restored.

The FTIR analysis can be used to investigate the evolution of the functional groups present in an aged binder when it is rejuvenated with additives. Referring to the study made by Cao et al. (Cao *et al.* 2018a), hereafter a picture showing the FTIR spectra of the waste cooking oil, the virgin binder and the rejuvenated one is reported (Fig. 15). Fig. 16 shows the FTIR spectra of the functional groups S=O, C=O and C-C in more detail. Additive and bitumen do not reach together during the rejuvenating process. In fact, the rejuvenated binder spectra are a union of those of the aged binder and the rejuvenator, without any new groups (Gong *et al.* 2016, Chen *et al.* 2018). In terms of carbonyl index ($I_{C=O}$) and sulphoxide index ($I_{S=O}$), both increased with aging and decreased by adding rejuvenators. This effect is related to the physical dilution of the binder.

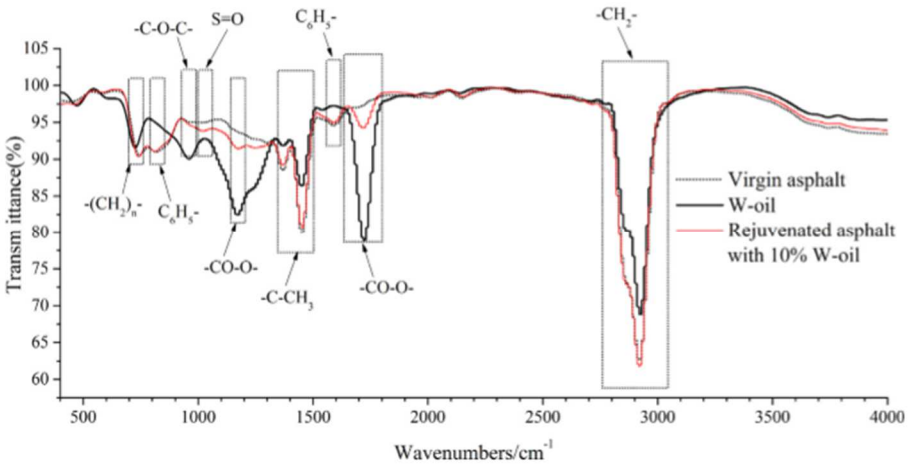

Figure 15 - FTIR spectra of WCO (W-oil), virgin and rejuvenated bitumen (reprinted from Reference (Cao et al. 2018) with the permission of Elsevier).

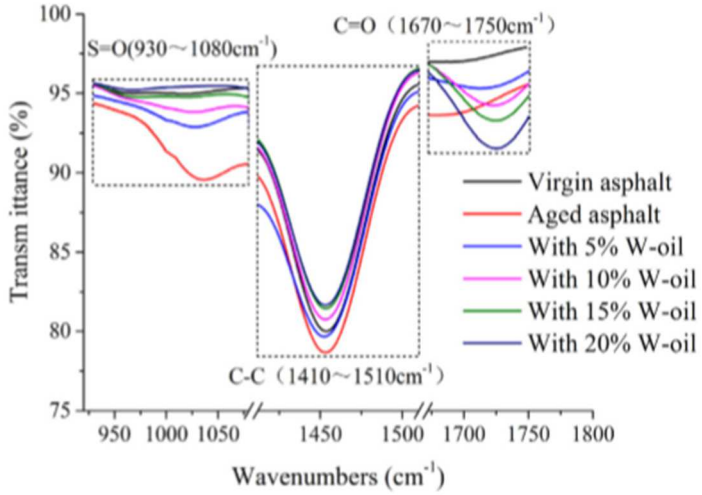

Figure 16 - FTIR spectra of S=O, C=O and C-C (reprinted from Reference (Cao et al. 2018) with the permission of Elsevier).

A study conducted by Noor et al. (Noor *et al.* 2020) focused on the analysis of the functional groups via FTIR when a biological or aromatic rejuvenator is added to a bituminous binder. Qualitative analyses were conducted by studying the spectra of the virgin bituminous binder,

the biological additive and the aromatic additive, in order to identify the representative functional groups. The functional groups identified in the bitumen are the same as those identified in the aromatic rejuvenator (both derived from petroleum). When the aromatic additive is added into the bitumen, there are no differences in the absorbance spectrum, as the functional groups are the same. On the other hand, when the biological rejuvenator is added, the resulting spectrum shows two distinct peaks in correspondence of the functional groups C=O (1744 cm^{-1}) and C-O (1162 cm^{-1}). Therefore, from the quantitative point of view, these bands can be a good reference for the identification of a specific biological rejuvenator in the bituminous binder.

Recently, Menapace et al. (Menapace *et al.* 2018) investigated the AFM images when adding tall oil to two different types of aged bitumen:

- TOAS: blend of virgin and aged bitumen extracted from Recycled Asphalt Shingles (RAS) coming from re-roofing or roof removal projects;
- MWAS: blend of virgin and aged bitumen extracted from RAS coming from the excess material obtained during the shingles production.

Regarding the TOAS-type bitumen, after long-term aging, there is a significant increase in roughness and a decrease in the phase contrast of the colloidal structure (Fig. 17). Bee structures appear in greater numbers but less defined than they were in virgin bitumen. The reduced size of the bee-shaped structures that have formed with aging indicates a relatively lower molecular mobility than for the virgin binder. Adding tall oil, there is a reduction of the dispersed domains and an increase of the matrix area. At the same time, a slight decrease in roughness and phase contrast are noted and the bee-structures are no longer visible. After re-aging (second PAV) of the rejuvenated binder, the surface of the matrix decreases, the roughness increases, the phase-contrast decreases and some bee-shaped structures reappear. It is interesting to understand how the bee-shaped structures come out again after the PAV re-aging, while they are not present in the rejuvenated blend. It is possible to hypothesize that the species used for the construction of the bee domains require a certain molecule agglomeration to create bee-shaped structures. The rejuvenator lowers the degree of association, thus breaks the bee-shaped structures originally present. Aging, on the other hand, helps the molecules to cluster again and reform the bee-shaped structures.

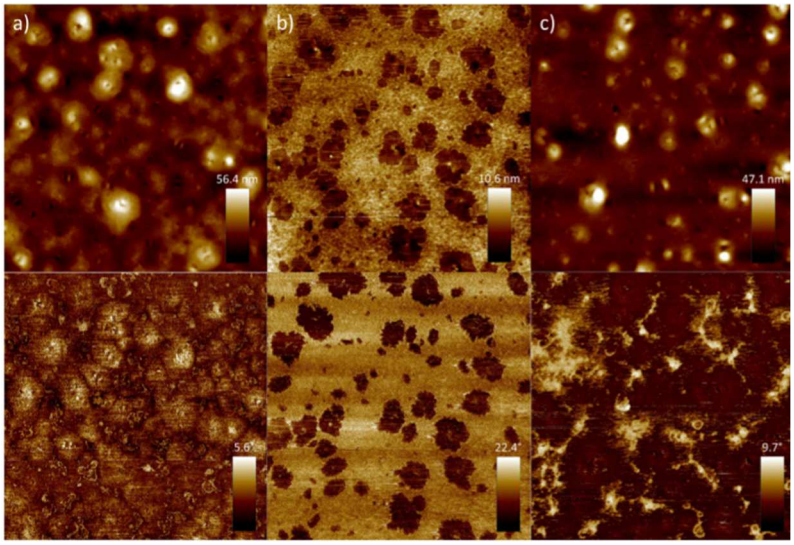

Figure 17 - - Height (above) and phase (below) images of aged TOAS binder (a), regenerated with tall oil (b) and re-aged (c) (reprinted from Reference (Menapace et al. 2018) with the permission of Elsevier).

In the MWAS bitumen, the long-term aging seems to form rippled structures that slightly different from the typical bees (Fig. 18). When the rejuvenator is used, the dispersed domains degenerate and on the binder surface as if they were liquid, to form a single interconnected phase. The rippled structures are still present, and the overall surface roughness slightly increases, while the phase-contrast shows a small decrease. After a second long-term aging process, numerous bee-shaped structures appear on the surface (c). The edges of these structures are not as smooth as in the original ones but show a more irregular conformation. This indicates that the molecules can hardly move and reach colloidal stability.

In conclusion, the rejuvenator (tall oil), through the separation of the agglomerates formed by aging, allows the attenuation or even elimination of the bee-shaped structures, which however reappear when the binder ages again.

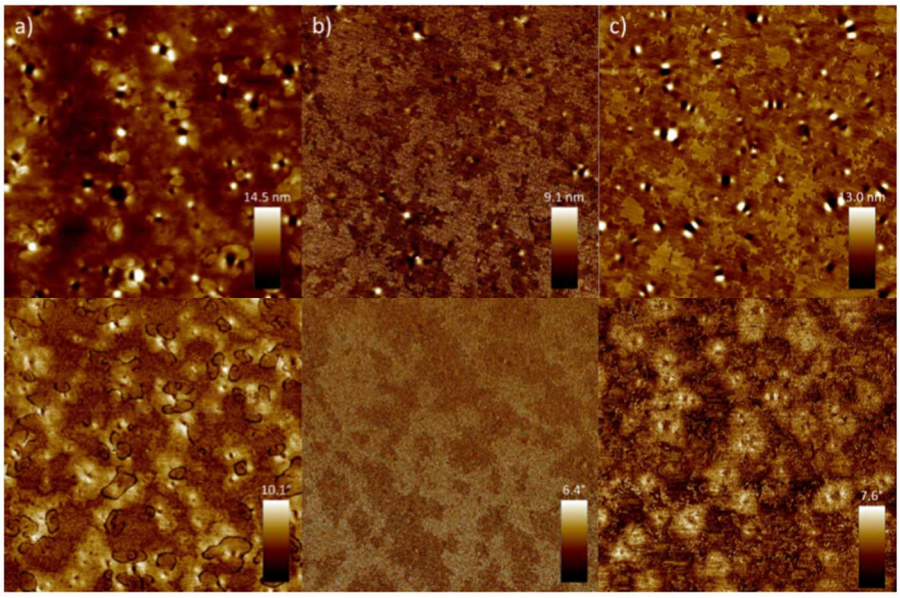

(a) **(b)** **(c)**

Figure 18 - Height (above) and phase (below) images of the MWAS binder aged (a), regenerated with tall oil (b) and re-aged (c) (reprinted from Reference (Menapace et al. 2018) with the permission of Elsevier).

More recently, Ganter et al. (Ganter *et al.* 2019), tried to evaluate the evolution of the bee structures during the aging and rejuvenating steps. For this purpose, 3 different rejuvenators, coming from bio (R1, R2) and oil (R3) sources are used. A PmB 25/55-55 bitumen was first short- and long-term aged (RTFOT + PAV) and then rejuvenated with the 3 additives listed before. They highlighted that the virgin binder displays clear bee-like structures and with increasing aging, the number of bees rises. The interesting aspect is that the addition of the three different rejuvenators causes a very different change in the surface morphology of the bitumen: size and quantities of the bee-like structure differ completely as a function of additive type and origin.

2.3.4. Aging of a rejuvenated bitumen (re-aging)

The growing use of RAP in the road sector is leading to new pavement mixtures composed not only of virgin materials but also of old recycled bitumen and rejuvenators. Therefore, it is very important to understand the changes that occur in the properties of an HRMA when it is subjected to aging during its service life (which indeed is a “second aging” or “re-aging”

for the RAP material). Hereafter, a literary review regarding the re-aging changes in the chemical and rheological properties of the recycled bitumen is provided.

Many studies have dealt with on the hot recycling of RAP and bitumen rejuvenation in the last decades. However, the bituminous mixtures that are in service in the road pavements worldwide are currently living their second or third life cycle. For this reason, researchers' efforts have recently focused on the characterization of the rejuvenated bitumen behaviour with re-aging, with different outcomes.

The second aging covers fundamental importance to understand the condition of the HRMA at the end of its second useful life. Continuous recycling of RAP would allow an increase in the circularity related to the road construction field. For this reason, in the next future, more studies regarding this aspect need to be carried out.

Generally, the second aging in a rejuvenated binder is less harmful with respect to the aging on a virgin bitumen. Based on the studies carried out by Mazzoni et al. (Mazzoni *et al.* 2018a) and Bocci et al. (Bocci *et al.* 2019), it is reasonable to expect that the HMA including a high amount of RAP and a rejuvenator suffers fewer aging phenomena and can be less stiff than an alike mixture with no RAP.

From the chemical point of view, in a recent study, Ingrassia et. al (Ingrassia *et al.* 2020) focused on evaluating the possibility of recycling binders already rejuvenated. Two virgin binders (one ordinary bitumen and a bio-binder) and two aged binders (one recovered from RAP and one "Bio-RAP" binder produced in the laboratory) were combined to reproduce the RAP hot recycling process. The chemical properties before and after aging were investigated using FTIR analysis through the evaluation of the $I_{C=O}$ and $I_{S=O}$ indices and an additional parameter, named chemical aging index AI_{FTIR}, and calculated with the following equation:

$$AI_{FTIR} \frac{(Ico + Iso)_{aged}}{(Ico + Iso)_{unaged}}$$

Basically, the analysis of AI_{FTIR} shows that the susceptibility to aging of recycled blends is significantly lower than that of the reference virgin binder. In fact, recycled bituminous blends (already containing a certain amount of oxidized binder) are less susceptible to further long-term aging.

Moreover, Sa-da-Costa et al. (Sá-da-Costa *et al.* 2017) tried to analyze, from the chemical point of view, the effects of aging on a rejuvenated bituminous binder. Several types of bitumen were analyzed in this study. As expected, an increase in the content of asphaltenes was found, confirming the oxidative transformations that contribute to increasing the polarity of the bitumen components in terms of SARA fraction. Furthermore, the oxidation of the bitumen involves a general increase in the carbonyl functional groups (C=O). Although precise correlations have not been found out, it can be stated that the chemical properties of an aged rejuvenated bitumen (second aging) are very close to that of an aged virgin binder (primary aging).

Ongel and Hugener (2015) investigated the effect of re-aging on a hard virgin bitumen, used to simulate a RA binder, rejuvenated with three types of additives. The results were compared with those of a virgin 70/100 penetration bitumen. The research showed that the aging of the virgin bitumen was slower than the re-aging of the rejuvenated bitumens. Ali et al. (2016) compared the shear modulus master curves of the binders extracted from mixtures including different percentages of RA, different rejuvenators and different re-aging levels (2 or 6 h at 153 °C). It was observed that the stiffness was lower for all of the rejuvenated binders than those for the control binder. This suggests that using asphalt binder rejuvenators when producing mixtures containing RA would result in an improved fatigue cracking resistance. Karki and Zhou (2016) tested virgin and rejuvenated bitumens after different PAV aging times and noted that rejuvenated blends reached damage initiation and significant cracking conditions at a much slower rate than the control blends did. Tabatabaee and Kurth (2017) used the Colloidal Instability Index (CII) as a parameter for monitoring the effect of re-aging on rejuvenated bitumen. The results showed that rejuvenator tested in the study had good aging stability, but the CII of the rejuvenated bitumen after re-aging for 40 h in the PAV resulted higher than for the original RA bitumen. Grilli et al. (2017) included a rejuvenator on PAV-aged bitumen and investigating the effect of a second PAV. It was noted that the aging effect on rejuvenated binders was slightly more detrimental than that on the virgin bitumen, since it entailed a higher variation of rheological parameters. Yin et al. (2017) studied the rejuvenator effectiveness on bituminous blends and mixtures with high RA contents, carrying out laboratory tests on binders and mixtures at different aging severities. The results showed that the rejuvenated materials (binders and mixtures) achieved equivalent or even better rheological properties and cracking resistance than those with an allowable amount of recycled materials per agency specifications but without rejuvenating agent.

However, as summarized in Table 7, the several research carried out about the topic of second aging or re-aging showed dissimilar findings. Therefore, it is still unclear if the bitumen performance against fatigue and thermal cracking is worse after re-aging (the more the aging process is extended, the more brittle the bitumen becomes) or after the first aging (as rejuvenation does not back-oxidize the bitumen, the already oxidized rejuvenated bitumen is less prone to further oxidize and consequently embrittle). Probably, it depends on the rejuvenator type (incompatible softeners, soluble softener or compatibilisers), dosage, effectiveness (under the same dosage and type, different products can more or less mobilize the RA binder) and the severity of the aging process (times and conditions, both in the laboratory and in the site).

Reference	**Bitumen presenting the more severe effects of aging**
Ongel & Hugener, 2015	Rejuvenated and re-aged bitumen
Ali et al., 2016	Virgin bitumen after first aging
Karki & Zhou, 2016	Virgin bitumen after first aging
Tabatabaee & Kurth, 2017	Rejuvenated and re-aged bitumen

Grilli et al., 2017	Rejuvenated and re-aged bitumen
Yin et al., 2017	Virgin bitumen after first aging
Mazzoni et al., 2018	Virgin bitumen after first aging
Bocci et al., 2019	Virgin bitumen after first aging
Koudelka et al., 2019	Rejuvenated and re-aged bitumen
Nsengiyumva et al., 2020	It depends on different variables

Table 7 - Summary of the literature review on re-aging after rejuvenation.

2.3.5. Discussion and summary

As explained in detail in the previous sections, bitumen aging involves different phenomena: loss of volatiles, oxidation, physical and steric hardening. These result in the unbalancing of the SARA fractions and the formation of large molecular agglomerates, which in turn affect the mobility of the fractions in the colloidal system and determine the binder embrittlement. In order to restore the properties that bitumen loses with aging, rejuvenators can be used.

A good rejuvenator can rebalance the SARA components and, despite oxidation is mainly irreversible, it can disrupt the asphaltene clusters and re-establish the proper molecular mobility. Above, different chemical analyses were described as tools to investigate bitumen aging and rejuvenation processes. Table 8 provides an overview of the discussed approaches to try to propose ideas for new research in this sector.

All the techniques showed promising results but, due to the limitations of each method, the contemporary use of different approaches is highly recommended to have a precise and clear overview of how bitumen ages and rejuvenates.

Moreover, the definition of multi-testing protocol for the characterization of the effects of aging and rejuvenation at a chemical level can represent the basis for the future application on more complex binders (polymer-modified bitumens, bitumens including extenders or nanoparticles).

Technique		**Investigation of aging**	**Investigation of rejuvenation**
AFM	Advantages	The bitumen chemo-morphological degradation with aging can be studied using AFM	The rejuvenation process proved to influence the surface morphology of the aged bitumen, specifically the bee-structures
	Limitations	Since the approach is very recent, there is still a gap of knowledge on associating the AFM phase evolution with other chemical and mechanical properties	The experimental approach is still at an early stage and further research is necessary to deeply understand how to exploit this powerful tool

FTIR	Advantages	It allows determining the severity of aging through the change of specific bands (particularly sulfoxide and carbonyl)	The presence of the rejuvenator in an HMA can be detected by comparing the spectra of the pure additive and the recovered bitumen.
	Limitations	It does not discriminate what happens to the bitumen colloidal system but mainly focuses on the oxidation effects	Since most additives have peculiar bands in correspondence to the sulfoxide and carbonyl bands, it is difficult to quantify the rejuvenator content in the recovered bitumen
TLC-FID	Advantages	The evolution of the SARA fractions with aging allows estimating the severity of the phenomena	It allows understanding the efficacy of the rejuvenation process in restoring the SARA proportioning
	Limitations	There is not a clear correlation between the SARA proportions and the bitumen mechanical behavior	Again, the main issue with this technique is related to the poor association between SARA proportions after rejuvenation and the effective improvement of the aged bitumen rheological properties
HP-GPC	Advantages	It allows quantifying the effects of SARA fraction shifting and the agglomeration of the asphaltenes due to aging	The analysis of the molecular weight distribution allows understanding if a rejuvenator can really detach the asphaltene clusters or only has a dilution effect
	Limitations	There is still uncertainty on how the different aging phenomena (oxidation, loss of volatiles, …) influence the molecular weight distribution	It could be used to estimate the degree of blending between aged and virgin bitumen with/without rejuvenators, but no precise procedures have been still defined.

Table 8- Advantages and limitations of the different techniques for the study of bitumen aging and rejuvenation.

The previous literary review highlighted that, despite extensive research have been moved to innovative and improved binders, there are still important aspects about neat bitumen that deserve to be studied to fully understand the complex chemistry of this material and somehow predict the behaviour of the bituminous mixtures when in service. In the light of the themes discussed above, future works should be addressed to:

- Combine the results of the chemical tests at the binder scale with the results of the mechanical and rheological tests at both binder and mixture scale. Understanding

what happens to the bitumen from the chemo-morphological point of view is fundamental but should be correlated to the corresponding effects on the material performance in order to have the research keen on the practical outcomes. To this goal, for instance, the IFSTTAR research team recently identified a relationship between the bitumen molecular weight distribution and the phase angle of the complex modulus and proposed a tool, the δ-method, to determine the molecular weight distribution from rheological tests (Themeli *et al.* 2015a). Within the RILEM TC 264-RAP, scientists are trying to find links between the mechanical characteristics of HRMA and the FTIR spectrum of the extracted bitumen, also aiming to estimate the presence or even the content of a rejuvenator in a mix from the FTIR binder spectrum.

- Evaluate new solutions to hinder, restrict, or slow down the bitumen aging. Several investigations showed that the use of a straight-run bitumen, instead of a visbreaker one, can reduce the aging susceptibility of an HMA both in the short- and in the long- term (Giavarini 1984, Giavarini and Saporito 1989, Bocci *et al.* 2018). However, poor attention is paid by road authorities, boards for standardization and HMA manufacturers on the bitumen origin and production process. To a similar scope, further research should also be focused on additives with antioxidant effect, i.e. with the ability to reduce the bitumen propensity to oxidation. Some products are currently available on the market with the declared effect of hindering bitumen oxidation, but scientific studies are required to deeply understand their behavior at both chemical and mechanical levels.
- Understand the interaction between old and fresh bitumen in hot recycling. The topics of RAP bitumen degree of activation (DoA) and RAP/virgin bitumen degree of blending (DoB) are actually among the most studied worldwide (Shirodkar *et al.* 2011, 2013, Coffey *et al.* 2013, Gundla and Underwood 2015, Stimilli *et al.* 2015, Ashtiani *et al.* 2018, Vassaux *et al.* 2019, Ding *et al.* 2018, Vassaux *et al.* 2018, Kaseer *et al.* 2019, Lo Presti *et al.* 2020). However, because of the huge complexity of the problem (which is influenced by many factors such as RAP bitumen content, nature and aging state; HMA production process; type, dosage and way of addiction of the rejuvenators; hauling, paving and compaction procedure…), univocal protocols to classify different RAP materials according to the DoA or to estimate the DoB during pavement construction have not been defined.
- Identify a method to allow precise quality controls on HRMA. This objective, which is maybe utopian, is one of the most crucial. Technical specifications currently provide controls on the HMA mechanical performance to limit the amount of RAP in the mix and encourage the use of rejuvenators. However, a solution to estimate how much RAP and how much rejuvenator have been included in a mix should be found, possibly including a series of physical, chemical, microscope and rheological analysis on the raw materials (RAP and its components, rejuvenator, virgin bitumen)

and the laboratory and plant-produced mixtures preliminarily to the full road construction.

Chapter 3. Research description and objectives

The present PhD. research programme wants to develop and investigate the above-mentioned topics. As already explained, the increasing bitumen cost, the growth of the traffic loads and the desire to find more sustainable paving practices are forcing agencies to identify new ways to maximize the re-use of recycled old pavements.

If RAP could theoretically be 100% recycled, its content in bituminous layers is still restricted in most countries mainly due to legislation limitations and technical issues. In particular, the stiffer and more brittle mixes, usually resulting from RAP addition, have raised concerns about the long-term properties of the pavement. Furthermore,in order to increase the amount of usable RAP, rejuvenating additives can be included in the mixtures.

The overall research activities discussed in this dissertation are carried out in the Department of Civil and Building Engineering and Architecture of the Polytechnic University of Marche and address the main issues related to hot recycling production techniques.

Among the various concerns in the use of RAP, the correct dosage and use of rejuvenator, the distillation process of virgin bitumen, mixing and compaction time and temperature are of great importance. Therefore, with the aim of moving towards a complete recycling of 100% even in the hot recycling technique, the present Phd. research wants to study and analyze the rheological, mechanical and performance properties of the HRMA changing the:

- type of rejuvenator;
- distillation process of the virgin bitumen;
- heating and mixing temperature;
- time spent in the oven of the loose mixture after the mixing phase.

In particular, the experimental program can be divided in two different step:

- 1st part: the purpose is to analyze the effectiveness of a rejuvenator on an aged bitumen extracted from RAP and to evaluate whether the oxidation is more or less severe on an already aged bitumen. This latter is carried out comparing the rheological properties of an aged bitumen before and after rejuvenation and subsequently also after a second aging (re-aging);
- 2nd part: it consists of the mechanical, performance and rheological characterization (ITSM, ITS, ITFT, complex modulus test) of HRMA containing 50% of RAP material. This part can, in turn, be divided into three phases:
    - comparison between 7 different additives of various kinds (available on the market and not);

- differences between a real-rejuvenator and a softening agent on HRMA fatigue performance
- evaluation of the mechanical and rheological properties of HRMA containing two different rejuvenators changing the following conditions:
  - virgin bitumen type: vis-breaking or straight-run;
  - heating and mixing temperature: 140°C, 170°C;
  - loose mixture high temperature exposure time (growing from 30 to 180 minutes).

The following scheme highlights the above-mentioned experimental program.

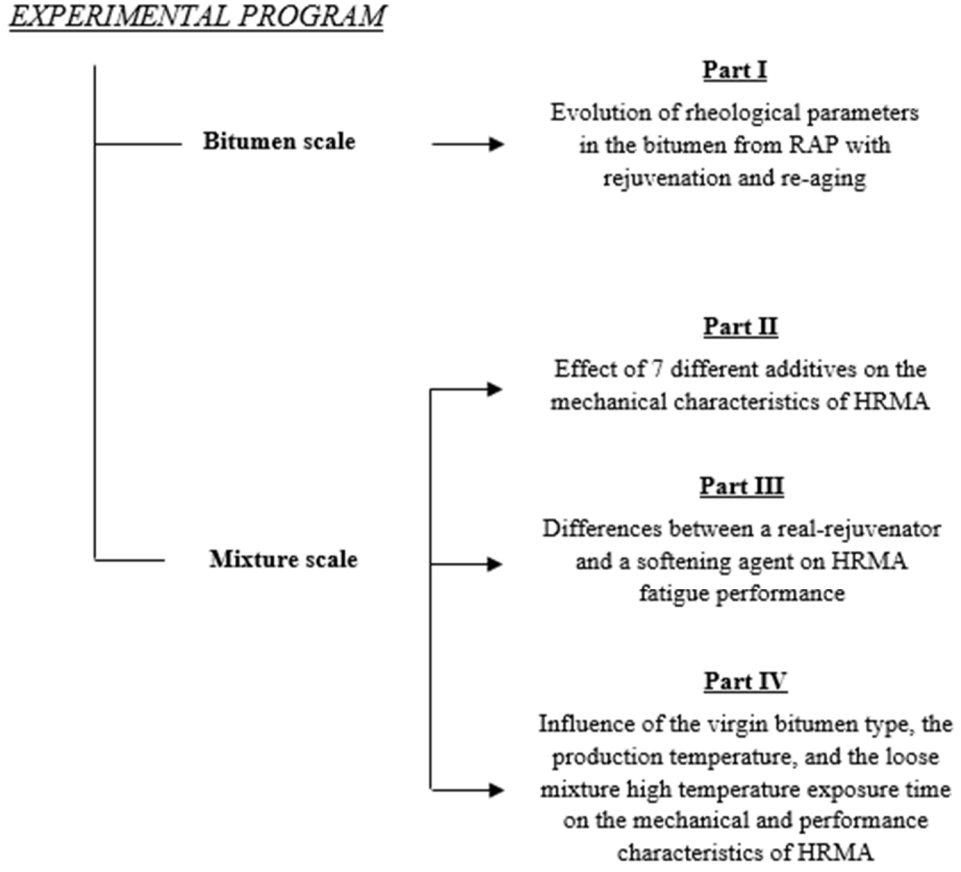

Figure 19 - Research program steps

Part I: Evolution of rheological parameters in the bitumen from RAP with rejuvenation and re-aging

Chapter 4. Introduction and experimental method

This part of the PhD program aims at analysing the evolution of the rheological behaviour of the aged bitumen extracted from RAP with rejuvenation (blending of virgin and RAP bitumen, with addition of a rejuvenator) and re-aging (representing the service life of the hot recycled mix). The complex modulus of the binders was measured through a DSR device, while RTFOT and PAV protocols were followed to reproduce the bitumen aging in the laboratory. Three rheological models (2S2P1D, modified CAM and generalized logistic sigmoidal) were used in order to study the evolution of their parameters in the various steps. In addition, the apparent molecular weight distribution (AMWD) of the bitumens, determined through δ-method, was analysed.

Therefore, the objective deals with the analysis of how the rheological parameters of an aged bitumen changes with rejuvenation and re-aging. To this aim, the hot recycling process was replicated in the laboratory at a binder scale by extracting the bitumen from the RAP milled from a French road. Then, this was blended with a rejuvenating agent and subsequently with virgin bitumen. Finally, the simulated hot recycled bitumen was re-aged in the laboratory in both the short-term and long-term steps.

The complex modulus tests were carried out on the virgin bitumen (VB), the bitumen recovered from the RAP (RB), the RAP bitumen blended with rejuvenator (RB+R) and afterwards virgin bitumen (RB+R+VB), and on the rejuvenated bitumen after short-term aging (RB+R+VB_STAG) and long-term aging (RB+R+VB_LTAG). Table 9 shows the tested materials and their codes.

The experimental data were interpolated using three different rheological models: 2S2P1D model, modified CAM model and generalized logistic sigmoidal model. The goal was to observe the effects of rejuvenation and re-aging on the model parameters, in order to quantify the changes in material behaviour and compare the rheological properties of a first-aged bitumen, represented by the bitumen extracted from RAP, and a re-aged bitumen. Moreover, the Apparent Molecular Weight Distribution (AMWD) of the bituminous blends was estimated through the application of the δ-method with the aim to better understand the effect of the rejuvenation process at a chemical structure level.

Bitumen type		Bitumen preparation
Code	**Name**	
VB	Virgin bitumen	The reference unaged bitumen 50/70
RB	RA bitumen	The bitumen extracted from the RA
RB+R	Rejuvenated bitumen	RB blended with 9% of rejuvenator by weight
RB+R+VB	Hot recycled bitumen	RB+R blended with virgin bitumen 50/70 in proportion 60/40
RB+R+VB-STAG	Short-term re-aged bitumen	RB+R+VB bitumen subjected to a short-term aging by means of RTFOT
RB+R+VB-LTAG	Long-term re-aged bitumen	RB+R+VB-STAG bitumen subjected to a long-term aging by means of PAV

Table 9 - Investigated bitumens

Chapter 5. Materials and specimen preparation

The virgin bitumen (VB) was a 50/70 pen bitumen with $55 \cdot 10^{-1}$ mm penetration at 25 °C and 52.1 °C softening point. The aged binder was extracted from the RAP using trichloroethylene and the rotary evaporator (Fig. 20), according to European standards EN 12697-1 (2020) and EN 12697-3 (2019). The RAP bitumen (RB) showed $11 \cdot 10^{-1}$ mm penetration at 25 °C and 77.1 °C softening point. The rejuvenator used in this research was a mineral oil-based material modified with an antioxidant compound (additive F – Fig. 21)). The physical properties of both the additive and the virgin binder are shown in Table 10.

The blend containing RAP bitumen and rejuvenator (RB+R) was manufactured by heating the bitumen at 130 °C, adding 9% of rejuvenator by aged bitumen weight and stirring for 30 s. Before cooling, a sample of RB+R was collected, then virgin bitumen (heated at 130 °C) was added and the blend (RB+R+VB) was stirred for another 30 s. The ratio of RB+R and VB was 60/40. The short-term aging was replicated in the laboratory by means of rolling thin film oven test (RTFOT) procedures (Fig. 22a). In accordance with EN 12607-1 (2015), the protocol provided a temperature of 163 °C and an aging time of 85 min. The long-term aging was simulated through pressure aging vessel (PAV) (Fig. 22b). According to EN 14769 (2013), a temperature of 100 °C and a pressure of 2.1 MPa were applied to the bituminous samples for 20 h. Table 10 summarized the tested bituminous blends and the preparation procedure.

Virgin bitumen		
Property	**Unit**	**Value**
Penetration @ T = 25 °C	10^{-1} mm	55
Ring and ball softening point	°C	52.1
Bitumen from RA		
Property	**Unit**	**Value**
Penetration @ T = 25 °C	10^{-1} mm	11
Ring and ball softening point	°C	77.1
Rejuvenator		
Property	**Unit**	**Value**
Density at 20 °C	g/cm3	0.87
Kinematic viscosity @ T = 25 °C	mPa·s	400
Kinematic viscosity @ T = 40 °C	mPa·s	69
Flash point	°C	> 260

Table 10 - Physical properties of virgin bitumen, RAP bitumen and rejuvenator.

(a)

(b)

Figure 20 - Bitumen extractor (a) and rotary evaporator (b)

Figure 21 - Rejuvenator used: additive F

(a)

(b)

Figure 22 - RTOFT (a) and PAV (b)

Chapter 6. Complex modulus: measurement, analysis and modelling

The rheological properties of the bitumens were determined using a dynamic shear rheometer (DSR, Fig. 23) in plate-plate configuration (diameter of 8 mm and gap of 2 mm for low and intermediate temperatures; diameter of 25 mm and gap of 1 mm for high temperatures), applying sinusoidal load curves in control-strain mode, according to EN 14770 (2012).

Figure 23 - Dynamic Shear Rheometer (DSR)

Preliminarily, the threshold of the linear viscoelastic (LVE) field (γ_{lim}) was determined through strain sweep tests. A constant frequency (f = 1.59 Hz) and a range of strains (γ = 0.003-3%) were applied for each temperature selected (T = 4, 16 and 28 °C) and the value of γ_{lim} was measured as the strain corresponding to a $|G^*|$ deviation equal to 95% of its initial value $|G^*_{in}|$. Then, frequency sweep tests were carried out at different temperatures for the characterization of bitumen viscoelastic properties. In particular, these tests were performed at a constant strain $\gamma = 0.5\% < \gamma_{lim}$ (enabling the application of time-temperature superposition principle) over a range of frequencies (from 0.1 to 10 Hz) and temperatures (from –6°C to 82 °C, with 6 °C intervals). Complying with EN 14770, the test protocol provided two repetitions for each test. In case of result dispersion ($|G^*|$ out of the range of 10%), a third repetition was carried out.

Figure 24 - 8mm and 25mm samples

The measured rheological data were plotted in the Black and Cole-Cole diagrams to evaluate the reliability of the experimental results, assess the time-temperature equivalency and thermo-rheologically simplicity for the tested bitumens, estimate the magnitude of the glassy asymptote and the preponderance of the viscous or elastic behaviour at the different temperatures investigated (Lesueur et al., 1996).

As resulted in the Black Diagrams depicted in the following sections, all the recovered bitumens were considered as thermo-rheologically simple and the time-temperature superposition principle (TTSP) was applied to determine complex modulus master curves and shift factor relationships. The rheological data were shifted with respect to time until the isothermal curves merge into a single smooth function at the reference temperature of 10 °C. The estimation of the temperature shift factors was carried out according to the closed form shifting algorithm (Gergesova et al., 2011), based on the minimization of the area between two successive isothermal curves. The rheological behaviour of the different materials in LVE was simulated by means of three models typically used in the field of bituminous binders and mixtures: the 2S2P1D model, the modified CAM model and the generalized logistic sigmoidal model.

6.1. 2S2P1D model

The 2S2P1D mechanical model (Olard and Di Benedetto 2003b) consists of the series of a linear dashpot, two parabolic elements and a spring of stiffness G_∞ - G_0, assembled in parallel with a second spring (G_0) (Figure 25).

In detail, according to the 2S2P1D model, the equation for complex modulus is given by Equation (1):

$$G^*(i\omega\tau) = G_0 + \frac{G_\infty - G_0}{1+\delta(i\omega\tau)^{-k}+(i\omega\tau)^{-h}+(i\omega\tau\beta)^{-1}} \qquad (1)$$

where G_0 is the static shear modulus when $\omega \to 0$ ($G_0 = 0$ for binders); G_∞ is the glassy shear modulus when $\omega \to \infty$; $\omega = 2\pi f$ is the angular frequency; i is the imaginary unit defined by $i^2 = -1$; τ is the characteristic time; δ, k and h are dimensionless constants ($0 < k < h < 1$); β is a function of the dashpot viscosity ($\eta = G_\infty \beta \tau$). Based on the TTSP, τ can be determined as in Equation (2):

$$\tau(T) = a_T \cdot \tau_0 \qquad (2)$$

where a_T is the shift factor at the temperature T and $\tau_0 = \tau(T_0)$ is determined at the reference temperature T_0.

Fig. 25 shows the correlation between the 2S2P1D model parameters and the shape of the curve in the Cole-Cole plot: the static (G_0) and glassy (G_∞) shear moduli represent the intersection with the real axis ($\phi = 0$), k and h are proportional to the angles that the curve generates with the real axis and δ defines the height of the pinnacle point.

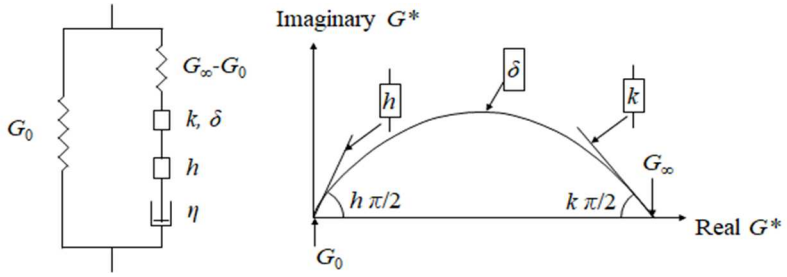

Figure 25 - Definition of 2S2P1D model and parameters.

6.2. Modified CAM model

The modified Christensen-Anderson-Marasteanu (mCAM) mathematical model was formulated by Bahia and co-workers (Bahia et al., 2001; Zeng et al., 2001) and includes separate equations for the norm and the phase angle of the complex modulus. In particular, the equation for complex modulus norm is given by Equation (3):

$$G^*(f') = G_e^* + \frac{G_g^* - G_e^*}{\left[1+\left(\frac{f_c}{f'}\right)^k\right]^{\frac{m_e}{k}}} \quad (3)$$

Where $G^*_e = G^*$ (f → 0) is the equilibrium complex modulus ($G^*_e = 0$ for bitumens), $G^*_g = G^*$ (f → ∞) is the glassy complex modulus, f_c is the location parameter with dimensions of frequency (crossover frequency), f' is the reduced frequency (function of both temperature and strain), k and m_e are dimensionless shape parameters.

Figure 26 illustrates the complex modulus master curve in Equation (2). As the G^*_e asymptote is zero for bitumens, the curve has a horizontal asymptote G_g^* at $f \to \infty$ and a diagonal viscous asymptote with a slope of m_e. The crossover frequency f_c represents the frequency at which the G^*_g and m_e asymptotes intercept. At this point, the distance between $G^*(f_c)$ and G^*_g is defined as rheological index (R) and results equal to $\frac{m_e}{k}\log 2$.

The phase angle of the complex modulus is given by Equation (4):

$$\phi(f') = 90I - (90I - \phi_m)\left\{1 + \left[\frac{\log(f_d/f')}{R_d}\right]^2\right\}^{-m_d/2} \quad (4)$$

where f_d is the location parameter with dimensions of frequency, corresponding to the value at the master curve inflection, ϕ_m is the phase-angle constant at the frequency f_d, R_d and m_d are shape parameters and I is a coefficient equal to 0 or 1 respectively for $f' \geq f^d$ and $f' \geq f^d$.

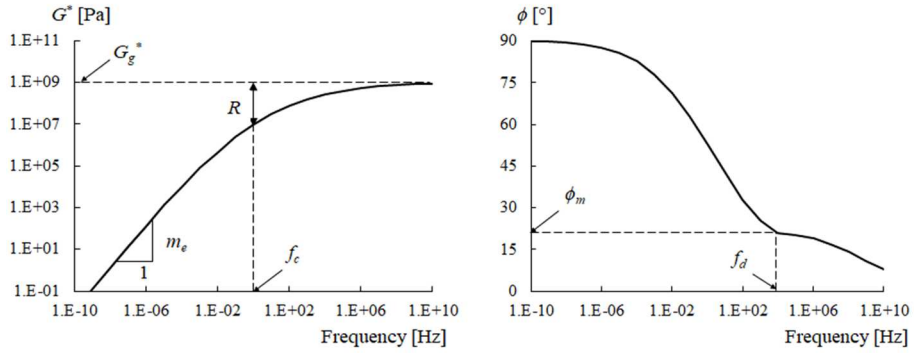

Figure 26- Definition of mCAM model parameters.

6.3. Generalized logistic sigmoidal model

The generalized logistic sigmoidal (GLS) model is the mathematical model presented in the Mechanistic-Empirical Pavement Design Guide (NCHRP 01-37A 2004). This sigmoidal model was developed by Pellinen et al. (2002) for bituminous mixtures; subsequently Rowe et al. (2009) applied it to binders and generalized it through the application of the Richards model (Richards 1959). The relationship between the norm of the complex modulus and the reduced frequency is given by Equation (5):

$$\log G^*(\omega) = \delta + \frac{\alpha}{\left[1+\lambda e^{[\beta+\gamma(\log\omega)]}\right]^{1/\lambda}} \tag{5}$$

where logω is the logarithm of the reduced frequency, δ is the lower asymptote (which is equal to zero for bitumens), α is the difference between the values of the upper and lower asymptote, λ, β and γ define the shape between the asymptotes and the location of the inflection point (Rowe, 2009). In particular, the parameter λ represents the difference between the standard and the generalized logistic sigmoidal model and allows the curve to take a non-symmetric shape (Figure 3). Rowe (2009) later employed the Kramers–Kronig equation by Booij and Thoone (1982) and numerically calculated phase angle values through Equation (6):

$$\phi(\omega) = 90 \cdot \frac{d\log G^*}{d\log\omega} = -90\alpha\gamma \frac{e^{[\beta+\gamma(\log\omega)]}}{\left[1+\lambda e^{[\beta+\gamma(\log\omega)]}\right]^{(1+1/\lambda)}} \tag{6}$$

Figure 27 shows the effect of each parameter in the $|G^*|$ and ϕ master curves trends.

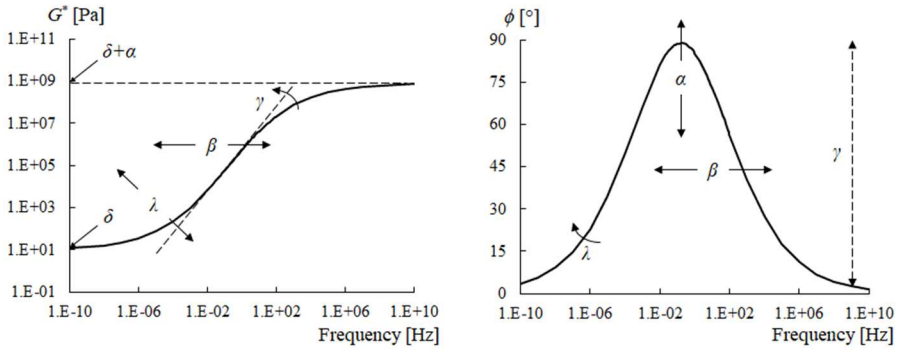

Figure 27 - Definition of modified GLS model parameters.

6.4. WLF model

The Williams-Landel-Ferry (WLF) law (Ferry 1980b) was used to model the shift factor trend with temperature. The temperature shift factors can be obtained using the Williams-Landel-Ferry (WFL) Equation (7) for bituminous materials:

$$log \frac{a_T(T)}{a_T(T_0)} = -\frac{C_1(T-T_0)}{C_2+(T-T_0)} \quad (7)$$

where a_T is the shift factor at temperature T, T_0 is the reference temperature, C_1 and C_2 are empirical constants.

6.5. Delta Method

The δ-method was developed by Themeli et al.(2015) as a tool to determine the apparent molecular weight distribution (AMWD) of the bituminous blends from the phase angle (ϕ) of the complex modulus.

Bitumen is considered as a mixture of groups of monodisperse molecular weight (MW). Each of them is characterized by a single relaxation frequency below which they relax and do not contribute to the mechanical response of the material. Schematically, it can be assumed that the unrelaxed molecules at a particular frequency are 'diluted' in a phase of relaxed molecules.

The basic assumption of the δ-method is that the phase angle (ϕ) of the complex modulus for a given frequency (ω_i) is proportional to the fraction of relaxed molecules at this frequency. In fact, when decreasing the oscillation frequency heavier and heavier molecules relax and become part of the 'diluted' phase determining, from the rheological point of view, a decrease

of $|G^*|$ and an increase in ϕ. In particular, this latter proved to be more sensitive to the MW of bitumen groups (Zanzotto *et al.* 1999).

Zanzotto et al. (1999) defined the relationship between the frequency ω and the MW obtained by vapour pressure osmometry. Assuming the proportionality between the cumulative molecular weight distribution (CMWD) curve and the ϕ master curve as in Equation (8)

$$CMWD = A + B \cdot \phi(MW) \tag{8}$$

the AMWD can be calculated through differentiation according to Equation (9) (Themeli *et al.* 2015b):

$$AMWD = \frac{d(CMWD)}{d(\log MW)} \tag{9}$$

In the present analysis, the AMWD was determined from the derivative of the continuous phase angle curve fitted with one of the previously described rheological models.

Chapter 7. Results and analysis

7.1. Identification of LVE region

The strain sweep tests were carried out on the bitumen extracted from the RA (RB) and on the rejuvenated bitumen after long-term aging (RB+R+VB_LTAG), as they were supposed to exhibit the worst condition in terms of brittleness. In fact, the harder the bitumen because of aging effects, the higher the $|G^*|$ values measured and the lower γ_{lim} (Grilli et al., 2017). Table 11 and Figure 28 show the results and allow identifying the threshold of LVE region, which resulted 1.45% and 1.73% respectively for RB and RB+R+VB_LTAG. Therefore, the strain value γ =0.5% (about one third of the minimum γ_{lim} value) was selected for the frequency sweep test implementation.

Bitumen	**Repet.**	**Temperature**					
		28 °C		**16 °C**		**4 °C**	
RB	N.	$\|G^*\|$ [Pa]	γ_{lim} (%)	$\|G^*\|$ (Pa)	γ_{lim} [%]	$\|G^*\|$ (Pa)	γ_{lim} [%]
	1	5.63E+06	1.61	1.92E+07	1.45	5.38E+07	1.72
	2	5.26E+06	1.84	1.83E+07	1.53	5.18E+07	1.65
RB+R+VB_ LTAG	N.	$\|G^*\|$ [Pa]	γ_{lim} (%)	$\|G^*\|$ (Pa)	γ_{lim} [%]	$\|G^*\|$ (Pa)	γ_{lim} [%]
	1	4.47E+06	2.23	1.44E+07	1.83	4.08E+07	1.73
	2	4.81E+06	2.00	1.54E+07	1.76	4.28E+07	1.88

Table 11 - Strain sweep test data for RB and RB+R+VB_LTAG.

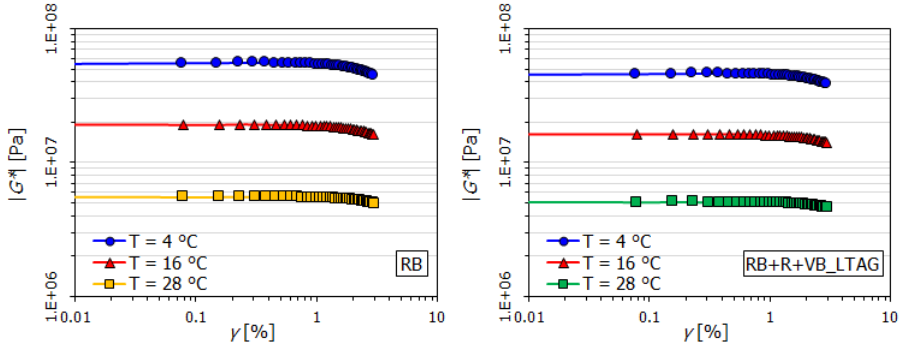

Figure 28 - Isotherm curves from strain sweep test for RB and RB+R+VB_LTAG.

7.2. Analysis of G* data on Black and Cole-Cole plots

Figures 29 and 30 depict the measured G^* data in the Black ($|G^*|$ vs ϕ) and Cole-Cole (G_2 vs G_1) diagrams. From the Black diagram, the variability of $|G^*|$ and ϕ can be observed. In particular, $|G^*|$ ranged between 23.5 Pa (VB) and 205 MPa (RB) while ϕ ranged between 18.5° (RB) and 89.15° (VB). Moreover, the G* data measured at different temperatures and frequencies well superimposed in the Black and Cole-Cole plots, allowing assuming the thermo-rheological simplicity of the bitumens and applying the time-temperature superposition principle (TTSP) to build the isothermal master curves of $|G^*|$ and ϕ.

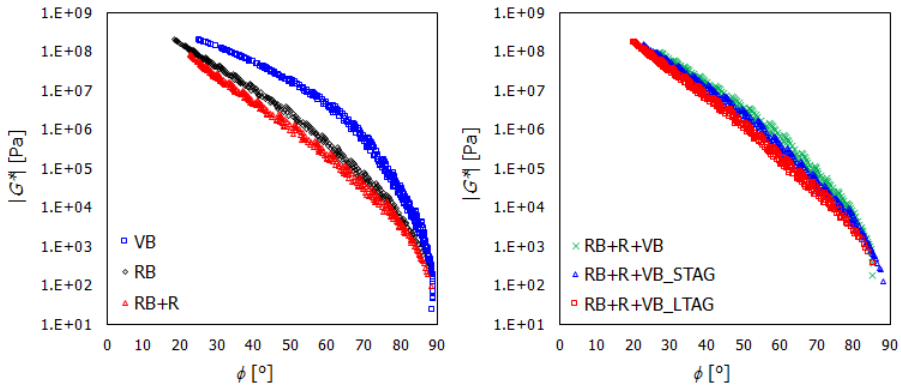

Figure 29 - Black space

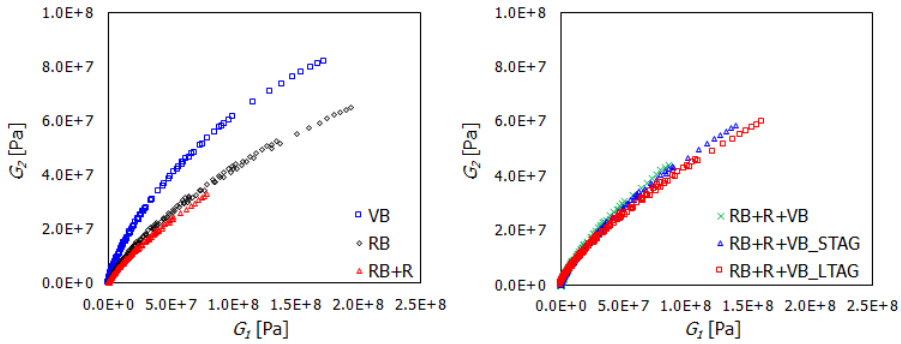

Figure 30 - Cole-Cole plot

The Black and Cole-Cole diagrams highlighted the different rheological behaviour of the tested bitumens. In particular, VB showed the typical trend of a neat bitumen, with G^* uniformly moving from a purely viscous ($|G^*| = 0$, $\phi = 90°$) to a purely elastic ($|G^*| \approx 1$ GPa, $\phi = 0°$) behaviour when decreasing temperature or increasing frequency. Differently, RB curves were positioned on the left and below VB curves in the Black and Cole-Cole diagrams, respectively, denoting a higher relevance of elastic component to detriment of the viscous component. The addition of the rejuvenator did not achieve substantial changes in the data trend, as the stiffness reduced (lower values of $|G^*|$) but the balance between elastic and viscous components did not vary. The re-aging determined again a leftward moving of the data in the Black space and a down- and rightward moving in the Cole-Cole plot, denoting an increase of $|G^*|$ and a further prevalence of elasticity against viscosity in the bitumen behaviour.

7.3. Effect of rejuvenation and re-aging on |G*| and ϕ master curves

Figure 31 depicts the master curves of $|G^*|$ for the tested bitumens at the reference temperature of 10 °C. The experimental data plotted in each graph of the figure are the same, while the interpolation was carried out using different rheological models (2S2P1D, mCAM or GLS). In particular, for 2S2P1D and GLS the model parameters were determined through the minimization of Equation (10), using the Solver feature of MS Excel:

$$\sum_{i=1}^{N}\left(\left[G_1^{exp}(\omega_i) - G_1^{model}(\omega_i)\right]^2 + \left[G_2^{exp}(\omega_i) - G_2^{model}(\omega_i)\right]^2\right) \qquad (10)$$

where G_1^{exp} and G_2^{exp} are respectively the real part and the imaginary part of the experimental G^* data, while G_1^{model} and G_2^{model} are respectively the real part and the imaginary part of the modelled G^* (Di Benedetto et al., 2004).

Differently, mCAM model parameters were determined my separately minimizing the sum of the distances between measured and modelled $|G^*|$ and the sum of the distances between measured and modelled ϕ. This was established because in mCAM model the $|G^*|$ and ϕ equations present different parameters (see Equations (3) and (4)). For all the models, a fixed value of the glassy asymptote (10^9 Pa) was imposed.

The results in Figure 31 showed that the stiffness of RB was higher than that of VB, particularly at low frequencies/ high temperatures. The addition of the rejuvenator determined a significant reduction of $|G^*|$ at all frequencies/temperatures, indicating a kind of vertical translation of the master curve but no changes in the shape. The $|G^*|$ master curve of RB+R+VB showed intermediate position and shape with respect to the master curves of VB and RB+R. The re-aging implied an increase in $|G^*|$, whose amplitude is comparable

between short- and long-term aging. The bitumen $|G^*|$ master curve at the end of the re-aging process resulted almost superimposed to that of RB (slightly higher $|G^*|$ values were observed at low frequencies/high temperatures).

From the graphs in Figure 31, it can be noted that the three rheological models well interpolated the experimental data. In particular, the little distances between the measured and modelled $|G^*|$ values proved a good effectiveness of the models in simulating the bitumen stiffness for all test conditions.

Figure 32 illustrates the master curves of ϕ at the reference temperature of 10 °C. Also in this figure, the experimental data in each graph are the same, while the curves represent the different rheological models (2S2P1D, mCAM or GLS).

The results showed that the phase angle of RB was lower than that of VB, particularly at low frequencies/ high temperatures. Differently from |G*|, when the rejuvenator was added the variation of ϕ was not as much significant, particularly at intermediate frequencies. The blending with VB allowed obtaining an increase in ϕ and the master curve of RB+R+VB resulted in an intermediate position between those of VB and RB+R. Finally, the ϕ values decreased again with re-aging, with a comparable extent determined by short-term and long-term processes.

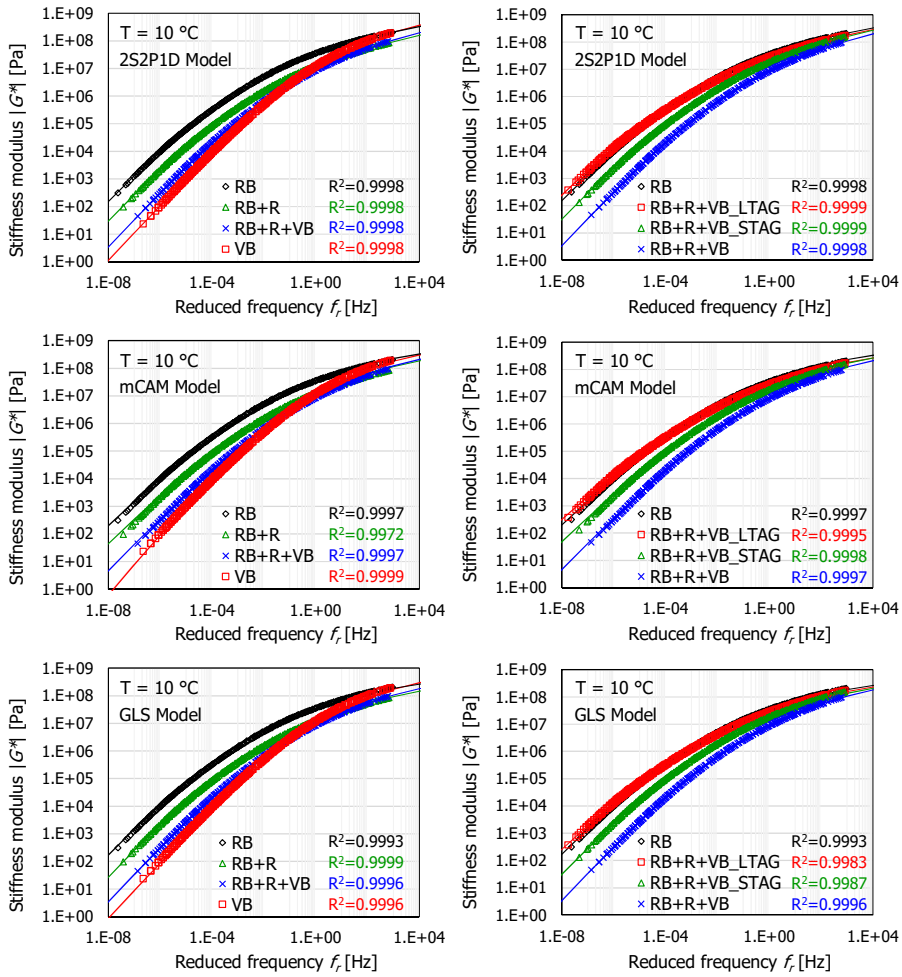

Figure 31 - |G| master curves at T = 10 °C with superposition of the different rheological models.*

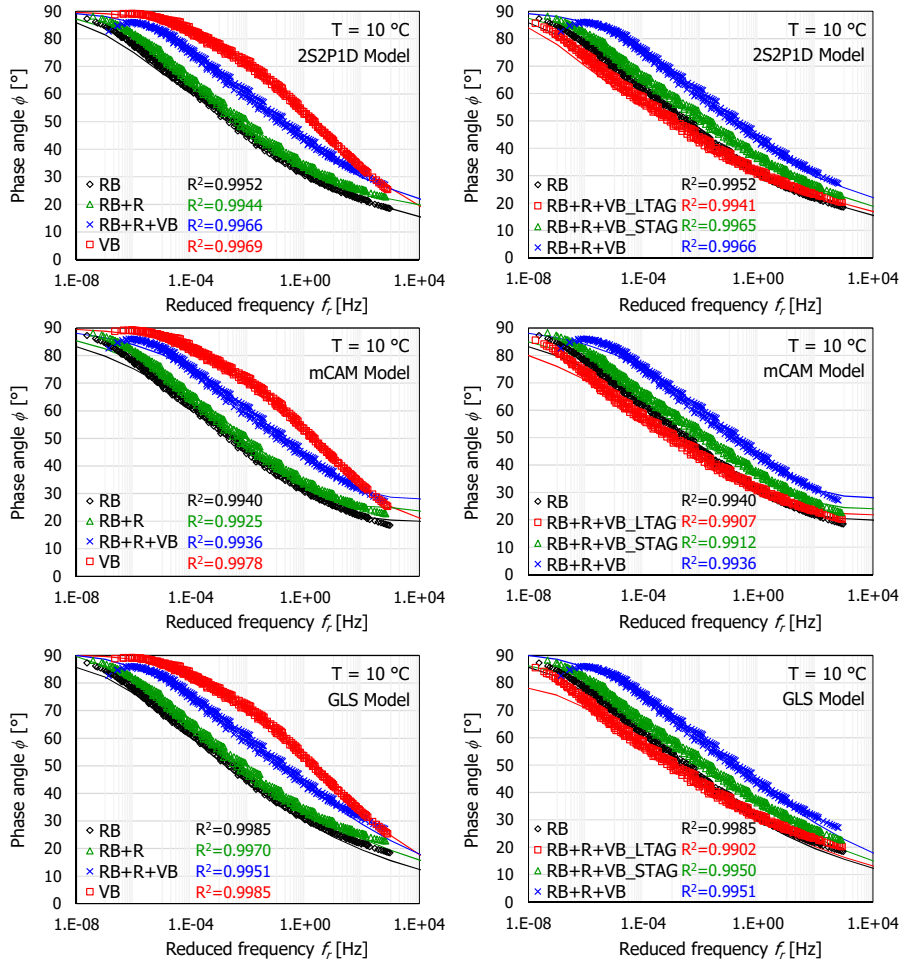

Figure 32 - ϕ master curves at T = 10 °C with superposition of the different rheological models.

The comparison between the measured data and the model curves allowed noticing a lower precision in the phase angle simulation with respect to the stiffness. In particular, the distance between experimental and modelled values increased when increasing bitumen aging severity, i.e. a more accurate estimation was obtained for VB and RB+R+VB while a lower precision was noted for RB, RB+R, RB+R+VB_STAG and RB+R+VB_LTAG. The 2S2P1D proved to be the most accurate model, with just a slight underestimation of ϕ (about 3° at maximum) observed for RB, RB+R and RB+R+VB_LTAG bitumens at high temperatures/low frequencies. The mCAM well modelled the ϕ values at intermediate

frequencies, but an underestimation of about 6° and on overestimation of 2° were respectively noticed at low frequencies/high temperatures and at high frequencies/low temperatures. The GLS model also provided an accurate ϕ simulation at intermediate frequencies but underestimated the phase angle at both low (approximately 7°) and high (approximately 4°) frequencies.

7.4. Evolution of the rheological model parameters with rejuvenation and re-aging

Figures 33 and 34 show the values of the parameters defined in the 2S2P1D, GLS and mCAM model equations (Equations from (1) to (6)). In particular, Figure 9 illustrates the values of the parameters h, k, β and τ_0 of the 2S2P1D model and the parameters α, β, γ and λ of the GLS model (the parameter δ is directly related to α, as the glassy asymptote $\alpha + \delta$ was fixed to 10^9 Pa). Figure 34 illustrates the parameters of the mCAM model, which are f_c, k, m_e and R for the norm of the complex modulus and f_d, δ_m, R_d and m_d for the phase angle.

A significant difference can be observed between the almost all the parameters of VB and RB provided by the different models. In the 2S2P1D, the aged bitumen from the RA showed lower k and h and higher β and τ_0 with respect to the virgin bitumen. The parameters k and h represent the order of derivation of the two fractional derivative elements included in the model and vary between 0 (purely elastic behaviour) and 1 (purely viscous behaviour). Therefore, the decrease of the k and h denoted the prevalence of elasticity over viscosity when increasing aging. At the same time, the increase of β and τ_0 reflected the lower relaxation ability of RB. In the mCAM, when moving from the VB to the RB the parameters f_c, k, m_e, f_d, and m_d decreased while the parameters R and R_d increased (the parameter δ_m was almost unaltered). This result is in agreement with different authors, which estimated the rate of aging of the bitumen with the rheological index R and the crossover frequency f_c of the mCAM model and reported the contemporary growth of R and decrease of f_c with aging (Cholewińska et al. 2018; Hao et al., 2017; King et al., 2012; Rowe et al., 2016). Indeed, this trend of the rheological index and the crossover frequency indicated a more gradual transition from the elastic behaviour to the viscous behaviour and a less sensitivity to frequency/temperature changes. In the GLS model, when comparing VB and RB higher values of β and γ and lower values of α and λ were observed for the latter, confirming the lower sensitivity to the variations of reduced frequency (flatter $|G^*|$ and ϕ master curves).

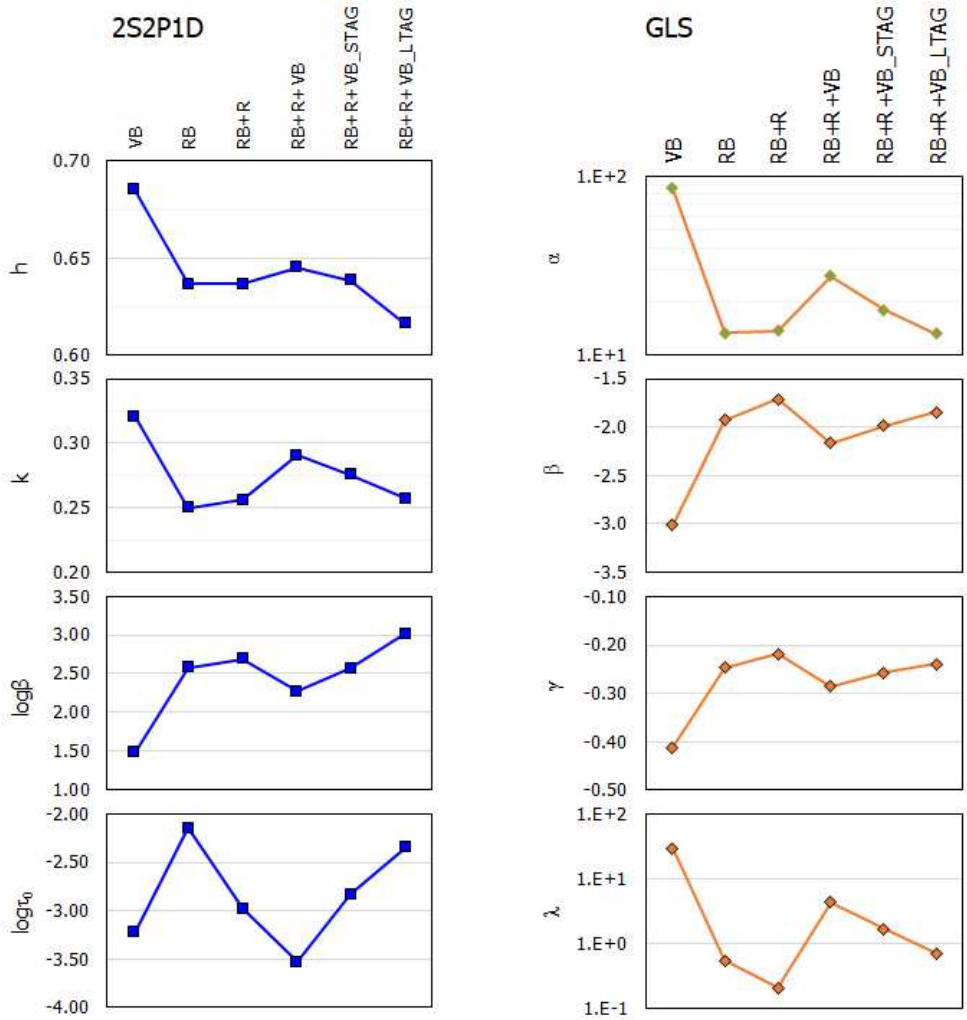

Figure 33 - Evolution of 2S2P1D and GLS model parameters with rejuvenation and re-aging.

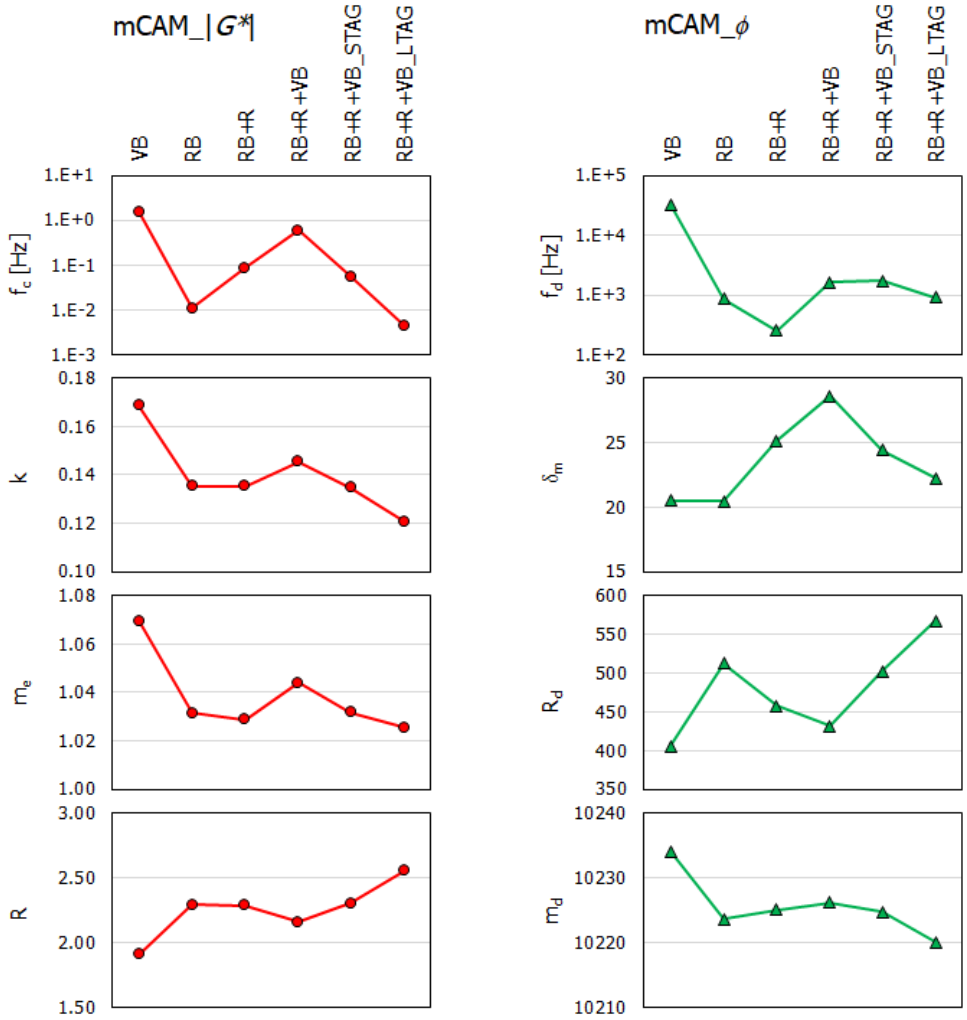

Figure 34 - Evolution of mCAM model parameters with rejuvenation and re-aging.

With the addiction of the rejuvenator, hypothesizing a full or partial restoration of the volatile components and disruption of the asphaltene clusters, the model parameters should have been intermediate between those of VB and RB. Differently, most of the parameters did not change. In the 2S2P1D model, only a decrease of τ_0 was noted while h, k and β were unaltered, confirming that the presence of the additive did not determine any change in the master curve

shape. In the GLS model, the parameter α was approximately the same between RB+R and RB, while the other parameters β, γ and λ were respectively higher, higher and lower for RB+R than for RB. This denoted that the GLS model parameters could not be precisely correlated with the effects of the rejuvenation process. In the mCAM model for the stiffness, the crossover frequency f_c of RB+R was indeed intermediate between those of VB and RB, confirming the shifting of the |G*| master curve, while the other parameters (k, m_e and consequently R) were constant. In the mCAM model for the phase angle, the rejuvenator addition pushed the parameters R_d and m_d closer to those determined for VB, but f_d had an opposite trend (values even lower than for RB) while δ_m was higher than for VB and RB.

When the rejuvenated bitumen and the virgin bitumen were blended, almost all the parameters from the different models showed intermediate values between those of RB+R and VB. The sole exceptions were represented by τ_0 of the 2S2P1D model, which showed a value even lower than for VB, and δ_m of the mCAM model, for which a significant trend could not be observed in general.

Finally, re-aging entailed a clear direction for all the parameters, which went towards the values determined for RB. In particular, in the 2S2P1D model the parameters k and h decreased while β and τ increased. The h and β parameters of RB+R+VB_LTAG (aged, rejuvenated and re-aged bitumen) resulted slightly worse (respectively lower and higher) than those of RB (aged bitumen), while k and τ were a little better (closer to those of VB). In the GLS model, α and λ decreased with re-aging while β and γ increased, showing values comparable to those of RB. In the mCAM model, f_c, k, m_e, f_d, δ_m and m_d decreased while R and R_d increased. Most of these parameters (f_c, k, m_e, R, R_d and m_d) had worse values than those of RB. In particular, it has to be remarked that the rheological index R resulted higher for RB+R+VB_LTAG than for RB, indicating that the recycled and re-aged bitumen likely suffered more severe aging effects.

To better evaluate how detrimental were the effects of aging on the bitumen extracted from the RA before and after rejuvenation and re-aging, the Glover Rowe (G-R) parameter was also investigated. The G-R parameter (Rowe et al., 2014) characterizes the stiffness and relaxation properties of a bitumen and assumes higher values when increasing brittleness and decreasing the resistance to non-load associated cracking. This parameter was calculated using the following Equation (11):

$$\text{G-R} = \frac{|G^*|(\cos\phi)^2}{(\sin\phi)^2} \tag{11}$$

where $|G^*|$ and ϕ are the modulus and phase angle at the temperature of 15 °C and angular frequency of 0.005 rad/s deduced from rheological models. Figure 34 shows the values of the Glover-Rowe (G-R) parameter determined for the tested bitumens through the different rheological models. In the graph, two lines represent the G-R values limiting the damage

onset zone (broken line, G-R = 180 kPa) and the significant cracking zone (full line, G-R = 450 kPa).

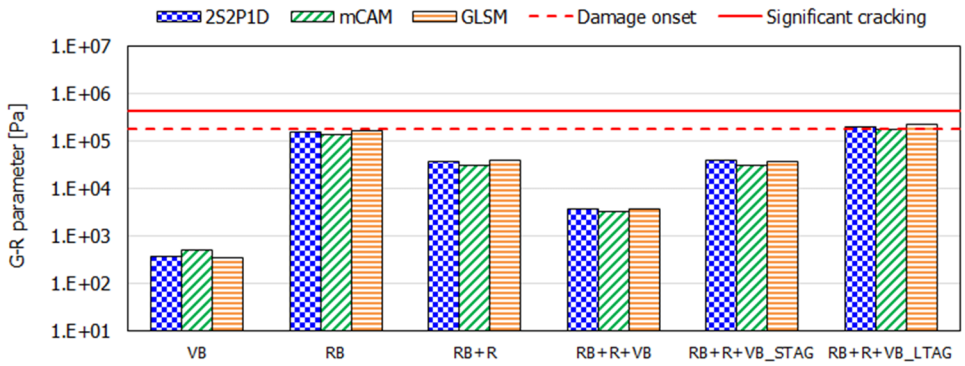

Figure 35 - G-R parameters determined through the different rheological models

As expected, the virgin bitumen showed a lower G-R value with respect to RB, whose G-R was slightly lower than the damage onset limit. The addiction of the rejuvenator and, even more, the blending with the virgin bitumen allowed decreasing the G-R and moving it away from the damage zone, but the value of VB could not be reached. When short- and long-term re-aging were applied, the G-R parameter again increased up to a final value that was slightly higher than that of RB and little above the damage onset limit.

The comparison of the G-R obtained through the different rheological models allowed observing that 2S2P1D and GLS models approximately provided the same values. Differently, the mCAM model showed higher G-R for the virgin binder but a slightly lower G-R for the other bitumens.

7.5. Variation of AMWD with rejuvenation and re-aging

The AMWD was estimated according to the previously described procedure by using the phase angle master curve defined through 2S2P1D model, which showed a higher accuracy in the experimental data interpolation for the entire investigated spectrum of reduced frequency.

The graphs in Figure 36 illustrate the concentrations of the molecular fractions as a function of their AMWD in Daltons (Da). It can be noted that most of the groups of virgin bitumen had AMW lower than 1000 Da. The spectrum of RB, compared to that of VB, was characterized by the reduction of the fractions with AMW < 500 Da (only a little peak at AMD ≈ 300 Da was observed) and the presence of molecules with higher weight

(approximately 1500 Da). These were the result of the asphaltene agglomeration in the aged bitumen.

When the rejuvenator was added to RB, the part of the low molecular weight fractions slightly increased, but the effect on high weight fractions was limited. In particular, the two peaks of RB at 800 and 1500 Da were almost unaltered, with only a little decrease of the AMW in the second peak from 1500 Da to 1300 Da. This result denoted that the rejuvenator probably restored part of the volatile components that RB lost with aging (as testified by the movement of the peak from 300 to 200 Da) but was not as effective in disrupting the asphaltene clusters. For this reason, the rejuvenator could be classified as a soluble or incompatible softener.

The further addition of VB determined the contemporary increase of the low molecular weight fractions (raising of the peak at AMW = 250 Da) and the decrease the high weight fractions (the high peaks of RB+R moved respectively from 800 to 700 Da and from 1300 to 1000 Da). After RTFOT+PAV, the content of low- and high-weight molecular groups in the rejuvenated bitumen respectively decreased and increased again. It has to be noted that the spectra of RB and RB+R+VB_LTAG were very similar. In particular:

- the peak at AMD = 300 Da was almost superimposable;
- the peak at AMW = 800 Da was present for both the bitumens but it had a lower height for RB+R+VB_LTAG;
- the last peak corresponded to a slightly different AMW (1500 Da for RB, 1650 Da for RB+R+VB_LTAG) and was taller for RB+R+VB_LTAG than for RB.

This confirmed that the recycled bitumen, at the end of the re-aging process, was in slightly worse condition than the original bitumen from the RA (as also indicated by the G* master curves and the rheological model parameters) and may show a higher brittleness and risk of low temperature cracking when in service.

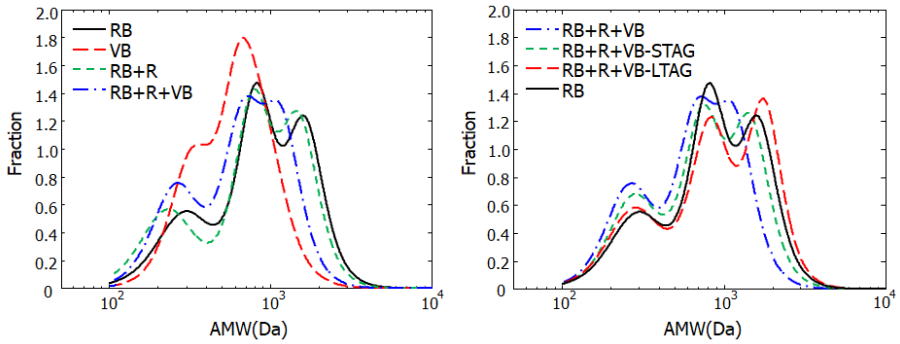

Figure 36 - Variation of AMWD with rejuvenation and re-aging.

Chapter 8. Conclusion

The present part of the PhD. program focused on the analysis of the rheological properties of the bitumen extracted from RAP when rejuvenated with a mineral oil additive and re-aged in the laboratory. In particular, the measured *G** data were interpolated using 2S2P1D, modified CAM and generalized logistic sigmoidal models with the aim to observe the variation of the different parameters with rejuvenation and re-aging. Moreover, the AMWD was determined using the δ-method to investigate the rejuvenator effect at a chemical level. The test results showed that:

- the addition of the rejuvenator determined a reduction of the stiffness and an almost negligible increase of the phase angle with respect to the RAP bitumen, while the blending with the virgin bitumen allowed both decreasing $|G^*|$ and increasing ϕ. The re-aging determined again an increase in the stiffness and a reduction of the viscous features in favour of the elastic ones;
- the 2S2P1D model provided a more precise interpolation of the complex modulus data than the other models, which showed inaccuracies in simulating the phase angle at low and high reduced frequencies;
- the parameters h and k of the 2S2P1D model decreased with aging (first aging in the case of RB, re-aging for the rejuvenated bitumen) and increased when VB was blended to the RAP bitumen; vice versa for τ_0 and β. When the rejuvenator was included in RB, only a decrease of τ was observed, denoting the $|G^*|$ master curve translation without changes in the shape;
- most of the parameters of the mCAM model (f_c, k, m_e, R, f_d, R_d and m_d) showed a clear trend when the bitumen aged and, with an opposite direction, when was blended with VB. The addiction of the rejuvenator to RB only determined an increase of f_c, while the effect on the other parameters was not significant or it was not possible to frame it in a general trend;
- the parameters β and γ of the GLS model increased with aging and decreased with the blending with VB, while α and λ showed an opposite behaviour. The parameter α did not change when the rejuvenator was added to RB, but the other parameters went in the same direction of aging, denoting an imprecise correlation with the effects of the rejuvenation process;
- the G-R parameters calculated with 2S2P1D and GLS models were comparable, while slightly lower G-R were obtained from the mCAM model in many cases;
- the δ-method provided to be very useful to understand the chemical mechanisms behind aging and rejuvenation. In particular, the aging entailed an increase of the high molecular weight fractions in the bitumen spectra, while the addition of VB restored part of the molecular groups with a low weight. The addiction of the

rejuvenator to RB had almost no effect on high weight fractions, denoting that the additive is probably a soluble or incompatible softener and cannot disrupt the asphaltene clusters.

In conclusion, the experimental approach based on the rheological modelling and the application of the δ-method resulted effective to understand the real contribution of the rejuvenator on the bitumen structure and compare the mechanical properties of the first-aged and the re-aged bitumens. Future activities of the research will involve other additives and longer aging times in order to validate the method before the implementation at a mix level.

Part II: Effect of 7 different additives on the mechanical characteristics of HRMA

Chapter 9. Introduction and experimental plan

As previously said, the distresses in the hot recycled bituminous mixtures including high RAP contents are mostly related to the aged binder. In order to increase the amount of RA in the mix, specific additives called rejuvenators can be included in the mixtures (Cao *et al.* 2018b, Joni *et al.* 2019). They are products aimed at restoring the aged asphalt binder to a state in which the RA can be introduced in new bituminous mixtures and sustain another pavement service life (Bocci, Prosperi, and Marsac 2020). Many laboratory and field studies demonstrated that successful use of rejuvenators can provide the desired pavement performance (Baghaee Moghaddam and Baaj 2016, Zaumanis *et al.* 2018).

In several countries (i.e. Italy), the use of high RAP contents is very tricky because it makes tough to meet the specifications, especially in terms of Indirect Tensile Strength (ITS). Moreover, it is largely known that the mixing procedure at the plant, and in particular the RA heating method, plays a large role in the mechanical characteristics of the mixture (Madrigal *et al.* 2017). Among the many issues, temperature is a key factor and only its correct definition for each component at each step results in a successful hot recycling (Bocci, Prosperi, Mair, *et al.* 2020). On the one hand, a low mix temperature can result in a poor mix workability and therefore in a high air voids content, reflecting on a higher risk of moisture damage, ravelling, rutting and cracking (Khan *et al.* 2013b). On the other hand, one of the commonest mistakes consists in raising the final temperature of the mix at the plant exit, in order to achieve a more effective softening of the RA bitumen and a higher mix workability. However, this can cause a more severe short-term aging for both virgin and RAP binders (Hofko, Falchetto, *et al.* 2017, Lolly *et al.* 2017), leading to a stiffer e more brittle mixture. In addition, the higher is the target mix temperature, the stronger is the virgin aggregate overheating (the RAP heating temperature is usually fixed according to the type of plant and the available equipment), the more severe is the thermal shock for the bitumen when it comes in contact with the aggregate particles (Mohajeri *et al.* 2016). Moreover, also the effectiveness of the rejuvenators could be influenced by the temperature at which the bituminous mixture comes out from the plant.

At the light of the discussed aspects, this second part of the PhD. program aimed at comparing seven additives in terms of their ability in mitigating the effects of the presence of RAP in the mix as a function of the production temperature. In particular, the focus of this research was to investigate the effect of the production temperature on bituminous mixtures, especially on those containing a high amount of RAP. Moreover, the effectiveness of seven different additives (coded with the letters A-G) as a function of the mix production temperature was evaluated.

The experimental programme preliminarily included the FTIR analysis on the additives to analyse the differences in their chemical composition. Then, bituminous mixtures containing

no RAP, 50% RAP and 50% RAP with additive were produced in the laboratory at 2 different temperatures: 140 °C or 170 °C. The air voids content (V_m) was measured to investigate the compactability of the mixtures while the Indirect Tensile Stiffness Modulus (*ITSM*) test and Indirect Tensile Strength (*ITS*) were performed to assess the mechanical characteristics. The Cracking Tolerance Index (*CTI*) defined by ASTM D8225-19, 2019 was also calculated from *ITS* test data to estimate the mix brittleness. In order to understand the influence of the mixing temperature and to rank the additives according to their efficacy, two indexes were defined:

- the rejuvenation index (RI), which represents the performance of the additive in minimizing the negative effects due to the presence of RA in the mix;
- the temperature index (TI), which represents the effect of the production temperature decrease from 170 °C to 140 °C.

The analysis of these indexes, calculated for *ITSM*, *ITS* and *CTI*, allowed the identification of the additive with the best performance.

MIX ID	RA CONTENT [% BY WEIGHT]	MIXING TEMPERATURE [°C]	ADDITIVE TYPE
00RA_170	0	170	-
50RA_170	50	170	-
50RA+A_170	50	170	A
50RA+B_170	50	170	B
50RA+C_170	50	170	C
50RA+D_170	50	170	D
50RA+E_170	50	170	E
50RA+F_170	50	170	F
50RA+G_170	50	170	G
00RA_140	0	140	-
50RA_140	50	140	-
50RA+A_140	50	140	A
50RA+B_140	50	140	B
50RA+C_140	50	140	C
50RA+D_140	50	140	D
50RA+E_140	50	140	E
50RA+F_140	50	140	F
50RA+G_140	50	140	G

Table 12 Definition of the codes and composition of the tested mixtures

Chapter 10. Material and specimen preparation

The bituminous mixtures were designed following the Italian specifications for a binder course. In particular, two mixtures were designed: one without RAP (0RAP) and one containing 50% RAP by aggregate weight (50RAP).

Two fractions of coarse limestone (12-16 and 6-12), limestone sand (0-6), filler and two fractions of RAP (0-8 and 8-16) (Fig. 37a-b) were used in this research. Bitumen extraction using trichloroethylene was carried out in order to determine the binder content and the "white curve" gradation of both RAP fractions. The binder contents were 4.8% and 5.1% by RAP weight for the 8-16 RA fraction and the 0-8 RA fraction, respectively. The aged binder extracted from the RAP using trichloroethylene (EN 12697-1) and the rotary evaporator (EN 12697-3) showed $13*10^{-1}$ mm penetration at 25 °C (EN 1426) and 77.1 °C softening point (EN 1427).

(a) **(b)**

Figure 37 - RAP 8-16 (a) and RAP 0-8 (b)

As previously mentioned, the mix design of the aggregates was carried out in order to obtain the gradation of a mix for binder course. Figure 38 shows that the gradation curves of the mixtures with and without RAP were similar and laid within the reference envelope given by the specifications.

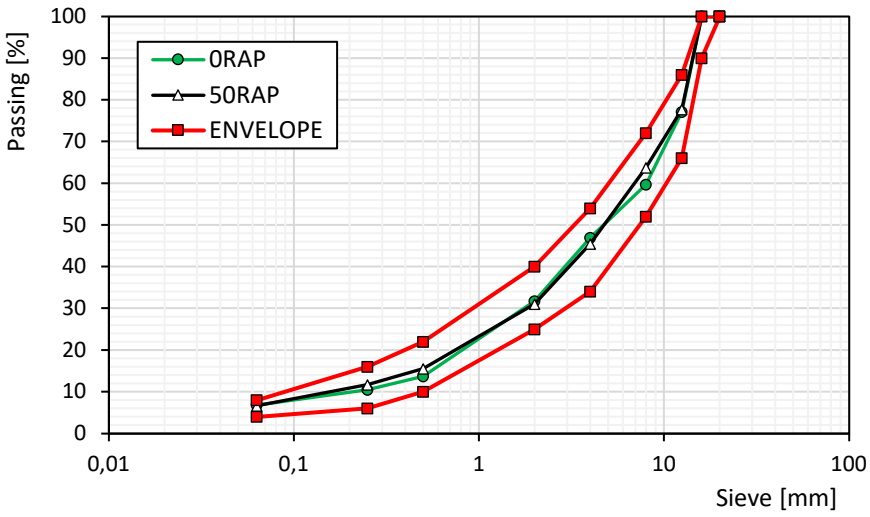

Figure 38 - Aggregate gradation of the mixtures with/without RAP

The binder was a 50/70 pen bitumen obtained as the residue from a visbreaking process, typically used in Italy for the production of bituminous mixtures. Visbreaking (i.e. viscosity breaking) is a relatively mild thermal cracking process operated at 455-510 °C and 0.3-2 MPa for a short residence time (1-3 min), which allows reducing the viscosity of residua without attempting coke formation and significant conversion to distillates (Speight 2012). This detail is significant as the research is part of a wider project in which also a bitumen obtained from a primary refinery process was investigated. For all the samples tested the total binder content fixed was 5.2% with respect to the weight of the mixture.

Seven different additives were used in this study, identified with letters from A to G. According to the classification proposed by Loise et al. (2019), they can be distinguished into:

- softening agents, also called fluidifying agents or rheological rejuvenators, which aim to reduce the viscosity of the aged bitumen by furnishing oily components to maltene. Flux oil, lube stock, slurry oil, belong to this category;
- real rejuvenators, which help to renovate the physical and chemical properties of the aged bitumen by restoring the original complex structure (hierarchical structures of asphaltenes).

The additives used (Fig. 39) in this research are commercialized as rejuvenators, except for additive E, which is declared as softening agent by the producer, and additive D, which is

supposed to contemporary be a rejuvenator and a softening agent. A brief description of the additives is reported hereafter while the physical characteristics are shown in Table 13:

- *Additive A*: it is a mix of different chemicals and consists of modified polyamines and vegetal oils;
- *Additive B*: it consists of a miscible crude tall oil derived from the processing of pine wood in the paper industry, and contains fatty acids, resin acids and unsaponifiable;
- *Additive C*: it is a cationic surfactant based on phosphoric esters dissolved in fatty acid esters and paraffinic oils;
- *Additive D*: it is a cationic surfactant based on phosphoric esters;
- *Additive E*: it consists of a cationic surfactant based on phosphoric esters with a structure characterized by long molecules consisting of a "polar" head and a "non-polar" tail;
- *Additive F*: it is a mineral oil modified with an antioxidant compound;
- *Additive G*: it is a vegetable oil (cashnew oil) modified with an antioxidant compound.

Figure 39 - additives used (Fig. 39) in this research

The additive content was fixed at 6% by RAP binder weight, as this is approximately the value that the manufacturing companies of the different products suggest. The only exception is additive E, whose content was 3% by RAP binder weight (about 1.5% by total bitumen weight) as indicated by the producer for this softening agent.

Among the ways to include the additives in the mixtures (Behnood 2019), two of them were used in this study (Fig. 40). Additives A, C, D, E, F and G were blended for 10 min with the

preheated (1 h) virgin binder, using a mechanical mixer (Fig. 40a). Subsequently, the virgin binder containing the additive was kept in the oven for 1 h before the mixing with the aggregates. Differently, additive B was sprayed on the RAP at room temperature (Fig. 40b). Then, the RAP damped with the additive was placed in the oven together with the other virgin materials to reach the mixing temperature.

(a) **(b)**

Figure 40 - addition and mixing of additives A, C, D, E, F, G in the virgin bitumen (a) - addition of rejuvenator B sprayed directly on the RAP (B)

ID	TYPE	Density @ T = 20 °C [g/cm^3]	Flash point [°C]	Kinematic viscosity @ T = 25 °C [mPa·s]
A	rejuvenator	0.80	> 150	45
B	rejuvenator	0.93	> 295	98
C	rejuvenator	0.95	> 180	53
D	rejuvenator/softening agent	0.96	> 190	150
E	softening agent	0.98	> 180	1020
F	rejuvenator	0.87	> 260	400
G	rejuvenator	0.97	> 240	600

Table 13 - Physical properties of the additives

The laboratory mixing procedure tried to simulate what could occur in the plant. According to EN 12697-35, the aggregates and the RAP have been heated in the oven at 140 °Cor 170 °C for 3 h while the virgin binder has been heated for 2 h. The materials were mixed using a mechanical mixer (Fig. 41a), initially entering only the coarse aggregates and the RAP, adding afterwards the bitumen and, in the end, the filler. The loose bituminous mixtures (Fig. 41b) have been kept in the oven for 30 min to reproduce the hauling time and uniform the temperature within the mix. Then, cylindrical specimens with 100 mm diameter were made using a Superpave gyratory compactor (EN 12697-31) at 100 revolutions (Fig. 41c).

(a) **(b)** **(c)**

Figure 41 - Mixing and compaction procedure

Chapter 11. Test methodology

In order to characterize the chemical composition of the additives, Fourier Transform Infrared Spectroscopy (FTIR) was used (Fig. 42). Infrared spectroscopy measures the infrared light absorbed by bonds in molecules when the infrared light has the same frequency as the vibration frequency of the bonds, enabling identification of chemical functionalities. The infrared spectrum represents the intensity of the spectral peaks, corresponding to the different bonds/functional groups, as a function of the wavenumber. The intensity of the peaks is a function of the concentration of the bonds/functional groups.

The FTIR measurements were performed in a Fourier Transform Infrared Spectrometer in Attenuated Total Reflectance (ATR) mode with a diamond crystal. The spectra were collected in the 4000–600 cm^{-1} wavenumber range with a resolution of 4 cm^{-1} and each final spectrum represented an accumulation of 16 spectra. The FTIR test allows to preliminary identify the chemical components of the additives from the peaks of the functional groups (Noor *et al.* 2020).

Figure 42 - FTIR test equipment

In order to assess the efficacy of the additives as a function of the mixing temperature, the volumetric and mechanical properties were evaluated on 4 specimens for each bituminous mixture.

The air voids content (V_m) was determined according to the EN 12697-8 from the maximum density, calculated on the basis of the aggregate and bitumen contents and densities (EN 12697-5) and the apparent bulk density, evaluated by dimensions (EN 12697-6 using Procedure D).

The Indirect Tensile Stiffness Modulus (*ITSM*) was determined through a non-destructive test according to EN 12697-26 - Annex C. The *ITSM* is the most popular form of non-destructive stress-strain measurement used to evaluate the elastic properties of bituminous mixtures and it is considered a very important performance parameter in pavement design (Cerni *et al.* 2017). The *ITSM* is defined as

$$ITSM = {F \cdot (v + 0{,}27)}/{(z + h)} \quad (11)$$

where F is the peak value of the applied vertical load; z is the amplitude of the horizontal deformation obtained during the load cycle; h is the mean thickness of the test specimen and v is the Poisson's ratio assumed to be 0.35 (Graziani *et al.* 2014). The test was performed in control deformation using the Nottingham Asphalt Tester (NAT – Fig. 43a). The magnitude of the applied force was adjusted by the system during the first ten conditioning pulses such that the specified target-peak transient diametral deformation of 3 μm was achieved. During testing, the rise time, which is the time taken for the applied load to increase from zero to a maximum value, was set at 124 ms. The test was performed after a 3-hour conditioning of the specimen at 20 °C.

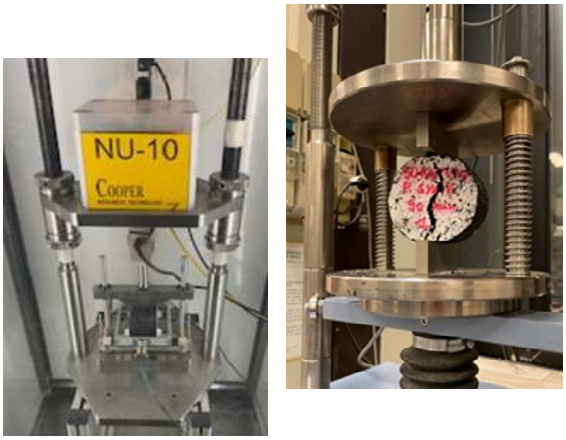

(a) **(b)**

Figure 43 - ITSM (a) and ITS (b) test equipment

In accordance with EN 12697-23, *ITS* (Fig. 43b) tests were carried out at 25 °C by imposing a constant deformation rate through the diametral line load until the force value decreases by 70% compared to the peak value. This type of loading produces a relatively uniform tensile stress acting perpendicularly to the applied load plane, and the specimen usually fails by splitting along with the loaded plane. Based on the maximum load carried by a specimen at failure, the *ITS* is calculated from the following equation:

$$ITS = \frac{2 \cdot F}{\pi \cdot L \cdot D} \quad (12)$$

where F is the peak value of the applied vertical load; L is the mean thickness of the test specimen and D is the specimen diameter.

Through this test, the Cracking Tolerance index (*CTI*) was also calculated for each specimen, according to ASTM D8225-19, 2019, since recent studies (F. Zhou, S. Im, L. Sun 2017) have shown that it is very sensitive to the presence of RA and rejuvenators. In particular, it tends to decrease as the presence of RA increases and to increase when using additives. Thus, the lower the *CTI*, the stiffer and the more brittle the bituminous mixture is.

The plot of the load versus displacement curve from *ITS* test was analysed to determine the *CTI* by the following equation:

$$CTI = \frac{t}{62} \cdot \frac{G_f}{\frac{P}{l}} \cdot \left(\frac{l}{D}\right) \tag{13}$$

where t and D are respectively the mean specimen thickness and diameter; the fracture energy G_f is the work of fracture (the area of the load vs. vertical displacement curve) divided by the area of cracking face ($t \cdot D$); l and P/l are the displacement and the slope of the load-displacement curve when the load is reduced to 75% of the peak.

$$\frac{P}{l} = \left|\frac{P_{85}+P_{65}}{l_{85}+l_{65}}\right| \tag{14}$$

Figure 44 illustrates how this slope is determined from the load-displacement curve.

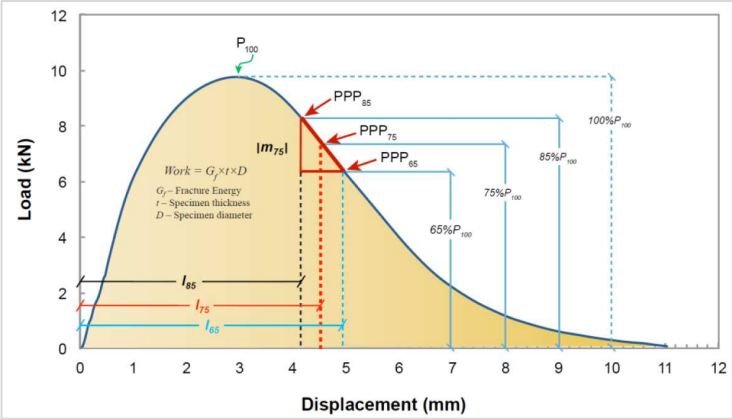

Figure 44 - Definition of the quantities for CTI calculation

To rank the additives, two indexes named Rejuvenation Index (RI) and Temperature Index (TI) were defined. In particular, $RI_{X,Add,Ti}$ is the rejuvenation index in percentage, calculated for the quantity X (average *ITSM*, *ITS* or log*CTI*) for the mix with the additive *Add* (A-G) produced at the temperature T_i (170 °C or 140 °C) and it was calculated as follows:

$$RI_{X,T_i,Add}[\%] = 100 \cdot \left(1 - \frac{X_{T_i,Add} - X_{T_i,0RA}}{X_{T_i,50RA} - X_{T_i,0RA}}\right) \quad (15)$$

where $X_{Ti,Add}$ is the value of the X calculated for the mix with the additive *Add* (A-G) produced at the temperature T_i, $X_{Ti,0RA}$ is the value of the *X* calculated for the mix no RAP produced at the temperature T_i and $X_{Ti,50RA}$ is the value of the *X* calculated for the mix 50%RA and no additives produced at the temperature T_i. The *RI* ranges between 0%, meaning that the additive has no effect and the properties of the mix with the additive are equal to those of the mix with 50% RAP and no additive, and 100%, corresponding to a perfect rejuvenation and analogous mix properties between 00RAP and 50RAP with additive. The temperature index $TI_{X,Mix}$, i.e. the percentage index calculated for the quantity *X* (average *ITSM*, *ITS* or log*CTI*) of the mixture *Mix* (00RAP, 50RAP or 50RAP with the different additives), was calculated through the following equation:

$$TI_{X,Mix}[\%] = 100 \cdot \frac{\left|X_{Mix,170°C} - X_{Mix,140°C}\right|}{X_{ref}} \quad (16)$$

where $X_{Mix,170°C}$ and $X_{Mix,140°C}$ are the values of the X calculated for the mixture *Mix* respectively produced at the temperature 170 °C and 140 °C, while X_{ref} is the reference value adopted for the comparison. Specifically, X_{ref} coincides with $X_{Mix,140°C}$ for *ITSM* and log*CTI*, while for *ITS* it has been assumed a fixed value of 1.06 MPa, corresponding to the intermediate value of the acceptability range provided by national specification.

Chapter 12. Results and discussion

12.1. Chemical characterization of the additives

Figure 45 shows the results from the FTIR analysis. It must be pointed out that in the graph, in order to ensure a better comparison, the additive spectra have been translated on the axis of the ordinates. Even if the ordinate axes do not have a precise scale, this procedure allowed a better evaluation of the peak frequencies and the identification of the analogies between the additives.

In the graph, the spectra of the additives have been positioned according to the similarities in the absorbance bands. On the bottom of the graph, the additive F had a very different spectrum with respect to the other additives. In particular, it is characterized by few bands, which denote the only presence of CH_2 (wavenumber 2920 cm^{-1}) and CH_3 (wavenumber 2950 cm^{-1}). The spectrum also indicated that the polymeric chains are quite short, with 11 or 12 atoms of carbon. Another feature of this spectrum is the absence of the C=O band at the wavenumber of 1742 cm^{-1}.

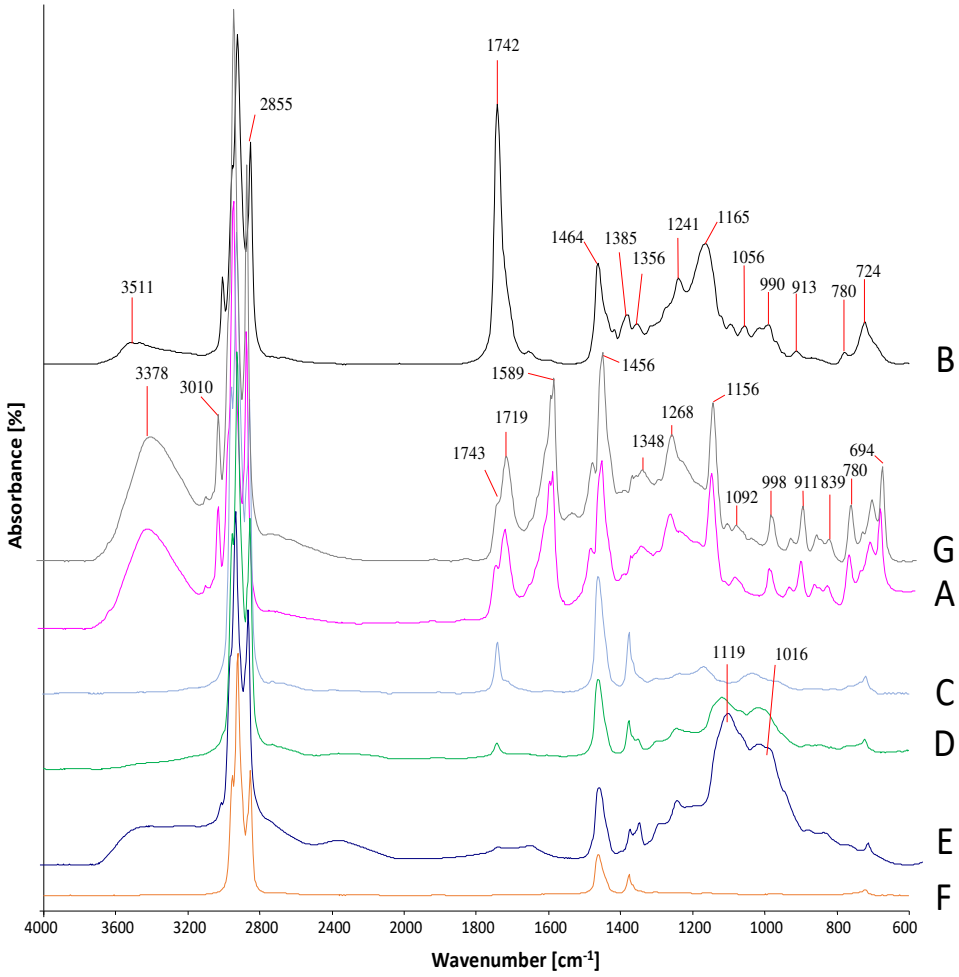

Figure 45 - Absorbance spectra of the additives

Moving upwards, the additive E, which is the only one that is commercialized as a softening agent, also showed a very small C=O band (1742 cm^{-1}), denoting a lower content of esters with respect to the other additives. In addition, differently from the other the additives (except form additive D), it presented large peaks between 1150 and 950 cm^{-1}, denoting a significant siloxane content. The additive C showed a spectrum similar to olefins, with long chains of carbon atoms. Differently from additive E, the peaks at the wavenumbers between 1150 and 950 cm^{-1} are not present (absence of siloxane) but it has a higher peak at 1742 cm^{-1} (C=O

ester band). The additive D presented an intermediate spectrum between additives C and E: the absorbance bands corresponded to the same wavenumbers, but in the areas around 1742 cm^{-1} and 1150-950 cm^{-1} the height was lower respectively than additive C and additive E.

Finally, on the top of the graph, the spectra of additives G, A and B presented many similarities: at the wavenumbers < 1200 cm^{-1} there are many absorbance bands, denoting a higher complexity of the additive chemical structure; in addition, they are characterized by peaks at 3010 cm^{-1} (corresponding to unsaturated compounds) and 1742 cm^{-1} (C=O ester band). This latter, in particular, is very high for additive B. Differently from additive B, additives A and G showed the absorbance bands at 1589 cm^{-1} and 3400 cm^{-1}, respectively corresponding to N–H bends and N-H stretches typical of amines.

12.2. Mechanical tests on the mixtures

Figures 46-49 show the average values of V_m, *ITSM*, *ITS*, and *CTI* measured for the specimens made with or without RAP, for the different additives and at both mixing temperatures (140 °C and 170 °C). The column height in the histograms represents the average of the values obtained for the tested specimens. Moreover, in order to ensure statistical validity, even data dispersion bars have been plotted. The lower and upper limits of these bars are respectively the minimum and maximum values obtained from that specific mixture.

Figure 46 highlights that the increase of the mixing temperature led to a reduction of the air voids content in the specimens, except for the mix including additive D. All the mixes were able to meet the Italian specifications (acceptability range of V_m is 3% - 6%), except for those including additive E, which showed an air voids content lower than the minimum. This result is consistent because E is a softening agent and its purpose is precisely to increase the workability and compactability of the bituminous mixture even at lower temperatures.

Figure 47 clearly shows the impact of the mixing temperature on the mix stiffness. Indeed, for all the tested mixes, the higher the temperature, the higher the *ITSM*. Moreover, for both mixing temperatures, the specimens including 50% RAP and no additive achieved the highest stiffness moduli (approximately 16000 MPa for the mixing temperature of 170 °C, about 12000 MPa for the mixing temperature of 140 °C), while the specimens containing no RAP had the lowest (approximately 7000 MPa for the mixing temperature of 170 °C, about 5500 MPa for the mixing temperature of 140 °C). The average *ITSM* of the mixtures including the additives was intermediate between that of 0RA mix and that of 50RAP mix.

When comparing the effectiveness of the different additives, it can be noted that additive E showed the lowest stiffness reduction with respect to 50RAP mix (particularly for the mixing temperature of 170 °C), confirming that the softening agent had low effect on the RAP rejuvenation and mix stiffness properties. However, it has to be considered that the additive content in this mix was a half with respect the others. For the mixing temperature of 170 °C, additives A, B, C, D, F and G showed a good effectiveness, especially additive G, which allowed the highest *ITSM* reduction to be achieved. For the mixing temperature of 140 °C,

specimens including additives A, B or G showed a higher performance (average *ITSM* lower than 9000 MPa) while the efficacy of additives C, D, E and F was slightly lower (average *ITSM* of about 9300-10100 MPa).

A similar outcome can be observed for *ITS*. Figure 48 shows that the *ITS* values were influenced by the mixing temperature: except for additive D, the higher the temperature, the higher the strength. The specimens including 50% RAP and no additive achieved the highest *ITS* values (respectively 2.1 MPa and 2.0 MPa for the mixing temperatures of 170 °C and 140 °C), while the specimens containing no RA had the lowest (approximately 1.45 MPa for the mixing temperature of 170 °C, about 1.20 MPa for the mixing temperature of 140 °C). All the mixes including an additive showed a reduction of the *ITS* with respect to 50RA mix. However, no one of the additives allowed complying with the Italian Specifications (ANAS 2016) in terms of *ITS* (acceptability range of 0.72 – 1.40 MPa) neither at 140 °C nor at 170 °C of mixing temperature. Even the mixture 0RA had an average *ITS* value greater than the maximum for the mixing temperature of 170 °C. Among the different additives, C, F and G showed a good effectiveness at both the mixing temperatures of 170 °C and 140 °C (ITS < 1.60 MPa for T = 170 °C, ITS < 1.50 MPa for T = 140 °C); B and D allowed a significant reduction of *ITS* to be achieved, but only for one mixing temperature (respectively 140 °C and 170 °C). Finally, the performance of additives A and E was fair, with *ITS* values of about 1.70 MPa at the mixing temperature of 140 °C and higher than 1.80 MPa at the mixing temperature of 170 °C.

Figure 49 shows the value of cracking tolerance index (*CTI*) for the different mixtures. It can be immediately noted that the increase of the mixing temperature from 140 °C to 170 °C determined a decrease of *CTI*, denoting a more brittle behaviour of the material. This result agrees with the scientific literature, which states that the higher the mixing temperature, the more severe is the short-term aging for the bitumen (Priyadharshini *et al.* 2013, Sarnowski *et al.* 2019). Therefore, temperature is a key factor in the production of bituminous mixtures, also when RAP is used, in order to avoid an excessive brittleness for the mixtures in service. Among the different mixes, the 00RAP achieved the highest *CTI* average values (about 75 and 90 respectively for the mixing temperatures of 170 °C and 140 °C), while the lowest were obtained for the mix including 50% RA and no additive (about 8 and 20 respectively for the mixing temperatures of 170 °C and 140 °C). All the additives were able to increase the *CTI* with respect to 50RAP mix. Additives B and G allowed the greatest increase (average *CTI* > 35 for the mixing temperatures of 170 °C, average *CTI* > 25 for the mixing temperatures of 140 °C). For the mixing temperatures of 170 °C additives A and E had the lowest performance (average *CTI* of about 15), while for the mixing temperatures of 140 °C additives A, C, D, E and F showed a similar *CTI* (approximately 30). At the light of the present results, *CTI* proved to be a useful and reliable parameter for the characterization of the bituminous mixtures with a high RAP content and for the evaluation of the rejuvenating efficacy of an additive, in particular if considering that it can be quickly and simply determined from *ITS* test data.

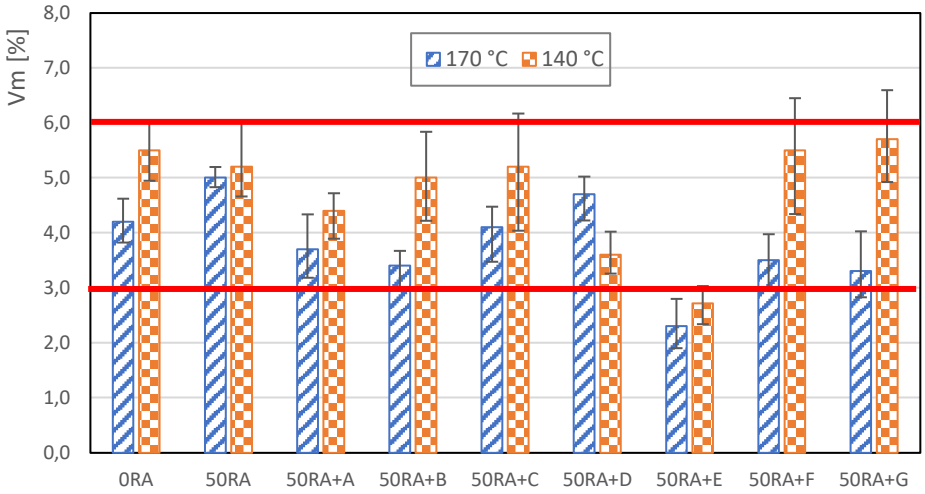

Figure 46 - Air voids contents of the mixtures for the different production temperatures

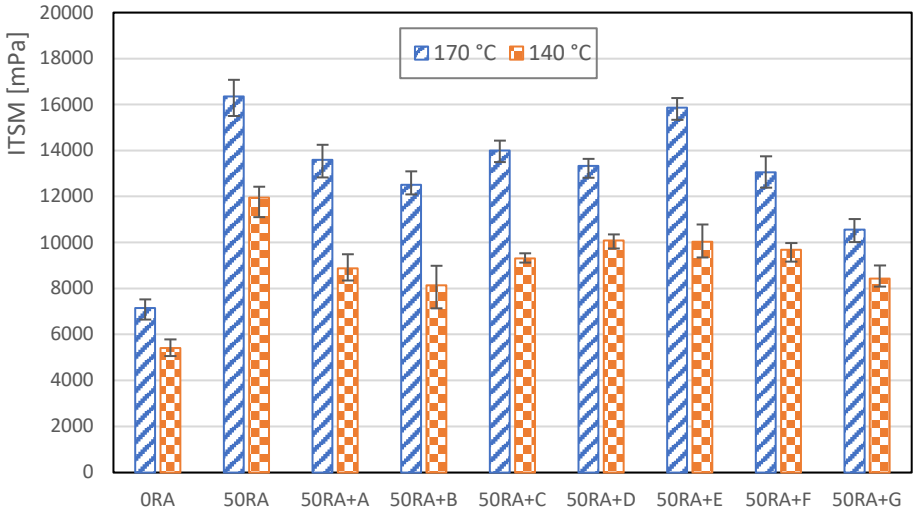

Figure 47 - Indirect tensile stiffness moduli of the mixtures for the different production temperatures

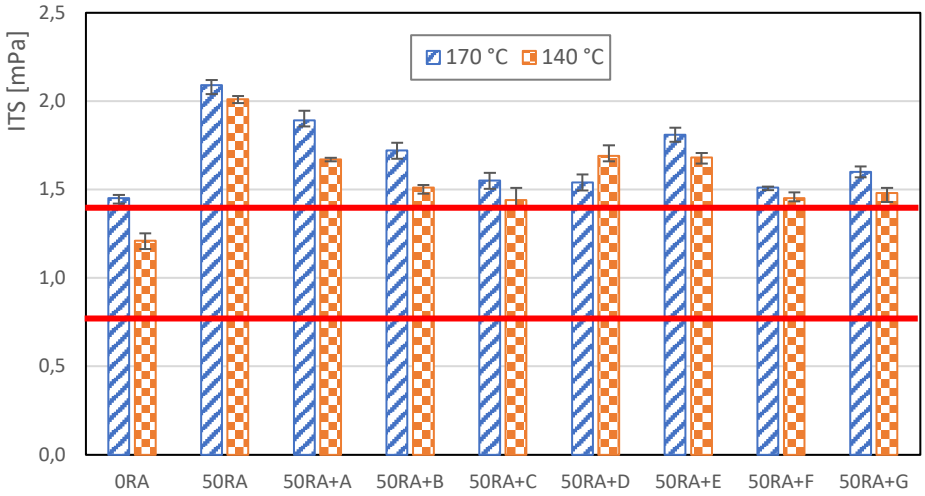

Figure 48 - Indirect tensile strengths of the mixtures for the different production temperatures

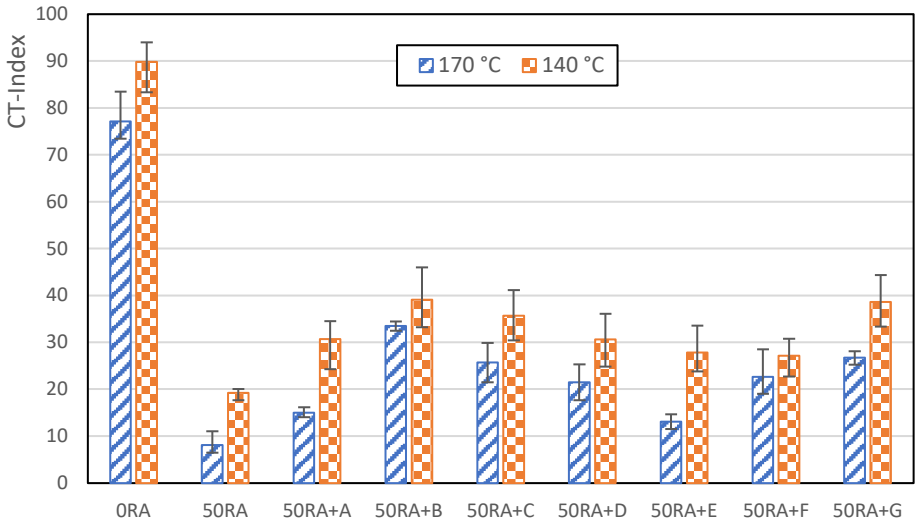

Figure 49 - Cracking tolerance indexes of the mixtures for the different production temperatures

12.3. Evaluation of Rejuvenation Index and Temperature Index

Table 14 shows the values of the rejuvenation index (*RI*) calculated for the different quantities *ITSM*, *ITS* and log*CTI* (considered in their average values) at the two mixing temperatures, for a total of 6 data per mix.

For each mixture, the average of the *RI* values and the standard deviation are reported in the table, in order to identify the additive with the best global performance. In addition, the *RI* values are plotted in a radar chart (Figure 50) to have visual feedback on the rejuvenating effect of the different additives. The higher the *RI* values, the wider the areas in the radar chart, the closer the behaviour to 00RAP mix. Vice versa, the lower the *RI*, the smaller the areas in the radar chart, the closer the behaviour to 50RAP mix.

From the results it can be observed that mixture including additive G showed the highest average *RI* (approximately 60%), denoting a good efficacy of the rejuvenation process (mechanical behaviour closer to that of the reference mix without RAP). In particular, the 50RA+G mix allowed high values of *RI* (> 45%) to be obtained for all the parameters at both the mixing temperatures, as also indicated by the low standard deviation and the regular shape of the hexagon in the radar chart.

In the ranking, the mixtures including additives B, C and F showed good *RI* average values (approximately between 50% and 55%): the 50RAP+B mix had a performance similar to 50RAP+G (this can probably be a consequence of the similar spectra observed in the FTIR analysis), but it showed lower *RI* values for *ITSM* and *ITS* at the mixing temperature of 170 °C; the 50RAP+C and 50RAP+F mixes were excellent in reducing *ITS* at both the mixing temperatures, but had a low influence on *ITSM* and *CTI*, which can also be observed by the high standard deviations.

The mixture including additive D had an average *RI* of 43.5%. The shape of the area in the radar chart was similar to those of 50RAP+C and 50RAP+F mixtures for the mixing temperature of 170 °C, but the additive D did not allow the same rejuvenating performance to be obtained for the mixing temperature of 140 °C, for which the *RI* values were lower.

Finally, the mixtures including additives A and E showed the lowest performance, with average *RI* respectively of about 35% and 27%, and single *RI* values always lower than 50%.

Additive	Mixing temperature = 170 °C			Mixing temperature = 140 °C			Average *RI* [%]	Standard Deviation
	RI_{ITSM} [%]	RI_{ITS} [%]	RI_{CTI} [%]	RI_{ITSM} [%]	RI_{ITS} [%]	RI_{CTI} [%]		
A	30.0	31.3	27.3	47.0	42.5	30.4	34.8	8.0
B	41.8	57.8	63.0	58.4	62.5	46.1	54.9	8.9
C	25.6	84.4	51.2	40.5	71.3	40.2	52.2	21.9
D	32.8	85.9	43.3	28.6	40.0	30.2	43.5	21.6
E	5.4	43.8	21.3	29.5	41.3	24.0	27.5	14.1
F	36.0	90.6	45.5	34.8	70.0	22.3	49.9	25.5
G	63.0	76.6	52.9	53.9	66.3	45.3	59.7	11.2

Table 14 - RI values of the mixtures including the different additives

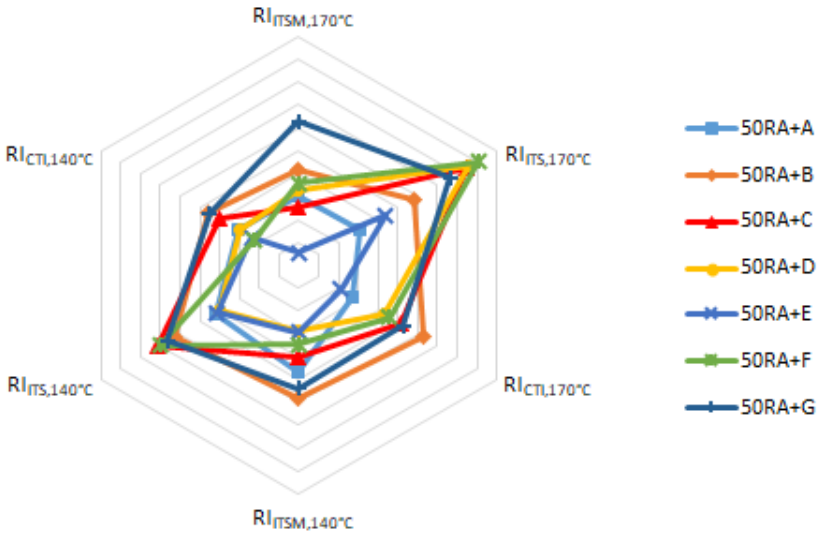

Figure 50 - Radar chart of the RI values

Table 15 shows the values of the temperature index (*TI*) calculated for the different quantities *ITSM*, *ITS* and log*CTI* (considered in their average values) of each mixture, including the reference 00RAP and 50RAP mixes. The average of the *TI* values and the standard deviation are also reported. In addition, the *TI* average values are plotted Figure 51. The parameter *TI* represents the effect on the mix properties of the mixing temperature reduction from 170 °C

to 140 °C: the lower *TI*, the more similar is the behaviour at the mixing temperatures of 170 °C and 140 °C.

From the results it can be noted that the mix without RAP had an average *TI* of about 20%. This was due to the more severe aging that the virgin bitumen in the mix experienced at 170 °C. The mix with 50% RAP and no additive showed a higher average *TI* (approximately 25%) with respect to the mix without RAP. This was probably related to the mobilization of a higher amount of aged bitumen from RA when increasing mixing temperature.

When analysing the *TI* of the mixture including the additives, the 00RAP and 50RAP mix were considered as a reference (broken lines are reported in Figure 40 in correspondence of the *TI* of 00RAP and 50RAP). The comparison with 50RAP mix, in particular, it allows discriminating if the different behaviour for the two mixing temperatures is effectively related to the presence of the additive. Through this interpretation, it can be noted that the mixes containing the additives A and E had a higher average *TI* than 50RAP mix (about 31%). For the additive E, this can be related to the fact that the softening agent reduced binder stiffness and viscosity at low mixing temperatures but could not rejuvenate the higher amount of RAP binder which was mobilized during mixing at 170 °C. However, it must also be considered that the dosage of additive E was half with respect to the other additives. For the additive A, the high *TI* can probably be explained with an excessive evaporation. In fact, the flash point of the additive A was rather low (Table 13) and it could have been partly lost during mixing at 170 °C.

Mixture	TI_{ITSM}	TI_{ITS}	TI_{CTI}	Average *TI*	Standard Deviation
00RAP	32.2	22.6	3.4	19.4	14.7
50RAP	36.8	7.5	29.2	24.5	15.2
50RAP+A	53.1	20.8	20.9	31.6	18.7
50RAP+B	53.9	19.8	4.2	26.0	25.4
50RAP+C	50.5	10.4	9.2	23.3	23.5
50RAP+D	32.3	14.2	10.3	18.9	11.7
50RAP+E	58.2	12.3	22.6	31.0	24.1
50RAP+F	34.9	5.7	5.5	15.3	16.9
50RAP+G	25.3	11.3	10.1	15.6	8.5

Table 15 - TI values of the different mixtures

The mixtures including additives B and C had an average *TI* comparable to that of 50RAP mix, indicating that the additives have a similar effect at both 140 °C and 170 °C. This result suggests that, when a higher amount of RAP bitumen is mobilized as a consequence of the higher mixing temperature, the dosage of the additive should be increased.

Finally, the mixtures including additive D and, especially, additives F and G had the lowest *TI* values, with averages (respectively 18.9%, 15.3% and 15.6% in the case of additive D, F

or G) that were even lower than for the 00RAP mix. In particular, the 50RAP+F and 50RAP+G mixes showed an excellent performance at high mixing temperature probably because of the effect of their antioxidant compound, which limited the oxidation of the binder, especially of the virgin unaged bitumen.

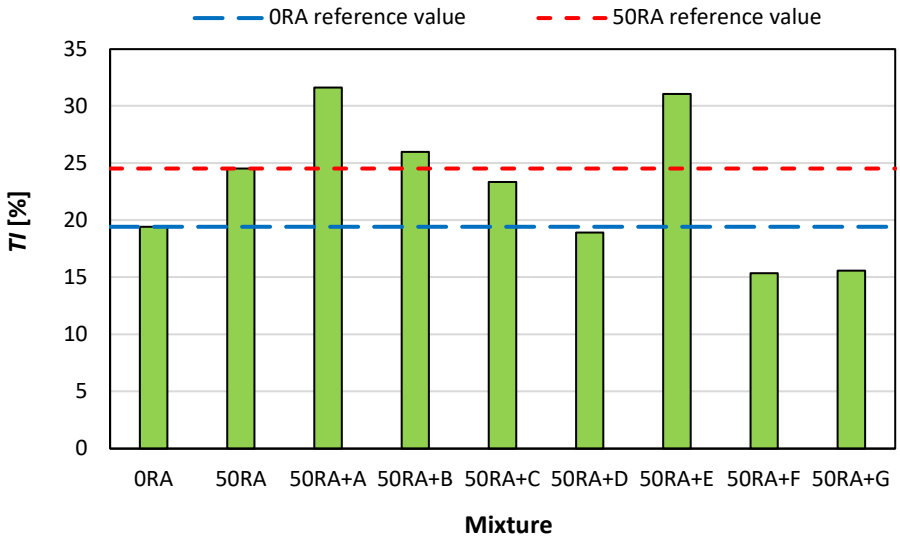

Figure 51 - Comparison of the average TI values

12.4. Discussion

In the following bulleted list, the additive behaviours are summarized, and the different products are ranked according to their average RI:

- Additive A - ranking position #6: the additive, characterized by the presence of esters, unsaturated compounds and amines, did not have a great efficacy in terms of *ITSM* and *ITS* reduction and *CTI* increase in the mix. Moreover, it was highly sensitive to the mixing temperature (lower performance at 170 °C), probably related to evaporation issues;
- Additive B - ranking position #2: the additive, characterized by a complex chemical structure where the noticeable content of esters stands out, was very effective in mitigating the effects related to the presence of 50%RA in the mix. In particular, the mix including additive B provided high values of *RI* for all the quantities at both the investigated mixing temperatures;
- Additive C - ranking position #3: the additive, characterized by long chains of carbon atoms and the presence of esters, allowed a high reduction of the mix *ITS* to

be obtained, in particular at the mixing temperature of 170 °C, but had a lower influence on the *ITSM* and *CTI* of the mix;

- Additive D - ranking position #5: the additive, characterized by a chemical structure comparable to additive C but including siloxane, allowed the mix to noticeable decrease the *ITS* for the mixing temperature of 170 °C, but was not as effective on the other properties;
- Additive E - ranking position #7: the additive, characterized by a significant siloxane content and the absence of esters, is the only that is declared as softening agent by the producer. In confirmation of this, the results showed that it allowed increasing the mix workability but had almost no rejuvenating effect;
- Additive F - ranking position #3: the additive, characterized by the only presence of CH_2 and CH_3 peaks in the FTIR spectrum, showed a behaviour comparable to additive C, with an important decrease of the mix *ITS* but a lower effect on *ITSM* and *CTI*;
- Additive G - ranking position #1: the additive, characterized by a chemical structure similar to additive A, with the presence of esters, unsaturated compounds and amines, allowed the best performance to be achieved. In particular, the mix including additive G showed high *RI* values for all the quantities and the mixing temperatures.

On the basis of the chemical analysis and result interpretation, it can be recognized that there is a kind of correlation between the performance of the additives and the presence of the ester band (C=O) in the FTIR spectrum. In fact, the additives in the highest position of the ranking (B, C, and G) were characterized by a marked peak at the wavenumber of 1742 cm^{-1}, in particular additive B. In the case of additive G, the ester band was shorter than for additive B, but the better rejuvenating behaviour can be justified by the antioxidant effect (not identifiable in the FTIR spectrum) that the product had, as proved by the temperature index values, which were lower than for the reference mix without RA. In support this assumption, the additive F, also including the antioxidant but not presenting the ester absorbance band in the FTIR spectrum, was effective at the mixing temperature of 170 °C, when oxidation was more severe, but did not show the same performance at the mixing temperature of 140 °C. Another key factor for the additives to achieve a good rejuvenation is avoiding its evaporation during mix production. This was probably the case of additive A, which has a similar chemistry than additive G but positioned on the bottom of the ranking. The simple evaluation of the Flash point can provide a quick indication if an additive presents a risk of evaporation. Finally, the different spectrum of additive E, which the results demonstrated to be a softening agent and not a rejuvenator, opens to the possibility of distinguishing between the two classed of additives through FTIR analysis. In fact, additive D, which is declared to be both a rejuvenator and a softening agent, presented blended chemical characteristics. Of course, this will have to be validated with a wider experimental campaign involving a large number of products.

Chapter 13. Conclusions

The present part of the PhD. program aims at evaluating the mechanical properties of bituminous mixtures including hot-recycled RAP as a function of the production temperature and ranking the rejuvenating effect of seven different additives.

The results obtained from the laboratory tests showed that the mixture containing 50% RAP had a higher stiffness and strength with respect to the mix produced with only virgin materials. The reduction of the mixing temperature from 170 °C to 140 °C determined an increase of the air voids content (approximately 1%) but also allowed a significant decrease of mix stiffness and strength with a contemporary increase of ductility. This was a consequence of the less severe short-term aging achieved on the virgin and RAP bitumen but it was likely due also to the mobilization of a lower amount of RAP binder.

The seven additives investigated in this research showed, in most cases, different chemical structures, which reflected in their rejuvenating performance. The effectiveness of the additives was assessed by measuring the *ITS* of the mixtures, as provided my Italian Specifications. In addition, the experimental program also included the determination of the *ITSM* and the *CTI*, which proved to be useful and reliable indicators to evaluate the effects of RAP rejuvenation and the variation of mixing temperature.

To make a ranking, a Rejuvenation Index *RI*, ranging from 0% (same performance of the mix with 50% of RAP and no additive) to 100% (same performance of the mix without RAP), was defined. Moreover, a Temperature Index *TI* was also introduced to represent the effect of the mixing temperature reduction and have a clearer understanding of the additive behaviour. This approach, based on simple and quick tests (i.e. *ITS* and *ITSM* tests), allowed the identification of the additives with the best rejuvenating performance (additives B, C, F and G) with a good accuracy and reliability.

In addition, the comparative analysis of the results from mechanical and chemical tests provided remarkable information about the characteristic properties of a good rejuvenator, particularly the presence of esters and the high flash point. The FTIR analysis also allowed to clearly distinguish between the chemistry of the softening agent and that of the other additives, encouraging to extend the investigation on more products in order to validate the method for additive classification.

In conclusion, the research showed that a high mixing temperature results in a stiff and brittle bituminous mixture, which can go out from the specification requirements even when no RAP is used. However, the mixing temperature of 140 °C has been identified by Ragni et al. (2019) as a lower limit for hot recycling technique, as below this temperature workability and compactability problems can occur and warm additives are needed.

Part III: Differences between a real-rejuvenator and a softening agent on HRMA fatigue performance

Chapter 14. Introduction and experimental program

One of the main issues in using RAP for the production of new asphalt pavement is related to the reduction of its fatigue resistance (Zhang, Ren, *et al.* 2019). Several studies have recently been carried out (Golchin and Mansourian 2017) trying to investigate this aspect. For example, some year ago, Vukosavljevic stated that fatigue life of field mixture decreased with the addition of RAP, in fact, adding 30% RAP significantly decreased the fatigue resistance (Vukosavljevic 2006). Trying to evaluate the fatigue performance of asphalt containing RAP using viscoelastic continuum damare (VECD) methos, even Norouzi et al conclude that the use of high amount of recycled material decreased the fatigue resistance (Norouzi *et al.* 2014). A year later, Mannan et al, showed that fatigue life of asphalt mixtures containing 35% RAP was lower than that of virgin asphalt mixtures (Mannan *et al.* 2015a). Contrary to what just said, Mangiafico et al measured the fatigue life of mixtures containing different amount of RAP (0, 20, 40 and 60%) and concluded that there was an optimum RAP content (20-40%) that increased the fatigue resistance of HRMA (Mangiafico *et al.* 2014). Even Tabakovic et al showed that asphalt mixtures containing up to 30% RAP improved the fatigue life of HMA as compared to the mixtures containing no RAP (Tabaković *et al.* 2010). Moreover, some years later, Ajideh et al evaluated the fatigue life of HRMA with 50% of RAP using scanning laser detection (SLD) technology and stated that specimens with 50% RAP exhibited equal or better fatigue performance compared to those with the control mix under the controlled-stress testing (Ajideh *et al.* 2013). Measuring the fatigue life of HMA containing different amount of RAP (0, 15, 25, 40%), Basueny et al. concluded that no general trend was observed between the amount of RAP and the number of cycles to reach fatigue failure. In addition, they highlighted that high fatigue resistance was observed when 40% of RAP is used (Basueny *et al.* 2016). Therefore, as can be seen, the influence of RAP in fatigue resistance is still uncertain and many studies will have to be carried out to have a more complete and clearer picture.

Moreover, as pointed out in previous chapters, according to different authors (Tabatabaee and Kurth 2017a, Loise *et al.* 2019, De Bock *et al.* 2020), rejuvenators can be classified, based on the effect, in softening agents (also called fluidifying agents or rheological rejuvenators), and real rejuvenators or compatibilizers, which help to renovate the physical and chemical characteristics of the bitumen through the disruption of the intermolecular associations between the asphaltenes.

In this context, this part of the experimental program aims to study the effect of RAP on fatigue performance of HRMA also analyzing any differences if a real rejuvenator or a softening agent is used. To achieve this goal two of the additives exposed in the previous part (E: softening agent and G: real rejuvenator) were used fixing the percentage of RAP (50%), the type of virgin bitumen (vis-breaking) and the production temperature (170 ° C).

Chapter 15. Material, specimen preparation and test methodology

The asphalt mixtures were designed following the Italian specifications for a binder course. In particular, two mixtures were designed: one without RAP (00RAP) and one containing 50% RAP by aggregate weight (50RAP), while the additives used were E and G. The additive content was fixed at 6% by RAP binder weight for both additives, following to the indications provided by the producers. The mix gradation (Fig. 38) and the bitumen content were the same as described in Chapter 10.

The laboratory mixing procedure follows the EN 12697-35. In particular, the aggregates and the RAP have been heated in the oven at 170 °C for 3 h while the virgin binder has been heated for 1 h. The materials were mixed using a mechanical mixer, initially entering only the coarse aggregates and the RAP, adding afterwards the bitumen and, in the end, the filler. Finally, the loose bituminous mixtures have been kept in the oven for 30 min. At the end of this time, cylindrical specimens with 100 mm diameter were made using a Superpave gyratory compactor (EN 12697-31) fixing the height of each specimen in order to obtain samples having an air voids content around 4%.

The Indirect Tensile Stiffness Modulus (ITSM) was used to firstly obtain the stiffness modulus of the mixtures, and the same procedure explained in Chapter 11 was followed.

In order to evaluate the fatigue performance, ITFT test were performed. The ITFT characterises the fatigue behaviour of bituminous mixtures under controlled load test conditions. The method main characteristic is that the force applied on the tested specimen is a constant load pulse that generates a steady (constant) horizontal stress in the specimen, thus letting the resulting strain increase as the asphalt mixture specimen fails through fatigue damage. Repeated applications of the vertical force will usually result in a crack along the vertical diameter; in stress control mode, failure corresponds with the fracture in two halves of the specimen. Fatigue life is usually determined as the number of load applications that cause the complete fracture of the asphalt specimen. The test parameters for the fatigue tests are:

- Test temperature: 20 °C;
- Poisson's ratio: 0.35
- Loading time: 0.1 s;
- Rest time: 0.4 s;
- Failure indication: 10 mm vertical deformation.

The maximum tensile stress σ_{max} (MPa) and the maximum tensile strain in the centre of the specimen ε_{max} (με) are:

$$\sigma_{max} = \frac{2P}{\pi * t * d} \quad (17)$$

$$\varepsilon_{max} = \left(\frac{2*\Delta H}{D}\right) * \left(\frac{1+3v}{4+\pi*v-\pi}\right) \quad (18)$$

Where P is the maximum load applied (N); t is the specimen thickness (40 mm); D is the specimen diameter (100 mm); ν is the Poisson's ratio (0.35); ΔH is the horizontal deformation (mm).

Nine specimens for each mixture were tested and the ε_0 vs N° cycles and σ vs N° cycles curves were drawn, where ε_0 is the horizontal strain after the first 100 cycles.

Chapter 16. Results and discussion

With regard to the specimens compaction, the number of revolutions required to reach the specified height were noted. Figure 52 shows the number of gyrations applied to each mixture. From the graph it can be observed that the number of gyrations was always lower than 120, denoting a good mix compactability for all the materials. In addition, it can be noted a little increase in workability when RAP is used. Moreover, as expected, the addition of a softening agent significantly reduced the number of gyrations required, synonym of a good increase in compactability.

When comparing the stiffness of the various mixtures (Figure 53), it can be noted that the lower ITSM values were obviously obtained from the virgin blend, while the higher ones from the specimens containing 50% of RAP without additives. The softening agent was unable to significantly lower the stiffness, while the real rejuvenator succeeded in part, but without getting close to the values of the virgin mixture. Probably to achieve ITSM values comparable to the mixtures produced without RAP, a higher dosage of rejuvenator was required.

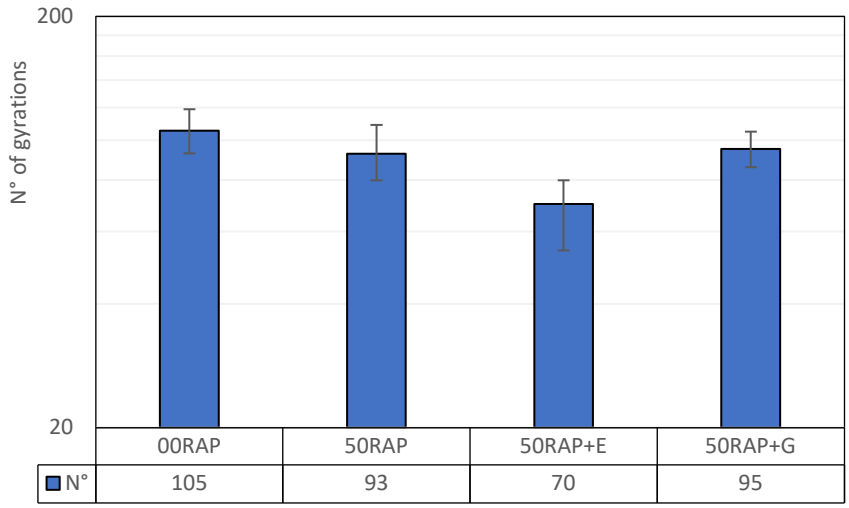

Figure 52 - Number of gyrations applied to each mixture

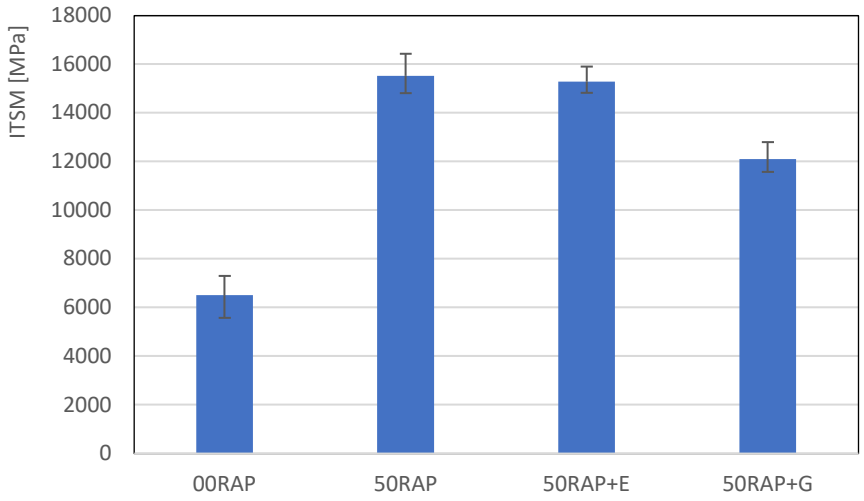

Figure 53 - ITSM values of the different mixtures

Two ways for drawing fatigue curves from the ITFT data were used, plotting the failure number of cycles as a function either of the applied horizontal stress or the horizontal strain after 100 cycles. According to the method of representation, the experimental data seem to provide conflicting deductions.

Considering the horizontal deformation versus the number of cycles graph (Figure 54), it was observed that the addition of RAP implied a downwards shift of the fatigue curve, denoting that, fixing a horizontal deformation, the fatigue performance decreased when RAP is used. By adding the softening agent, no particular changes are noticed, while, using the real rejuvenator, the fatigue performance of asphalt tended to get closer to that of the virgin mixture, but without reaching them.

Analysing the horizontal stress versus the number of cycles graph (Figure 55), it can be seen how the addition of RAP caused a shift of the fatigue curve up and to the right side, leading to observe that, fixing the same cyclic stress applied, the RAP led to an increase in fatigue performance. Moreover, on the one hand, by adding the real rejuvenator it was possible to notice a shift of the fatigue curve towards that obtained from the mixtures produced with no recycled material, symptom that such additive was really effective in the rejuvenation of the RAP aged bitumen. On the other hand, using the softening agent, a further upward and rightward shift was noted, sign of how such additive had not been able to produce any rejuvenating effect on the recycled mixture.

ITFT @20°C						
	00RAP			***50RAP***		
SAMPLE	ε_0	*σ [kPa]*	*N° cycles*	ε_0	*σ [kPa]*	*N° cycles*
1	216	700	7500	127	800	25206
2	188	600	8636	140	900	19046
3	244	700	3566	95	600	127000
4	150	500	32526	113	700	58166
5	188	600	10286	104	700	85296
6	187	600	10686	126	800	39096
7	150	500	55076	122	800	40346
8	228	700	4000	129	800	33386
9	130	500	68866	133	900	20056

Table 16 - ITFT data of the mixtures with no additives

ITFT @20°C						
	50RAP+E			***50RAP+G***		
SAMPLE	ε_0	*σ [kPa]*	*N° cycles*	ε_0	*σ [kPa]*	*N° cycles*
1	132	900	20106	187	800	5996
2	117	800	52056	131	600	31926
3	97	700	166500	170	700	10686
4	96	700	133500	141	600	28556
5	109	800	52606	175	800	6266
6	108	800	56866	166	700	11036
7	127	900	27136	136	600	33326
8	96	700	133500	188	800	6416
9	133	900	24156	115	600	85556

Table 17 - ITFT data of the mixtures with additives

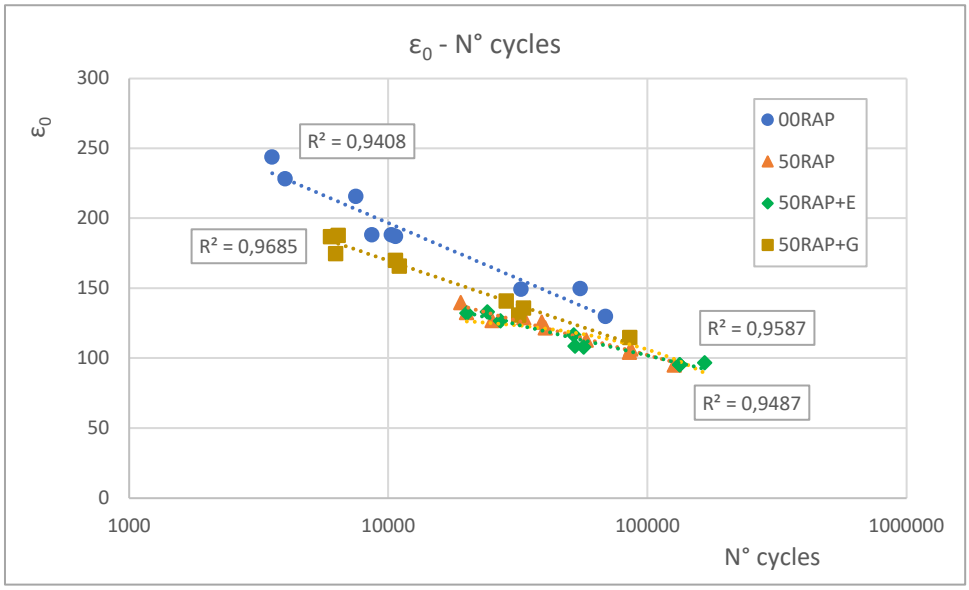

Figure 54 – Initial horizontal strain vs number of cycles chart

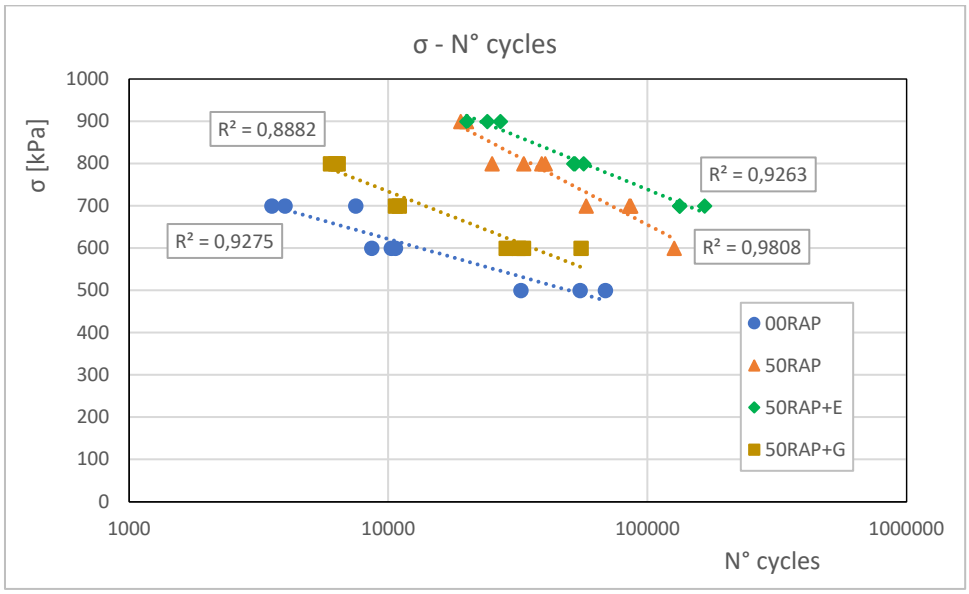

Figure 55 - Stress vs number of cycles chart

Chapter 17. Conclusions

The present part of the PhD. program aims at evaluating the fatigue performance of bituminous mixtures including high amount RAP as a function of the type of the additives used. For this purpose, two RAP content (0 and 50%) and two additives (a real rejuvenator and a softening agent) were chosen and ITFT tests were performed after analysing the workability and the indirect tensile stiffness modulus of the mixture.

In the light of what has been stated in the previous chapters we can conclude that:

- analyzing the number of revolutions needed to reach the air void content equal to 4%, the mixture containing 50% of RAP with the softening agent achieved the greatest workability. Slightly lower was the workability of the blends containing recycled material with no additives and with the real rejuvenator, while the lowest workability resulted from the mixture of virgin materials only.
- Comparing the stiffness of the various mixtures, it can be noted that the lower ITSM values were obviously obtained from the virgin mixture, while the higher ones from the specimens containing 50% of RAP without additives. The softening agent was unable to significantly lower the stiffness, while the real rejuvenator succeeded in part, but without getting close to the values of the virgin mixture. Probably to achieve ITSM values comparable to the mixtures produced without RAP, a higher dosage of rejuvenator was required.
- As regards the results of the fatigue tests, considering the horizontal deformation versus the number of cycles graph, it was observed that the addition of RAP decreased the fatigue resistance and, only the real rejuvenator was able to bring the fatigue curve close to that of the virgin mixture. On the contrary, analysing the horizontal stress versus the number of cycles graph, the addition of RAP caused an increase in fatigue performance. Moreover, by adding the real rejuvenator it was possible to notice a shift of the fatigue curve towards that obtained from the mixtures produced with no recycled material. Finally, using the softening agent, it was found that such additive had not been able to produce any effect on the recycled mixture.

Finally, given the difference in the results depending on the type of graph analysed, it can be stated that the ITFT test was not able to fully represent and investigate the effects of RAP and rejuvenators in the fatigue performance of HRMA. Since fatigue resistance is one of the main issues to be faced when RAP is used, it is essential to use a suitable test to fully understand how the recycled material affects such performance. It will be the subject of future studies to perform further fatigue tests using different test methodologies such as fatigue tests in traction-compression mode to be processed with the Simplified Viscoelastic Continuum Damage Model (S-VECD model) developed by Underwood e al. (Underwood *et al.* 2012).

Part IV: Influence of the virgin bitumen type, the production temperature and the loose mixtures time spent in the oven after the mixing phase on the mechanical and performance characteristics of HRMA

Chapter 18. Introduction and experimental program

As said in the previous sections, in order to produce HMA with high amounts of RAP, the use of a rejuvenator is needed. The main purpose is to restore the properties of the aged asphalt binder to levels comparable to those of the virgin one [8].

As well as the type and content of the rejuvenators (Zaumanis, Mallick, Poulikakos, *et al.* 2014, Bocci *et al.* 2017), the mechanical properties of the HRMA depend on other factors such as the amount of RAP (Kamil Arshad *et al.* 2018); the content, type and aging degree of the bitumen contained into the RAP (Ozer *et al.* 2009, Reyes-Ortiz *et al.* 2012, De Lira *et al.* 2015); the degree of binder activation and blending (Lo Presti *et al.* 2020); the RAP heating procedure during HRMA production (Bocci, Prosperi, Mair, *et al.* 2020, Ma *et al.* 2020) and the type of the virgin bitumen used (neat or polymer-modified, soft binders) (Tarsi *et al.* 2020). However, two further variables influence the performance of HRMA but that is often neglected or underestimated: the virgin bitumen production process and the HRMA manufacturing temperature. Regarding the type of virgin binder used, a recent study shows that virgin bitumens having the same Performance Grade (PG) but obtained from different oil sources will not always lead to mixtures that perform the same (Mogawer *et al.* 2020). Moreover, together with the oil source (that can hardly be managed even by the refineries), also the type of distillation process to which the crude oil is subjected can influence the characteristics of the final mixture. During the distillation, the various phases of the crude oil are separated due to the difference in its boiling and condensing temperatures (Paliukaitė *et al.* 2014). A typical distillation process involves a first step in which the lighter components are separated, subjecting the crude oil to a temperature of about 350 °C at atmospheric pressure. The residue of the first step is subjected to a higher temperature, around 350-425 °C, under a controlled pressure ranging from 1 kPa to 10 kPa. The residue of the second process is called straight-run bitumen (Giavarini 1981). Moreover, if the residue of this second process is subjected to another step of thermal distillation at temperatures between 455 °C and 510 °C, visbreaker bitumen is produced (Speight 2012). Vis-breaking allows refineries to reduce the amount of the residue produced, as it allows the further recovery of lighter products such as diesel and gas. This penalizes the quality of the bitumen that is obtained, which is more rigid, brittle and susceptible to aging (Giavarini and Saporito 1989). Some years ago, Giavarini (Giavarini 1984) studied visbreaker (VB) and straight-run (SR) bitumens obtained from the same crude oil. He repeated tests such as penetration and softening immediately and after 1 year, during which all bitumens were subjected to the same treatment (i.e. controlled heating to simulate aging) and stored under the same conditions in the laboratory. He found out that the effect of aging was much more pronounced for the VB. In particular, starting from average penetration values of 175 dmm and 155 dmm for the SR and VB bitumen respectively, the average penetration decrease for the VB binder was more than 90 dmm, against about 40 dmm for the SR. Moreover, the penetration index, which was

originally about the same for both kinds of bitumen, became appreciably lower for the VB, indicating that the characteristics of VB products change significantly during storage.

Summarizing, the products derived from visbreaking show higher temperature susceptibility, lower oxidation resistance and more rapid changes in properties. Considering the amount of VB bitumens that are marketed in Europe, more detailed and recent information is needed on the differences between such binders and straight-run ones, and on the correlations between the severity of the visbreaking process and the stability of the bitumen. Very often, pavement technologists distinguish bitumen only by penetration index or PG, without considering the distillation process from which it derives, which greatly affects the characteristics of HMA and its aging.

Lastly, temperature plays an essential role in bitumen aging, as it can accelerate chemical modifications (Hofko, Cannone Falchetto, *et al.* 2017). For this reason, it is fundamental to avoid bitumen overheating, which means containing the temperatures during HMA manufacturing. In particular, this can cause a more severe short-term aging for both virgin and RAP binders (Lolly *et al.* 2017), leading to stiffer and excessively brittle mixtures. In the HMA plants, the virgin aggregates are often overheated, as a function of the target mix temperature, the RAP content and the temperature and humidity of the RAP when it is introduced into the mix. The stronger the aggregate overheating is, the more severe is the thermal shock for the bitumen when it meets the aggregate particles. Moreover, also the effectiveness of the rejuvenators can be influenced by the temperature at which the HRMA is produced. On the other hand, a low mix temperature can result in poor workability and therefore in a high air voids content, reflecting on a higher risk of moisture damage, raveling, rutting and cracking (Khan *et al.* 2013b).

Therefore, with the aim to deeper investigate the above highlighted variables that influence the mechanical and performance characteristics of HRMA, two of the seven additives, studied in the previous section, were analysed.

In particular, the main goal of this part of the PhD program was to evaluate the evolution of the volumetric (Air Voids content), mechanical (ITS and ITSM tests), chemical (FTIR test) and rheological (master curves) properties of HRMA changing the type of rejuvenator (coded with the letters A and B), the origin of the virgin bitumen (Visbreaker and Straight-run SR), the pre-heating and mixing temperature (140-170 °C) and a heating time of the loose mixture after mixing growing from 30 to 180 minutes. Mixtures made using 50% of RAP are produced together with reference virgin HMA manufactured without recycling materials. The different mixtures were identified using the following characters:

XRAP(**+*R***)**_B_T_t**

Where X is the percentage of RAP (0-50%), R is the rejuvenator used (A-B), B is the origin of the virgin bitumen (VB-SR), T is the pre-heating and mixing temperature (140-170°C) and t is the heating time of the loose mixture (30, 90, 180 min).

It should be pointed out that for the evaluation of the rheological properties (master curves), only specimens compacted after 30 min were produced and tested.

Chapter 19. Material and sample preparation

The bituminous mixtures were designed following the Italian specifications for a binder course. In particular, two mixtures were designed: one without RAP (00RAP) and one containing 50% RAP by aggregate weight (50RAP), while the additives used were A and B. The additive content was fixed at 6% and 9% by RAP binder weight respectively for rejuvenators A and B, according to the indications provided by the producers. The mix gradation (Figure 38) and the bitumen content were the same as described in Chapter 10.

The laboratory mixing procedure follows the EN 12697-35. In particular, the aggregates and the RAP have been heated in the oven at 140 °C or 170 °C for 3 h while the virgin binder has been heated for 1 h. The materials were mixed using a mechanical mixer, initially entering only the coarse aggregates and the RAP, adding afterwards the bitumen and, in the end, the filler. Finally, the loose bituminous mixtures have been kept in the oven for different times (30, 90 and 180 min). At the end of each time, cylindrical specimens with 100 mm diameter were made using a Superpave gyratory compactor (EN 12697-31) fixing the height of each specimen in order to obtain samples having an air voids content around 4%.

With regard to the specimens compacted after 30 min, the number of revolutions required to reach the specified height were noted. Figure 56 shows the number of gyrations applied to each specimen, were 1 and 2 represent two samples produced for each mixture. From the graph it can be observed that the number of gyrations was always lower than 120, denoting a good mix compactability for all the materials, even for high RAP contents and low mixing temperatures. In addition, it can be noted that the decrease of the mix temperature from 170 °C to 140 °C did not largely affect the compactability. Indeed, the mixtures with VB showed a lower number of gyrations for the mixing temperature of 170 °C, while the mixtures with SR resulted slightly more compactable at 140 °C. In general, it was observed that the presence of RAP determined an increase in the number of gyrations, due to the higher binder viscosity and thus lower compactability, while the use of rejuvenators allowed the number of gyrations to be decreased.

In order to obtain the specimens for the dynamic modulus test, the following procedure was used. When cooled to room temperature, the specimens were cored to a diameter of 75 mm. Then, the thickness of 15 mm was cut from the top and the bottom of the cylinders. Each face was leveled using a two-component resin in order to obtain a final eight about 120 mm and a perfectly smooth plane for testing. Finally, 3 pairs of strikers were glued on the lateral surface of the specimens in order to fix the linear variable displacement transformers (LVDT). The steps of the specimen preparation are shown in Figure 57.

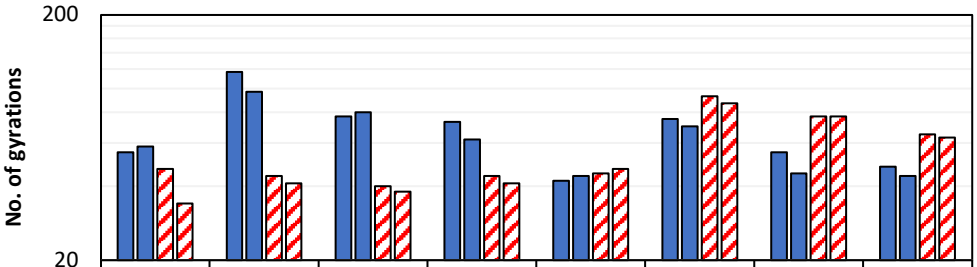

	00RAP_VB	50RAP_VB	50RAP+A_VB	50RAP+B_VB	00RAP_SR	50RAP_SR	50RAP+A_SR	50RAP+B_SR
140 °C_1	55	117	77	73	42	75	55	48
140 °C_2	58	97	80	62	44	70	45	44
170 °C_1	47	44	40	44	45	93	77	65
170 °C_2	34	41	38	41	47	87	77	63

Figure 56 - Number of gyrations applied to each specimen

Figure 57 - Preparation of the specimen for the dynamic modulus test

Chapter 20. Test methodology

Regarding the traditional tests (ITS, ITSM) and the calculation of the CT-index, the procedures were the same of those followed in the previous part of the Phd Program (Chapter 11). Moreover, in order to provide a statistical validation to the results of the tests performed, the test results were also subjected to one-way (influence of time) and two-way (influence of temperature and type of the bitumen) analysis of variance (ANOVA) at a 0.05 significance level (Avsenik *et al.* 2016, Khodadadi *et al.* 2020).

For what concern the dynamic modulus test, the complex modulus E^* of the specimens was measured through uniaxial cyclic compression tests. A servo-hydraulic universal testing machine (UTM-30) was used. The load cell was used to monitor axial stress, while the axial strain was measured on the middle part of the specimen (measuring base of 70 mm) using three LVDT placed 120° apart. A haversine compression loading was applied to obtain a target vertical strain amplitude of 50 microstrain ($50 \cdot 10^{-6}$ mm/mm). Four temperatures (5 °C, 20 °C, 35 °C and 50 °C) and eight frequencies (ranging between 0.1 and 20 Hz) were tested. Two samples of each mixture were tested.

In order to fit the E^* data, the 2S2P1D rheological model was used (Olard and Di Benedetto 2003a). The model consists of a series of a linear dashpot, two parabolic elements and a spring of stiffness E_∞ - E_0, assembled in parallel with a second spring (E_0) (Figure 58). The mathematical representation of the model can be described by the following expression:

$$E^*(i\omega t) = E_0 + \frac{E_\infty - E_0}{1+\delta(i\omega\tau)^{-k}+(i\omega\tau)^{-h}+(i\omega\beta\tau)^{-1}} \quad (19)$$

where ω is the frequency, k and h are the parabolic element constants ($0 < k < h < 1$), E_0 is the static modulus when $\omega \to 0$, E_∞ is the glassy modulus when $\omega \to \infty$, δ is a dimensionless shape factor, β is a parameter proportional to the dashpot viscosity η ($\eta = G_\infty \cdot \beta \cdot \tau$), I the unit imaginary number and τ is characteristic time. Based on the time-temperature superposition principle (TTSP), τ can be determined as in Equation (20):

$$\tau(T) = a_T \cdot \tau_0 \quad (20)$$

where a_T is the shift factor at the temperature T and $\tau_0 = \tau(T_0)$ is the characteristic time at the reference temperature T_0 (equal to 20 °C).

In order to fit this model with the experimental data, the application of the TTSP is required. This principle states that the same rheological characteristics can be obtained at different temperatures by multiplying frequencies with a shift factor. This latter was defined using the William, Landel and Ferry (WLF) equation (Williams *et al.* 1955):

$$\log(a_T) = \frac{-C_1 * (T - T_0)}{(C_2 + T - T_0)} \quad (21)$$

where C_1 and C_2 are constants, T is the temperature, and T_0 is the reference temperature.

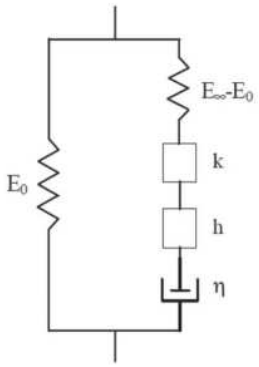

Figure 58 - 2S2P1D model (Olard and Di Benedetto 2003a)

Figure 59 highlights the correlation between the 2S2P1D model parameters and the shape of the master curve in the Cole-Cole plot: the static (E_0) and glassy (E_∞) shear moduli represent the intersection with the axis ($\phi = 0$), k and h are proportional to the angles that the curve generates with the real axis and δ defines the height of the pinnacle point (Carpani *et al.* 2021).

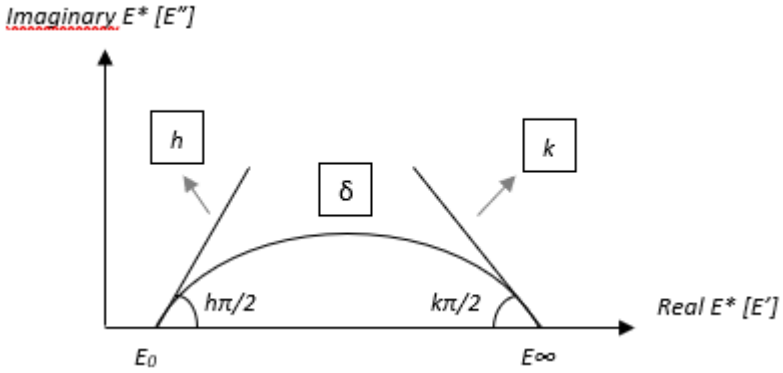

Figure 59 - Definition of the 2S2P1D parameters

With the aim to obtain the 2S2P1D constants, the superposition of the experimental data to the model was achieved by minimizing the following sum of errors for each measured temperature and frequency:

$$Error = \left(\frac{|E^*|_c - |E^*|_m}{|E^*|_c}\right)^2 + \left(\frac{\phi_c - \phi_m}{\phi_c}\right)^2 \quad (22)$$

where $|E^*|_c$ and $|E^*|_m$ are respectively the calculated and measured norm of the complex modulus and ϕ_c and ϕ_m are respectively the calculated and measured phase angles.

Identical values of h, k, δ, β and τ_0 were assumed for the two specimens of the same mixtures as they are commonly associated with the properties of the binder phase, thus exhibit a small sample-to-sample variability (Graziani *et al.* 2019).

During the last years, Glover–Rowe (*G-R*) parameter has been used to evaluate the stiffness and relaxation characteristics of bitumen and correlated to the field performance of asphalt pavements (Rowe *et al.* 2014, Menapace *et al.* 2018, Kleiziene *et al.* 2019). This index is calculated from the values of $|G^*|$ and ϕ at the temperature of 15 °C and the angular frequency of 0.005 rad/s. Ogbo et al. (Ogbo *et al.* 2019) proposed to use the mixture-based G-R parameter to assess the intermediate-temperature cracking resistance of the mixtures directly from the Black Space (ϕ vs $|E^*|$) data. Different from the binders, the temperature/frequency combination that is pointed out in the original *G-R* formulation (15 °C and 0.005 rad/s, i.e. 0.0008 Hz) was considered unsuitable for the mixtures. In fact, E^* is not directly measured at these temperatures and frequencies. Moreover, this combination is located in the high temperature/low-frequency part of the phase angle master curve, where the aggregate skeleton has a great influence on the rheological behavior. For these reasons, mixture-based G-R parameter was formulated according to Equation 5:

$$G\text{-}R = |E^*| \frac{(\cos \phi)^2}{\sin \phi} \tag{23}$$

where $|E^*|$ and ϕ are the norm and phase angle of the complex modulus measured at 20 °C and 5 Hz.

At the end of the mechanical test, FTIR test on bitumen extracted from different type of mixture were carried out. Infrared spectroscopy measures the infrared light absorbed by bonds in molecules when the infrared light has the same frequency as the vibration frequency of the bonds, enabling identification of chemical functionalities. The FTIR measurements were performed in a Fourier Transform Infrared Spectrometer in Attenuated Total Reflectance (ATR) mode with a diamond crystal. The spectra were collected in the 4000–600 cm^{-1} wavenumber range with a resolution of 4 cm^{-1} and each final spectrum represented an accumulation of 16 spectra. In order to evaluate the effect of the time spent in the oven, all the bitumen extracted from the mixtures made using the vis-breaking binder at 170 °C were analyzed. Moreover, to evaluate the influence of the bitumen type and the mixing temperature, the spectra of the HRMA made either at 170 ° C or 140 °C after 30 minutes of re-heating were compared. With the aim to quantify the effects of bitumen oxidation, two indices have been introduced:

- Carbonyl index: $I_{C=O} = \frac{A_{1690}}{Aref}$
- Sulphoxide index: $I_{S=O} = \frac{A_{1030}}{Aref}$

where A_{1690} is the area of the C=O peak centered at 1690 cm-1, A_{1030} is the area of the S=O peak centered at centered at 1030 cm-1 and A_{ref} is the area of the reference ethylene and methyl peaks, respectively centered at 1460 and 1375 cm-1 (Dony *et al.* 2017). When increasing the aging, the heights and the areas of the peaks in correspondence of the wave numbers of 1690 cm^{-1} and 1030 cm^{-1} increase, so even the two indices increase (Nivitha *et al.* 2015, Mikhailenko *et al.* 2016b, Gabrielle do Nascimiento Camargo *et al.* 2020, Yan *et al.* 2020). Moreover, a recent study (Poulikakos *et al.* 2019) proposed the Chemical Aging Index (CAI), calculated as $I_{C=O}$ plus $I_{S=O}$, in order to better understand the variation of both indices during aging.

Chapter 21. Result and discussion

21.1. Mechanical tests on the mixtures

Figures 56 highlight the influence of the heating time of the loose mixtures depending on the RAP content and the type of rejuvenator. In particular, independently from mix type (with or without RAP/rejuvenator), bitumen origin (VB or SR) and mixing temperature (140 °C or 170 °C), increasing the time spent in the oven, the ITS and ITSM increases, while the CT-Index decreases. Moreover, increasing the temperature to 170 °C seemed to amplify this effect of time, in fact, the slope of the lines of the mixtures made at 170 °C (Figures 60b, 60d) were higher than those made at 140 °C (Figures 60a, 60c).

Figures 61 are drawn with the aim to investigate the effect of both the type of the virgin bitumen and the pre-heating temperature. The mixing temperature influenced the mix properties, in particular, the mixtures made at 170 °C (dotted lines) achieved higher ITS and ITSM and lower CT-Index values with respect to the ones manufactured at 140 °C (solid lines). Moreover, since the slope of the purple lines (straight-run) appeared to be lower with respect to the blue ones (vis-breaking), using a straight-run bitumen seemed to reduce the effect of the heating time of the loose mixtures.

The experimental data obtained were analysed using both one and two-way ANOVA test in order to statistically validate the conclusions just drawn. Table 18-19 summarizes the ANOVA tests performed. In particular, Table 18 shows that the mechanical properties (ITSM, ITS and CT-index) statistically varied (significance < 0.05) when increasing the conditioning time in the oven, independently from mix type (with or without RAP/rejuvenator), bitumen origin (VB or SR) and mixing temperature (140 °C or 170 °C). Moreover, through the two-factor ANOVA test, it was possible to evaluate the influence of both the temperature and the bitumen.

Two parameters, called bitumen and T factor, are introduced in Table 19, and represent respectively the statistical significance of the mixing temperature and the bitumen type. For the mixtures with 50% RAP, both the bitumen type and the mixing temperature influence the mix properties (ITSM, ITS and CT-index) with a level of confidence of 95% (significance < 0.05). The mixtures with no RAP conditioned for 30 min showed statistically comparable (significance > 0.05) values of ITSM independently from bitumen type and mixing temperature. ITS and CT-index were influence by the bitumen origin (significance < 0.05) but not by mixing temperature (significance > 0.05). When the conditioning in the oven was prolonged to 90 min or 180 min, both bitumen type and mixing temperature influenced (significance < 0.05) the mechanical properties of the mixes without RAP.

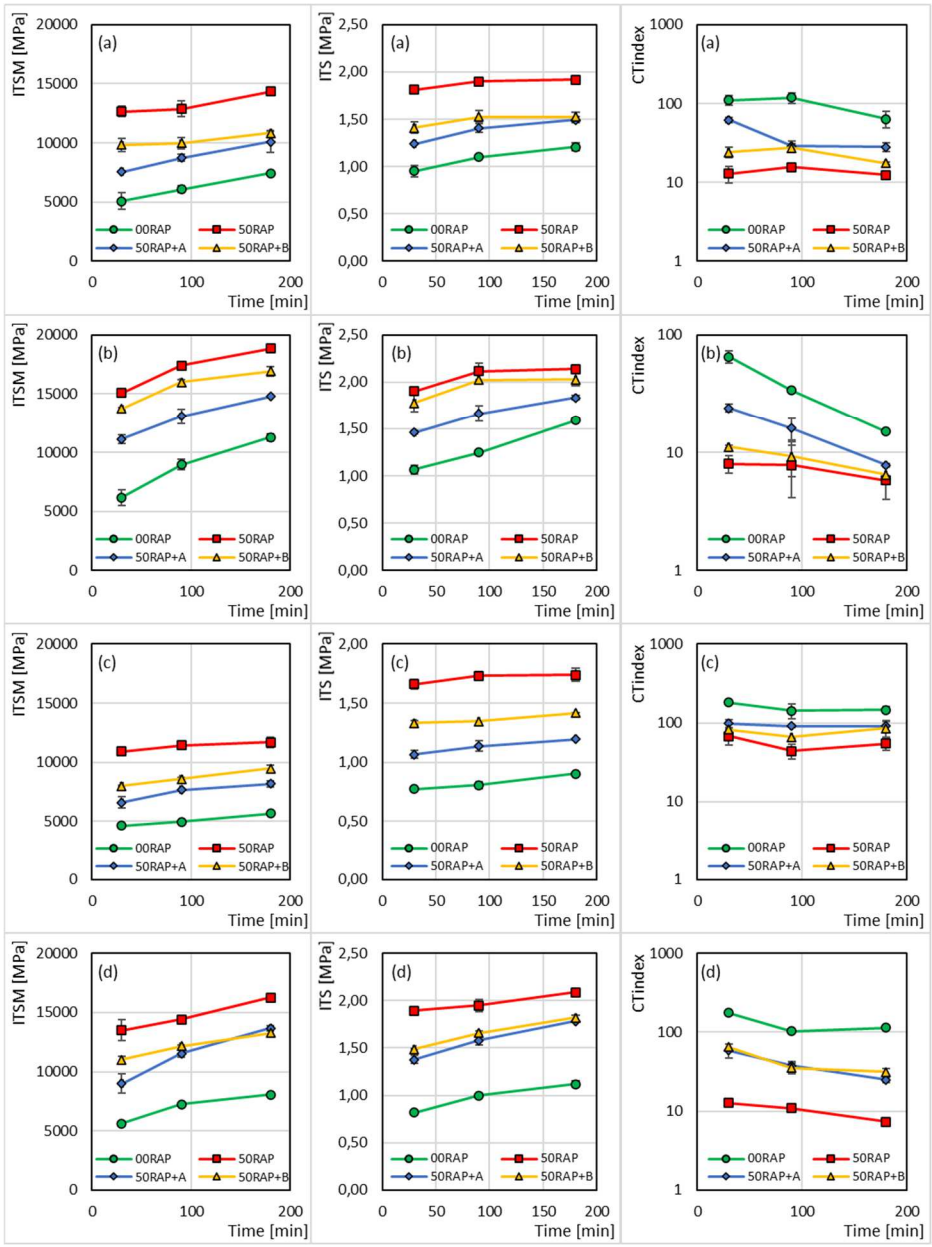

Figure 60 - Effect of the heating time changing RAP percentage and rejuvenator type: (a) VB, 140 °C; (b) VB, 170 °C; (c) SR, 140 °C; (d) SR, 170 °C.

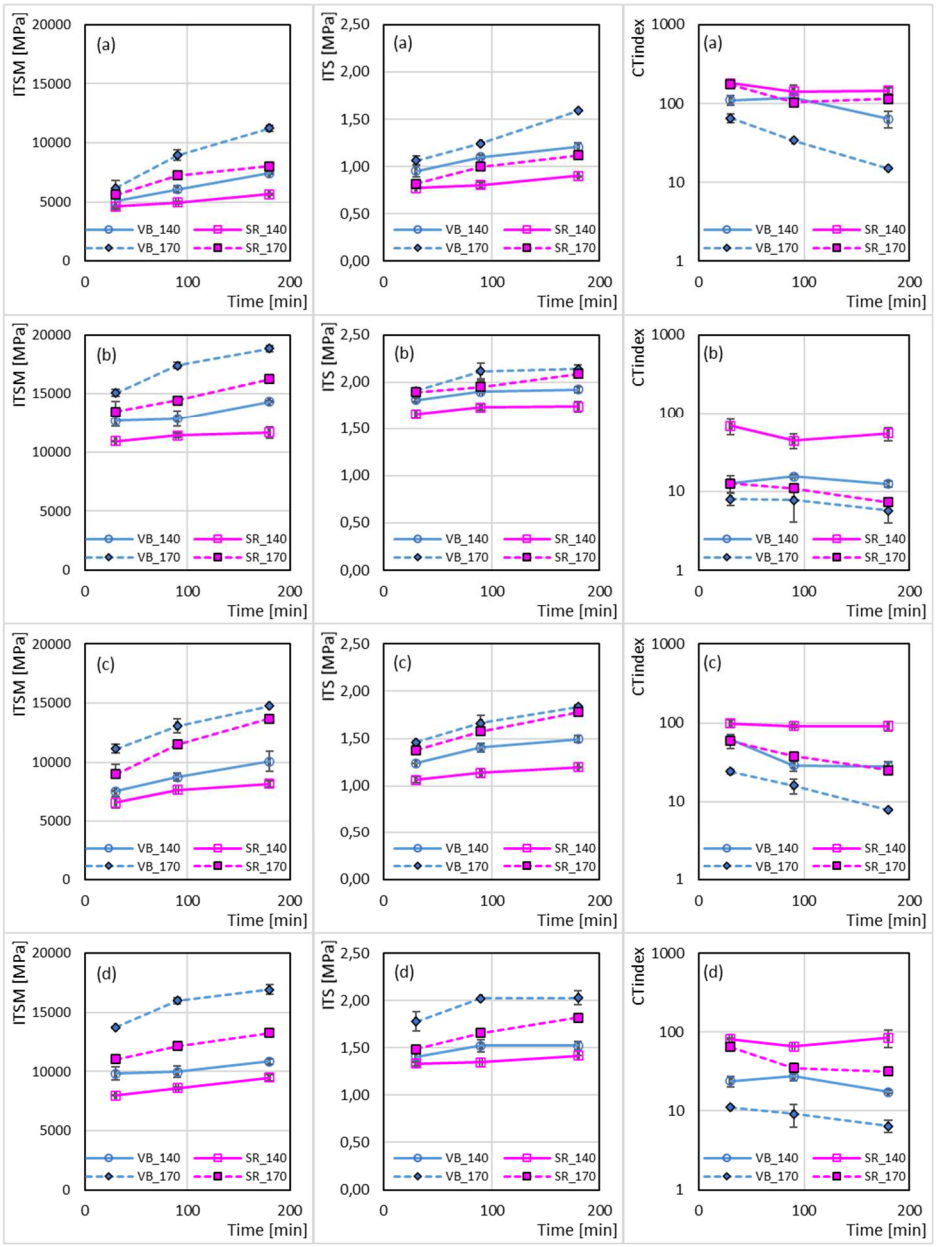

Figure 61 - Effect of the heating time changing type of the virgin bitumen and the pre-heating temperature: (a) 00RAP; (b) 50RAP; (c) 50RAP+A; (d) 50RAP+B

	ITSM	ITS	CT-index
30 min vs 90 min	0,00001	0,00001	0,0003
90 min vs 180 min	0,0005	0,001	0,0308

Table 18 - Result of the one-way ANOVA test to evaluate the statistical significance of the influence of the time spent in the oven of the loose mixtures.

	ITSM		ITS		CT-index	
	Bitumen factor	*T factor*	*Bitumen factor*	*T factor*	*Bitumen factor*	*T factor*
00RAP-30	0,3474	0,0947	0,0049	0,1041	0,0010	0,0688
00RAP-90	0,0074	0,0008	0,0003	0,0020	0,0583	0,0251
00RAP-180	0,0001	0,0001	0,0001	0,0004	0,0008	0,0157
50RAP-30	0,0331	0,0087	0,0479	0,0046	0,0196	0,0193
50RAP-90	0,0048	0,0006	0,0406	0,0182	0,0341	0,0150
50RAP-180	0,0008	0,0001	0,0344	0,0016	0,0318	0,0842
50RAP+A-30	0,0405	0,0045	0,0107	0,0007	0,0156	0,0123
50RAP+A-90	0,0240	0,0004	0,0363	0,0036	0,0006	0,0015
50RAP+A-180	0,0300	0,0004	0,0013	0,0001	0,0045	0,0035
50RAP+B-30	0,0017	0,0003	0,0361	0,0115	0,0001	0,0106
50RAP+B-90	0,0008	0,0001	0,0014	0,0003	0,0009	0,0026
50RAP+B-180	0,0011	0,0001	0,0221	0,0005	0,0240	0,0345

Table 19 - Result of the two-way ANOVA test to evaluate the statistical significance of the influence of the mixing temperature and the type of the bitumen.

21.2. Evaluation of the FTIR test results

Figure 64 depicts the influence of the re-heating time of the loose mixtures while figure 65 draws the influence of the mixing temperature and the bitumen type on the FTIR spectra.

However, to have a deeper understanding of how these variables affect the chemical composition of HRMA figures 62-63 are required. Moreover, figure 63 highlights the effect of the re-heating time on the evolution of the sum of the Ico and Iso indexes. What can be seen is that the high temperature exposure time clearly increased the sum of the indices, and,

for each time, the addition of RAP led to a substantial increase in this sum. Furthermore, both rejuvenators were unable to lower that parameter at all.

Regarding the effects of the production temperature and the type of the virgin bitumen, it was decided to evaluate not the sum but the individual indices separately because, while to evaluate the effect of the re-heating time the sum of the parameters was very representative, changing temperature and type of bitumen can result in a simultaneous growth of a parameter and a decrease in other one. For this reason, in this case, evaluating both indices separately were considered more appropriate. As results in figure 63, in the mixtures made with RAP, the carbonyl index seems to increase with increasing temperature and using an SR bitumen, while where no recycled material is added, Ico increases with the temperature but decreases by using SR bitumen. Moreover, the sulphoxide index always decreases with temperature while the use of SR bitumen seems to decrease it when there is no RAP and increase it when recycled materials are included.

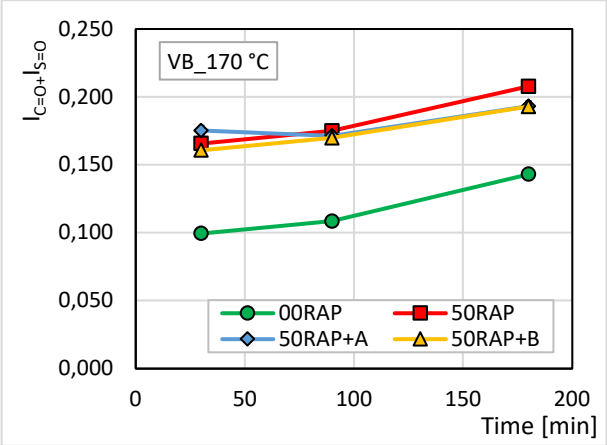

Figure 62 - Influence of the re-heating time on the sum of the Ico and Iso parameters

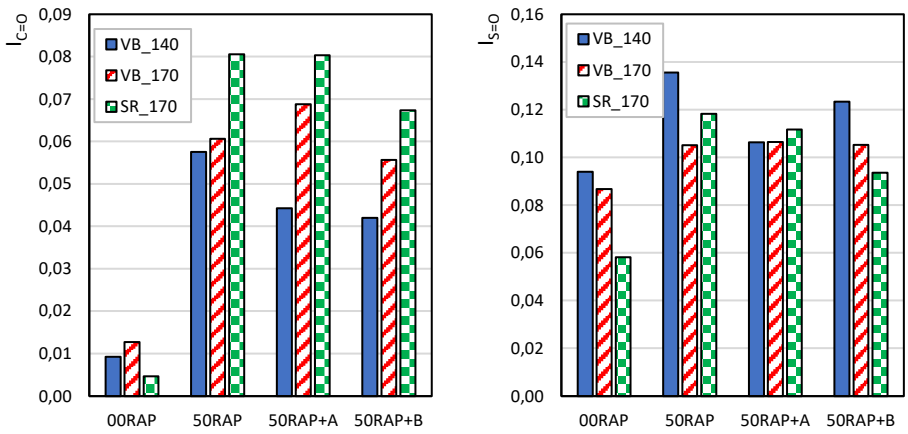

Figure 63 - Influence of the mixing temperature and the type of the virgin bitumen on the Ico and Iso parameters

From the figure 60-61 it can be seen that additives display new bands on the FTIR spectra. In particular, despite both rejuvenators display the band at 1740 cm^{-1} additive B has it much more evident. This evidence can be easily explained since, as can be seen from figure 45, it has a spectrum with this very pronounced band. Moreover, rejuvenator A causes the formation of bands at 3511 cm^{-1} typical of the amines contained therein.

Therefore, hypothetically, by analyzing the spectrum of the rejuvenators and studying a calibration curve for each additive it would be possible to evaluate the percentage of additive added in HRMA even after its production and compaction. Such test could be crucial to the checks that contractors carry out on the contracting companies.

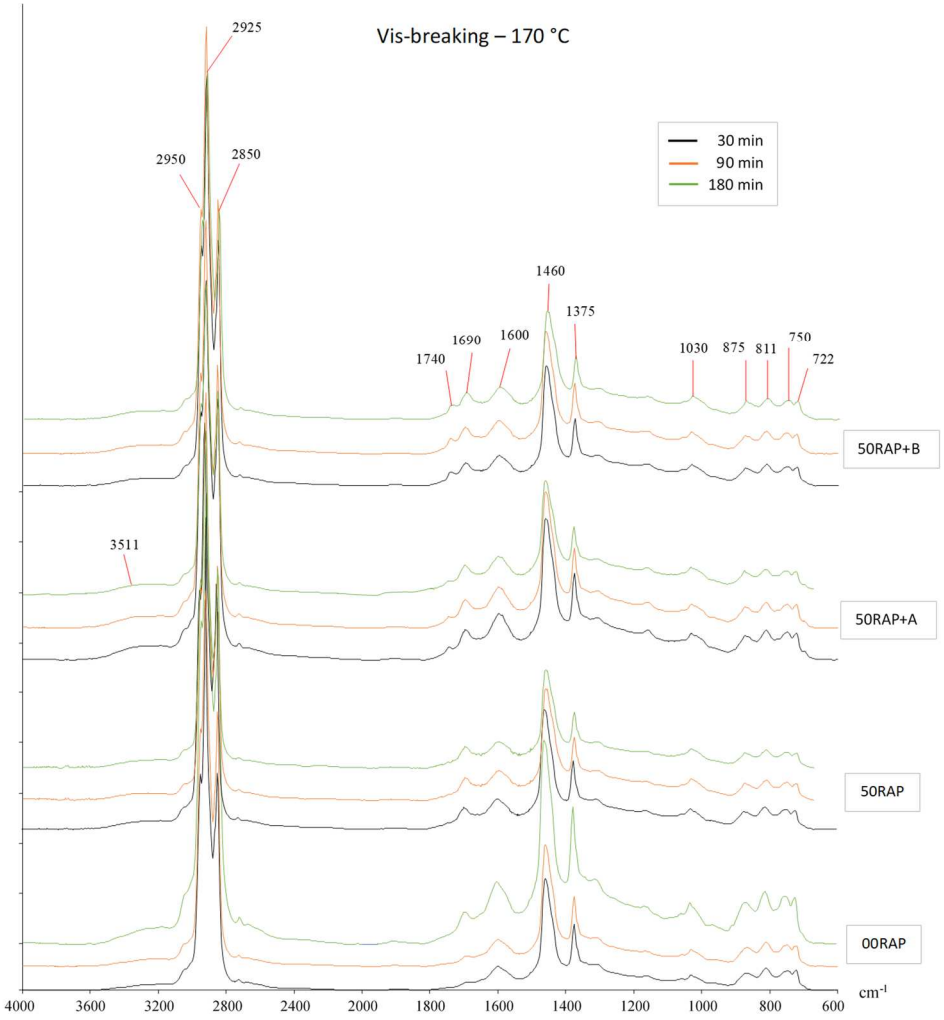

Figure 64 - Influence of the re-heating time on the FTIR spectra

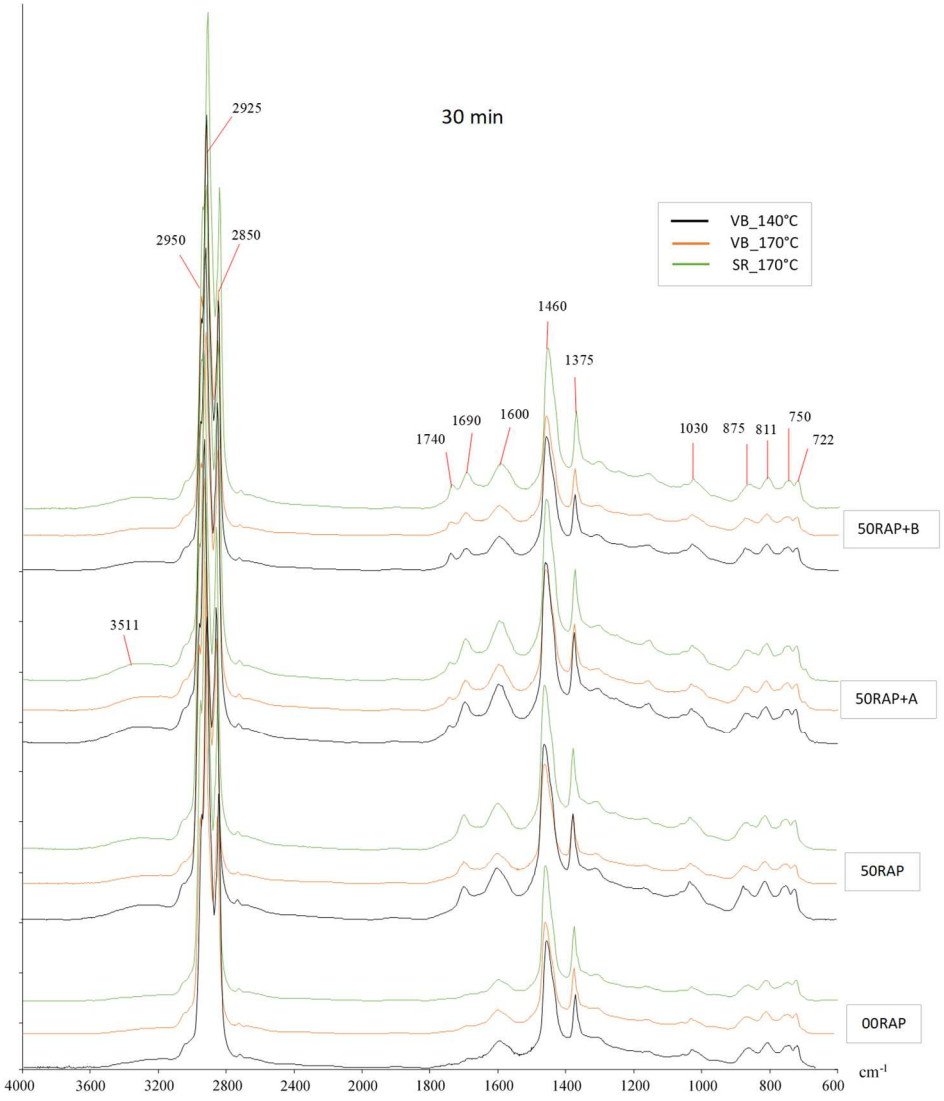

Figure 65 - Influence of the mixing temperature and the bitumen type on the FTIR spectra

21.3. Ageing and cooling of HRMA during hauling and paving

Once the ageing and stiffening of the loose HMA conditioned in the oven were assessed, field studies were carried out in order to check if the same behaviour also occurs on site during the hauling phase. At the same time, the study aimed at verifying if any temperature segregation happens as a function of truck bed type, when the lay-down site is far from the plant. For this purpose, four different batch plants (A, B, C and D) operating in the Autonomous Province of Bolzano (northern Italy) were selected to produce HRMA. In each plant, the loose mixtures were dumped into two different kinds of trucks (normal and insulated) which have travelled around the nearby roads for 3 h, in order to simulate the hauling phase. Every 1 h, they came back to the plant and temperature of the HRMA was evaluated using probe and infrared thermometers. In addition, infrared thermal camera was used to check the temperature segregation on the surface of the loose mixture inside the truck bed (Figure 66a). During each stop, some HRMA was sampled from the truck bed at 50 cm depth and compacted using a shear gyratory compactor (SGC) providing 100 mm diameter and 100 revolutions according to EN 12697-31 and subsequentially evaluated using ITSM and ITS test. Finally, the HRMA was laid down using a paving machine (Figure 66b). During this phase, temperatures were checked in order to evaluate any temperature segregation in the road surface. After few days, cores were taken out from the pavement for laboratory testing. Table 20 reports the data set available for each batch plant. On the specimens and cores, air voids content, indirect tensile stiffness modulus, indirect tensile strength and cracking tolerance index were determined.

The HRMA temperature was determined by using both infrared and probe thermometers. The first uses the amount of infrared energy emitted by the HRMA and its emissivity to evaluate, within a certain range, its actual temperature. They are sometimes called non-contact thermometers or temperature guns, to describe the device ability to measure temperature from a distance. The second is a thermometer that has a pointy metal stem that can be inserted into the loose mixture. The temperature probe was introduced into the loose mixture, orthogonally to the surface, for a depth of about 2 cm. This kind of measurement requires approximately 2 minutes to reach the thermal equilibrium and obtain a consistent value of the mix temperature. In addition, a thermographic camera was used to investigate the temperature variation of the mixtures into the truck and during the paving operations. The electromagnetic spectrum encompasses radiation from gamma rays, X-rays, ultraviolet, a thin region of visible light, infrared, terahertz waves, microwaves, and radio waves. All objects emit a certain amount of black body radiation as a function of their temperature. The higher the object temperature, the more infrared radiation (with wavelengths approximately between 1000 nm and 14000 nm) is emitted as black body radiation. The thermographic camera can detect this radiation in a way similar as an ordinary camera detects the visible light. The contemporary use of multiple devices for temperature monitoring allowed analyzing different aspects: the infrared and probe thermometers recorded the mix temperature in specific points and gave information of the local behavior, while the thermographic camera showed the

temperature of the entire construction site highlighting the dissimilarities between different areas of the truck bed and the pavement surface.

(a) ***(b)***

Figure 66 - Pictures from the field investigation: (a) temperature measurement; (b) HMA delivery to the paver.

		Plant A	Plant B	Plant C	Plant D
Truck	**Normal**	X	X	X	X
	Insulated	X	X		
Specimens compacted on site	**After 0 h hauling**	X	X	X	X
	After 1 h hauling	X	X	X	X
	After 2 h hauling	X	X	X	X
	After 3 h hauling	X	X	X	X
Cores		X		X	X
Specimens compacted in the lab after reheating		X			

Table 20 - Data set available for each HMA plant.

21.3.1. Evaluation of temperatures during hauling and paving

The trials in the plants A, B C and D were carried out between October 2018 and April 2019. In the chosen days, the average of air temperature measured during the experimentation was

about 15 °C and the weather was sunny. Table 21 shows, for each system, the hours when the loose mixtures were produced and sampled from the truck bed, and the average temperatures measured on the top corner (C), inside the truck bed (B) and on the loose mixture sampled from the truck body at 50 cm depth (L).

Plant	Truck			Production	1st Sampling	2nd Sampling	3rd Sampling	4th Sampling
A	Normal	Hours		9:00	9:12	10:08	11:04	11:27
		T [°C]	C	-	146	121	98	87
			B	-	184	175	171	168
			L	-	165	160	152	146
	Insulated	Hours		9:00	9:40	10:37	11:33	12:27
		T [°C]	C	-	143	124	105	101
			B	-	178	182	170	165
			L	-	165	160	163	154
B	Normal	Hours		8:45	8:52	9:59	10:56	12:30
		T [°C]	C	-	152	112	100	94
			B	-	181	186	184	175
			L	-	150	138	131	110
	Insulated	Hours		8:45	9:21	10:25	11:25	12:30
		T [°C]	C	-	133	106	92	96
			B	-	182	185	180	172
			L	-	165	151	131	111
C	Normal	Hours		9:00	9:15	10:08	11:13	12:18
		T [°C]	C	-	135	101	90	87
			B	-	185	183	178	174
			L	-	147	160	137	117
D	Normal	Hours		8:00	8:15	9:22	10:24	11:18
		T [°C]	C	-	151	109	97	85
			B	-	188	188	186	182
			L	-	169	130	129	109

Table 21 - Temperatures measured during production and loose mix sampling.

The average temperatures measured during the paving phases are shown in Table 20. Moreover, the time elapsed between the production of the mixtures and their lay-down is

reported. In the table, the codes “N” and “I” respectively indicate the normal and the insulated trucks.

	A		B		C	D
	N	I	N	I	N	N
Time elapsed between production and lay-down [min]	210	242	203	230	242	196
Temperature of the loose mix into the paver [°C]	-	-	180	172	121	170
Surface HMA temperature after lay-down (probe) [°C]	-	-	161	140	106	152
Surface HMA temperature after lay-down (infrared) [°C]	-	-	146	181	142	171
Temperature of outside of the truck bed [°C]	-	-	62	155	55	62
Temperature of bottom of the truck bed [°C]	-	-	55	-	75	81

Table 22 - Temperatures measured during paving operations.

The data in Table 21 show that the cooling of the mix inside the truck bed (B) was very low (10 °C after about 3 hours). Moreover, there was no significant difference between the normal and the insulated trucks. Probably, the tarpaulin which protected the top of the normal truck bed allowed avoiding the cooling on the material surface as similarly to the case of the insulated truck. Differently, the temperatures on the top corner (C) and those measured on the loose mix (L) considerably decreased (respectively up to 66 °C and 60 °C). For plant A, the insulated truck proved to reduce the heat loss, particularly on the truck corner. However, for plant B the lower precision in the measurement did not allow confirming this assumption.

From Table 22 it can be noted that the mix produced at plant B showed a comparable temperature into the paver if hauled with normal or insulated truck. Some temperature differences between the different truck types were observed after the laying. As both the probe and infrared thermometers measured the temperature in localized positions of the road surface, this result was probably related to thermal segregation of the material during hauling. It was difficult to evaluate the influence of the truck type from the temperature determined on the pavement surface. However, the noticeably different temperature outside the truck bed was a sign of the insulated truck ability to preserve the HMA heat during the 3 hours from production to paving.

21.3.2. Thermal image analysis

The pictures taken with the infrared camera were of considerable interest. Figures 67 and 68 show the most significant images for the evaluation of HMA cooling and temperature segregation during hauling phase.

The strong external cooling compared to the almost zero cooling of the HMA batch determined a huge temperature segregation at the paving site, as evidenced by the

measurements with the probe and infrared thermometers and by the photos with the thermal imaging camera. In particular, Figure 67a highlights that 3 h after mix production, near the corner of the normal truck the loose HMA cooled rather quickly, showing a large temperature difference (approximately 30 °C) between the material in contact with the edge and that in the centre of the truck bed. Differently, in the case of insulated truck (Figure 67b), this temperature segregation was less severe (temperature variation of about 10 °C).

Figure 68 shows that, during the paving, there was a huge difference in the HMA temperature on the pavement surface (higher than 30 °C). This was probably due to the inability of the paving machine to re-mix the loose HMA and disperse the colder parts among the warmer mass. The temperature segregation can negatively affect the HMA compaction, especially in the construction of thin layers (i.e. surface layers) where the colder portions can hardly be heated by the surrounding material, even if much warmer. If the temperature of the colder parts drops below the minimum temperature necessary for a good compaction (typically about 130 - 140 °C for HMA with polymer modified bitumen), high porosity areas, more susceptible to rapid degradation (in particular cracking and ravelling), can occur.

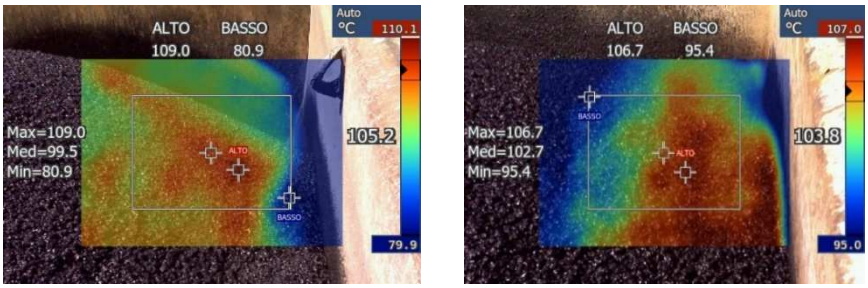

(**a**) (**b**)

Figure 67 - Pictures of the bed corner taken with infrared camera 3 h after production: (a) Normal truck; (b) Insulated truck

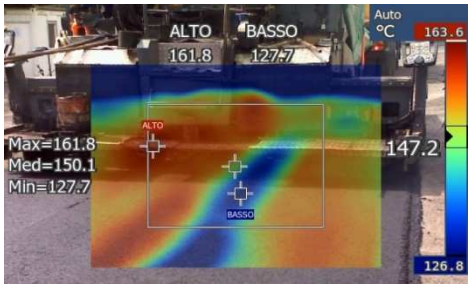

Figure 68 - Picture taken with infrared camera showing the paver laying the HMA from plant A hauled with normal truck.

21.3.3. Mechanical tests

Figures 69-72 show the average values of V_m, *ITSM*, *ITS* and CT_{index} measured for the specimens compacted in plant (immediately after the sampling of the loose asphalt), in the laboratory (after re-heating) and for the cores.

The bar-chart in Figure 69 shows that there was no significant difference in the voids contents of the specimens from the HMA produced in plant A, B and C. In particular, the air voids content of these samples, compacted with SGC in the plant was about 2-3%, independently from sampling time and truck type. Differently, the specimens from the HMA produced in plant D showed a higher V_m, approximately 4-5%, but also in this case the influence of sampling time was not very high. This result indicates that the eventual increase in binder viscosity achieved in the truck, due to bitumen ageing or cooling, did not affect the mix compactability, as observed for the HMA produced in the laboratory (Figure 70). The specimens compacted after re-heating showed a higher air voids content (4.2% on average), indicating a certain decrease in mix workability.

The V_m values of the cores showed different trends for the plants A-D: for plants A and B the air voids content of the cores was higher than that of the specimens, for plant C it was comparable, while for plant D it was lower. Moreover, for the HMA produced in plant A there was a significant difference in V_m as a function of the truck type (8% for normal truck, 5.5% for insulated truck), while for the mix produced in plant B the truck type had no influence on V_m (about 4.5%). As the voids content of each core represent the condition of the pavement in the exact place where the cores were taken, the absence of a clear trend and the higher data dispersion probably reflected the temperature segregation and localized cooling observed with the thermal camera.

Figure 70 shows that, for all the plants, the *ITSM* values of the specimens compacted in site were always about 4000 MPa, independently from the truck type and time spent in the truck during the hauling phase. Even *ITS* (Figure 71) and CT_{Index} (Figure 72) were approximately constant with sampling time, even if a slight variability between the mixes produced in the different plants was observed. It is very interesting to note that this result was opposite to what observed in the mix produced in the laboratory (Figure 4), where ITSM increased as a function of the conditioning time in the oven at 180 °C. The reason for this is probably in the fact that, in the laboratory, the small amount of HMA in the oven (some kilograms) allowed oxygen to come into contact with most of the loose mix, favoring binder oxidation and loss of volatiles. In site, the HMA was taken out from the truck bed at 50 cm depth from the batch surface, where the temperature remained almost constant, and the material was repaired by the one above. In such conditions, the batch surface was exposed to external condition, but the core was basically isolated and neither oxidation nor loss of volatile could occur, hindering the ageing of the HMA.

The cores showed lower *ITSM* and *ITS* and higher CT_{index} with respect to the specimens from the same plant, compacted in site, probably related to different air voids content. Instead, for the HMA compacted in the laboratory after re-heating at 170 °C, the stiffness modulus

considerably increased (growth greater than 100%). At the same time, *ITS* noticeably increased (up to 2.1 MPa) and CT_{Index} felt (lower than 30). This result confirmed that a severe ageing happened during the HMA re-heating in the oven.

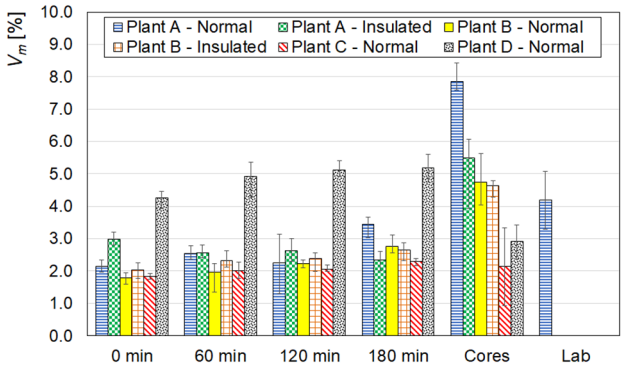

Figure 69 - Vm of the mixes produced at the plants: field- and lab-compacted specimens and cores

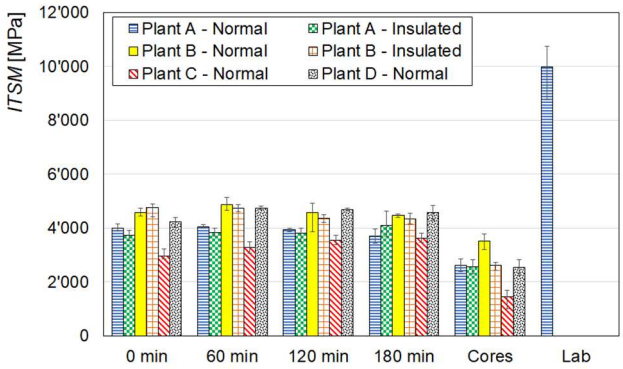

Figure 70 - ITSM of the mixes produced at the plants: field- and lab-compacted specimens and cores

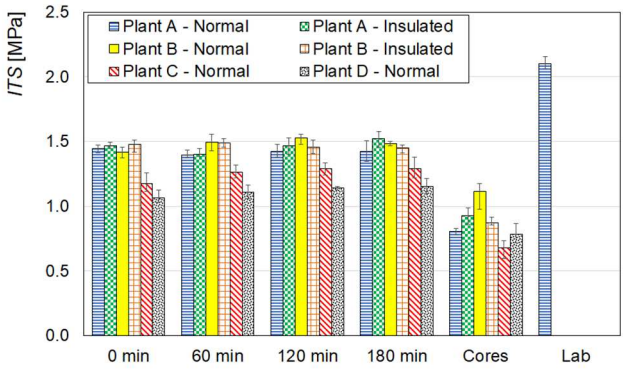

Figure 71 - ITS of the mixes produced at the plants: field- and lab-compacted specimens and cores

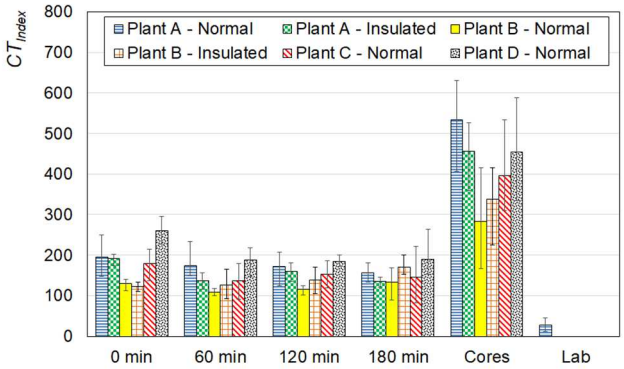

Figure 72 - CTIndex of the mixes produced at the plants: field- and lab-compacted specimens and cores

At the light of the results obtained the following conclusions can be drawn:

- the temperature monitoring proved that the mix inside the truck bed did not significantly cool after 3 hours hauling (temperature decrease between 6°C and 16 °C), while the temperatures on the top corner of the truck and those measured on the sampled loose mix considerably decreased (approximately 60 °C cooling);
- the thermal camera images highlighted a large temperature segregation at the paving site, with discrepancies higher than 30 °C both on the truck bed (normal truck) and on the road surface after paving. However, in the case of insulated truck the severity of this phenomenon was reduced;

- HRMA compactability, stiffness, strength and cracking tolerance did not change when increasing hauling time. Differently from laboratory oven (where most of the HRMA volume was exposed to air), the core of the HRMA in the truck bed was basically isolated by the surface material and neither oxidation nor loss of volatile could occur, hindering the ageing of the bitumen;
- when the loose HRMA was re-heated and compacted in the laboratory, ITSM and ITS (respectively +150% and +50%) considerably increased, whereas CTIndex decreased (-84%), denoting that a severe ageing happened through this specimen preparation procedure.

The research demonstrated that HRMA handling in the laboratory, during quality assurance and quality controls, is extremely important, since keeping the material in the oven for a prolonged time or re-heating it may significantly affect the test results. Moreover, the plant trial showed that cooling and temperature segregation represent a higher risk for HRMA than ageing. So, the use of insulated trucks (to avoid temperature segregation) and remixing material transfer vehicles is recommended in the case of long hauling distances.

21.4. Rheological tests on the mixtures

21.4.1. Rheological behavior

To validate the thermorheologically simple behavior of the mixtures, the Black (Figure 73) and Cole–Cole (Figures 74) diagrams are plotted. From the Black diagrams, the variability of $|E^*|$ and ϕ can be noted. In particular, $|E^*|$ approximately ranged between 150 MPa and 25'500 MPa for the mixtures with VB, between 50 MPa and 25'000 MPa for the mixtures with SR, independently from the mixing temperature (140 °C or 170 °C). The phase angle ϕ ranged between 4° and 35° for the mixtures with VB, between 4° and 48° for the mixtures with SR. In general, the maximum value of $|E^*|$ (measured at 5 °C and 20 Hz) was comparable among the different mixtures and ranged between 18'300 MPa (mix 00RAP_SR_170, specimen #2) and 25'500 MPa (mix 50RAP_VB_170, specimen #1). Differently, some differences can be observed in the phase angle and in the stiffness modulus at high test temperatures (35 °C and 50 °C). In particular, the presence of RAP led to a global decrease in ϕ at all temperatures and an increase in the |E*| at high temperatures. These differences are more remarkable when the straight-run bitumen and the higher mixing temperature are used.

The graphs in Figures 73 and 74 show that, even if the data are slightly scattered and a certain sample-to-sample variability can be observed, the E^* values measured at different frequencies and temperatures align on a single smooth curve for each specimen. Therefore, the thermoreologically simplicity is confirmed for all the tested mixtures, thus the TTSP can be applied.

The Black and Cole-Cole diagrams were also used for the first estimation of glassy and static asymptotes to be put into the 2S2P1D model before the error numerical minimization. In particular, the Black diagram allowed estimating the glassy modulus (E_∞) as the intersection of the prolongation of the top data with the y-axis. For all the samples tested the glassy modulus ranges between 42 and 48 GPa. Using the Cole-Cole diagram the static modulus (E_0) is determinable as the intersection of the data with the x-axis (enlarged plots on the upper right side of the graphs in Figure 74). The estimation of E_0 changed a lot depending on the RAP content, the rejuvenator A or B, the type of virgin bitumen and the mixing temperature. In particular, E_0 ranged between 35 MPa and 195 MPa, respectively obtained for a specimen of the mix 00RAP_SR_140 and a specimen on the mix 50RAP_VB_170.

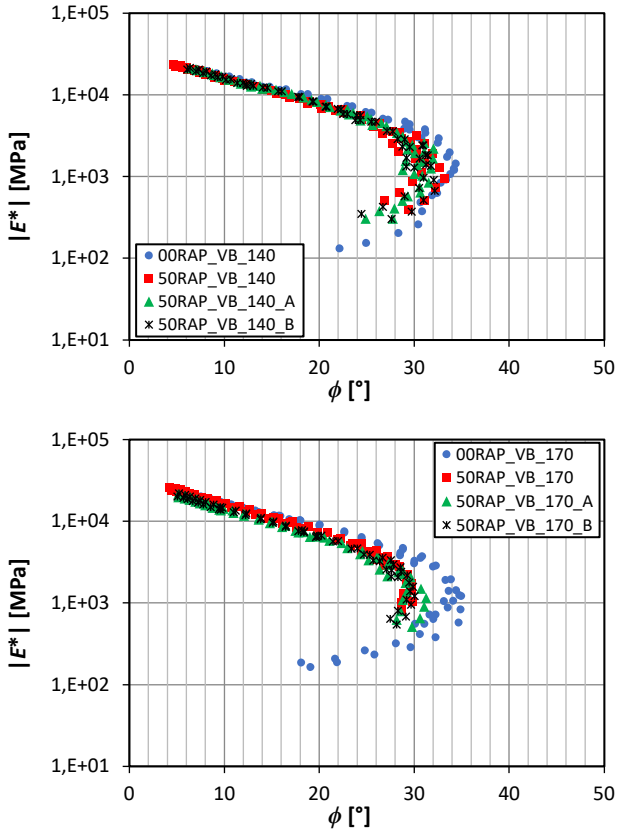

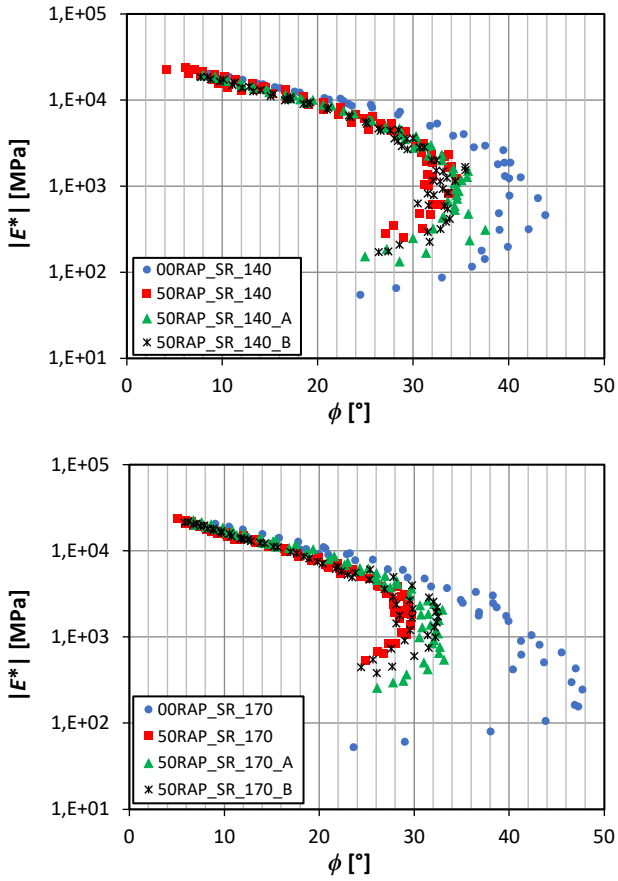

Figure 73 - Black diagrams

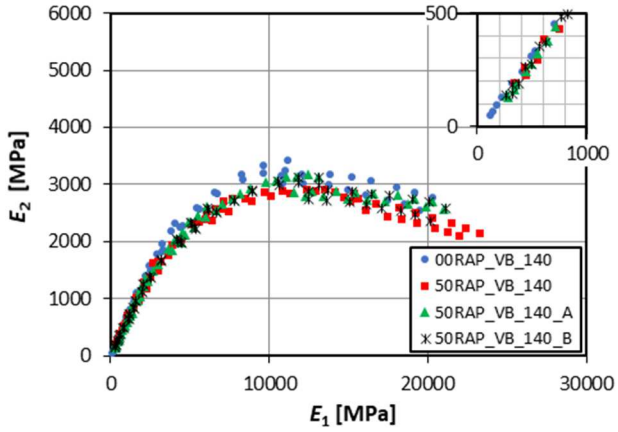
6000
5000
4000
3000
2000
1000
0
E_2 [MPa]
0
10000
20000
30000
E_1 [MPa]
500
0
0
1000
00RAP_VB_140
50RAP_VB_140
50RAP_VB_140_A
50RAP_VB_140_B

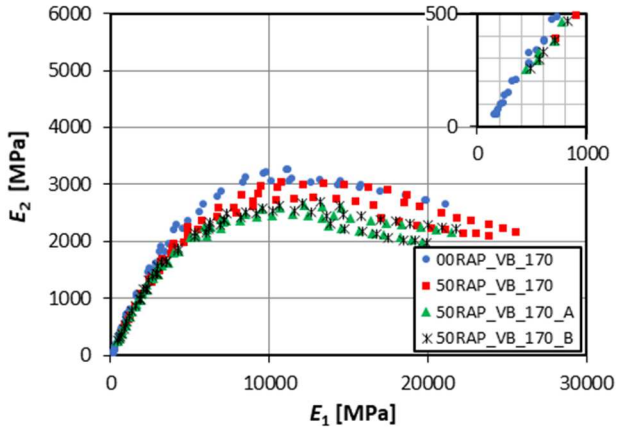
6000
5000
4000
3000
2000
1000
0
E_2 [MPa]
0
10000
20000
30000
E_1 [MPa]
500
0
0
1000
00RAP_VB_170
50RAP_VB_170
50RAP_VB_170_A
50RAP_VB_170_B

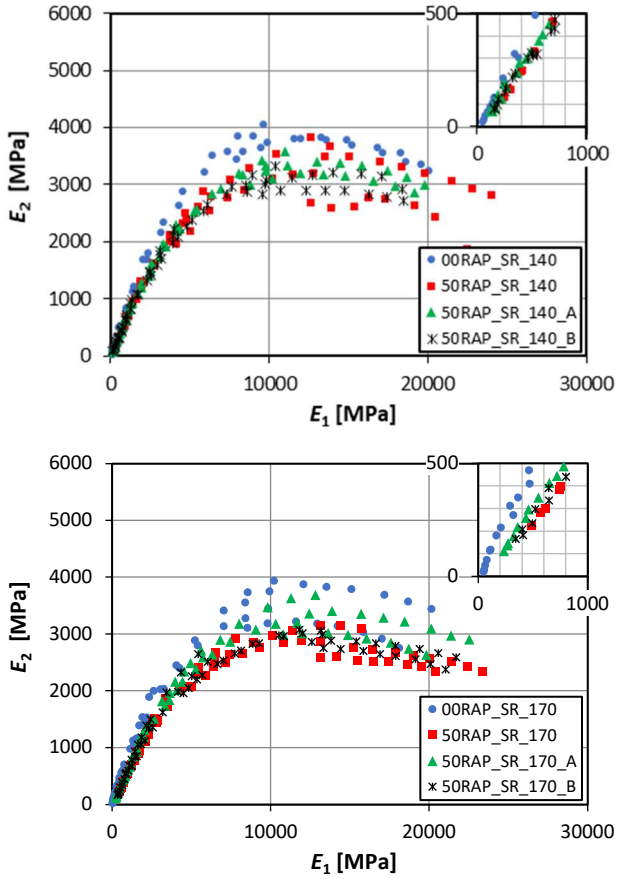

Figure 74 - Cole-Cole diagrams

21.4.2. Application of the 2S2P1D model

Assessed the validity of the TTSP, the temperature shift factors were applied to the complex modulus data to obtain the $|E^*|$ and ϕ master curves at the reference temperature of 20 °C. The shift factors were estimated through the closed-form shifting (CFS) algorithm, which provides the minimization of the area between two successive isothermal curves (Gergesovam *et al.* 2011).

Figure 75 shows the $|E^*|$ master curves superimposed to the 2S2P1D model. For all the mixtures tested, the addition of RAP induced an evident shift of the master curve upwards, while the rejuvenators were able to take it back downwards in an intermediate position with

respect to the two boundary cases. The mixing temperature had an amplifying effect on these shifts. In fact, the higher the mixing temperature, the more the distance between the 00RAP and the 50RAP mixtures. Moreover, it can be noted that, for both mixing temperatures, the use of straight-run bitumen led to an increase in the gap between the mixes made with and without RAP. No remarkable differences were visible between the two rejuvenators, except when straight-run bitumen and a temperature of 170 °C were used: in this case rejuvenator A seemed to be more efficient than rejuvenator B.

The phase angle is an indicator of the viscous properties of the material evaluated. For a purely elastic material, $\phi = 0°$ and for purely viscous material, $\phi = 90°$. Therefore, evaluating the variation of this parameter as the RAP content, rejuvenator type and mixing temperature vary is fundamental to better understand the evolution of the rheological characteristics of the HRMA compared to those of a mix made with only virgin materials. Consistently with the results obtained for the $|E^*|$ master curves, from Figure 76, it can be observed that using 50RAP led to a downward flattening and a leftward shift of the phase angles. Therefore, the 50RAP was found to be less viscous than the 00RAP. As the viscous features allow the material to dissipate the stress-energy and relax, the decrease in viscosity entails an increase in brittleness. The addition of the rejuvenators left the shape and position of the phase angle master curves almost unchanged (only a slight increase of the ϕ values can be noted), meaning that the effect of the additive is mainly to reduce the stiffness of the HRMA, without fully restoring the rheological characteristics. Moreover, the differences in the shape and position of the ϕ master curves between the mixtures made with and without RAP seemed to increase when mixing temperature increased and when straight-run bitumen was used.

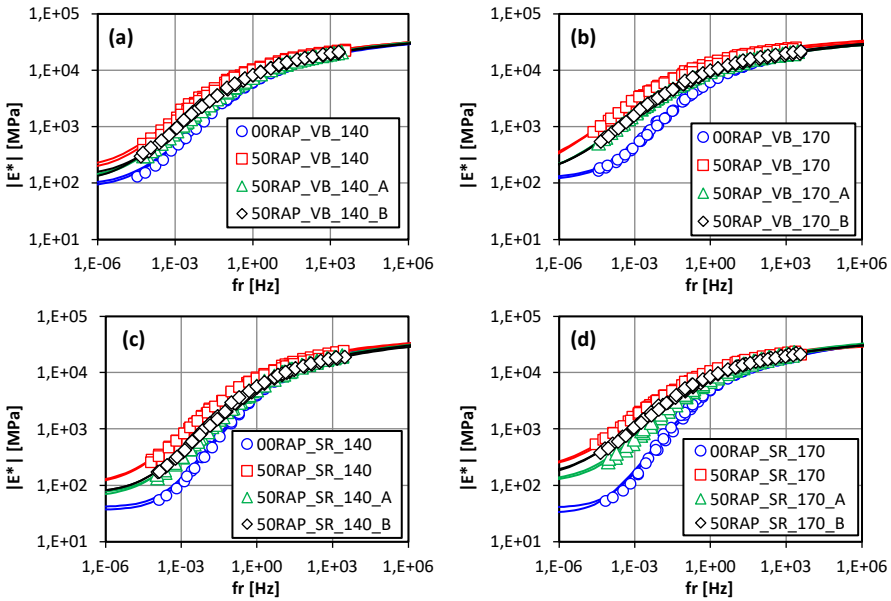

Figure 75 - Master curves of $|E^*|$: (a) visbreaker bitumen, 140 °C; (b) visbreaker bitumen, 170 °C; (c) straight-run bitumen, 140 °C; (d) straight-run bitumen, 170 °C.

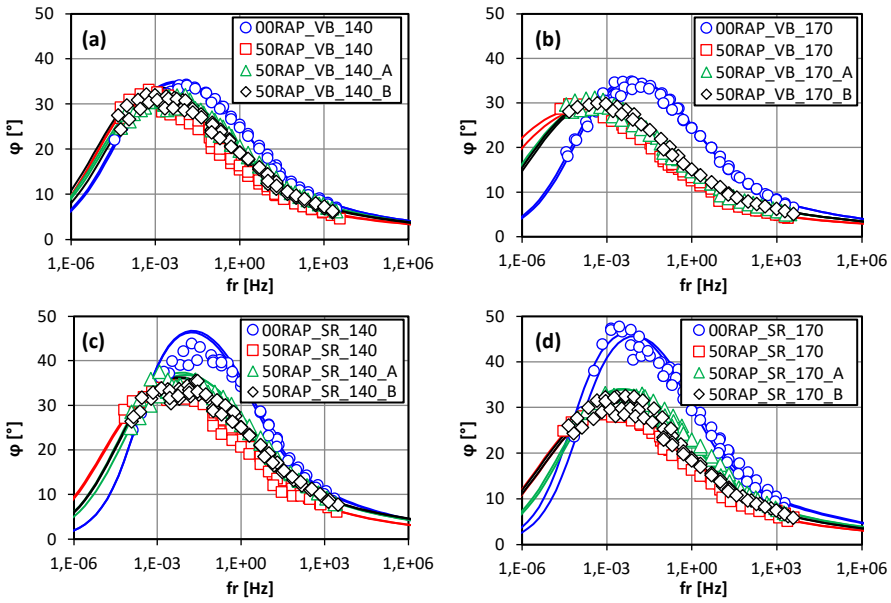

Figure 76 - Master curves of ϕ: (a) visbreaker bitumen, 140 °C; (b) visbreaker bitumen, 170 °C; (c) straight-run bitumen, 140 °C; (d) straight-run bitumen, 170 °C.

In order to allow a clearer understanding of the influence of the bitumen production process and the mixing temperature on the $|E^*|$ and ϕ master curves, these are represented by plotting the same mixtures (00RAP, 50RAP, 50RAP+A and 50RAP+B) in separated pictures (Figures 77 and 78). In this way, with the equivalent mixture composition, the differences in the complex modulus can be directly related to the mixing temperature and the type of virgin bitumen used. From Figure 73a and Figure 74a it can be noted that the mixtures with visbreaker bitumen had almost identical master curves of $|E^*|$ and ϕ for both the mixing temperatures of 140 °C and 170 °C. The master curves of the HMA with straight-run bitumen showed noticeably lower stiffness and higher phase angle with respect to the HMA with VB, especially at low frequencies/high temperatures. Moreover, for the SR bitumen, a slight increase in $|E^*|$ and a decrease in ϕ were observed when increasing the mixing temperature from 140 °C to 170 °C (even if for one of the 00RAP_SR_170 specimens the peak of the phase angle was higher). In the result interpretation, it is important to consider that the rheological behavior of the unaged VB and SR bitumens, tested with the dynamic shear rheometer in previous research (Bocci *et al.* 2018), was almost identical. Therefore, it can be deduced that the VB bitumen had already suffered severe short-term aging at the mixing temperature of 140 °C and a temperature increase did not determine a further worsening of the performance. On the other hand, the SR bitumen showed a significantly lower aging

sensitivity in the short-term, but the rise of the mixing temperature to 170 °C resulted slightly more detrimental.

Figures 77b and 78b show the $|E^*|$ and ϕ master curves of the mixtures including 50% RAP. It can be observed that, comparing the behavior of the mixtures with different virgin binders, the SR bitumen allowed obtaining lower $|E^*|$ and higher ϕ with respect to VB. However, the difference between the performances of the mixtures with SR and with VB was lower in the case of HRMA with 50RAP than in the case of HMA without RAP. The most interesting result deals with the effect of the mixing temperature on the specimen rheological properties: the mix stiffness noticeably increased and the phase angle noticeably decreased when increasing the mixing temperature from 140 °C to 170 °C, both in the case of VB and SR bitumens. These results are related to the different short-term aging of the virgin bitumen only in a small part, as the influence of the mixing temperature was low for the mixtures with no RAP. So, they could be explained by hypothesizing that at the mixing temperature of 170 °C a higher percentage of RAP bitumen has melted and blended with the virgin one. The higher aged/virgin bitumen ratio of the "active" binder in the mix can be considered responsible for the stiffer and less viscous behavior of the mixtures produced at 170 °C.

This assumption was confirmed by the graphs in Figures 77c-d and 78c-d, plotting the $|E^*|$ and ϕ master curves of the mixtures including the rejuvenator. Indeed, these mixtures containing 50% RAP also showed a significant sensitivity to the production temperature, providing higher stiffness and lower phase angle values for the mixing temperature of 170 °C, regardless of the virgin bitumen and rejuvenator type. In general, for the mixtures including 50% RAP (with or without rejuvenator), the master curves of the specimens made at 170 °C with the SR bitumen were very close to those of the specimens made at 140 °C with the VB bitumen.

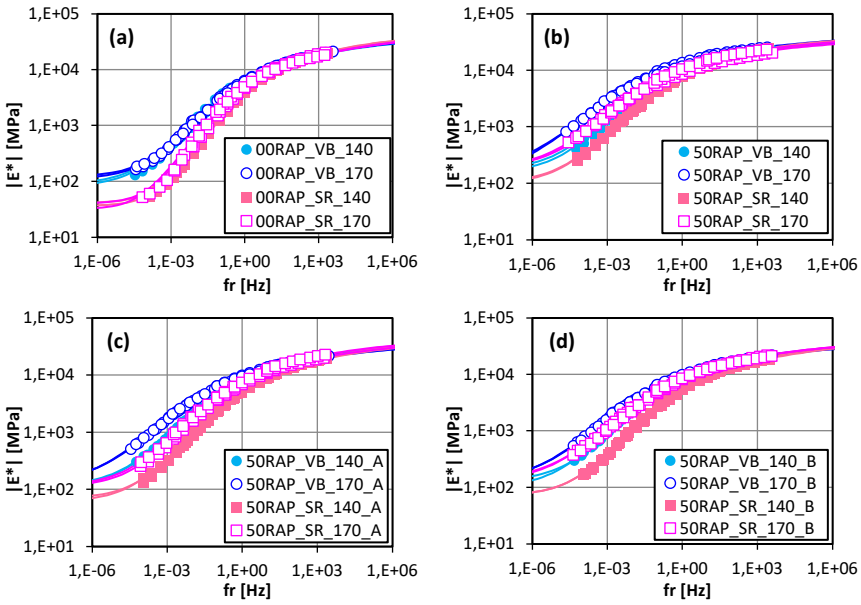

Figure 77 - Master curves of $|E^*|$: (a) 00RAP; (b) 50RAP; (c) 50RAP+A; (d) 50RAP+B.

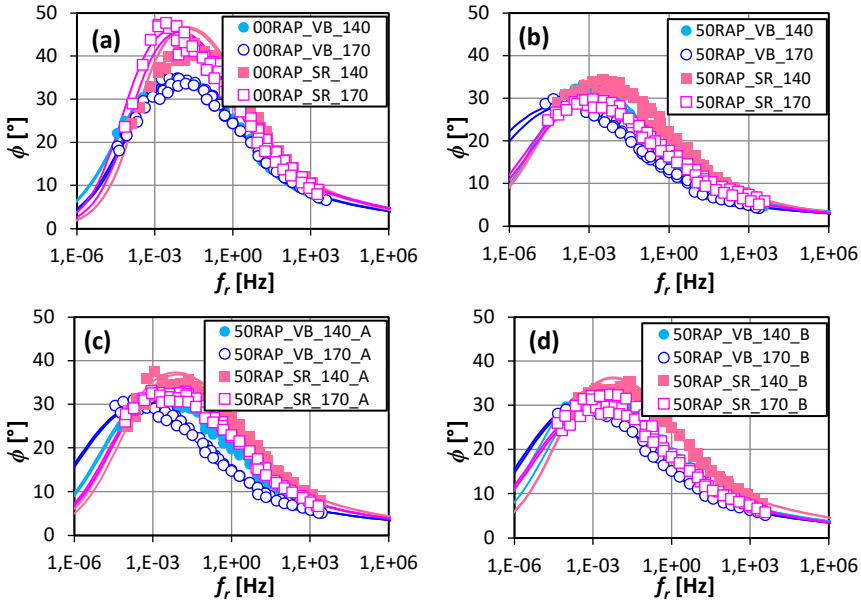

Figure 78 - Master curves of ϕ: (a) 00RAP; (b) 50RAP; (c) 50RAP+A; (d) 50RAP+B.

21.4.3. Analysis of rheological parameters

The values of the 2S2P1D model (E_∞, E_0, h, k, δ, β, τ_0) and Glover-Rowe (G-R) parameters are shown in Figure 75.

Figures 79a and 79b respectively depict the values of the glassy and viscous asymptotes of the E^* master curves using the 2S2P1D model. From the graphs, it can be noted that comparable values of E_∞ were obtained for the different mixtures (approximately around 45 GPa) except for the mix 50RAP_VB_170 which provided an E_∞ value of about 50 GPa. Differently, E_0 was sensitive to the presence of RAP/rejuvenator, the virgin bitumen type and the production temperature. In particular, E_0 values were higher in the case of higher mixing temperature, presence of 50% RAP in the mix and use of visbreaker bitumen. The presence of the rejuvenator allowed decreasing the viscous asymptote value, but not achieving the performance of the mixes without RAP. It has to be highlighted that the experimental data did not allow reaching the asymptotic trend of the model at low reduced frequencies, as the "softer" mix condition investigated was T = 50 °C, f = 0.1 Hz, so the values of E_0 represent a mere estimation. However, a significant result and a good correlation with the physical behavior of the different materials were obtained. In addition, the specimen-to-specimen variability was very low in the case of both E_∞ and E_0 approximation.

Figures 79c-d show the values of h and k, representing the parabolic elements in the 2S2P1D model. In particular, for both parameters, using RAP and increasing mixing temperature led to lower h and k, while there is a very slight increase in these parameters by adding the rejuvenators. The decrease of h and k values corresponds to the flattening of the curves in the Cole-Cole plot, denoting the more inhibited viscous features. No remarkable changes were noted between the two rejuvenators added. Moreover, it can be observed that the differences just mentioned were less marked when the visbreaker bitumen was used.

The values of δ (Figure 79e) showed a low variability among the tested mixtures when VB bitumen was used, ranging between 0.03 and 0.06. Differently, for the mixtures including SR bitumen, the parameter δ slightly increased when 50% RAP was included in the mix (up to 0.165) and decreased when adding the rejuvenators.

The values of β (Figure 79f) did not provide a significant trend as a function of RAP/rejuvenator presence, bitumen type and mixing temperature. Moreover, it has to be remarked that the parameter β resulted very high ($> 10^6$) and a further increase did not entail either change in the master curve shape or reduction of the error between calculated and measured E^*. This suggests that the viscous damper in the 2S2P1D model was so viscous that it could be equated to a rigid element and the analogical model could be reduced to an Huet-Sayegh (2S2P) (Sayegh 1967).

Figure 79g shows that higher values of $\log\tau_0$ (lower in absolute value) were obtained when RAP was used, denoting lower relaxation ability. The addition of rejuvenator led to a decrease (increase if considering the absolute value) of the characteristic time up to values even lower than those of the mixtures made without RAP. This trend was noted for both

mixing temperatures, but it was more remarkable when the SR bitumen was used. No differences between the two rejuvenators were found.

Finally, Figure 79h shows that the *G-R* parameter ranged between 11'000 MPa and 90'000 MPa for the different mixtures, resulting in about 5 orders higher than for binders. The addition of 50% RAP to the mixture led to a noticeable increase of the *G-R* parameter while the addition of rejuvenators allowed lowering the *G-R*, but never reaching those of the mixture produced without RAP. Moreover, for all the mixtures investigated, the straight-run bitumen showed lower *G-R* values with respect to the visbreaker. The increase of the mixing temperature induced a significant increase of the *G-R* for all the mixtures except for those produced without RAP using the visbreaker bitumen, confirming what was observed for the master curves (Figures 77 and 78). Rejuvenator A seemed to be slightly more effective in reducing the *G-R* values for both the bitumen types and both the mix production temperatures.

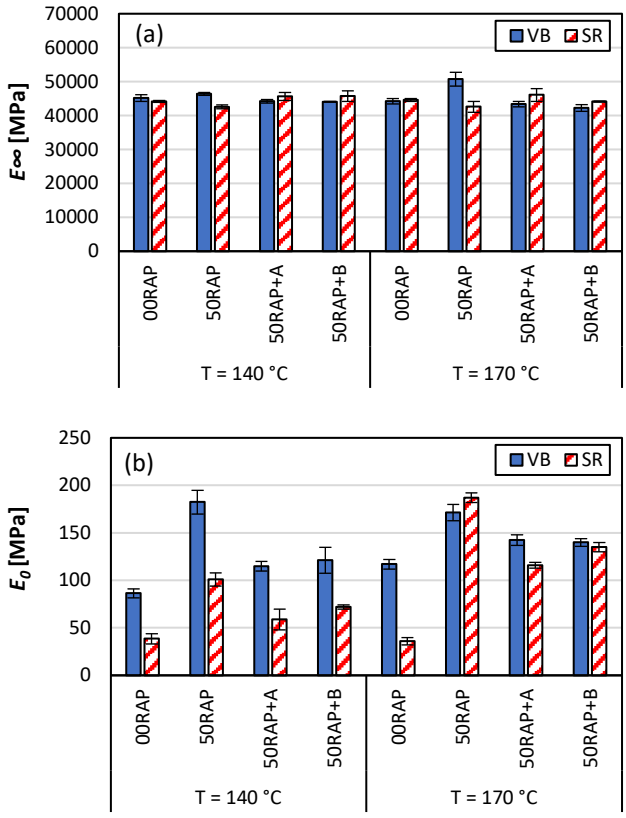

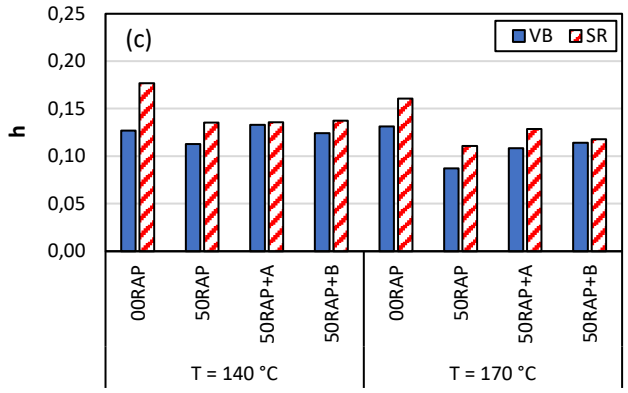
(c)
VB
SR
h
0,25
0,20
0,15
0,10
0,05
0,00
00RAP
50RAP
50RAP+A
50RAP+B
00RAP
50RAP
50RAP+A
50RAP+B
T = 140 °C
T = 170 °C

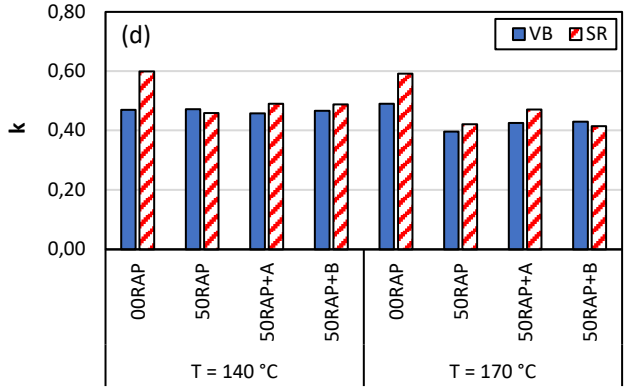
(d)
VB
SR
k
0,80
0,60
0,40
0,20
0,00
00RAP
50RAP
50RAP+A
50RAP+B
00RAP
50RAP
50RAP+A
50RAP+B
T = 140 °C
T = 170 °C

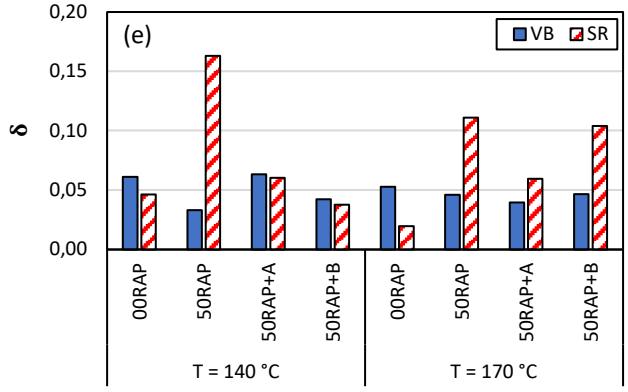
(e)
VB
SR
δ
0,20
0,15
0,10
0,05
0,00
00RAP
50RAP
50RAP+A
50RAP+B
00RAP
50RAP
50RAP+A
50RAP+B
T = 140 °C
T = 170 °C

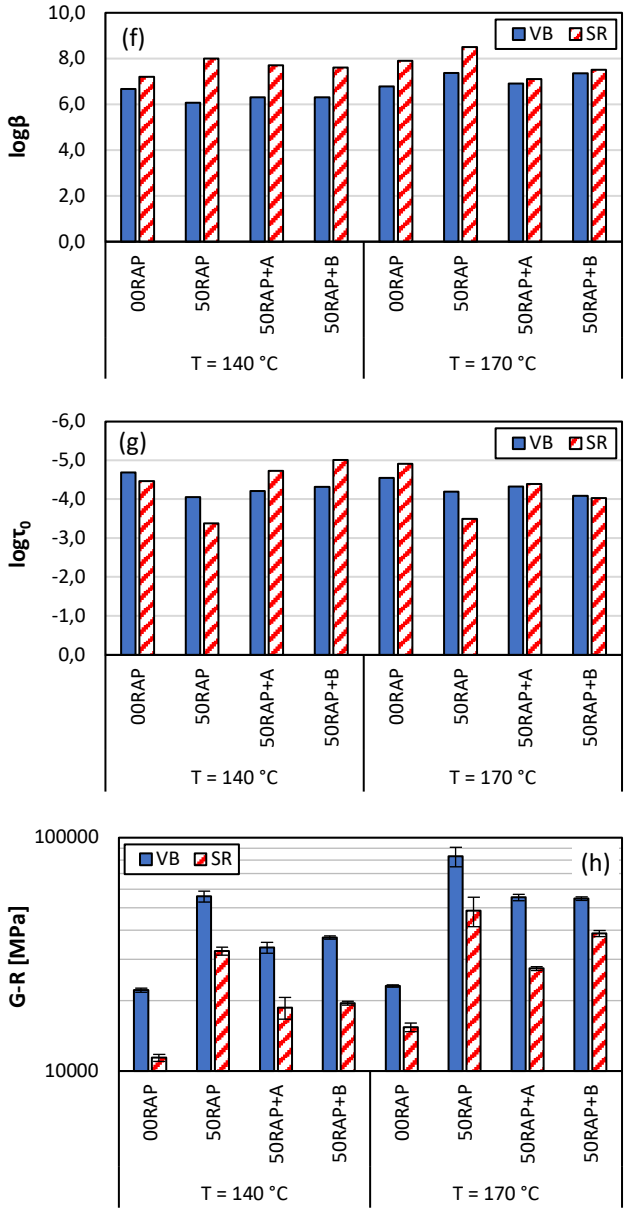

Figure 79 - Rheological parameters changing the mixture composition, the temperature and the type of the virgin binder used

Chapter 22. Conclusions

The present part of the Phd thesis aimed at evaluating the influence of the mixing temperature (140°C or 170°C) and the origin of the neat bitumen (visbreaker vs straight-run), the type of the rejuvenator (A, B) and the re-heating time of the loose mixture (from 30 to 180 minutes) on the mechanical and rheological characteristics of an HRMA made using 50% of RAP.

For what concern the mechanical tests the following conclusions can be drawn:

- The mixing temperature influenced the mix properties, in particular, the mixtures made at 170 °C (dotted lines) achieved higher ITS and ITSM and lower CT-Index values with respect to the ones manufactured at 140 °C.
- The time in the oven clearly increased the sum of the Ico and Iso indices. In the mixtures made with RAP, the carbonyl index seems to increase with increasing temperature and using an SR bitumen, while where no recycled material is added, Ico increases with the temperature but decreases by using SR bitumen. Moreover, the sulphoxide index always decreases with temperature while the use of SR bitumen seems to decrease it when there is no RAP and increase it when recycled materials are included.
- Additives display new bands on the FTIR spectra. In particular, rejuvenator B shows an important band at 1740 cm-1 while rejuvenator A causes the formation of bands at 3511 cm-1.
- HRMA compactability, stiffness, strength and brittleness did not change when increasing hauling time. Differently from laboratory oven (where most of the HRMA volume was exposed to air), the core of the HRMA in the truck bed was basically isolated by the surface material and neither oxidation nor loss of volatile could occur, hindering the ageing of the bitumen;

Regarding the rheological tests, the measured complex modulus data were interpolated using the 2S2P1D model in order to observe the variation of the master curves shape and the rheological parameters. Based on the results presented in this paper, the following conclusions can be illustrated:

- All the tested specimens showed a thermorheologically simple behaviour, which could be well simulated through the 2S2P1D model.
- The addition of RAP in the mixtures induced a pronounced upwards shift of the $|E^*|$ master curve. The rejuvenators were able to take it back downwards in an intermediate position between the master curves of the 00RAP and 50RAP mixes. No remarkable differences were visible between the two rejuvenators, except when straight-run bitumen and a mixing temperature of 170°C were used, where rejuvenator A seemed to be more efficient.

- When including 50% RAP, the phase angles master curves tended to flatten and shift leftward. The addition of rejuvenators left the shape and position of the ϕ master curves almost unchanged, meaning that the effect of the additive was mainly to reduce the stiffness of the HRMA, without fully restoring its rheological characteristics.
- The different master curves of the mixtures without RAP produced with VB or SR bitumen indicated a higher sensitivity to the short-term aging for VB than for SR. Also, the mixtures with VB including RAP/rejuvenators showed higher stiffness and lower phase angle compared to the analogous mixtures with SR.
- The mixing temperature lowly influenced the rheological behavior of the mixtures without RAP while it had a high impact on the mixtures including 50% RAP. This denoted that the mixing temperature increase did not determine a significant worsening of the short-term aging for the virgin bitumen but probably entailed the mobilization of a higher amount of the aged bitumen from the RAP.
- The parameters E_∞, δ and β of the 2S2P1D model showed a low significance in representing the evolution of the mix rheological properties as a function of the different variables (presence of RAP/rejuvenator, origin of virgin bitumen and mixing temperature). The parameters E_0, h, k and τ_0 had a more relevant variation when RAP and, afterward, rejuvenators were used, but they were lowly representative of the different behavior when varying bitumen type and mix production temperature. The Glover-Rowe parameter, in the formulation proposed by Ogbo et al. (Ogbo *et al.* 2019) for bituminous mixtures, proved to be effective in summarizing the changes in the complex modulus with the different factors.

Summary of the overall experimental study

Chapter 23. Concluding Remarks

The experimental study described in this dissertation was developed with the aim to scientifically verify how to produce recycled HMA with high RAP content without penalizing the pavement in terms of performance. The main properties of asphalt mixtures directly related to the major distresses typical of flexible pavements (i.e. rutting, fatigue and thermal cracking) were deeply investigated through a wide set of chemical, rheological and mechanical tests carried out on several different materials.

The first part of the program aimed at analysing the evolution of the rheological behaviour of the aged bitumen extracted from RAP with rejuvenation (blending of virgin and RAP bitumen, with addition of a rejuvenator) and re-aging (representing the service life of the hot recycled mix). The complex modulus of the binders was measured through a DSR device, while RTFOT and PAV protocols were followed to reproduce the bitumen aging in the laboratory. Three rheological models (2S2P1D, modified CAM and generalized logistic sigmoidal) were used in order to study the evolution of their parameters in the various steps. In addition, the apparent molecular weight distribution (AMWD) of the bitumens, determined through δ-method, was analysed. Therefore, the objective deals with the analysis of how the rheological parameters of an aged bitumen changes with rejuvenation and re-aging. To this aim, the hot recycling process was replicated in the laboratory at a binder scale by extracting the bitumen from the RAP. Then, this was blended with a rejuvenating agent and subsequently with virgin bitumen. Finally, the simulated hot recycled bitumen was re-aged in the laboratory in both the short-term and long-term steps. This experimental approach based on the rheological modelling and the application of the δ-method resulted effective to understand the real contribution of the rejuvenator on the bitumen structure and compare the mechanical properties of the first-aged and the re-aged bitumens. In particular, the addition of the rejuvenator determined a reduction of the stiffness and an almost negligible increase of the phase angle with respect to the RAP bitumen, while the blending with the virgin bitumen allowed both decreasing $|G^*|$ and increasing ϕ. The re-aging determined again an increase in the stiffness and a reduction of the viscous features in favour of the elastic ones. Moreover, the δ-method proved that the aging entailed an increase of the high molecular weight fractions in the bitumen spectra, while the addition of VB restored part of the molecular groups with a low weight. The addiction of the rejuvenator to RB had almost no effect on high weight fractions, denoting that the additive is probably a soluble or incompatible softener and cannot disrupt the asphaltene clusters.

The second part of the PhD. program aimed at comparing seven additives in terms of their ability in mitigating the effects of the presence of RAP in the mix as a function of the production temperature. In particular, the focus of this research was to investigate the effect of the production temperature on bituminous mixtures, especially on those containing a high amount of RAP. Moreover, the effectiveness of seven different additives as a function of the mix production temperature was evaluated. The experimental programme preliminarily included the FTIR analysis on the additives to analyse the differences in their chemical

composition. Then, bituminous mixtures containing no RAP, 50% RAP and 50% RAP with additive were produced in the laboratory at 2 different temperatures: 140 °C or 170 °C. The air voids content (Vm) was measured to investigate the compactability of the mixtures while the Indirect Tensile Stiffness Modulus (ITSM) test and Indirect Tensile Strength (ITS) were performed to assess the mechanical characteristics. The Cracking Tolerance Index (CTI) defined by ASTM D8225-19, 2019 was also calculated from ITS test data to estimate the mix brittleness. In order to understand the influence of the mixing temperature and to rank the additives according to their efficacy, two indexes were defined: the rejuvenation index (RI), which represents the performance of the additive in minimizing the negative effects due to the presence of RAP in the mix and the temperature index (TI), which represents the effect of the production temperature decrease from 170 °C to 140 °C. The analysis of these indexes, calculated for ITSM, ITS and CTI, allowed the identification of the additive with the best performance. The results obtained from the laboratory tests showed that the mixture containing 50% RAP had a higher stiffness and strength with respect to the mix produced with only virgin materials. The reduction of the mixing temperature from 170 °C to 140 °C determined an increase of the air voids content (approximately 1%) but also allowed a significant decrease of mix stiffness and strength with a contemporary increase of ductility. This was a consequence of the less severe short-term aging achieved on the virgin and RAP bitumen but it was likely due also to the mobilization of a lower amount of RAP binder. The seven additives investigated in this research showed, in most cases, different chemical structures, which reflected in their rejuvenating performance. The effectiveness of the additives was assessed by measuring the ITS of the mixtures, as provided my Italian Specifications. In addition, the experimental program also included the determination of the ITSM and the CTI, which proved to be useful and reliable indicators to evaluate the effects of RAP rejuvenation and the variation of mixing temperature. In addition, the comparative analysis of the results from mechanical and chemical tests provided remarkable information about the characteristic properties of a good rejuvenator, particularly the presence of esters and the high flash point. The FTIR analysis also allowed to clearly distinguish between the chemistry of the softening agent and that of the other additives, encouraging to extend the investigation on more products in order to validate the method for additive classification.

The following part of the PhD. program aims at evaluating the fatigue performance of bituminous mixtures including high amount RAP as a function of the type of the additives used. For this purpose, two RAP content (0 and 50%) and two additives (a real rejuvenator and a softening agent) were chosen and ITFT tests were performed after analysing the workability and the indirect tensile stiffness modulus of the mixture.

In the light of what has been stated in the part regarding the fatigue performance, we can conclude that analyzing the number of revolutions needed to reach the air void content equal to 4%, the mixture containing 50% of RAP with the softening agent achieved the greatest workability. Slightly lower was the workability of the blends containing recycled material with no additives and with the real rejuvenator, while the lowest workability resulted from the mixture of virgin materials only. Comparing the stiffness of the various mixtures, it can be noted that the lower ITSM values were obviously obtained from the virgin mixture, while

the higher ones from the specimens containing 50% of RAP without additives. The softening agent was unable to significantly lower the stiffness, while the real rejuvenator succeeded in part, but without getting close to the values of the virgin mixture. Probably to achieve ITSM values comparable to the mixtures produced without RAP, a higher dosage of rejuvenator was required.

As regards the results of the fatigue tests, considering the horizontal deformation versus the number of cycles graph, it was observed that the addition of RAP decreased the fatigue resistance and, only the real rejuvenator was able to bring the fatigue curve close to that of the virgin mixture. On the contrary, analysing the horizontal stress versus the number of cycles graph, the addition of RAP caused an increase in fatigue performance. Moreover, by adding the real rejuvenator it was possible to notice a shift of the fatigue curve towards that obtained from the mixtures produced with no recycled material. Finally, using the softening agent, it was found that such additive had not been able to produce any effect on the recycled mixture.

Finally, given the difference in the results depending on the type of graph analysed, it can be stated that the ITFT test was not able to fully represent and investigate the effects of RAP and rejuvenators in the fatigue performance of HRMA. Since fatigue resistance is one of the main issues to be faced when RAP is used, it is essential to use a suitable test to fully understand how the recycled material affects such performance. It will be the subject of future studies to perform further fatigue tests using different test methodologies such as fatigue tests in tension-compression mode to be processed with the Simplified Viscoelastic Continuum Damage Model (S-VECD model) developed by Underwood e al. (Underwood *et al.* 2012).

The main goal of the last part of the PhD program was to evaluate the evolution of the volumetric (Air Voids content), mechanical (ITS and ITSM tests), chemical (FTIR test) and rheological (master curves) properties of HRMA changing the type of rejuvenator (coded with the letters A and B), the origin of the virgin bitumen (Visbreaker VB and Straight-run SR), the pre-heating and mixing temperature (140-170 °C) and a heating time of the loose mixture after mixing growing from 30 to 180 minutes. Mixtures made using 50% of RAP are produced together with reference virgin HMA manufactured without recycling materials. For what concern the mechanical, the mixing temperature influenced the mix properties, in particular, the mixtures made at 170 °C (dotted lines) achieved higher ITS, ITSM, Ico and Iso values and lower CT-Index values with respect to the ones manufactured at 140 °C. The time in the oven clearly increased the sum of the Ico and Iso indices. Additives display new bands on the FTIR spectra. In particular, rejuvenator B shows an important band at 1740 cm-1 while rejuvenator A causes the formation of bands at 3511 cm-1. Moreover, HRMA compactability, stiffness, strength and brittleness did not change when increasing hauling time. Differently from laboratory oven (where most of the HRMA volume was exposed to air), the core of the HRMA in the truck bed was basically isolated by the surface material and neither oxidation nor loss of volatile could occur, hindering the ageing of the bitumen. Regarding the rheological tests, the addition of RAP in the mixtures induced a pronounced upwards shift of the |E*| master curve. The rejuvenators were able to take it back downwards

in an intermediate position between the master curves of the 00RAP and 50RAP mixes. No remarkable differences were visible between the two rejuvenators, except when straight-run bitumen and a mixing temperature of 170°C were used, where rejuvenator A seemed to be more efficient. When including 50% RAP, the phase angles master curves tended to flatten and shift leftward. The addition of rejuvenators left the shape and position of the ϕ master curves almost unchanged, meaning that the effect of the additive was mainly to reduce the stiffness of the HRMA, without fully restoring its rheological characteristics. The different master curves of the mixtures without RAP produced with VB or SR bitumen indicated a higher sensitivity to the short-term aging for VB than for SR. The mixing temperature lowly influenced the rheological behaviour of the mixtures without RAP while it had a high impact on the mixtures including 50% RAP.

In conclusion, a high mixing temperature, the use of visbreaker bitumens and a high permanence in the oven proved to amplify the differences between 00RAP and 50RAP mixtures and limit the effectiveness of the rejuvenators. Therefore, using a reasonably low mixing temperature (enough to make the bitumen workable) and a good SR virgin bitumen plays a fundamental role in the production of an HRMA that achieves optimal rheological and mechanical characteristics and is therefore durable over time without suffering from cracking issues.

Lists of 3-years Ph.D. publications

Bocci, E., Prosperi, E. - Recycling of reclaimed fibers from end-of-life tires in hot mix asphalt. Journal of Traffic and Transportation Engineering (English Edition), Volume 7, Issue 5, October 2020, Pages 678-687 https://doi.org/10.1016/j.jtte.2019.09.006

Bocci, E., Prosperi, E. - Analysis of different reclaimed asphalt pavements to assess the potentiality of RILEM cohesion test. Mater Struct 53, 117 (2020). https://doi.org/10.1617/s11527-020-01551-3

Bocci, E., Prosperi, E., Mair V., Bocci M. - Ageing and cooling of hot-mix-asphalt during hauling and paving—a laboratory and site study. Sustainability 2020, 12(20), 8612 https://doi.org/10.3390/su12208612

E. Prosperi, E. Bocci, A Review on Bitumen Aging and Rejuvenation Chemistry: Processes, Materials and Analyses. Sustainability 2021, 13(12), 6523, https://doi.org/10.3390/su13126523

E. Bocci, E. Prosperi, P. Marsac - Evolution of rheological parameters and apparent molecular weight distribution in the bitumen from reclaimed asphalt with rejuvenation and re-ageing, Road Material and Pavement Design, 2021, https://doi.org/10.1080/14680629.2021.1994449

E. Prosperi, E. Bocci, M. Bocci - Evaluation of the rejuvenating effect of different additives on bituminous mixtures including hot-recycled RA as a function of the production temperature, Road Material and Pavement Design, 2022, https://doi.org/10.1080/14680629.2021.2002179

E. Bocci, E. Prosperi, P. Marsac - Rheological modelling of the bitumen from reclaimed asphalt with rejuvenation and re-ageing, RILEM Bookseries, 2022, 27, pp. 1579–1585, https://doi.org/10.1007/978-3-030-46455-4_200

References

A. E. Martin, Z.Z., 2015. Evaluating the Effects of Recycling Agents on Asphalt Mixtures with High RAS and RAP Binder Ratios. *NCHRP Report 927*, (9–58).

Afanasieva, N., Alvarez, M., and Ortiz, M., 2002. Rheological characterization of aged asphalt. *Ciencia, Tecnologia y Futuro 2 (3)*, 121–134.

Ahmad, T., Ahmad, N., Jamal, M., Badin, G., and Suleman, M., 2020. Investigation into possibility of rejuvenating aged asphalt binder using mustard oil. *International Journal of Pavement Engineering*, 0 (0), 1–16.

Ajideh, H., Bahia, H., Carnalla, S., and Earthman, J., 2013. Evaluation of fatigue life of asphalt mixture with high rap content utilizing innovative scanning method. *Airfield and Highway Pavement: Sustainable and Efficient Pavements*, 1112–1121.

Al-Shujairi, A.O., Al-Taie, A.J., and Al-Mosawe, H.M., 2021. Review on applications of RAP in civil engineering. *IOP Conference Series: Materials Science and Engineering*, 1105 (1), 012092.

Ali, A.W., Mehta, Y.A., Nolan, A., Purdy, C., and Bennert, T., 2016a. Investigation of the impacts of aging and RAP percentages on effectiveness of asphalt binder rejuvenators. *Constr. Build. Mater.*, 110, 211–217.

Ali, A.W., Mehta, Y.A., Nolan, A., Purdy, C., and Bennert, T., 2016b. Investigation of the impacts of aging and RAP percentages on effectiveness of asphalt binder rejuvenators. *Construction and Building Materials*, 110, 211–217.

Ameri, M., Mansourkhaki, A., and Daryaee, D., 2018. Evaluation of fatigue behavior of high reclaimed asphalt binder mixes modified with rejuvenator and softer bitumen. *Constr. Build. Mater.*, 191, 702–712.

American Society for Testing and Materials, 2018. *ASTM D4124-09: Standard Test Method for Separation af Asphalt into Four Fractions*.

ANAS, 2016. Capitolato Speciale di Appalto - Norme Tecniche per l'esecuzione del contratto - Parte 2.

Anwar, W., Ahmad, N., Khitab, A., Faizan, M., Tayyab, S., Saeed, M., and Imran, M., 2021. Performance augmentation of asphalt binder with multi-walled carbon nanotubes. *In*: *the Institution of Civil Engineers: Transport, Volume 174, Issue 2*. 130–141.

Araújo, M.F.A.S., Lins, V.C.F., and Pasa, V.M.D., 2011. Effect of Ageing on Porosity of Hot Mix Asphalt. *Brazilian Journal of Petroleum and Gas*, 5 (1), 011–018.

Ashtiani, M.Z., Mogawer, W.S., and Austerman, A.J., 2018. A Mechanical Approach to Quantify Blending of Aged Binder from Recycled Materials in New Hot Mix Asphalt Mixtures. *Journal of the Transportation Research Board*, 2672(28), 107–118.

Asli, H., Ahmadinia, E., Zargar, M., and Karim, M.R., 2012. Investigation on physical

properties of waste cooking oil – rejuvenated bitumen binder. *Constr. Build. Mater.*, 37, 398–405.

ASTM D8225-19, 2019. Standard Test Method for Determination of Cracking Tolerance Index of Asphalt Mixture Using the Indirect Tensile Cracking Test at Intermediate Temperature.

Avsenik, L., Klinar, D., Tušar, M., and Perše, L.S., 2016. Use of modified slow tire pyrolysis product as a rejuvenator for aged bitumen. *Construction and Building Materials*, 120, 605–616.

Azahar, W.N.A.W., Jaya, R.P., Hainin, M.R., Bujang, M., and Ngadi, N., 2016. Chemical modification of waste cooking oil to improve the physical and rheological properties of asphalt binder. *Constr. Build. Mater.*, 126, 218–226.

Baghaee Moghaddam, T. and Baaj, H., 2016. The use of rejuvenating agents in production of recycled hot mix asphalt: A systematic review. *Construction and Building Materials*, 114, 805–816.

Bahia, H.U., Hanson, D.I., Zeng, M., Zhai, H., Khatri, M.A., and Anderson, R.M., 2001. Characterization of Modified Asphalt Binders in Superpave Mix Design. *NCHRP Report 459*.

Basueny, A., Carter, A., Perraton, D., and Vaillancourt, M., 2016. Laboratory evaluation of complex modulus and fatigue resistance of asphalt mixtures with RAP. *In*: *8th RILEM International Symposium on Testing and Characterization of Sustainable and Innovative Bituminous Materials*. 521–532.

Bearsley, S., Forbes, A., and Haverkamp, R.G., 2004. Direct observation of the asphaltene structure in paving-grade bitumen using confocal laser-scanning microscopy. *Journal of Microscopy*, 215 (2), 149–155.

Bearsley, S.R. and Haverkamp, R.G., 2007. Age hardening potential of tall oil pitch modified bitumen. *Road Mater. Pavement Des.*, 8 (3), 467–481.

Behnood, A., 2019. Application of rejuvenators to improve the rheological and mechanical properties of asphalt binders and mixtures: A review. *Journal of Cleaner Production*, 231, 171–182.

Di Benedetto, H., Sauzéat, C., Delaporte, B., and Olard, F., 2004. Linear viscoelastic behaviour of bituminous materials: From binders to mixes. *Road Materials and Pavement Design*, 5 (December 2014), 163–202.

Bocci, E., Cardone, F., and Grilli, A., n.d. Mix design and volumetric analysis of hot recycled bituminous mixtures using a bio-additive. *In*: *AIIT International Congress on Transport Infrastructure and Systems*. Rome, Italy, 267–274.

Bocci, E., Grilli, A., Bocci, M., and Gomes, V., 2017. Recycling of high percentages of reclaimed asphalt using a bio-rejuvenator – a case study. *In*: *6th Eurasphalt & Eurobitume Congress*. Prague, Czech Republic.

Bocci, E., Mazzoni, G., and Canestrari, F., 2018. Ageing of rejuvenated bitumen in hot recycled bituminous mixtures : influence of bitumen origin and additive type. *Road Mater. Pavement Des.*, 20, S127–S148.

Bocci, E., Mazzoni, G., and Canestrari, F., 2019. Ageing of rejuvenated bitumen in hot recycled bituminous mixtures : influence of bitumen origin and additive type. *Road Materials and Pavement Design*, 20 (sup1: EATA Granada), S127–S148.

Bocci, E. and Prosperi, E., 2020. Analysis of different reclaimed asphalt pavements to assess the potentiality of RILEM cohesion test. *Materials and Structures*, 53 (5).

Bocci, E., Prosperi, E., Mair, V., and Bocci, M., 2020. Ageing and cooling of hot-mix-asphalt during hauling and paving—a laboratory and site study. *Sustainability (Switzerland)*, 12 (20), 1–16.

Bocci, E., Prosperi, E., and Marsac, P., 2020. Rheological modelling of the bitumen from reclaimed asphalt with rejuvenation and re-ageing. *In*: *RILEM International Symposium of Bituminous Materials - Lyon*. Lyon.

De Bock, L., Vansteenkiste, S., and Vanelstraete, A., 2020. *Categorisation and analysis of rejuvenators for asphalt recycling*.

Booij, H.C. and Thoone, G.P.J.M., 1982. General of Kramers-Kronig transforms and some approximations of relations between viscoelastic quantities. *Rheological Acta*, 21, 1–15.

Borghi, A., Jimenez del Barco Carrion, A., Lo Presti, D., and Giustozzi, F., 2017. Effects of laboratory aging on properties of biorejuvenated asphalt binders. *J. Mater. Civ. Eng.*, 29 (10).

Boussingault, J.B., 1837. *Mémoire sur la composition des bitumes, Ann. Chim. Phys, V. 64*.

Branthaver, J.F. Petersen, J.C. Robertson, R.E. Duvall, J.J. Kim, S.S. Harnsberger, P.M. Et Al, 1994. *Binder Characterization and Evaluation – vol. 2 Chemistry, SHRP Report A-368. Washington D. C.: National Research Council*.

Brett, A.., Willis, J.R., and Ross, T.C., 2019. Asphalt Pavement Industry Survey on Recycled Materials and Warm-Mix Asphalt Usage:2018. *Information Series 138 (9th edition).*, 2019 (September).

Cao, X., Wang, H., Cao, X., Sun, W., Zhu, H., and Tang, B., 2018a. Investigation of rheological and chemical properties asphalt binder rejuvenated with waste vegetable oil. *Construction and Building Materials*, 180, 455–463.

Cao, X., Wang, H., Cao, X., Sun, W., Zhu, H., and Tang, B., 2018b. Investigation of rheological and chemical properties asphalt binder rejuvenated with waste vegetable oil. *Construction and Building Materials*, 180, 455–463.

Carpani, C., Bocci, E., and Bocci, M., 2021. Rheological and performance characterisation of the bitumen recovered from different emulsions for cold mixtures. *Road Materials and Pavement Design*, 22, 214–231.

Carpenter, S. and Wolosick, J., 1980. Modifier Influence in the Characterization of Hot-Mix Recycled Material. *In*: *Transportation Research Record 777*. TRB: Washington, DC, USA.

Cavalli, M.C., Mazza, E., Zaumanis, M., and Poulikakos, L.D., 2019. Surface nanomechanical properties of bio-modified reclaimed asphalt binder. *Road Materials and Pavement Design*, 0 (0), 1–17.

Cavalli, M.C., Zaumanis, M., Mazza, E., Partl, M.M., and Poulikakos, L.D., 2018. Effect of ageing on the mechanical and chemical properties of binder from RAP treated with bio-based rejuvenators. *Composites Part B: Engineering*, 141, 174–181.

Celauro, C., Saroufim, E., Mistretta, M.C., and F.P., L.M., 2020. Influence of short-term aging on mechanical properties and morphology of polymer-modified bitumen with recycled plastics from waste materials. *Polymers*, 12 (9), 1–21.

Cerni, G., Bocci, E., Cardone, F., and Corradini, A., 2017. Correlation Between Asphalt Mixture Stiffness Determined Through Static and Dynamic Indirect Tensile Tests. *Arabian Journal for Science and Engineering*, 42 (3), 1295–1303.

Chávez-Valencia, L.E., Manzano-Ramírez, A., Alonso-Guzmán, E., and Contreras-García, M.E., 2007. Modelling of the performance of asphalt pavement using response surface methodology-the kinetics of the aging. *Building and Environment*, 42 (2), 933–939.

Chen, A., Liu, G., Zhao, Y., Li, J., Pan, Y., and Zhou, J., 2018. Research on the aging and rejuvenation mechanisms of asphalt using atomic force microscopy. *Construction and Building Materials*, 167, 177–184.

Chen, J.-S., Chen, S.-F., Liao, M.-C., and Huang Shuo, W., 2015. Laboratory evaluation of asphalt blends of recycling agents mixed with aged binders. *J. Mater. Civ. Eng.*, 27 (4).

Cheraghian, G. and Wistuba, M.., 2021. Effect of Fumed Silica Nanoparticles on Ultraviolet Aging Resistance of Bitumen. *Nanomaterials*, 11 (454).

Cheraghian, G. and Wistuba, M.P., 2020. *Ultraviolet aging study on bitumen modified by a composite of clay and fumed silica na-noparticles." Scientific Reports 10, no. 1*.

Cholewińska, M., Iwański, M., and Mazurek, G., 2018. The impact of ageing on the bitumen stiffness modulus using the CAM model. *The Baltic Journal of Road and Bridge Engineering*, 13 (1), 34–39.

Coffey, S., Dubois, E., Mehta, Y., Nolan, A., and Purdy, C., 2013. Determining the impact of degree of blending and quality of reclaimed asphalt pavement on predicted pavement performance using pavement ME design. *Construction and Building Materials*, 48, 473–478.

Coleri, E. and Sreedhar, S., 2019. Strategies to Improve Performance of Reclaimed Asphalt Pavement- Recycled Asphalt Shingle Mixtures. *International Journal of Pavement Engineering*.

Copeland, A., 2011. *Reclaimed Asphalt Pavement in Asphalt Mixtures: State of the Practice*.

USA.

Corbett, L.W., 1969. Composition of Asphalt Based on Generic Fractionation, Using Solvent Deasphaltening, Elution-Adsorption Chromatography, and Densimetric Characterization. *Analytical Chemistry*, 41 (4), 576–579.

Cortés, C., Pérez-Lepe, A., Fermoso, J., Costa, A., Guisado, F., Esquena, J., and Potti, J.J., 2010. Envejecimiento foto-oxidativo de betunes asfálticos. Comunicación 21,. *In*: *V Jornada Nacional ASEFMA*. 227–238.

Cuciniello, G., Leandri, P., Filippi, S., Lo Presti, D., Polacco, G., Losa, M., and Airey, G., 2021. Microstructure and rheological response of laboratory-aged SBS-modified bitumens. *Road Materials and Pavement Design*, 22 (2), 372 – 396.

Dell'Antonio Cadorin, N. Victor Staub de Melo, J., Borba Broering, W., Luiz Manfro, A., and Salgado Barra, B., 2021. Asphalt nanocomposite with titanium dioxide: Mechanical, rheological and photoactivity performance. *Construction and Building Materials*, 289.

Dharmesh, M., 2015. Use of Recycled Asphalt Pavement in Asphalt Plants. *NBM&CW*.

Ding, Y., Huang, B., and Shu, X., 2018. Blending efficiency evaluation of plant asphalt mixtures using fluorescence microscopy. *Construction and Building Materials*, 161, 461–467.

Dony, A., Colin, J., Bruneau, D., Drouadaine, I., and Navarro, J., 2013. Reclaimed asphalt concretes with high recycling rates: changes in reclaimed binder properties according to rejuvenating agent. *Constr Build Mater*, 41, 175–181.

Dony, A., Ziyani, L., Drouadaine, I., Pouget, S., Faucon-Dumont, S., Simard, D., Mouillet, V., Poirier, J.E., Gabet, T., Boulange, L., Nicolai, A., and Gueit, C., 2017. MURE National Project: FTIR spectroscopy study to assess ageing of asphalt mixtures. *In*: *6th Eurasphalt & Eurobitume Congress*. Prague, Czech Republic.

EAPA, 2018. Asphalt in figures. *In*: *EAPA*. Brussels, Belgium, 1–9.

Ecker, A., 2001. The application of Iatroscan-tecnique for analysis of bitumen. *Petroleum and Coal*, 51–53.

Elkashef, M., Williams, R.C., and Cochran, E.W., 2019. Thermal and cold flow properties of bio-derived rejuvenators and their impact on the properties of rejuvenated asphalt binders. *Thermochim. Acta*, 671, 48–53.

EN 12607-1, 2015. Bitumen and bituminous binders - Determination of the resistance to hardening under the influence of heat and air - Part 1: RTFOT method.

EN 12697-1, 2020. *Bituminous mixtures - Test methods for hot mix asphalt - Part 1: Soluble binder content*.

EN 12697-3, 2019. *Bituminous mixtures - Test methods for hot mix asphalt - Part 3: Bitumen recovery: Rotary evaporator*.

EN 14769, 2013. Bitumen and bituminous binders - Accelerated long-term ageing conditioning by a Pressure Ageing Vessel (PAV).

EN 14770, 2012. *Bitumen and bituminous binders - Determination of complex shear modulus and phase angle - Dynamic Shear Rheometer (DSR)*.

F. Zhou, S. Im, L. Sun, T.S., 2017. Development of an IDEAL Cracking Test for Asphalt Mix Design, Quality Control and Quality Assurance. *Road Mater. Pavement Des.*, 18, 405–427.

Fahrenfort, J. and Visser, W.M., 1962. On the determination of optical constants in the infrared by attenuated total reflection. *Spectrochimica Acta*, 18 (4), 1103–1116.

Farooq, M.A., Mir., M.S., and Sharma, A., 2018. Laboratory study on use of RAP in WMA pavements using rejuvenator. *Constr. Build. Mater.*, 168, 61–72.

Feng, Z., Cai, F., Yao, D., and Li, X., 2021. Aging properties of ultraviolet absorber/SBS modified bitumen based on FTIR analysis. *Construction and Building Materials*, 273.

Fernandes, S.R.M., Silva, H.M.R.D., and Oliveira, J.R.M., 2018. Recycled stone mastic asphalt mixtures incorporating high rates of waste materials. *Constr. Build. Mater.*, 187, 1–13.

Fernández-Gómez, W.D. and Rondón Quintana, H. Reyes, F., 2013. A review of asphalt and asphalt mixture aging. *Ingeniería e Investigación*, 33 (1).

Ferry, J.D., 1980a. *Viscoelastic Properties of Polymers, 3rd Edition*. NY.

Ferry, J.D., 1980b. *Viscoelastic Properties of Polymers, 3rd Edition*.

Fini, E.H., Buabeng, F.S., Abu-Lebdeh, T., and Awadallah, F., 2016. Effect of introduction of furfural on asphalt binder ageing characteristics. *Road Materials and Pavement Design*, 17 (3), 638–657.

Fischer, H.R., Dillingh, E.C., and Hermse, C.G.M., 2014. On the microstructure of bituminous binders. *Road Materials and Pavement Design*, 15 (1), 1–15.

Frolov, I.N., Bashkirceva, N.Y., Ziganshin, M.A., Okhotnikova, E.S., and Firsin, A.A., 2016. The steric hardening and structuring of paraffinic hydrocarbons in bitumen. *Petroleum Science and Technology*, 34 (20), 1675–1680.

Gabrielle do Nascimiento Camargo, I., Hofko, B., Mirwald, J., and Grithe, I., 2020. Effect of Thermal and Oxidative Aging on Asphalt Binders Rheology and Chemical Composition. *Materials*, 13 (4438).

Gaestel, C., Smadja, R., and Lamminan, K.A., 1971. Contribution à la connaissance des propriétés des bitumes routiers. *Rev. Gen. Routes Aérodromes*, 466, 85–95.

Ganter, D., Franzka, S., Shvartsman, V. V., and Lupascu, D.C., 2020. The phenomenon of bitumen 'bee'' structures–bulk or surface layer–a closer look'. *International Journal of Pavement Engineering*, 0 (0), 1–9.

Ganter, D., Mielke, T., Maier, M., and Lupascu, D.C., 2019. Bitumen rheology and the

impact of rejuvenators. *Construction and Building Materials*, 222, 414–423.

Garcia, A., Schlangen, E., van de Ven, M., and Sierra-Beltran, G., 2010. Preparation of capsules containing rejuvenators for their use in asphalt concrete. *J. Hazard. Mater.*, 184 (1), 603–611.

Gergesova, M., Zupančič, B., Saprunov, I., and Emri, I., 2011. The closed form t-T-P shifting (CFS) algorithm. *Journal of Rheology*, 55 (1), 1–16.

Gergesovam, M., Zupančič, B., Saprunov, I., and Emri, I., 2011. The Closed Form t-T-P Shifting (CFS) Algorithm. *Journal of Rheology*, 55, 1–16.

Giavarini, C., 1981. Stability of bitumens produced by thermal processes. *Fuel*, 60 (5), 401–404.

Giavarini, C., 1984. Visbreaker and straight-run bitumens. *Fuel*, 63 (11), 1515–1517.

Giavarini, C. and Saporito, S., 1989. Oxidation of visbreaker bitumens. *Fuel*, 68 (7), 943–946.

Gökalp, I. and Emre Uz, V., 2019. Utilizing of Waste Vegetable Cooking Oil in bitumen: Zero tolerance aging approach. *Construction and Building Materials*, 227.

Golchin, B. and Mansourian, A., 2017. Evaluation of fatigue properties of asphalt mixtures containing reclaimed asphalt using response surface method. *International Journal of Transportation Engineering*, 4 (4), 335–350.

Gong, M., Yang, J., Zhang, J., Zhu, H., and Tong, T., 2016. Physical-chemical properties of aged asphalt rejuvenated by bio-oil derived from biodiesel residue. *Constr. Build. Mater.*, 105, 35–45.

Graziani, A., Bocci, E., and Canestrari, F., 2014. Bulk and shear characterization of bituminous mixtures in the linear viscoelastic domain. *Mechanics of Time-Dependent Materials*, 18 (3), 527–554.

Graziani, A., Mignini, C., Bocci, E., and Bocci, M., 2019. Complex modulus testing and rheological modeling of cold-recycled mixtures. *Journal of Testing and Evaluation*, 48 (1).

Grilli, A., Bocci, E., and Bocci, M., 2015. Hot recycling of reclaimed asphalt using a bio-based additive. *In*: *8th International RILEM-SIB Symposium*. Ancona.

Grilli, A., Bocci, M., Cardone, F., Conti, C., and Giorgini, E., 2013. Laboratory and in-plant validation of hot mix recycling using a rejuvenator. *International Journal of Pavement Research and Technology*, 6 (4), 364–371.

Grilli, A., Iorio Gnisci, M., and Bocci, M., 2017. Effect of ageing process on bitumen and rejuvenated bitumen. *Construction and Building Materials*, 136, 474–481.

Gundla, A. and Underwood, S., 2015. Evaluation of in situ RAP binder interaction in asphalt mastics using micromechanical models. *International Journal of Pavement Engineering*, 18(9), 798–810.

Han, M., Muhammad, Y., Wei, Y., Zhu, Z., Huang, J., and Li, J., 2021. A review on the development and application of graphene based materials for the fabrication of modified asphalt and cement. *Construction and Building Materials*, 285.

Hao, G., Huang, W., Yuan, J., Tang, N., and Xiao, F., 2017. Effect of aging on chemical and rheological properties of SBS modified asphalt with different compositions. *Construction and Building Materials*, 156, 902–910.

Hesp, S.A.M., Iliuta, S., and Shirokoff, J.W., 2007. Reversible aging in asphalt binders. *Energy and Fuels*, 21 (2), 1112–1121.

Hofko, B., Cannone Falchetto, A., Grenfell, J., Huber, L., Lu, X., Porot, L., Poulikakos, L.D., and You, Z., 2017. Effect of short-term ageing temperature on bitumen properties. *Road Materials and Pavement Design*, 18 (March), 108–117.

Hofko, B., Eberhardsteiner, L., Füssl, J., Grothe, H., Handle, F., Hospodka, M., Grossegger, D., Nahar, S.N., Scarpas, A., and M., S.J., 2016. Impact of maltene and asphaltene fraction on mechanical behavior and microstructure of bitumen. *Materials and Structures*, 49, 829–841.

Hofko, B., Falchetto, A.C., Grenfell, J., Huber, L., Lu, X., Porot, L., You, Z., Falchetto, A.C., Grenfell, J., Huber, L., Lu, X., and Porot, L., 2017. Effect of short-term ageing temperature on bitumen properties. *Road Materials and Pavement Design*, 18 (Sup2: EATA2017), 108–117.

Holýa, M. and Remišováa, E., 2019. Analysis of influence of bitumen composition on the properties represented by empirical and viscosity test. *Transportation Research Procedia*, 40, 34–41.

Hou, X., Lv, S., Chen, Z., and Xiao, F., 2018. Applications of Fourier transform infrared spectroscopy technologies on asphalt materials. *Measurement: Journal of the International Measurement Confederation*, 121 (March), 304–316.

Huang, B., Li, G., Vukosavljevic, D., Shu, X., and Egan, B., 2005. Laboratory Investigation of Mixing Hot-Mix Asphalt with Reclaimed Asphalt Pavement. *In*: *Transportation Research Record 1929*. TRB: Washington, DC, USA.

Hugener, M., Partl, M.N., and Morant, M., 2014. Cold asphalt recycling with 100% reclaimed asphalt pavement and vegetable oil-based rejuvenators. *Road Mater. Pavement Design*, 15(2), 239–258.

Hunter, R.., Self, A., and Read, J., 2015. *The Shell Bitumen Handbook, Sixth edition*. UK.

Ingrassia, L.P., Lu, X., Ferrotti, G., Conti, C., and Canestrari, F., 2020. Investigating the "circular propensity" of road bio-binders: Effectiveness in hot recycling of reclaimed asphalt and recyclability potential. *Journal of Cleaner Production*, 255.

Joni, H.H., Al-Rubaee, R.H.A., and Al-zerkani, M.A., 2019. Rejuvenation of aged asphalt binder extracted from reclaimed asphalt pavement using waste vegetable and engine oils. *Case Studies in Construction Materials*, 11, e00279.

Kamil Arshad, A., Awang, H., Shaffie, E., Hashim, W., and Abd Rahman, Z., 2018. Performance Evaluation of Hot Mix Asphalt with Different Proportions of RAP Content. *E3S Web of Conferences*, 34, 1–8.

Karki, P. and Zhou, F., 2016. Effect of Rejuvenators on Rheological, Chemical, and Aging Properties of Asphalt Binders Containing Recycled Binders. *Transportation Research Record: Journal of the Transportation Research Board*, 2574, 74–82.

Karlsson, R. and Isacsson, U., 2003a. Application of FTIR-ATR to Characterization of Bitumen Rejuvenator Diffusion. *Journal of Materials in Civil Engineering*, 15 (2), 157–165.

Karlsson, R. and Isacsson, U., 2003b. Investigations on Bitumen Rejuvenator Diffusion and Structural Stability. *Asphalt Paving Technology: Association of Asphalt Paving Technologists-Proceedings of the Technical Sessions*, 72, 463–501.

Karlsson, R. and Isacsson, U., 2006. Material-related aspects of asphalt recycling - State-of-the-art. *Journal of Materials in Civil Engineering*, 18 (1), 81–92.

Kaseer, F., Arámbula-Mercado, E., and Martin, A.E., 2019. A Method to Quantify Reclaimed Asphalt Pavement Binder Availability (Effective RAP Binder) in Recycled Asphalt Mixes. *Transportation Research Record: Journal of the Transportation Research Board*.

Van Den Kerkhof, E., 2015. Warm waste asphalt recycling in Belgium—30 years of experience and full confidence in the future. *In*: *5th Eurasphalt & Eurobitume Congress,*. Instambul, Turkey.

Kezhen, Y., Yang, P., and Lingyun, Y., 2020. Use of tung oil as a rejuvenating agent in aged asphalt: Laboratory evaluations. College of Civil Engineering, Hunan University, Changsha 410082, China.

Khan, R., Grenfell, J., Collop, A., Airey, G., and Gregory, H., 2013a. Moisture damage in asphalt mixtures using the modified SATS test and image analysis. *Construction and Building Materials*, 43, 165–173.

Khan, R., Grenfell, J., Collop, A., Airey, G., and Gregory, H., 2013b. Moisture damage in asphalt mixtures using the modified SATS test and image analysis. *Construction and Building Materials*, 43, 165–173.

Khodadadi, M., Moradi, L., Dabir, B., Moghadas Nejad, F., and Khodaii, A., 2020. Reuse of drill cuttings in hot mix asphalt mixture: A study on the environmental and structure performance. *Construction and Building Materials Volume 256, 30 September 2020, 119453*, 256 (30).

King, G., Anderson, M., Hanson, D., and Blankenship, P., 2012. Using black space diagrams to predict Age-induced cracking. *7th RILEM International Conference on Cracking in Pavements*, 453–463.

Kleiziene, R., Panasenkiene, M., and Vaitkus, A., 2019. Effect of aging on chemical

composition and rheological properties of neat and modified bitumen. *Materials*, 12 (24).

de Klerk, A., 2020. *Unconventional oil: Oilsands*. Future Energy: Improved, Sustainable and Clean Options for Our Planet. Elsevier Ltd.

Koots, J.A. and Speight, J.G., 1975. Relation of petroleum resins to asphaltenes. *Fuel*, 54 (3), 179–184.

Koudelka, T., Coufalik, P., Fiedler, J., Coufalikova, I., Varaus, M., and Yin, F., 2019. Rheological evaluation of asphalt blends at multiple rejuvenation and aging cycles. *Road Materials and Pavement Design*, 20 (sup:1), 3–18.

Kowalski, J.K., Krol, B.J., Bankowski, W., Radziszewski, P., and Sarnowski, M., 2017. Thermal and fatigue evaluation of asphalt mixtures containing RAP treated with a bio-agent. *Appl. Sci.*, 7 (3), 2016.

Krishnan, J.M. and Rajagopal, K.R., 2003. Review of the uses and modeling of bitumen from ancient to modern times. *Applied Mechanics Reviews*, 56 (2), 149–214.

Król, J.B., Kowalski, K.J., Niczke, L., and Radziszewski, P., 2016. Effect of bitumen fluxing using a bio-origin additive. *Constr. Build. Mater.*, 114, 194–203.

Kuchiishi, A.K., Vasconcelos, K., and Bariani Bernucci, L.L., 2019. Effect of mixture composition on the mechanical behaviour of cold recycled asphalt mixtures. *International Journal of Pavement Engineering*, 0 (0), 1–11.

Lamontagne, J., Dumas, P., Mouillet, V., and Kister, J., 2001. Comparison by Fourier transform infrared (FTIR) spectroscopy of different ageing techniques: Application to road bitumens. *Fuel*, 80 (4), 483–488.

Lee, C., Terrel, R., and Mahoney, J., 1983. Test for Efficiency of Mixing of Recycled Asphalt Paving Mixtures. *In*: *Transportation Research Record 911*. TRB: Washington, DC, USA.

Lee, J., Denneman, E., and Choi, Y., 2015. *Maximising the Re-use of Reclaimed Asphalt Pavement - Outcomes of Year Two: RAP Mix Design; Technical Report AP-T286-15*. Sydney, Australia.

Lee, N., Chou, C.P., and Chen, K.Y., 2012. Benefits in energy savings and CO2 reduction by using reclaimed asphalt pavement. *In*: *Transportation Research Board 91st Annual Meeting*.

Leroy, G., 1989. Bitumen analysis by thin layer chromatography (IATROSCAN). *In*: *4th Eurobitume Congress*. Madrid.

Lesueur, D., 2009. The colloidal structure of bitumen: Consequences on the rheology and on the mechanisms of bitumen modification. *Advances in Colloid and Interface Science*, 145 (1–2), 42–82.

Lesueur, D., Gerard, J., Claudy, P., Letoffe, J., Planche, J., and Martin, D., 1996. A structure-

related model to describe asphalt linear viscoelasticity. *Journal of Rheology*, 40 (5), 813–836.

Li, H., Dong, B., Wang, W., Zhao, G., Guo, P., and Ma, Q., 2019. Effect of Waste Engine Oil and Waste Cooking Oil on Performance Improvement of Aged Asphalt. *Applied Sciences*.

Li, Z., Fa, C., Zhao, H., Zhang, Y., Chen, H., and Xie, H., 2020. Investigation on evolution of bitumen composition and micro-structure during aging. *Construction and Building Materials*, 244, 118322.

Lin, P., Liu, X., Apostolidis, P., Erkens, S., Ren, S., Xu, S., Scarpas, T., and Huang, W., 2021. On the rejuvenator dosage optimization for aged SBS modified bitumen. *Construction and Building Materials*, 271.

De Lira, R.R., Cortes, D.D., and Pasten, C., 2015. Reclaimed asphalt binder aging and its implications in the management of RAP stockpiles. *Construction and Building Materials*, 101, 611–616.

Liu, H., Fu, L., Jiao, Y., Tao, J., and Wang, X., 2017. Short-Term Aging Effect on Properties of Sustainable Pavement Asphalts Modified by Waste Rubber and Diatomite. *Sustainability*, 9 (996).

Loise, V., Caputo, P., Porto, M., Calandra, P., Angelico, R., and Rossi, C.O., 2019. A review on Bitumen Rejuvenation: Mechanisms, materials, methods and perspectives. *Applied Sciences (Switzerland)*, 9 (20).

Lolly, R., Zeiada, W., Souliman, M., and Kaloush, K., 2017. Effects of Short-Term Aging on Asphalt Binders and Hot Mix Asphalt at Elevated Temperatures and Extended Aging Time, 07010.

Lu, H., Talon, Y., and Redelius, P., 2008. Aging of bituminous binders – laboratory tests and field data. *In*: *4th Euroasphalts and Eurobitumen Congress, European Asphalt Pavement Assotiation*.

Lu, X. and Isacsson, U., 2002. Effect of ageing on bitumen chemistry and rheology. *Construction and Building Materials*, 16, 15–22.

Lu, X., Langton, M., Olofsson, P., and Redelius, P., 2005. Wax morphology in bitumen. *Journal of Materials Science*, 40, 1893–1900.

Lu, X., Sjövall, P., Soenen, H., Blom, J., and Makowska, M., 2021. Oxidative aging of bitumen: a structural and chemical investigation. *Road Materials and Pavement Design*.

Ma, X., Leng, Z., Wang, L., and Zhou, P., 2020. Effect of reclaimed asphalt pavement heating temperature on the compactability of recycled hot mix asphalt. *Materials*, 13 (16), 1–13.

Madrigal, D.P., Iannone, A., Martìnez, A.H., and Giustozzi, F., 2017. Effect of mixing time and temperature on cracking resistance of bituminous mixtures containing reclaimed

asphalt pavement material. *Journal of Materials in Civil Engineering*, 29 (8).

Maharaj, R., Harry, V., and Mohamed, N., 2015. The rheological properties of Trinidad asphaltic materials blended with waste cooking oil. *Prog. Rubber Plast. Recycl. Technol.*, 31(4), 265–279.

Al Mamun, A., Wahhab, A.H.I., and Dalhat, M.A., 2020. Comparative Evaluation of Waste Cooking Oil and Waste Engine Oil Rejuvenated Asphalt Concrete Mixtures. *Arabian Journal for Science and Engineering*, 45 (10), 7987–7997.

Mangiafico, S., Sauzéat, C., Di Benedetto, H., Pouget, S., Olard, F., Planque, L., and VanRooijen, R., 2014. Statistical analysis of influence of mix design parameters on mechanical properties of mixes with reclaimed asphalt pavement. *Transportation Research Record: Journal of the Transportation Research Board, No 2445*, 29–38.

Mannan, U.A., Islam, M.R., and Tarefder, R.A., 2015a. Effects of recycled asphalt pavements on the fatigue life of asphalt under different strain levels and loading frequencies. *International Journal of Fatigue*, 78, 72–80.

Mannan, U.A., Islam, R., and Tarefder, R.A., 2015b. Fatigue Behavior of Asphalt Containing Reclaimed Asphalt Pavements Effects of recycled asphalt pavements on the fatigue life of asphalt under different strain levels and loading frequencies. *INTERNATIONAL JOURNAL OF FATIGUE*, 78 (May), 72–80.

Martinez, G. and Caicedo, B., 2005. Asfalticas, Efecto de la radiacion ultravioleta en el envejecimiento de ligantes y mezclas. *In*: *Congresso Ibero-Latinoamericano del Asfalto CILA XIII*. San Josè de Costa Rica.

Masson, J.F., Leblond, V., and Margeson, J., 2006. Bitumen morphologies by phase-detection atomic force microscopy. *Journal of Microscopy*, 221 (1), 17–29.

Masson, J.F., Price, T., and Collins, P., 2001. Dynamics of bitumen fractions by thin-layer chromatography/flame ionization detection. *Energy and Fuels*, 15 (4), 955–960.

Mastrofini, D. and Scarsella, M., 2000. The application of rheology to the evaluation of bitumen ageing. *Fuel*, 79.

Mazzoni, G., Bocci, E., and Canestrari, F., 2018a. Influence of rejuvenators on bitumen ageing in hot recycled asphalt mixtures. *Journal of Traffic and Transportation Engineering (English Edition)*, 5 (3), 157–168.

Mazzoni, G., Bocci, E., and Canestrari, F., 2018b. Influence of rejuvenators on bitumen ageing in hot recycled asphalt mixtures. *Journal of Traffic and Transportation Engineering (English Edition)*, 5 (3).

Menapace, I., Garcia Cucalon, L., Kaseer, F., Arámbula-Mercado, E., Epps Martin, A., Masad, E., and King, G., 2018. Effect of recycling agents in recycled asphalt binders observed with microstructural and rheological tests. *Construction and Building Materials*, 158, 61–74.

Mikhailenko, P., Bertron, A., and Ringot, E., 2016a. Methods for analyzing the chemical

mechanisms of bitumen aging and rejuvenation with FTIR spectrometry. *RILEM Bookseries*, 11 (October), 203–214.

Mikhailenko, P., Bertron, A., and Ringot, E., 2016b. Methods for Analyzing the Chemical Mechanisms of Bitumen Aging and Rejuvenation with FTIR Spectrometry. *In*: *8th RILEM International Symposium on Testing and Characterization of Sustainable and Innovative Bituminous Materials. RILEM Bookseries, vol. 11*. doi:10.1007/978-94-017-7342-3_17.

Milad, A., Taib, A.M., Ahmeda, A.G.F., Solla, M., and Yusoff, N.I.M., 2020. A review of the use of reclaimed asphalt pavement for road paving applications. *Jurnal Teknologi*, 82 (3), 35–45.

Miró, R., Martínez, A.H., Moreno-Navarro, F., and Rubio-Gámez, C., 2015. Effect of ageing and temperature on the fatigue behaviour of bitumens. *Materials and Design*, 86, 129–137.

Mirwald, J., Werkovits, S., Camargo, I., Maschauer, D., Hofko, B., and Grothe, H., 2020. Understanding bitumen ageing by investigation of its polarity fractions. *Construction and Building Materials*, 250, 118809.

Mogawer, W., Bennert, T., Daniel, J.S., Bonaquist, R., Austerman, A., and Booshehrian, A., 2012. Performance characteristics of plant produced high RAP mixtures. *Road Materials and Pavement Design*, 13 (SUPPL. 1), 183–208.

Mogawer, W.S., Austerman, A., Roque, R., Underwood, S., Mohammad, L., and Zou, J., 2015. Ageing and rejuvenators: evaluating their impact on high RAP mixtures fatigue cracking characteristics using advanced mechanistic models and testing methods. *Road Mater. Pavement Des.*, 16 (Suppl., 1–28.

Mogawer, W.S., Stuart, K.D., Austerman, A., and Ahmed, S., 2020. Influence of Reclaimed Asphalt Pavement (RAP) Source and Virgin Binder Source on RAP Specifications and Balanced Mix Design. *In*: *Association of Asphalt Paving Technologist (AAPT) - 95th Annual Meeting*.

Mohajeri, M., Molenaar, A.A.A., and van de Ven, M.F.C., 2016. Blending simulation of RA and virgin binders in hot recycled mixtures. *RILEM Bookseries*, 11, 891–901.

Mokhtari, A., David Lee, H., Williams, R.C., Guymon, C.A., Sholte, J.P., and Schram, S., 2017. A novel approach to evaluate fracture surfaces of aged and rejuvenator-restored asphalt using cryo-SEM and image analysis techniques. *Constr. Build. Mater.*, 133, 301–313.

Moretti, L., Fabrizi, N., Fiore, N., and D'andrea, A., 2021. Mechanical characteristics of graphene nanoplatelets-modified asphalt mixes: A comparison with polymer-and not-modified asphalt mixes. *Materials*, 14 (91).

Mortazavi, M. and Moulthrop, J.S., 1993. The SHRP Materials Reference Library, SHRP Report A-646, 228.

Mouillet, V., Lamontagne, J., Durrieu, F., Planche, J.P., and Lapalu, L., 2008. Infrared microscopy investigation of oxidation and phase evolution in bitumen modified with polymers. *Fuel*, 87 (7), 1270–1280.

Nayak, P. and Sahoo, U.C., 2017. A rheological study on aged binder rejuvenated with Pongamia oil and Composite castor oil. *Int. J. Pavement Eng.*, 18 (7), 595–607.

NCHRP 01-37A, 2004. *Guide for mechanistic-empirical design of new and rehabilitated pavement structures*.

Nellensteyn, F.J., 1924. The constitution of asphalt. *J Inst Pet Technol*, 10, 311–325.

Newcomb, D.E., Brown, E.R., and Epps, J.A., 2007. *Designing HMA Mixtures with High RAP Content: A Practical Guide*. NAPA: Lanham, MD, USA.

Nivitha, M.R., Prasad, E., and Krishnan, J.M., 2015. Ageing in modified bitumen using FTIR spectroscopy Ageing in modified bitumen using FTIR spectroscopy. *International Journal of Pavement Engineering*, 17 (7), 565–577.

Noor, L., Wasiuddin, N.M., Mohammad, L.N., and Salomon, D., 2020. Use of Fourier Transform Infrared (FT-IR) Spectroscopy to Determine the Type and Quantity of Rejuvenator Used in Asphalt Binder. *Recent Developments in Pavement Engineering. GeoMEast 2019. Sustainable Civil Infrastructures*, 1, 70–84.

Norouzi, A., Sabouri, M., and Kim, Y.R., 2014. Evaluation of the fatigue performance of asphalt mixtures with high RAP content. *Journal of Tylor and Francis Group*, 1069–1077.

Noureldin, S. and Wood, L., 1987. Rejuvenator Diffusion in Binder Film for Hot-Mix Recycled Asphalt Pavement. *In*: *Transportation Research Record 1115*. TRB: Washington, DC, USA.

Nsengiyumva, G., Haghshenas, H.F., Kim, Y., and Kommidi, S.R., 2020. Mechanical-Chemical Characterization of the Effects of Type , Dosage , and Treatment Methods of Rejuvenators in Aged Bituminous Materials. *Transportation Research Record: Journal of the Transportation Research Board*, 2674 (3), 126–138.

Ogbo, C., Kaseer, F., Oshone, M., Sias, J.E., and Martin, A.E., 2019. Mixture-based rheological evaluation tool for cracking in asphalt pavements. *Road Materials and Pavement Design*, 20 (sup1), S299–S314.

Olard, F.. and M.R.M. a and Di Benedetto, H., 2003a. General "2S2P1D" Model and Relation Between the Linear Viscoelastic Behaviours of Bituminous Binders and Mixes. *Road Materials and Pavement Design*, 4(2), 185–224.

Olard, F. and Di Benedetto, H., 2003b. General "2S2P1D" Model and Relation Between the Linear Viscoelastic Behaviours of Bituminous Binders and Mixes. *Road Materials and Pavement Design*, 4 (2), 185–224.

Oliver, J., 1975. Diffusion of Oil sin Asphalts; Report No. 9. *In*: *Australian Road Research Board*. Vermont South, Victoria, Australia.

Ongel, A. and Hugener, M., 2015. Impact of rejuvenators on aging properties of bitumen. *Construction and Building Materials*, 94, 467–474.

Osmari, P.H., Aragao, F.T.S., Leite, L.F.M., Simao, R.A., da Motta, L.M.G., and Kim, Y.-R., 2017. Chemical, microstructural, and rheological characterization of binders to evaluate aging and rejuvenation. *Transport. Res. Rec.*, 2632 (1), 14–24.

Ozer, H., Al-Qadi, I.L., Carpenter, S.H., Aurangzeb, Q., Roberts, G.L., and Trepanier, J., 2009. Evaluation of RAP impact on hot-mix asphalt design and performance. *Asphalt Paving Technology: Association of Asphalt Paving Technologists-Proceedings of the Technical Sessions*, 78, 317–348.

Pahlavan, F., Hung, A.M., Zadshir, M., Hosseinnezhad, S., and Fini, E.H., 2018. Alteration of π-Electron Distribution to Induce Deagglomeration in Oxidized Polar Aromatics and Asphaltenes in an Aged Asphalt Binder. *ACS Sustainable Chemistry and Engineering*, 6 (5), 6554–6569.

Pahlavan, F., Mousavi, M., Hung, A.M., and Fini, E.H., 2018. Characterization of oxidized asphaltenes and the restorative effect of a bio-modifier. *Fuel*, 212, 593–604.

Pahlavan, F., Samieadel, A., Deng, S., and Fini, E., 2019. Exploiting Synergistic Effects of Intermolecular Interactions to Synthesize Hybrid Rejuvenators to Revitalize Aged Asphalt. *ACS Sustainable Chemistry and Engineering*, 7 (18), 15514–15525.

Paliukaitė, M., Vaitkus, A., and Zofka, A., 2014. Evaluation of bitumen fractional composition depending on the crude oil type and production technology. *9th International Conference on Environmental Engineering, ICEE 2014*, (January).

Pellinen, T.., Witczak, M.W., and Bonaquist, R.F., 2002. Asphalt Mix Master Curve Construction using Sigmoidal Fitting Function with Non-Linear Least Squares Optimization Technique. *In*: *Proceedings of 15th ASCE Engineering Mechanics Conference*.

Petersen, J.C., 1984. Chemical Composition of Asphalt As Related To Asphalt Durability: State of the Art. *Transportation Research Record*, 13–30.

Petersen, J.C., 2009. Review of the Fundamentals of Asphalt Oxidation: Chemical, Physicochemical, Physical Property, and Durability Relationships. *TRB Transportation Research Circular E-C140 - Transportation Research Board*.

Pfeiffer, J.P. and Saal, R.N.J., 1940. Asphaltic bitumen as colloid systems. *The Journal of Physical Chemistry*, 44, 139–149.

Polacco, G., Filippi, S., Merusi, F., and Stastna, G., 2015. A review of the fundamentals of polymer-modified asphalts: Asphalt/polymer interactions and principles of compatibility. *Advances in Colloid and Interface Science*, 224, 72–112.

Poulikakos, L.D., Cannone Falchetto, A., Wang, D., Porot, L., and Hofko, B., 2019. Impact of asphalt aging temperature on chemo-mechanics. *RSC Advances*, 11602–11613.

Lo Presti, D., Vasconcelos, K., Orešković, M., Pires, G.M., and Bressi, S., 2020. On the

degree of binder activity of reclaimed asphalt and degree of blending with recycling agents. *Road Materials and Pavement Design*, 21 (8), 2071–2090.

Priyadharshini, Y., Maheshwari, S., Padmarekha, A., and Krishnan, J.M., 2013. Effect of Mixing and Compaction Temperature on Dynamic Modulus of Modified Binder Bituminous Mixtures. *Procedia - Social and Behavioral Sciences*, 104, 12–20.

Radenberg, M., Boetcher, S., and Sedaghat, N., 2016. Effect and efficiency of rejuvenators on aged asphalt binder German experiences. *In*: *6th Eurasphalts and Eurobitume Congress*. Prague, Czech Republic.

Ragni, D., Ferrotti, G., Lu, X., and Canestrari, F., 2019. Influence of chemical additives for warm mix asphalts on the short-term ageing of a plain bitumen. *Road Materials and Pavement Design*, 20 (sup1), S34–S48.

Rathore, M., Zaumanis, M., and Haritonovs, V., 2019. Asphalt Recycling Technologies: A Review on Limitations and Benefits. *IOP Conference Series: Materials Science and Engineering*, 660 (012046).

Redelius, P. and Soenen, H., 2015. Relation between bitumen chemistry and performance. *Fuel*, 140, 34–43.

Reyes-Ortiz, O., Berardinelli, E., Alvarez, A.E., Carvajal-Muñoz, J.S., and Fuentes, L.G., 2012. Evaluation of Hot Mix Asphalt Mixtures with Replacement of Aggregates by Reclaimed Asphalt Pavement (RAP) Material. *Procedia - Social and Behavioral Sciences*, 53, 379–388.

Richards, F.J., 1959. A Flexible Growth Function for Empirical Use. *Journal of Experimental Botany*, 10 (29), 290–300.

Richardson, C., 1910. *The Modern Asphalt Pavement, 2nd Ed.*

Roberts, F.L., Kandhal, P.S., Brown, E.R., Lee, D.Y., and Kennedy, T.W., 1996a. *Hot Mix Asphalt Materials, Mixture Design and Construction. 2nd Ed.*

Roberts, F.L., Kandhal, P.S., Brown, E.R., Lee, D.Y., and Kennedy, T.W., 1996b. *Hot Mix Asphalt Materials, Mixture Design and Construction, 2nd ed.* USA.

Rodriguez-Fernandez, I., Cavalli, M.C., Poulikakos, L., and M., B., 2020. Recyclability of asphalt mixtures with crumb rubber incorporated by dry process: A laboratory investigation. *Materials*, 13 (12).

Romera, R., Santamaria, A., Pena, J., Munoz, M., Barral, M., Garcia, E., and Janez, V., 2006. Rheological aspects of the rejuvenation of aged bitumen. *Rheol. Acta*, 45 (4), 474–478.

Rosinger, A., 1914. Beiträge zur Kolloidchemie des Asphalts. *Kolloid-Z*, 15, 177–179.

Rostler, F.S., 1965. *Fractional Composition: Analytical and Functional Significance. In Bituminous Materials: Asphalts, Tars, and Pitches*. Vol. 2. New York.

Rowe, G., 2009. Phase angle determination and interrelationships within bituminous materials. *Proceedings of 7th International RILEM Symposium on Advanced Testing*

and Characterization of Bituminous Materials, Rhodes, Greece, (1), 43–52.

Rowe, G., Barry, J., and Crawford, K., 2016. Evaluation of a 100% Rap Recycling Project in Fort Wayne, Indiana. *8th RILEM International Symposium on Testing and Characterization of Sustainable and Innovative Bituminous Materials*, 941–951.

Rowe, G., Baumgardner, G., and Sharrock, M., 2009. Functional forms for master curve analysis of bituminous materials. *Proceedings of 7th International RILEM Symposium on Advanced Testing and Characterization of Bituminous Materials, Rhodes, Greece*, (1), 81–92.

Rowe, G.M., King, G., and Anderson, M., 2014. The Influence of Binder Rheology on the Cracking of Asphalt Mixes in Airport and Highway Projects. *Journal of Testing and Evaluation*, 42(5).

Rzek, L., Ravnikar Turk, M., and Marjan, T., 2020. Increasing the rate of reclaimed asphalt in asphalt mixture by using alternative rejuvenator produced by tire pyrolysis. *Construction and Building Materials*, 232.

Sá-da-Costa, M., António Correia, D., and Farcas, F., 2017. Life cycle of bitumen: ageing-regeneration-ageing. *In*: *6th Eurasphalts and Eurobitume Congress*. Prague, Czech Republic.

Santagata, E., Baglieri, O., Dalmazzo, D., and Tsantilis, L., 2016. Experimental investigation on the combined effects of physical hardening and chemical ageing on low temperature properties of bituminous binders. *RILEM Bookseries*, 11, 631–641.

dos Santos, S., Partl, M.N., and Poulikakos, L., n.d. Newly observed effects of water on the microstructures of bitumen surface. *Construction and Building Materials*, 71, 618–627.

Santos, S. Dos, Poulikakos, L.D., and Partl, M.N., 2016. Crystalline structures in tetracosane-asphaltene films. *RSC Advances*, 6 (47), 41561–41567.

Sarnowski, M., Kowalski, K.J., Król, J.B., and Radziszewski, P., 2019. Influence of overheating phenomenon on bitumen and asphalt mixture properties. *Materials*, 12 (4).

Sayegh, G., 1967. Viscoelastic Properties of Bituminous Mixtures. *In*: *2nd International Conference on Structural Design of Asphalt Pavements*. Ann Arbor, MI, 743–755.

Sharma, M.K. and Yen, T.F., 1994. *Asphaltene Particles in Fossil Fuel Exploration, Recovery, Refining, and Production Processes*.

Shirodkar, P., Mehta, Y., Nolan, A., Dubois, E., Reger, D., and McCarthy, L., 2013. Development of blending chart for different degrees of blending of RAP binder and virgin binder. *Resources, Conservation and Recycling*, 73, 156–161.

Shirodkar, P., Mehta, Y., Nolan, A., Sonpal, K., Norton, A., Tomlinson, C., and Sauber, R., 2011. A study to determine the degree of partial blending of reclaimed asphalt pavement (RAP) binder for high RAP hot mix asphalt. *Construction and Building Materials*, 25(1), 150–155.

Siddiqui, M.N. and Ali, M.F., 1999. Studies on the aging behavior of the Arabian asphalts. *Fuel*, 78 (9), 1005–1015.

Solanki, P., Zaman, M., Adje, D., and Hossain, Z., 2015. Effect of Recycled Asphalt Pavement on Thermal Cracking Resistance of Hot-Mix Asphalt. *Int. J. Geomech*, 15, 1–9.

Somé, C., Pavoine, A., Chailleux, E., Andrieux, L., DeMArco, L., Philippe Da, S., and Stephan, B., 2016. Rheological behaviour of vegetable oil-modified asphaltite binders and mixes. *In*: *6th Eurasphalt & Eurobitume Congress*. Prague, Czech Republic.

Speight, J.G., 2004. Petroleum asphaltenes. Part 1. Asphaltenes, resins and the structure of petroleum. *Oil Gas Science Technology*, 59, 467–477.

Speight, J.G., 2012. Visbreaking: A technology of the past and the future. *Scientia Iranica*, 19 (3), 569–573.

Stimilli, A., Virgili, A., and Canestrari, F., 2015. New method to estimate the "re-activated" binder amount in recycled hot-mix asphalt. *Road Materials and Pavement Design*, 16(sup1), 442–459.

Struik, L., 1978. *Physical Hardening in Amorphous Polymers and Other Materials*.

Sun, G., Li, B., Sun, D., Yu, F., and Hu, M., 2021. Chemo-rheological and morphology evolution of polymer modified bitumens under thermal oxidative and all-weather aging. *Fuel*, 285.

Tabaković, A., Gibney, A., McNally, C., and Gilchrist, M.D., 2010. Influence of recycled asphalt pavement on fatigue performance of asphalt concrete base courses. *Journal of Materials in Civil Engineering*, 22, 643–650.

Tabatabaee, H.A. and Kurth, T.L., 2017a. Analytical investigation of the impact of a novel bio-based recycling agent on the colloidal stability of aged bitumen. *Road Materials and Pavement Design*, 0 (0), 1–10.

Tabatabaee, H.A. and Kurth, T.L., 2017b. Analytical investigation of the impact of a novel bio-based recycling agent on the colloidal stability of aged bitumen. *Road Materials and Pavement Design*, 18 (Sup2:EATA 2017), 131–140.

Tachon, N., 2008. Nouveaux types de liants routiers a hautes performances, a teneur en bitume reduite par addition de produits organiques issus des agroressources. Doctoral Thesis. L'Institut National Polytechnique de Toulouse, France.

Tarpoudi Baheri, F., Rico Luengo, M., Schutzius, T.M., Poulikakos, D., and Poulikakos, L.D., 2020. The effect of additives on water condensation on bituminous surfaces. *In*: *ISBM Lyon*.

Tarsi, G., Tataranni, P., and Sangiorgi, C., 2020. The challenges of using reclaimed asphalt pavement for new asphalt mixtures: A review. *Materials*, 13 (18).

Tarsi, G., Varveri, A., Lantieri, C., Scarpas, A., and Sangiorgi, C., 2018. Effects of Different

Aging Methods on Chemical and Rheological Properties of Bitumen. *Journal of Materials in Civil Engineering*, 30 (3), 04018009.

Tauste, R., Moreno-Navarro, F., Sol-Sánchez, M., and Rubio-Gámez, M.C., 2018. Understanding the bitumen ageing phenomenon: A review. *Construction and Building Materials*, 192, 593–609.

Tebaldi, G., Dave, E., Marsac, P., Muraya, P., Hugener, M., Pasetto, M., Graziani, A., and Grilli, A., 2012. Classification of recycled asphalt pavement (RAP) material. *In*: *2nd International Symposium on Asphalt Pavement & Environment,*. Fortaleza, Brasil.

Tebaldi, G., Dave, E. V., Cannone Falchetto, A., Hugener, M., Perraton, D., Grilli, A., Lo Presti, D., Pasetto, M., Loizos, A., Jenkins, K., Apeagyei, A., Grenfell, J., and Bocci, M., 2018. Recommendation of RILEM TC237-SIB: protocol for characterization of recycled asphalt (RA) materials for pavement applications. *Materials and Structures/Materiaux et Constructions*, 51 (6), 1–8.

Themeli, A., Chailleux, E., Farcas, F., Chazallon, C., and Migault, B., 2015a. Molecular weight distribution of asphaltic paving binders from phase- angle measurements. *Road Mater. Pavement Des.*, 16(S1), 228–244.

Themeli, A., Chailleux, E., Farcas, F., Chazallon, C., and Migault, B., 2015b. Molecular weight distribution of asphaltic paving binders from phase- angle measurements, 16 (S1), 228–244.

Thurston, R.R. and Knowles, E.C., 1941. Asphalt and Its Constituents. Oxidation at Service Temperatures. *Industrial & Engineering Chemistry*, 33 (3), 320–324.

Tran, N., Taylor, A., and Willis, R., 2012. *Effect of Rejuvenator on Performance Properties of HMA Mixtures with High RAP and RAS Contents: NCAT Report 12-05*. ; National Center for Asphalt Technology: Auburn, AL, USA.

Traxler, R.R., 1963. Durability of asphalts cements. *In*: *Asphalt Paving Technol. 32*. 44–58.

Underwood, B., Baek, C., and Kim, Y., 2012. Simplified viscoelastic continuum damage model as platform for asphalt concrete fatigue analysis. *Transportation Research Record*, (2296), 36–45.

Vassaux, S., Gaudefroy, V., Boulangé, L., Pevere, A., Michelet, A., Barragan-Montero, V., and Mouillet, V., 2019. Assessment of the binder blending in bituminous mixtures based on the development of an innovative sustainable infrared imaging methodology. *Journal of Cleaner Production*, 215, 821–828.

Vassaux, S., Gaudefroy, V., Boulangé, L., Soro, L.J., Pévère, A., Michelet, A., and Mouillet, V., 2018. Study of remobilization phenomena at reclaimed asphalt binder/virgin binder interphases for recycled asphalt mixtures using novel microscopic methodologies. *Construction and Building Materials*, 165, 846–858.

Vukosavljevic, D., 2006. Fatigue characteristics of field HMA surface mixtures containing recycled asphalt pavement (RAP). University of Tennessee.

Walther, A., Cannone Falchetto, A., and Wang, D., 2020. Performance Characteristics of in Plant Mixed Stone Mastic Asphalt SMA Using Different Rejuvenators. *In*: *Asphalt Paving Technology: Association of Asphalt Paving Technologists-Proceedings of the Technical Sessions*.

Wang, H., Lu, G., Feng, S., Wen, X., and Yang, J., 2019. Characterization of Bitumen Modified with Pyrolytic Carbon Black from Scrap Tires. *Sustainability*, 11, 16–31.

West, R.C., 2010. Reclaimed Asphalt Pavement Management: Best Practices. *In*: *National Center for Asphalt Technology of Auburn University*. Auburn, Alabama.

West, R.C., 2015. Best Practices for RAP and RAS Management. *In*: *National Center for Asphalt Technology of Auburn University*.

West, R.C. and Copeland, A., 2015. High RAP Asphalt Pavements: Japan Practice - Lessons Learned. *National Asphalt Pavement Association Information Series*, 139, 62.

Williams, M.L., Landel, R.F., and Ferry, J.D., 1955. The Temperature Dependence of Relaxation Mechanisms in Amorphous Polymers and Other Glass-Forming Liquids. *ournal Americans Chemical Society*, 77, 3701–3707.

Willis, J.R., Turner, P., Julian, G., Taylor, A.J., Tran, N., and De Padula, G.F., 2012. *Effects of Changing Virgin Binder Grade and Content on Rap Mixture Properties. Report No. 12-03*. Auburn, AL, USA,.

Wu, S., Pang, L., Liu, G., and Zhu, J., 2010. Laboratory Study on Ultraviolet Radiation Aging of Bitumen. *Journal of Materials in Civil Engineering*, 22 (8), 767–772.

Wu, Z., Zhang, C., Xiao, P., Li, B., and Kang, A., 2020. Performance Characterization of Hot Mix Asphalt with High RAP Content and Basalt Fiber. *Materials*, 13 (3145).

Xiao, F. and Amirkhanian, S.N., 2009. HP-GPC Approach to Evaluating Laboratory Prepared Long-Term Aged Rubberized Asphalt Binders. *Proceedings of GeoHunan International Conference*, 41043 (July), 42–48.

Xu, Q., Zhang, Z., Zhang, S., Wang, F., and Yan, Y., 2014. Molecular structure models of asphaltene in crude and upgraded bio-oil. *Chem. Eng. Technol.*, 37 (7).

Yan, Y., Yang, Y., Ran, M., Zhou, X., Zou, L., and Guo, M., 2020. Application of Infrared Spectroscopy in Prediction of Asphalt Aging Time History and Fatigue Life. *Coatings*, 10 (959).

Yang, X., Mills-Beale, J., and You, Z., 2017. Chemical characterization and oxidative aging of bio-asphalt and its compatibility with petroleum asphalt. *J. Clean. Prod.*, 142, 1837–1847.

Yin, F., Kaseer, F., Arámbula-Mercado, E., and Epps, M., 2017. Characterising the long-term rejuvenating effectiveness of recycling agents on asphalt blends and mixtures with high RAP and RAS contents. *Road Materials and Pavement Design*, 18 (sup:4), 273–292.

Zadshir, M., Oldham, D.J., Hosseinnezhad, S., and Fini, E.H., 2018. Investigating bio-

rejuvenation mechanisms in asphalt binder via laboratory experiments and molecular dynamics simulation. *Construction and Building Materials*, 190, 392–402.

Zanzotto, L., Stastna, J., and Ho, S., 1999. Molecular weight distribution of regular asphalts from dynamic material functions, 32, 224–229.

Zargar, M., Ahmadinia, E., Asli, H., and Karim, M.., 2012. Investigation of the possibility of using waste cooking oil as a rejuvenating agent for aged bitumen. *J. Hazard. Mater.*, 223, 254–258.

Zaumanis, M., Boesiger, L., Kunz, B., Cavalli, M.C., and Poulikakos, L., 2019. Determining optimum rejuvenator addition location in asphalt production plant. *Construction and Building Materials*, 198, 368–378.

Zaumanis, M., Cavalli, M.C., and Poulikakos, L.D., 2018. Effect of rejuvenator addition location in plant on mechanical and chemical properties of RAP binder. *International Journal of Pavement Engineering*, 21 (4), 507–515.

Zaumanis, M., Mallick, R., and Frank, R., 2014a. Evaluation of different recycling agents for restoring aged asphalt binder and performance of 100% recycled asphalt. *Mater. Struct.*

Zaumanis, M. and Mallick, R.B., 2014. Review of very high-content reclaimed asphalt use in plant-produced pavements: State of the art. *Int. J. Pavement Eng.*, 16, 39–55.

Zaumanis, M. and Mallick, R.B., 2015. Review of very high-content reclaimed asphalt use in plant-produced pavements: State of the art. *International Journal of Pavement Engineering*, 16 (1), 39–55.

Zaumanis, M., Mallick, R.B., and Frank, R., 2013. Evaluation of rejuvenator's effectiveness with conventional mix testing for 100% reclaimed asphalt pavement mixtures. *Transp. Res. Rec.*, 2370.

Zaumanis, M., Mallick, R.B., and Frank, R., 2014b. 100% recycled hot mix asphalt: A review and analysis. *Resources, Conservation and Recycling*, 92, 230–245.

Zaumanis, M., Mallick, R.B., and Frank, R., 2016. 100% Hot Mix Asphalt Recycling: Challenges and Benefits. *Transportation Research Procedia*, 14, 3493–3502.

Zaumanis, M., Mallick, R.B., Poulikakos, L., and Frank, R., 2014. Influence of six rejuvenators on the performance properties of reclaimed asphalt pavement (RAP) binder and 100% recycled asphalt mixtures. *Constr. Build. Mater.*, 71.

Zeng, M., Bahia, H.U., Zhai, H., and Turner, P., 2001. Rheological modeling of modified asphalt binders and mixtures. *Journal of the Association of Asphalt Paving Technologists*, 70, 403–441.

Zeng, M., Li, J., Zhu, W., and Xia, Y., 2018. Laboratory evaluation on residue in castor oil production as rejuvenator for aged paving asphalt binder. *Constr. Build. Mater.*, 189, 568–575.

Zeng, W., Wu, S., Wen, J., and Chen, Z., 2015. The temperature effects in aging index of

asphalt during UV aging process. *Constr. Build. Mater.*, 93, 1125–1131.

Zhang, C., Ren, Q., Qian, Z., and Wang, X., 2019. Evaluating the effects of high RAP content and rejuvenating agents on fatigue performance of fine aggregate matrix through DMA flexural bending test. *Materials*, 12 (9), 1–15.

Zhang, J., Sun, H., Jiang, H., Xu, X., Liang, M., Hou, Y., and Zhanyong, Y., 2019. Experimental assessment of reclaimed bitumen and RAP asphalt mixtures incorporating a developed rejuvenator. *Construction and Building Materials*, 215, 660–669.

Zhang, M., Wang, X., Zhang, W., and Ding, L., 2020. Study on the Relationship between Nano-Morphology Parameters and Properties of Bitumen during the Ageing Process. *Materials*, 13 (1472).

Zhang, R., You, Z., Wang, H., Ye, M., Yap, Y.K., and Si, C., 2019. The impact of bio-oil as rejuvenator for aged asphalt binder. *Constr. Build. Mater.*, 196, 134–143.

Zhao, K., Wang, Y., Chen, L., and Li, F., 2018. Diluting or dissolving? The use of relaxation spectrum to assess rejuvenation effects in asphalt recycling. *Constr. Build. Mater.*, 188, 143–152.

Zhou, F., Hu, S., Das, G., and Scullion, T., 2011. High RAP Mixes Design Methodology with Balanced Performance. *In*: *FHWA/TX-11/0-6092-2*. Texas Transportation Institute: College Station, TX, USA,.

Zupanick, M. and Baselice, V., 1997. Characterizing asphalt volatility. *Transportation Research Record*, (1586), 1–9.